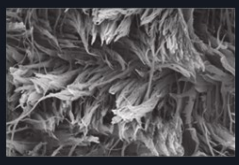
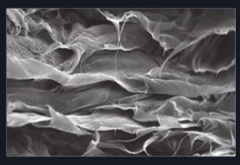
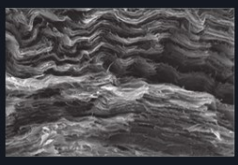

Volume 34 TOPICS IN GEOBIOLOGY Series Editors: Neil H. Landman and Peter J. Harries

Chitin
Formation and Diagenesis

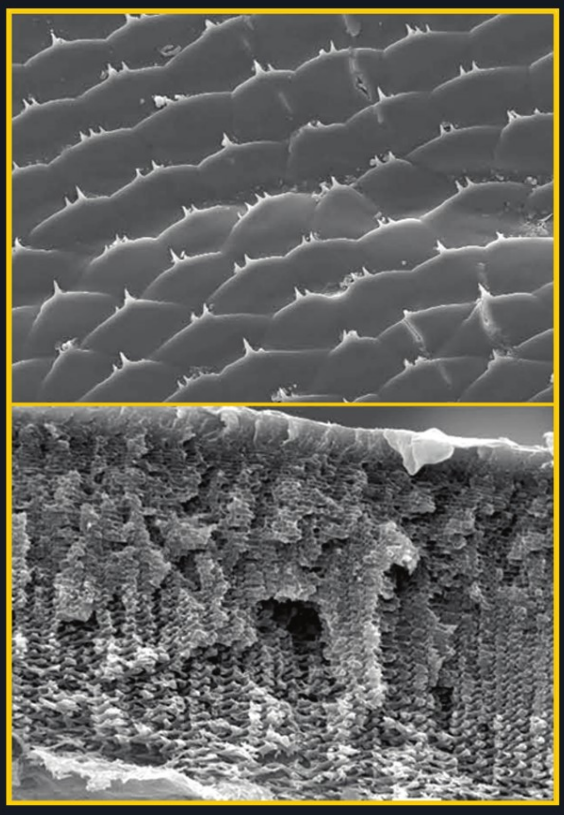

Edited by

Neal S. Gupta

Springer

Chitin

Aims and Scope Topics in Geobiology Book Series

Topics in Geobiology series treats geobiology – the broad discipline that covers the history of life on Earth. The series aims for high quality, scholarly volumes of original research as well as broad reviews. Recent volumes have showcased a variety of organisms including cephalopods, corals, and rodents. They discuss the biology of these organisms-their ecology, phylogeny, and mode of life – and in addition, their fossil record – their distribution in time and space.

Other volumes are more theme based such as predator-prey relationships, skeletal mineralization, paleobiogeography, and approaches to high resolution stratigraphy, that cover a broad range of organisms. One theme that is at the heart of the series is the interplay between the history of life and the changing environment. This is treated in skeletal mineralization and how such skeletons record environmental signals and animal-sediment relationships in the marine environment.

The series editors also welcome any comments or suggestions for future volumes.

Series Editors
Neil H. Landman, landman@amnh.org
Peter Harries, harries@shell.cas.usf.edu

For other titles published in this series, go to
http://www.springer.com/series/6623

Chitin

Formation and Diagenesis

Neal S. Gupta
Editor

Springer

Editor
Neal S. Gupta
Indian Institute of Science Education and Research
Mohali, India
sngupta@iisermohali.ac.in

ISBN 978-90-481-9683-8 e-ISBN 978-90-481-9684-5
DOI 10.1007/ 978-90-481-9684-5
Springer Dordrecht Heidelberg London New York

Library of Congress Control Number: 2010935490

Cover illustrations: Top: Fracture surfaces of the crusher claw tested in wet state and of joint membranes taken from the claws and tested in dry and wet. Photo credit by Christoph Sachs and Helge Fabritius. Centre: SEM of surface and cross section of cockroach cuticle (top) and thickness of cuticle (bottom). Scale in microns. Photo credit by Neal S. Gupta

Printed on acid-free paper

Springer is part of Springer Science+Business Media (www.springer.com)

Preface

There are several books on properties of chitin and associated biomolecules and their biochemical significance. However, the present volume, 'Chitin: Formation and Diagenesis' deals with a wide variety of biogeochemical and organic geochemical aspects of this vital macromolecule written by leading authors and experts in the field.

Chapter 1 deals with chitin nanostructures in living organisms and observes that the occurrence of a chitin-producing system is an ancestral condition present in a number of phyla that supported many organisms during the Cambrian explosion. Current research in the chapter states that chitinous nanostructures are important in order to understand the roles of chitin in vivo, as well as to prepare materials for medical and veterinary applications. Chapter 2 focuses on chitin in the exoskeletons of arthropods. Arthropods use chitin and various proteins as basic materials of their cuticle which form the exoskeletons. The exoskeleton is composed of skeletal elements with physical properties that are adapted to their function and the eco-physiological strains of the animal. These properties are achieved by forming elaborate microstructures that are organized in several hierarchical levels. Additionally, the properties are influenced by variations in the chemical composition of the cuticle, for instance by combining the organic material with inorganic nano-particles. Thus, there is an emphasis in the chapter right from ancient design to novel material science. Chapter 3 covers recent advances in pretreatment chemistry for AMS radiocarbon dating of insects, including isolation of polymeric chitin or chitin monomers. The uses of chitin dates, in particular the archaeological and palaeoenvironmental applications, are also discussed. Problems with the radiocarbon dating of insects, including contamination, degradation, and the often observed offset between dates of insect remains and surrounding organic material, are addressed along with potential solutions. Chapter 4 discusses that stable isotope ratios in chitin are firmly imprinted during biopolymer biosynthesis and reflect dietary, metabolic, and environmental influences. Additionally, chemically preserved archeological chitin are isotopically compatible with modern chitin from comparable environments and new analytical stable isotope techniques with reduced sample size requirements open opportunities to utilize geologically preserved chitin in paleoenvironmental studies. Chapter 5 provides data that show intra- and interspecimen D/H variation in modern water beetles that may relate to systematic

variations in chitin biosynthesis during exoskeleton development. A discussion of existing hydrogen-isotope studies of chitin are presented, including recent advances in hydrogen-isotope analysis that can enhance sample throughput. Chapter 6 provides data on mass spectral investigation of chitin using pyrolysis–GC–MS and characteristic peaks using solid state ^{13}C NMR and scanning transmission x-ray microscopy (STXM) coupled to C,N,O-XANES to facilitate identification of compounds and characteristic peaks for future studies. In Chapter 7 analysis of fossils using a range of mass spectrometric and spectroscopic methods have shown that preserved cuticles include significant amounts of aliphatic hydrocarbon component at times with an aromatic component that is very different to the composition of the cuticle of the living arthropod. Analysis of successively older fossil material reveals that this transformation to an aliphatic composition is gradual and perhaps time dependant. Taphonomic incubation experiments demonstrate that lipids such as fatty acids are incorporated into the decaying chitin protein exoskeleton as early as a few weeks contributing to the aliphatic component. This is supported by chemolytic analysis of fossils that reveal presence of fatty acyl moieties in the macromolecule. Chapter 8 introduces a unique hydrothermal experimental study by comparison of the products derived from maturation of different pre-treated plant and arthropod tissues demonstrates that solvent-extractable and hydrolysable lipids are precursors of the generated aliphatic macromolecular material. Thus, the experiments indicate that labile alkyl compounds can be a source of the insoluble aliphatic component of fossil organic matter in the absence of a resistant aliphatic precursor in the living organism.

Mohali, India Neal S. Gupta

Acknowledgements

Even though I had the privilege and fortune to edit this volume on biogeochemical significance of chitin, several people need to be thanked, as without them it would have been impossible to assemble this. Each chapter has been carefully peer reviewed and I am grateful to the following people for it: Dr. Jennifer A. Tripp (University of Scranton), Dr. Shuhei Ono (MIT), Dr. Darren Gröcke (University of Durham), Dr. Weifu Guo (Carnegie Institution of Washington), Dr. Alok K. Gupta (University of Allahabad), Professor Roger Summons (MIT). Professor Derek Briggs (Yale University) is thanked for discussions regarding outlining the chapters and content of the volume. Dr. Neil Landman is thanked for useful comments from time to time and for correspondence in tracking the progress of the volume. Mrs. Judith Terpos is thanked for guiding me in the production of the volume. I also thank the host universities where I worked in order to compile the volume. They are Yale University, New Haven, CT, USA, MIT, Cambridge, MA, USA and the Carnegie Institution of Washington, Washington D.C., USA. I thank my father Professor Alok K. Gupta for the motivation to complete it in time and my wife Mrs. Mary Gupta for being very patient during the entire process.

Mohali, India Neal S. Gupta

Contents

Contributors

George D. Cody
Geophysical Laboratory, Carnegie Institution of Washington,
Washington, DC 20015, USA
gcody@ciw.edu

Scott A. Elias
Department of Geography, Royal Holloway University of London,
Egham, Surrey TW20 0EX, UK
s.elias@rhul.ac.uk

Helge Fabritius
Department Microstructure Physics and Metal Forming,
Max-Planck-Institut für Eisenforschung, Max-Planck-Str. 1,
40237 Düsseldorf, Germany
h.fabritius@mpie.de

Martin Friák
Department Computational Materials Design,
Max-Planck-Institut für Eisenforschung, Düsseldorf, Germany
m.friak@mpie.de

Darren R. Gröcke
Department of Earth Sciences, Durham University,
Science Labs, Durham DH1 3LE, UK
d.r.grocke@durham.ac.uk

Neal S. Gupta
Indian Institute of Science Education and Research, Transit Campus MGSIPAP,
Complex Sector 26, Chandigarh 160 019, Mohali, India
sngupta@iisermohali.ac.in

Maarten van Hardenbroek
Institute of Environmental Biology, Palaeoecology,
Laboratory of Palaeobotany and Palynology,
Utrecht University, Budapestlaan 4, 3584 CD Utrecht, The Netherlands
m.r.vanhardenbroek@uu.nl

Thomas F. G. Higham
Oxford Radiocarbon Accelerator Unit, Research Laboratory for Archaeology and the History of Art, University of Oxford, Oxford OX1 3QY, UK
thomas.higham@rlaha.ox.ac.uk

Riccardo A. A. Muzzarelli
Professor Emeritus of Enzymology, University of Ancona, Ancona, Italy
muzzarelli.raa@gmail.com

Jörg Neugebauer
Department Computational Materials Design,
Max-Planck-Institut für Eisenforschung, Düsseldorf, Germany
neugebauer@mpie.de

S. Nikolov
Institute of Mechanics, Bulgarian Academy of Sciences,
Acad. G. Bontchev Str., Bl. 4, 1113 Sofia, Bulgaria
sv.nikolov@imbm.bas.bg

Dierk Raabe
Department Microstructure Physics and Metal Forming, Max-Planck-Institut für Eisenforschung, Max-Planck-Str. 1, 40237 Düsseldorf, Germany
d.raabe@mpie.de

C. Sachs
Department of Mechanical Engineering, MIT, 77 Massachusetts Ave.,
Cambridge, MA 02139-4307, USA
csachs@mit.edu

Peter E. Sauer
Department of Geological Sciences, Indiana University,
Bloomington, IN 47405-1405, USA
pesauer@indiana.edu

Arndt Schimmelmann
Department of Geological Sciences, Indiana University, 1001 East 10th Street,
Bloomington, IN 47405-1405, USA
aschimme@indiana.edu

Roger E. Summons
Department of Earth Atmospheric and Planetary Sciences,
Massachusetts Institute of Technology, Cambridge, MA 02139, USA
rsummons@mit.edu

Jennifer A. Tripp
Department of Chemistry and Biochemistry, San Francisco State University,
San Francisco, CA 94132, USA
tripp@sfsu.edu

Chapter 1
Chitin Nanostructures in Living Organisms

Riccardo A.A. Muzzarelli

Contents

Abstract In living organisms, chitin synthase present in chitosomes promotes the polymerization of N-acetylglucosamine, then the native chitin is assembled into nanocrystals. The latter cluster into long chitin-protein fibers that form a planar network whose spacings are filled up with pigments, nano-sized inorganic compounds and other substances. In certain cases quinones contribute to the mechanical strength by tanning. Elaborated but robust structures are present in arthropods, chitons, yeasts, fungi, diatoms, corals and sponges. The occurrence of a chitin-producing system is an ancestral condition observable in a number of phyla. Chitin supported many organisms during the Cambrian life explosion. Current research on the chitinous nanostructures is today important in order to understand the roles of chitin in vivo, as well as to prepare materials for medical and veterinary applications, in particular composites for filling bone defects, hemostatic bandages for emergency management of bleeding, and non-wovens for the ordered regeneration of wounded tissues.

R.A.A. Muzzarelli (✉)
Professor Emeritus of Enzymology, University of Ancona, Ancona, Italy
e-mail: muzzarelli.raa@gmail.com

N.S. Gupta (ed.), *Chitin*, Topics in Geobiology 34,
DOI 10.1007/978-90-481-9684-5_1, © Springer Science+Business Media B.V. 2011

Keywords Chitin • Chitin synthase • Crustaceans • Insects • Diatoms • Sponges • Chitons • Nanofibrils

1.1 Introduction

Early descriptions of the presence of crystalline chitin fibrils in the integuments and organs of arthropods are those by Richards (1951), Runham (1961), Rudall (1955), Rudall and Kenchington (1973) and Brown (1975) among others. The subject has been further dealt with in a chapter of the first book devoted to chitin (Muzzarelli 1977), in the books by Hepburn (1976), Neville (1975, 1993), Muzzarelli et al. (1986), Stankiewicz and VanBergen (1998), Jollès and Muzzarelli (1999) and Muzzarelli (1993, 1996, 2001). Recent chapters and reviews include those by Pont Lezica and Quesada-Allue (1990), Giraud-Guille et al. (2004), Kurita (2006) and Kumar et al. (2004).

The natural associations of chitins with other biopolymers often recur in the cited literature as well as in numerous research articles: for example, most preparations of hyaluronan have chitooligomers at their reducing end, that act as templates for hyaluronan synthesis (Varki 1996). Likewise, composite materials of chitin with inorganic compounds are frequently dealt with in recent publications (Muzzarelli and Muzzarelli 2002b).

Scope of the present chapter is to describe some of the most impressive chitin-based nanostructures of living organisms, to report on their performances at the biochemical and biomechanical levels, and to mention the technological importance of some chitin-based items that mimic natural nanostructures.

1.2 Biosynthesis and Characteristic Properties of Chitins

Ruiz-Herrera's discovery that chitin microfibrils were generated in fungi prompted the investigation of the intracellular location of chitin synthase (EC 2.4.1.16, UDP-2-acetamido-2-deoxy-D-glucose: chitin 4-beta-acetamidodeoxy-D-glucosyltransferase), a member of the family 2 of glycosyltransferases. The polymerization of N-acetylglucosamine requires UDP-N-acetylglucosamine as a substrate and one divalent cation, usually Mg^{2+}, as a co-factor: the product is chitin, the linear polysaccharide of beta-(1–4)-linked 2-acetamido-2-deoxy-D-glucopyranose units. In collaboration with Bracker, he identified chitosomes as the major reservoir of chitin synthetase in fungi. Peculiar in size, buoyant density and membrane thickness, the fungal chitosome exhibited the characteristic reversible dissociation into 16S subunits (Hanseler et al. 1983). The 16S subunits are the smallest molecular entities that retain chitin synthase activity, so that further dissociation leads to inactivity. Structural and enzymatic characteristics are in favor of the chitosome being poised for exocytotic delivery rather than endocytotic recycling. Chitosomes were originally

described in fungi (Leal-Morales et al. 1988, 1994; Ziman et al. 1996; Chuang and Schekman 1996) and appear as specialized intracellular compartments different from secretory vesicles, because they have a unique lipid and protein composition (Bracker et al. 1976; Hernandez et al. 1981). The chitosome represents the main vehicle for delivering the membrane-integral enzyme chitin synthase to the cell surface, nevertheless many aspects are enigmatic such as the role of proteins encoded by the reported chitin synthase genes in the structure or function of chitosome, and the integration with the cell surface to construct the organized microfibrillar scaffold of the cell wall (Bartnicki-Garcia 2006).

Ruiz-Herrera and Bartnicki-Garcia (1974) were able to synthesize chitin nanofibrils in vitro with the aid of a "soluble" chitin synthase preparation from *Mucor rouxii* (Fig. 1.1); the x-ray diffraction spectra indicated that the crystallinity degree of the nanofibrils obtained in vitro via the natural biosynthetic route was most similar to that of chitin from yeast cell walls of *M. rouxii*. Incidentally, it should be underlined that the natural biosynthesis of chitin duplicated in vitro has nothing in common

Fig. 1.1 Electron micrograph of chitin microfibrils synthesized in vitro by a soluble enzyme from the yeast form of *Mucor rouxii*. The sample was washed with cold 1 N NaOH to remove the enzyme, mounted, and shadow cast with Pd at 19°C (× 50,000) (Courtesy of Salomon Bartnicki-Garcia)

with the artificial synthesis of oligomeric chitin by chitinase-catalyzed polymerization of chitobiose oxazoline, or by other techniques involving organic media (Sakamoto et al. 2000; Yoon 2005).

Chitin biosynthesis takes place in three steps: in the first one the enzyme catalytic domain facing the cytoplasmic site forms the polymer; the second step involves the translocation of the nascent polymer across the membrane and its release into the extracellular space, and the third step completes the process as single polymers spontaneously assemble to form crystalline microfibrils. In subsequent reactions the microfibrils combine with other sugars, proteins, glycoproteins and proteoglycans to form fungal septa and cell walls as well as arthropod cuticles and peritrophic matrices, notably in crustaceans and insects. The present knowledge of the structure, topology and catalytic mechanism of chitin synthases is rather limited: gaps remain in understanding biosynthesis, enzyme trafficking, regulation of enzyme activity, translocation of chitin chains across cell membranes, fibrillogenesis and the interaction of microfibrils with other components of the extracellular matrix. However, clearer views of chitin synthase function and its regulation are being provided by cumulating genomic data on chitin synthase genes and new experimental approaches (Merzendorfer 2006).

Conserved acidic units of the donor and acceptor binding sites that could be negatively charged under physiological conditions play a functional role as a base in a nucleophilic substitution reaction leading to the formation of the glycosidic bond. Chitin synthase is a processive enzyme, i.e. it remains bound to the polymer through many polymerization steps that add single GlcNAc units to the non-reducing end of the growing polymer. The directionality of this synthesis was recently re-investigated and confirmed using electron crystallography applied to reducing-end labeled beta-chitin from vestimentiferan Lamellibrachia satsuma tubes and nascent beta-chitin microfibrils from the diatom *Thalassiosira weissflogii*. The microfibrils were extruded with their reducing end away from the biosynthetic loci, an orientation consistent only with elongation through polymerization at the non-reducing end of the growing chains. Such a chain-extension mechanism, which has also been demonstrated for cellulose and hyaluronan, appears to be general for glycosyltransferases that belong to the glycosyl transferase 2 family (Imai et al. 2003). The initiation of chain assembly seems to involve a covalently bound primer to which the incoming sugar moiety is transferred (Merz et al. 1999). Figure 1.2 shows the detection of chitin in thin sections of budding yeast with gold markers (Horisberger and VonLanthen 1977), since then a widely adopted technique.

1.2.1 Alpha-Chitin: The 3D Hydrogen Bonded Polymorph

Chitin is a common constituent not only of the crustacean exoskeleton, but of the arthropod cuticle in general, including insects, chelicerates, and myriapods. It also occurs in mollusk shells and fungal cell walls. All chitins are made of chitin nanofibrils (crystallites) embedded into a less crystalline chitin. Alpha-Chitin is the most

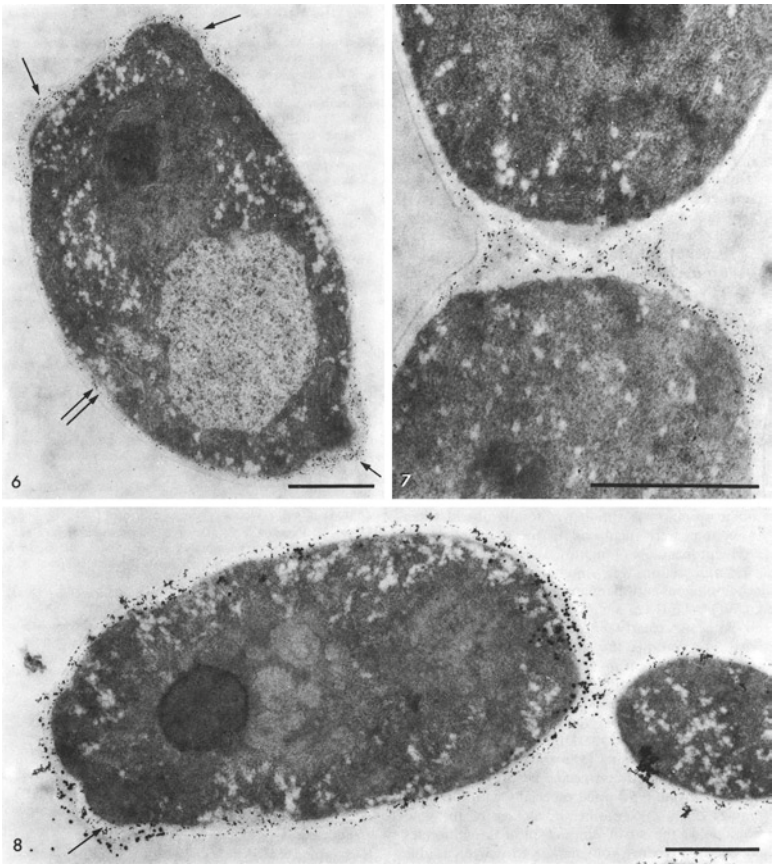

Fig. 1.2 *Candida utilis* sections; *bars* represent 1 μm. **6**, the presence of chitin is detected in the scars (*arrows*) and in the cell wall near the plasmalemma (*double arrows*) marked with wheat germ agglutinin-Au-I. **7**, the forming septum of *C. utilis* marked with WGA-Au-I. **8**, sections marked simultaneously with anti-mannan antibodies-Au-I and WGA-Au-II. The *arrow* indicates the presence of mannan in the bud scar (small granules Au-I 5 nm) accompanying chitin (large granules Au-II 26 nm) (Horisberger and VonLanthen 1977)

abundant polymorph; it occurs in fungal and yeast cell walls, in the crustacean exoskeletons, as well as in the insect cuticle. Studies on the crystallographic texture of the crystalline alpha-chitin matrix in the biological composite material forming the exoskeleton of the lobster *Homarus americanus* have shown that everywhere in the carapace the texture is optimized in such a way that the same crystallographic axis of the chitin matrix is parallel to the normal to the local tangent plane of the carapace. Notable differences in the texture are observed between hard mineralized parts and soft membranous parts (Raabe et al. 2005abc, 2006).

The hard chitinous tissues found in some invertebrate marine organisms are paradigms for robust, lightweight materials. Examples are the oral grasping spines of Chaetognaths, *Sagitta* in particular (Saito et al. 1995; Bone et al. 1983), the

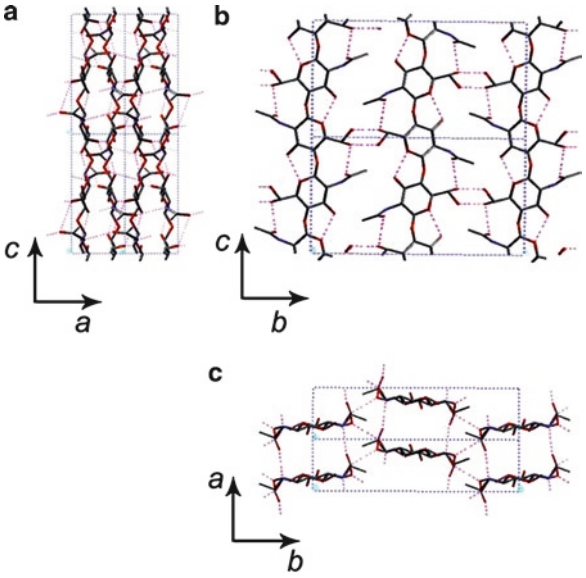

Fig. 1.3 Structure of alpha-chitin: (**a**) ac projection; (**b**) bc projection; (**c**) ab projection. The structure contains a statistical mixture of two conformations of the $–CH_2OH$ groups (Original data by Minke and Blackwell 1978. Reprinted from Rinaudo 2006. Copyright 2006, with permission from Elsevier)

granular chitin in the epidermis of nudibranch gastropods (Martin et al. 2007) and the filaments of the seaweed *Phaeocystis* (Chretiennot-Dinet et al. 1997). These uncommon alpha-chitins are interesting for structural studies since they present remarkably high crystallinity and absence of pigments, proteins and calcite.

In the proposed crystal structures of *alpha-chitin* (Fig. 1.3), the chitin chains are organized in sheets where they are tightly held by a number of intra-sheet hydrogen bonds. This tight network, dominated by the rather strong C–O…NH hydrogen bonds, maintains the chains at the distance of about 0.47 nm along the a axis of the unit cell. It is important to note that in the alpha-chitin there are also some inter-sheet hydrogen bonds along the b axis of the unit cell, involving the hydroxymethyl groups of adjacent chains (Fig. 1.3): this peculiar feature is not found in the structure of beta-chitin (vide infra) (Minke and Blackwell 1978; Noishiki et al. 2003; Rinaudo 2006).

While chitin is usually found in stiff extracellular coatings typified by the arthropod exoskeleton, it is not associated with the soft, flexible mollusk skin. However, in nudibranch gastropods (Opisthobranchia, Mollusca) chitin occurs as intracellular granules that fill the epidermal cells of the skin and the epithelial cells of the stomach. Granular chitin does not depress the suppleness and flexibility of such tissues. The identity of chitin was demonstrated by the use of an antibody raised in rabbits against crab chitin: the antibody revealed that the spindles in the epidermal cells were immunoreactive, as well as the radula teeth and the cuticles of the head alimentary tract. More information on the chemical composition of the spindles

was obtained after hydrolysis with HCl, and by degradation with chitinase and N-acetylglucosaminidase: the obtained N-acetylglucosamine was silylated for gas-chromatographic and mass spectrometry determination. Raman and infrared spectrometry data supported the chitin identification.

In response to nematocysts fired by tentacles of prey Cnidaria, the epidermal cells of eolid nudibranchs (Aeolidacea) release masses of chitin granules, which then form aggregates with the nematocyst tubules, having the effect of insulating the animal from the dangerous consequences of the Cnidaria tentacles: thus, the specialized epidermis enables nudibranchs to live with and feed on Cnidaria. Sandbag-like cells filled with chitin granules exhibit some advantages, compared to the rigid chitin exoskeleton of arthropods: there is no need for periodic molts, and damages in the skin is repaired by cell proliferation in a fast, locally circumscribed regeneration process (Martin and Walther 2003). The slugs without shells move, bend and swim with a flexible skin, waving their rhinophores and cerata on contact with their prey's tentacles. Notwithstanding the success story of the rigid exoskeletons of arthropods, the chitin-bearing specialized skin enabled nudibranchs to invade an aversive biotic niche and take advantage of abundant food (Martin et al. 2007).

The main constituents of the beak of the jumbo squid, *Dosidicus gigas*, are chitin fibers (15–20 wt.%) and histidine- and glycine-rich proteins (40–45%). Notably absent are mineral phases, metals and halogens. Despite being fully organic, beak hardness and stiffness are at least twice those of the most competitive synthetic organic materials, and comparable to those of *Glycera* and *Nereis* jaws. Furthermore, the combination of hardness and stiffness makes the beaks more resistant to plastic deformation than virtually all metals and polymers. In fact the closure forces exerted by the mandibular muscles of some species are large enough to crush the shells of gastropods. Moreover, the presence of intact beaks in the stomachs of squid predators indicates a high resistance to proteolysis.

The 3,4-dihydroxy-L-phenylalanine and abundant histidine content in the beak proteins as well as the pigmented hydrolysis-resistant residue testify cross-linking via quinone tanning. A high cross-linking density between the proteins and chitin may be the most important determinant of hardness and stiffness in the beak. Even after prolonged hydrolysis, some aminoacids remain in the chitin; while this is a general situation at the aminoacid trace level, the data for the *Dosidicus gigas* chitin indicate the presence of substantial amounts of 15 aminoacids with prevalent percentages of glycine, alanine and histidine (Miserez et al. 2007).

Knowledge about cephalopod beaks has emerged largely from ecological and population studies, interest in the dietary habits of their predators, and growing importance for the fish industry. The rostral (tip) region is unmistakably the hardest part; in contrast, the back of the lateral wall and the wing have mechanical characteristics similar to soft cartilaginous tissues with a hydrogel-like texture. Their properties also appear to be correlated with coloration, hardness increasing with level of pigmentation. The cephalopod beaks consist of chitin fibers embedded in a protein matrix. Alkali deproteinization treatments of *Octopus vulgaris* beak rostra indicate chitin levels of about 6–7% but enzymatic studies on the beaks of *Loligo*

species suggest about 20%. These studies also indicate that the beaks are devoid of minerals, metal ions and halogens. The aminoacid composition of a near-tip beak sample was dominated by glycine (26%), alanine (14%) and histidine (ca. 10%). Other notable constituents detected were DOPA and glucosamine. The only crystalline phase in the beaks was alpha-chitin, manifested by the intense peaks at 2theta = 9° and 19° [associated with the (002) and the combination of (101) and (004) reflections, respectively] and the weaker peaks at 12, 23 and 27° [due to (012), (103) and (031) reflections]. In contrast, the beta-chitin exhibits only two broad peaks, at 8° and 19°. From the corresponding chemical analysis, the chitin mass fraction was estimated to be 15–20% with no detectable levels of metals or halogens. The nature of the remaining 35–40% of the beaks is unknown.

The presence of chitin, His-rich proteins and catechols (i.e. DOPA) in *Dosidicus* beaks suggests intriguing parallels with insect cuticles. All hard insect cuticles contain some chitin, with concentrations between 15% and 30% of dry weight. Like cellulose, chitin is stiff in tension (Terbojevich et al. 1991) and, especially when oriented with the axis of loading, contributes to the reinforcement of the protein matrix (Fig. 1.4). Beak proteins are glycine-, histidine- and alanine-rich. Overall, insect cuticles are also glycine- and alanine-rich. Although the global histidine content of cuticles rarely stands out, the enrichment of histidine near the C-terminal region of cuticular proteins and its role as a sclerotizing agent have been emphasized. Chitin is traditionally viewed as extensively H-bonded to cuticular proteins through histidyl residues to form stable glycoprotein complexes.

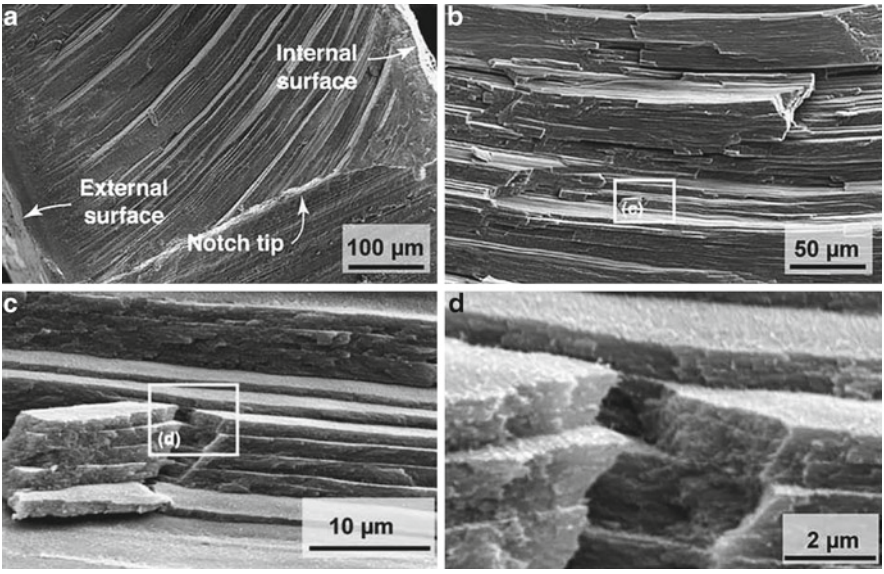

Fig. 1.4 Scanning electron micrographs of fracture surfaces of squid beak, in the near-tip regions where the material exhibits a largely lamellar microstructure. The lamellae are typically 2–3 µm thick and are aligned parallel with the long axis of the beak. Progressively increasing magnifications (Reprinted from Miserez et al. 2007. Copyright 2007, with permission from Elsevier)

In other analyses of hydrolyzed insect cuticle, however, covalent cross-links of catechols coupled to both histidine and glucosamine (presumably from chitin) were evident. The abundance of histidine in *Dosidicus* beaks more closely resembles *Nereis* and *Glycera* jaw compositions than insect cuticle (Miserez et al. 2007).

1.2.2 Beta-Chitin: The 2D Hydrogen Bonded Polymorph

Beta-Chitin is found in association with proteins in squid pens: the structural characteristics of chitin from *Illex argentinus* were defined recently and were in agreement with data for *Ommastrephes bartrami*. The dry pen contains 31% chitin whose viscosity average molecular weight calculated from the intrinsic viscosity is over 2 MDa, the crystallinity index derived from x-ray spectra is 75%; the characteristics of the beta polymorph appear in the CP-MAS ^{13}C-NMR spectrum in terms of configurations of C^3 and C^5 resulting from the different hydrogen bonds established. The degree of acetylation was found to be 0.96 (Cortizo et al. 2008). As shown in Fig. 1.5, beta-chitin lacks hydrogen bonds in the b direction, and therefore it is more susceptible than alpha-chitin to intra-crystalline swelling, acid hydrolysis even at low acid concentrations, and removal of scarcely crystalline fractions.

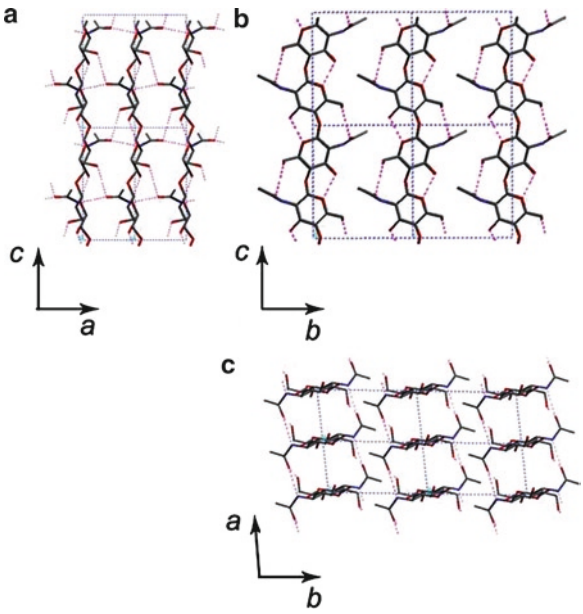

Fig. 1.5 Structure of anhydrous beta-chitin: (**a**) ac projection; (**b**) bc projection; (**c**) ab projection. A major point of difference from alpha-chitin is the absence of hydrogen bonds in the b direction (Reprinted from Rinaudo 2006. Copyright 2006, with permission from Elsevier)

Beta-chitin occurs also in the tubes synthesized by pogonophoran and vestimentiferan worms mentioned above, in aphrodite chaetae as well as in the lorica of protozoa like *Eufolliculina uhligi*: the lorica of the latter contains ribbon-like alkali-resistant fibrils that exhibit the x-ray diffraction pattern typical of beta-chitin. The lorica material seems to be generated in numerous vesicles that release their initially amorphous content by exocytosis; microfibril formation takes place outside the cell. Microfibril formation is prevented when loricae are secreted in dilute solutions of Calcofluor White and Congo Red, as it is known for chitin. After extraction with 20% NaOH the lorica retains its shape but a meshwork of 20 nm wide flattened fibrils becomes observable (Mulisch et al. 1983).

The kinetics of chitin synthesis in *Eufolliculina uhligi* and the influence of the inhibitors diflubenzuron and nikkomycin were analysed by Schermuly et al. (1996) by fluorescence microscopy after staining with monoclonal anti-chitin and FITC-coupled secondary antibody. The feeding stage (trophont) of *E. uhligi* incorporated tritiated N-acetylglucosamine into intracellular chitin for about 2 h, before cell division initiated. Said inhibitors reduced the incorporation of N-acetylglucosamine into chitin, but did not influence chitin deposition when applied to swarmers. In contrast, the quantity of chitin was drastically reduced in the loricae of swarmers derived from trophonts already exposed to the inhibitors.

Among the ciliates the cyst walls of *Blepharisma undulans* and *Pseudomicrothorax dubius* examined with wheat germ agglutinin-gold conjugate were found to contain 3-nm fibrils of chitinous nature. Pretreatment of the sections with chitinase inhibited labeling. The apostome *Hyalophysa chattoni* secretes a phoretic cyst wall composed of chitin, mucopolysaccharides and protein. These results obtained from phylogenetically distant species confirm that chitin synthesis is an ancestral feature of ciliated protozoa (Mulish and Hausmann 1989; Landers 1991). An exhaustive search of the crystal structure of beta-chitin recently made by Yui et al. (2007) confirmed the original structure proposed by Gardner and Blackwell in 1974.

The pens of the squids *Loligo sanpaulensis* and *Loligo plei* have become available in considerable amounts from the fisheries in Brazil, for the extraction of beta-chitin. Due to the low content of inorganic compounds the demineralization step is skipped and a two-step alkaline treatment was deemed adequate to produce beta-chitin with low ash contents (<0.7%). Indeed, the inorganic contents were particularly low: Ca < 10.4 ppm, Mg < 2.5 ppm, Mn < 3.1 ppm and Fe < 1.8 ppm (Lavall et al. 2007; Chandumpai et al. 2004). Similarly, beta-chitin and the corresponding chitosan have been isolated from the pens of *Loligo lessoniana* and *Loligo formosana*; they have been chemically characterized to qualify a potential chitin source.

1.3 Chitin in Insects

Insect chitin is a secretion product of epidermal, tracheal or midgut epithelial cells. Electron microscopy studies using *Calpodes* epidermal cells showed densely stained areas at the tips of microvilli referred to as plasma membrane plaques: because the plaques were only observed during cycles of cuticle formation, they

were considered as clusters of chitin synthesizing enzymes (Binnington 1985; Locke 1991). In accordance with the predicted site of epidermal chitin synthesis, immuno-histochemistry using polyclonal anti-chitin synthase antibodies showed strong labeling within the apical region of the epidermis from the cockroach *Periplaneta americana* (Merzendorfer and Zimoch 2003). Similar results have been obtained for midgut epithelial cells that produce the chitin found in the peritrophic matrix, shown in Fig. 1.6 (Lehane 1997).

Hopkins and Harper (2001) used transmission electron microscopy and wheat germ agglutinin-gold staining to visualize newly secreted chitinous material in lepidopteran

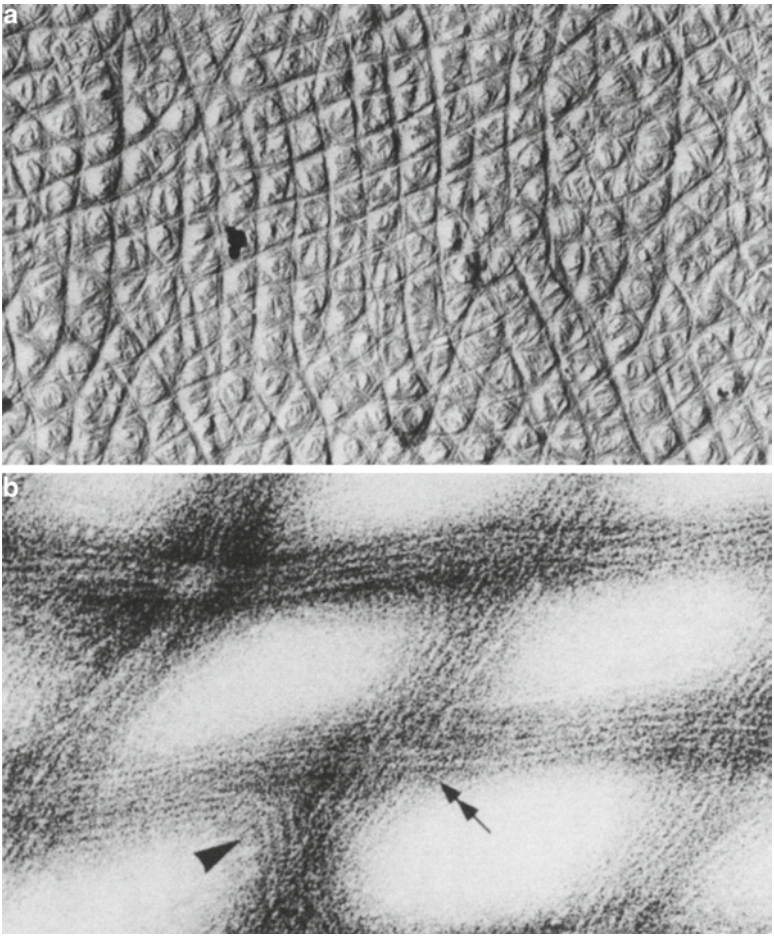

Fig. 1.6 (**a**) Nanofibrillar bundles are regularly arranged within the peritrophic matrix of the larva of *Tipula* sp. (× 22,000). (**b**) The arrangement of nanofibril bundles of the peritrophic matrix of *Forficula auricularia* (× 270,000). The *double arrowhead* indicates a region of felting; the *single arrowhead* indicates individual nanofibrils sharply changing course. Diameters of individual nanofibrils are 2–6 nm; length ca. 500 nm; one bundle contains ten or more parallel nanofibrils. Reprinted, with permission Lehane (1997). www.annualreviews.org

midgut sections: the secretion product was found on the microvillar apical surface but also within the apical region of microvilli. In line with these findings, in-situ hybridization performed with cryosections of the *Manduca* larval midgut demonstrated that chitin synthase is expressed in brush border of columnar cells. Immunohistochemistry using polyclonal anti-chitin synthase antibodies further showed that the enzyme is indeed localized at the brush border but restricted to apical tips of microvilli. Confocal laser scanning microscopy has unveiled vesicular structures in the cytoplasm of columnar cells that undergo immunological reaction with the anti-chitin synthase antibodies.

The vesicles may be on their way from the Golgi apparatus to the apical tips of microvilli (Zimoch and Merzendorfer 2002), however, the vesicles also may resemble fungal chitosomes. Similar observations were made on cell-free precipitates from crude extracts of the red flour beetle *Tribolium castaneum*: chitin synthase produced a network of long microfibrils 10–80 nm thick, aligned in parallel. The microfibrils were associated with particles approximately 50–250 nm in diameter, interpreted as insect chitosomes (Cohen 1982); analogous observations were made on the biosynthesis of chitin by the brine shrimp (Horst 1981). The fungal chitin synthase isoforms Chs1p and Chs3p are distributed between the plasma membrane and chitosomes, which may therefore serve as an endosomal reservoir of these enzymes (Ziman et al. 1996). Thus, insect chitin synthases may also reside in different membrane compartments: in the apical plasma membrane and in the membranes of different endosomal compartments such as transport vesicles or chitosomes (Merzendorfer 2006). Chitin synthase is also assisted by other enzymes such as the glutamine-fructose-6-phosphate aminotransferase (EC 2.6.1.16) as elucidated in early studies on *Locusta migratoria* (Surholt 1975). Radiochemical techniques helped elucidate the metabolism of ^{14}C-glucose, for example in the blowfly *Phormia regina* and mechanical testing helped characterize the honeybee *Apis mellifera* cuticle at different developmental ages (Tate and Wimer 1974; Thompson and Hepburn 1978).

Of course the newly secreted amorphous chitin undergoes crystallization as soon as the conditions recur for the formation of the tissue, which are: alpha or beta polymorph requirements, need for controlled partial deacetylation, cross-linking to other biopolymers, and quinone tanning. Chitin nanofibril deposition is tuned to permit morphogenesis and tissue growth. Thus, as a consequence, the microfibers are made of chitin nanocrystals regularly arranged in a chitin matrix of lower degree of crystallinity. When thin sections of the fly *Rhyssa persuosaria* ovipositor are properly oriented with the axis of the ovipositor parallel to the electron microscope beam, the chitin crystallites in cross section are seen as an array of small dark dots of about 2 nm in width, embedded in a clear matrix assigned to the non-diffracting substances (proteins). The distribution of the crystallites follows a nearly hexagonal pattern with distances from center to center of approximately 7 nm (Giraud-Guille et al. 1990). Deviations from this behavior are observed for specialized tissues essentially made of chitin crystallites alone, such as the grasping spines of the worm *Sagitta* (alpha-chitin) and the flotation filaments of the diatom *Thalassiosira fluviatilis* (beta-chitin).

1.3.1 Sclerotization of the Insect Cuticles

In insects the sclerotization of cuticles is particularly important for the mechanical properties of the wings. The native insect cuticle was studied at several different stages throughout its sclerotization process (also known as tanning). As tanning proceeds, the catechols react with the proteins via a chemo-enzymatic process catalyzed by an oxidase. The catechols are hydrophobic components and hence the water content of the cuticle decreases as tanning proceeds. Changes in mechanical properties take place as a function of the ratio of quinone as demonstrated on *Sarcophaga bullata* larvae by Sugumaran and Lipke (1983) who proposed a clear reaction scheme: the sclerotizing catechol is oxidized to the quinone by cuticular polyphenol oxidase, thus exoskeletal proteins probably add on to the quinone by a Michaelis 1,4-addition reaction; the catechol-protein adduct is enzymatically oxidized again to quinone that in turn generates protein-protein cross-links.

Elytra from the beetles *Tribolium castaneum* and *Tenebrio molitor* (yellow mealworm) were tested by dynamic mechanical analysis. In *T. castaneum,* an economically important agricultural pest, it was possible to use RNA interference techniques to selectively suppress laccase gene expression during sclerotization in order to test the role of laccase in cuticle tanning. The fracture stress of the fully tanned elytra was 45 ± 12 MPa; stiffness was very high as shown by the Young's modulus of 1.67 GPa, and the elastic modulus was 4.86 GPa. Laccase silencing accompanied by water loss resulted in cuticles with poor fracture stress and strain, proving quantitatively that laccase plays a major role in tanning as well as showing that water loss alone is not responsible for the superior mechanical properties of fully tanned insect cuticle.

Within the cuticle the chitin is assembled into nanofibres about 3 nm in diameter and about 300 nm long, each containing 19 molecular chains (Atkins 1985). Although it has never been specifically measured, the stiffness of these nanofibres is at least 150 GPa, based on the observation that cellulose is about 130 GPa and the extra bonding in the chitin crystallite is going to stiffen it further. Given the fact that in aqueous suspension chitin nanofibres are highly thixotropic and liquid crystalline (Murray and Neville 1998), it seems that stiffness and thixotropy are crucial properties for the self-assembly of the components of the cuticle. The number of chitin chains in the nanofibre is probably close to a minimum for internal stability of the crystallite; hence the nanofibres present the maximum surface area for interfacial interactions.

The complexation of the remaining proteins with the chitin seems to be fairly consistent in that even in the softest of cuticles a drastic treatment (with boiling 5% NaOH) is required to remove the protein from the chitin. X-ray diffraction of the ovipositor of the wood wasp *Megarhyssa* suggested that the proteins surround the chitin in a regular manner (Blackwell and Weih 1980). Later work on this ovipositor, allied with more careful molecular modeling and the analysis of the crystalline structure of the chitin nanofibril, suggested that the protein is attached only to the 010 faces and that the other faces of the nanofibril are bare of bound protein.

The explanation of stiffening of cuticle (tanning, sclerotisation) was suggested long ago (Pryor 1940) : as soon as the old cuticle has been shed, the epidermal cells secrete a variety of substituted o-diphenols. They are converted into the more reactive quinone form and, supposedly, cross-link the proteins making the matrix stiff, hydrophobic, insoluble and chemically inert.

There are various chemo-enzymatic models today inspired to the quinone tanning hypothesis originally elaborated by entomologists: they are mainly based on the use of chitosan that is much more reactive than chitin, and range from removal of phenols from industrial waters (Yamada et al. 2006), to innovative textile fibers (Sampaio et al. 2005, Freddi et al. 2006), high-performance coatings (Uyama and Kobayashi 2006), delivery of vitamins (Muzzarelli and Muzzarelli 2002a; Muzzarelli et al. 1994, 2003), and biofabrication of biosensors that meld the molecular recognition capabilities of biochemistry with the signal processing capabilities of electronic devices (Yi et al. 2005; Miscoria et al. 2006; Abdullah et al. 2006, Lu et al. 2006).

The research on quinone sclerotization has removed the belief that the cuticle can be stiffened simply by the alteration of the water content (Vincent 1980): however the control of stiffness remains in general a matter of manipulating the water content (Vincent 1990). In some cuticles the insect can increase the water content so that the modulus decreases. This happens in the blood-sucking bug *Rhodnius*, for instance, which can change the pH of the cuticle from about 7 to below 6, thereby increasing the charge density of the cuticular protein and increasing the cuticular water content from about 26% to 31%, dropping its stiffness from 250 to 10 MPa and increasing its extensibility from 10% to more than 100% (Reynolds 1975).

Moreover, since nearly all adult insects fly, they must have a very efficient and lightweight exoskeleton. Information is available about the mechanical properties of cuticle: the Young's modulus for soft cuticles is about 1 kPa to 50 MPa, of sclerotised cuticles 1–20 GPa; and for one of its components, the chitin nanofibril, the Young's modulus is more than 150 GPa. Experiments based on fracture mechanics have not been performed although the layered structure probably provides some toughening. The structural performance of wings and legs has been measured, but the consequences of buckling remain unknown. The insect wing undergoes millions of cycles, flexing or buckling on each cycle, but nothing is known of fatigue.

Studies on a number of orders (Orthoptera, Phasmida, Lepidoptera, Hymenoptera and Coleoptera) revealed that the reinforcement against wear and tear is achieved by impregnating the sclerotised cuticle of the mandible with heavy metals such as Zn, Mn, or Fe (Quicke et al. 1998). These metals are present in relatively large amounts up to 16% of dry mass of the mandibular cutting edges and increase their hardness significantly (Schofield et al. 2002, 2003). How the incorporation of metals into the cuticle hardens and stiffens the cuticle is not yet understood (Vincent and Wegst 2004), but transition metal ions coordinate the functional groups of chitin (and other biopolymers) thus acting as cross-linkers (Muzzarelli and Tubertini 1969).

The remarkable mechanical performance and efficiency of cuticle can be analysed and compared with those of other materials using material property charts and material indices. Charts have been elaborated to show: (1) stiffness per unit weight

(Young's modulus vs. density); (2) elastic hinges and elastic energy storage per unit weight (specific Young's modulus vs. specific strength); (3) fracture resistance under various loading conditions (Young's modulus vs. toughness); (4) wear resistance (Vicker's hardness). In conjunction with a structural analysis of cuticle these charts help to understand the relevance of microstructure (fibre orientation effects in tendons, joints and sense organs, for example) and shape (including surface structure) of this fibrous composite for a given function. With modern techniques of analysis of structure and material, and emphasis on nanocomposites and self-assembly, insect cuticle should be the archetype for composites at all scale levels.

Current knowledge of cuticle derives from the application of biochemistry to the structure formation, and from the application of principles of materials science to the natural structures. Technical benefit can be gained from both these streams: from the disruption of the normal biochemical reactions we can acquire control of pest insects. Development of biomimetic materials susceptible of industrial exploitation may be found in the design optimisation that is perceived in biological materials: adhesive-free and reversible attachment systems, wear resistant articulations with variable frictional properties, functional surfaces, mechano-sensors, hardening and stiffening of polymers through metal incorporation, specific fibre alignment for wear resistant surfaces, fatigue and fracture resistance, are examples. The use of chitin nanofibrils in composite design for improved mechanical properties is another (Muzzarelli and Muzzarelli 2005). Usefully large structures can be generated in this way as indicated by the size of some marine crustaceans and of the insects which flew in the forests of the Carboniferous era.

1.4 Chitin in Crustaceans

Crustaceans and insects protect themselves from predators and pathogens by secreting an exoskeleton that provides mechanical support to the body, armor against predators, and defense against pathogens while permitting mobility through the formation of joints and attachment sites for muscles. The matrix, made of four superimposed layers and composed of chitin associated with proteins, is produced by an underlying monolayer of epidermal cells that also secrete modest quantities of lipids in the epicuticle, and carothenoids in the pigmented layer.

Chitin fibers in crustacean shells are associated with carbonate that diffuse and precipitate after the fibrous component has been excreted and stabilized; carbonic anhydrase, is synthesized in relation with the control of calcification: maximum activity is attained during the initial stages of calcification in producing carbonate ions. Analogous phenomena occur with collagen fibers and calcium phosphate in bones. In these tissues, the supporting organic component is made of preformed nanometer to micrometer-size elongated particles arranged into supramolecular structures with geometry analogous to that of some liquid crystals. In compact bones, arthropod cuticles and plant cell walls, these structures exhibit the macroscopic features of a cholesteric phase, except fluidity. In most cases, collagen, chitin and

cellulose can be extracted from the biological tissues and dispersed in aqueous media to form colloidal suspensions. At appropriate concentrations, liquid crystalline phases can be identified, indicating that rod-like or spindle-like particles tend to align cooperatively in these systems. The particles are rigid and their shape is constant throughout the phase diagram. This helps understand the influence of various parameters, such as concentration, pH, and ionic strength on the behavior of the suspensions (Li et al. 1996, 1997; Nair and Dufresne 2003).

The arthropod cuticle is a multilayered extracellular matrix produced by the epidermis during embryogenesis and molting. The amphipod crustacean *Parhyale hawaiensis* had a common ancestor with *Drosophila* about 510 million years ago. Molecularly and histologically, cuticle differentiation has been extensively investigated in the embryo of the insect *Drosophila melanogaster*: the establishment of the layers of the *Parhyale* juvenile cuticle is largely governed by mechanisms observed in *Drosophila*, e.g. the synthesis and arrangement of chitin in the inner procuticle are separate processes. The analysis of *Parhyale* cuticle differentiation allows the characterization of the cuticle production and organization factors. *Parhyale* embryogenesis is completed after 240 h post-fertilization (hpf); this period has been subdivided into 30 stages. Cuticle differentiation has been observed to start around stage 26 (S26) at 180 hpf. To trace the cellular mechanisms of cuticle differentiation in the *Parhyale* embryo, Havemann et al. (2008) have analyzed the ultrastructure of the cuticle of staged embryos from 120 hpf (S21) to 240 hpf (S30), shown in Fig. 1.7.

Chitin synthesis and orienting factors are conserved between insects (*Drosophila*) and crustaceans (*Daphnia*). Arthropod chitin is synthesised and extruded to the extracellular space by the large glycosyltransferase chitin synthase that resides in the apical plasma membrane of epidermal cells (chitin synthase-1) or in the epithelium of the midgut (chitin synthase-2). In a similar search with the amino acid sequence of *Drosophila* chitin synthase-1, it was found that the *Daphnia* genome encodes a third protein with a chitin synthase signature. A review of the literature concerning cuticle structure supports the conclusion that the epicuticle has been more sensitive to selective forces during evolution than have the envelope and the procuticle.

The carapace of decapod crustaceans is a biological multiphase nano-composite consisting of an organic matrix (crystalline chitin and non-crystalline proteins) and biominerals (calcite, phosphate). The synchrotron measurements of the crystalline

Fig. 1.7 (continued) disrupted manually (S25). SEM. (**c**) As detected with gold-conjugated WGA (*black dots*), this layer contains chitin (S24), TEM, cross section. (**d**) In tangential section, the apical plasma membrane during chitin synthesis carries regularly spaced microvillus-like structures (mv) with electron-dense tips called plaques (S25), TEM, tangential section entering from the cuticle at the *right* side into the epidermal cell (*left*). (**Inset d'**) Longitudinally sectioned microvillus-like structures (egg eggshell), TEM, longitudinal section. (**e**) In early S26, the apical plasma membrane of the epidermal cells is smooth and chitin production is terminated (EC embryonic cuticle), TEM, cross section. Bars 100 μm (**a**), 3 μm (**b**), 1 μm (**c**–**e**) (Havemann et al. 2008)

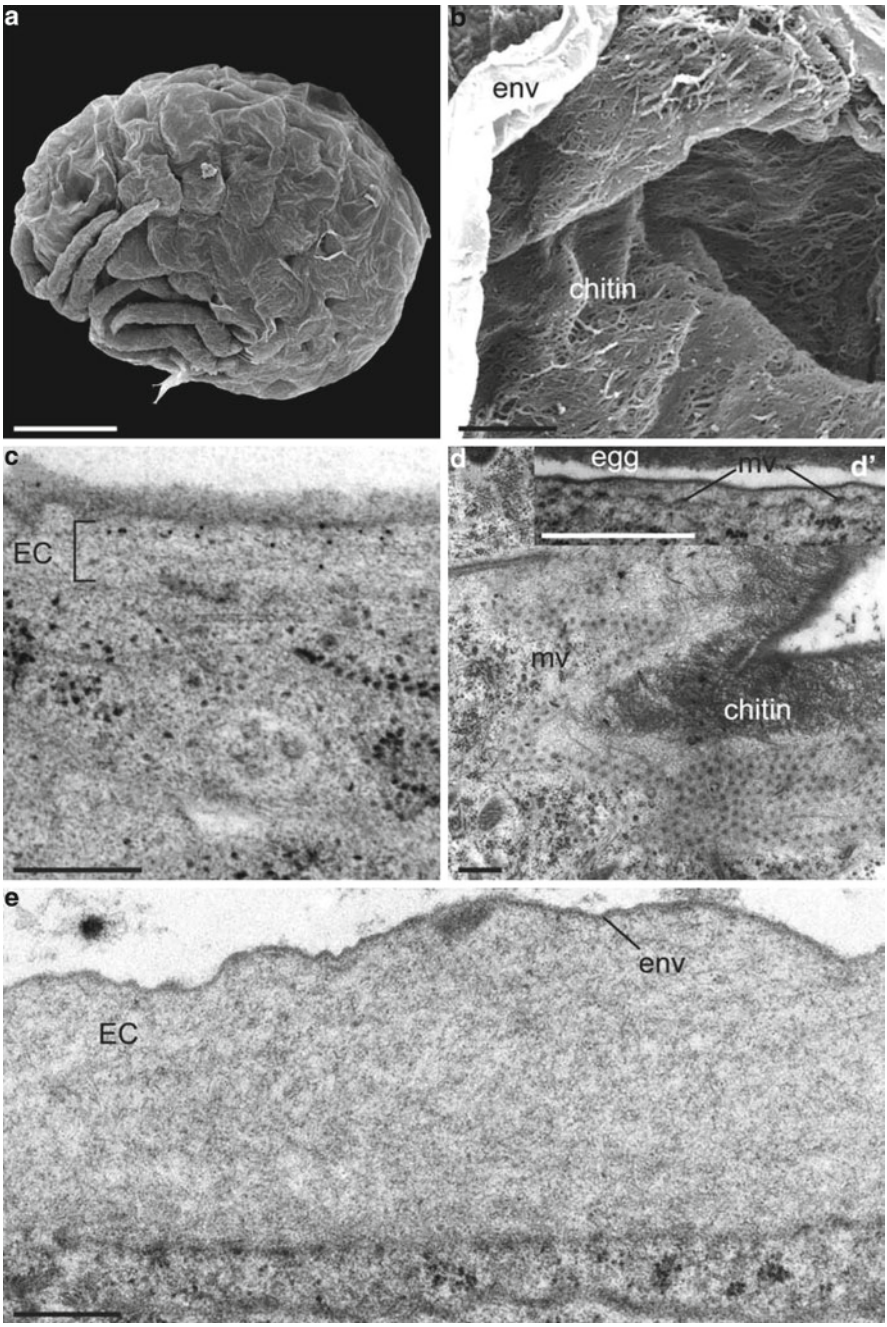

Fig. 1.7 Differentiation of the embryonic cuticle of the amphipod crustacean *Parhyale hawaiensis*. (**a**) A wrinkled membrane covers the embryos at stage S25). (**b**) Randomly oriented fibres with diameter of 100 nm are tightly packed underneath the membrane (env envelope) that has been

chitin and of the biominerals embedded in the chitin-protein matrix (in case of lobster and crab) reveal strong textures. The horseshoe crab does not seem to contain notable amounts of crystalline minerals. The Debye-Scherrer images of the lobster specimen suggest that the biominerals form clusters of crystals with similar crystallographic orientation, and TEM images support this suggestion. The crystallographic texture of the chitin is arranged with its longest cell axis parallel to the normal of the surface of the exoskeleton. In order to grow, the animals must replace their old exoskeleton periodically by a new one in a process termed molting. Before the old cuticle is shed, a new, thin and not yet mineralized cuticle is secreted by the epidermal cells, and then the animals expand and the new soft cuticle is completed and mineralized (Raabe et al. 20075abc, 2006).

As can be seen in Fig. 1.8, the smallest sub-units in the structural hierarchy of the cuticle of the lobster *H. americanus* are the chitin macromolecules. They are arranged in an antiparallel fashion forming alpha-chitin, that prevails in the exoskeleton of large crustaceans; 18–25 of these chains together form nanofibrils of diameter ca. 2–5 nm and length ca. 300 nm. These nanofibrils cluster to form long chitin–protein fibers with diameters between 50 and 350 nm. The fibers assemble in planar honeycomb shaped arrays.

Ultra-thin sections of the organic matrix, in crab carapaces and in compact bone osteons as well, reveal typical arced patterns that however do not result from authentic curved filaments. In an ideal representation, the molecular directions are drawn as parallel and equidistant straight lines on a series of rectangles and from one card to the next, the lines turn by a small and constant angle. Series of nested arcs appear on oblique sides of the model, just as they appear in microscopy after

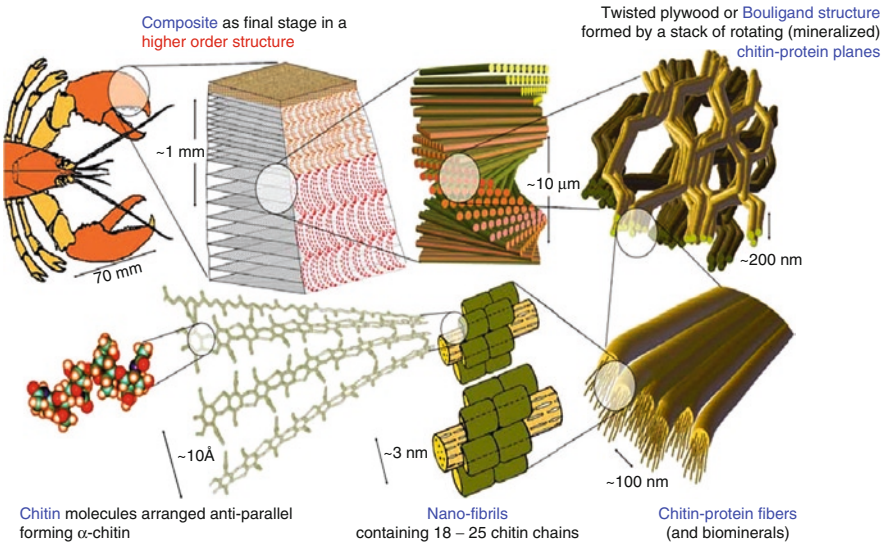

Fig. 1.8 Hierarchical microstructure of the cuticle of the lobster *H. americanus* (Reprinted from Raabe et al. 2005b). Copyright 2005, with permission from Elsevier)

sectioning of the material. Another consequence of the twisted plywood arrangement is the presence of periodic extinctions when the sections are viewed in polarized light microscopy, with a planar disposition observed in the crab cuticle (Giraud-Guille et al. 2004). This helical arrangement is revealed by the fingerprint patterns typical of cholesteric liquid crystals. The distance between two dark bands corresponds to a 180° rotation of the molecular orientations and corresponds to the half-cholesteric pitch. A stack that has been rotated from one plane to another by 180° about its normal is referred to as a Bouligand or plywood layer (Fig. 1.8).

Characteristic for the lobster cuticle is the presence of a well-developed pore canal system with many such canals penetrating the plywood structure. The pore canals contain long soft tubes. The fibers of each chitin–protein plane are arranged around the cavities of the pore canals, building a structure that resembles a twisted honeycomb. In the hard parts of the lobster, the exo- and endo-cuticles are mineralized with calcium carbonate in the form of small crystallites a few nanometers in diameter (Raabe et al. 2007; Chen et al. 2008).

1.4.1 Isolation of Crustacean Nanofibrils

Suspensions of chitin crystallites form cholesteric phases. Revol and Marchessault (1993) investigated the effects of pH and ionic strength on the proportion of nematic phase in biphasic samples and found few changes because the contribution of the crystallites themselves is large. Attempts to compare experimental data to theoretical predictions were also made using Onsager's treatment and showed a reasonable qualitative agreement.

Suspensions of chitin crystallites were prepared by acid hydrolysis of technical grade crab chitin. Similar results could also be obtained with shrimp as well as a variety of other chitin sources. Typically, 5 g of dry chitin powder were treated with 100 ml 3 M HCI at the boil (104°C) for 1 h. The sample was then washed with distilled water by successive low-speed centrifugation-dilution cycles until the supernatant reached a pH of about 2. At this pH, the coarse dispersion from the residue of the shell fragments begins to convert spontaneously into a colloidal suspension. The washing was continued by dialysis against distilled water to neutrality. Due to acid hydrolysis of the sample, a 30–40% mass loss occurs after 1 h of HCl treatment. To promote dispersion, aliquots of the preparation were sonicated for 1 min.

The main difference between this process proposed by Revol and Marchessault (1993) and by Revol et al. (1996), and the one proposed by Belamie et al. (2004) is that the change of the suspending medium and the concentration of the suspensions were achieved by ultracentrifugation rather than dialysis.

Aqueous suspensions of nanocrystals can be prepared by acid hydrolysis of the purified polysaccharide: the effect of this treatment is to dissolve the chitin regions of low lateral order so that the insoluble, highly crystalline residue may be converted into a stable suspension by subsequent vigorous mechanical shearing action.

For cellulose and chitin, the monocrystals appear as rod-like nanofibrils whose dimensions depend on the biological source (in the case of starch they consist of platelet-like nanoparticles). Titrations of suspensions at 0.6 and 3.1 wt.% provided consistent values of respectively 1.60×10^{-4} and 1.66×10^{-4} mol NaOH necessary to titrate 1 g of chitin. This corresponds to nearly 1.0×10^{20} amino groups per gram of particles.

Alpha-Chitin from shrimp shells was subjected to extensive hydrolysis in boiling 3 M hydrochloric acid. X-ray diffraction data indicated an increase in chitin crystallinity after hydrolysis, as the less-ordered chitin domains were digested. Line broadening data were used to measure crystallite size and particle size in the chitin nanocrystals. Congo Red adsorption was used to measure the specific surface area of the chitin nanocrystals, which was found to be 347 m^2/g, compared to 124 for chitin fibres, 249 for pulp cellulose nanocrystals, 272 for bacterial cellullose nanocrystals, and 88 for pulp fibres (Goodrich and Winter 2007). The nanofibrils are slightly cationic (1 g is titrated with 0.16 mmol NaOH). In water, the protonated amino groups and their counter-ions form an electrical double layer around the crystallites; perturbation of the layer by solvents or electrolytes promotes reversible aggregation. The isolated chitin nanocrystals are pure and exempt from residual proteins and minerals.

For HCl concentrations between 0.01 and 0.5 mM and chitin concentrations below 2.5 wt.%, the samples remain completely isotropic and show no birefringence. Beyond 2.5 wt.% and up to 4 wt.% chitin, the liquid appears bright in polarized light, and within a few days, a birefringent phase settles at the bottom of the tubes, separated from an upper isotropic one by a sharp interface. When the chitin concentration is further increased, the samples are entirely anisotropic. The boundaries of the biphasic domain only slightly change in this HCl concentration range. Samples in the range 2.5–10.0 mM HCl only showed complete phase separation. Samples prepared with 0.01 M HCl and beyond never exhibited bulk phase separation, in test tubes, in the range of chitin concentration investigated. Instead, the birefringence increased continuously from dark to very bright samples when viewed between crossed polaroids.

At the beginning of the treatment for the isolation of chitin nanofibrils, a rapid weight loss is observed which is attributed to preferential hydrolysis of non-crystalline chitin into soluble oligomers and monomers. Progressively, a plateau is reached, when only the more crystalline material remains, as shown by X-ray diffraction. After 1 h treatment, the mass loss is close to 40% of the initial weight. If one aims at producing only dilute colloidal dispersions of crystallites, less hydrolysis time is required and hence less weight loss is produced. In such a case, the crystallites are much longer, and a gel exhibiting a nematic order is easily obtained by a colloid mill treatment followed by any process which increases the concentration. For spontaneous liquid crystalline phase separation into a two-phase system, isotropic-anisotropic, a minimum hydrolysis time of about 1 h is required.

In water, the protonated amino groups and their counterions form an electrical double layer around the crystallites, which prevents flocculation thus yielding a stable colloidal suspension.

The electron diffractogram of the preparation corresponds to the alpha-chitin crystal structure: thus, the acid hydrolysis treatment does not change the original crystalline structure of the sample. Unlike that of cellulose the HCl hydrolysis of chitin does not encourage crystallite aggregation into spindle-like bundles. Instead, as the hydrolysis proceeds, free amino groups are uncovered and in their protonated state they provide the electrostatic repulsion which stabilizes the suspension.

1.5 Chitin in Chitons

With the aid of chemical methods, the presence of chitin was demonstrated in the Cephalopods shells (*Sepia, Loligo, Spirula*) (Meyer 1913, 1942; Turek 1933; Lotmar and Picken 1950; Rudall 1955) and also in the radula of Gastropods (Toth and Zechmeister 1939; Rudall 1955). Some years later, Jeuniaux (1963, 1965) adopted a more specific and sensitive enzymatic method that he had developed (Jeuniaux 1958, 1959) for the determination of chitin in other molluskan classes, and found that chitin amounts to 12% of the organic matter in *Acanthochites discrepans*, 3% in *Helix pomatia* and 7% in *Aplysia depilans*, whilst in the oyster *Ostrea edulis* it is well below 1% of the decalcified matter. Chitin was found not only in Cephalopod shells, but also in mother-of-pearl, pseudo-nacreous layers, and often in the periostracum and prismatic layers of Gastropod and Bivalve shells. The constant presence of chitin in the organic matrix associated with mother-of-pearl emphasizes the homology of the chitinous structure in the whole phylum of Mollusca: therefore the participation of chitin in the building of the organic matrix of the various shell structures was related to taxonomic aspects insofar as it gives an indication of the homogeneity of taxa, and ecological characteristics because chitin is high in burrowing species and very low in the shells of fixed or free species (Goffinet and Jeuniaux 1979).

Polyplacophorans, or chitons, are an important group of molluscan invertebrates deemed to have retained many plesiomorphic features of the molluscan body plan. Polyplacophoran trochophore larvae possess several peculiar features including modifications of the ciliated prototrochal cells, the position of the eyes or ocelli, epidermal calcareous spicules, and a collection of serially reiterated epidermal shell plates (Henry et al. 2004). The dorsal integument of the girdle of the chiton *Mopalia muscosa* is covered by a chitinous cuticle about 0.1 mm thick: within the cuticle are fusiform spicules composed of a central mass of pigment granules surrounded by a layer of calcium carbonate crystals. Tapered, curved chitinous hairs pass through the cuticle and protrude above the surface (Leise and Cloney 1982).

Many of the 24 extant species of the chiton genus *Mopalia* are conspicuous, large-bodied and ecologically important today, but pre-Pleistocene fossils for the genus are rare. A combined analysis of four gene regions (16S and COI mtDNA, 18S and 28S rDNA) was used to estimate the phylogenetic relationships of *Mopalia* species and to analyse the group's biogeography and patterns of speciation. Those data were used to distinguish between two alternative interpretations of the fossil

record: it was concluded that the observed rates in *Mopalia* are consistent with a Miocene origin for the genus. Given this age for the group and assuming a molecular clock, most speciation events in *Mopalia* are inferred to have occurred on average 5 Mya before present, mainly along the western North American coast (Kelly and Eernisse 2008).

Modern chitons possess a highly conserved skeleton of eight shell plates (valves) surrounded by spicules or scales, and fossil evidence suggests that the chiton skeleton has changed little since the first appearance of the class in the Late Cambrian period (about 500 million years before present). However, the Palaeozoic problematic taxon Multiplacophora, in spite of having a more complex skeleton, shares several derived characters with chitons. The enigmatic status of the Multiplacophora is due in part to the fact that its members had an exoskeleton of numerous calcium carbonate valves that usually separated after death. An articulated specimen from the Carboniferous period (about 335 million years before present) of Indiana reveals that multi-placophorans had a dorsal protective surface composed of head and tail valves, left and right columns of overlapping valves (five on each side), and a central zone of five smaller valves, all surrounded by an annulus of large spines. Thus the highly conserved body plan of living chitons belies the broad disparity of this clade during the Palaeozoic era (Vendrasco et al. 2004).

Seriality of organs in supposedly independent molluscan lineages, i.e., in chitons and the deep-sea living fossil monoplacophorans, was assumed to be a relic of ancestral molluscan segmentation and was commonly accepted to support a direct relationship with annelids. Molecular data on monoplacophorans, analyzed together with the largest data set of mollusks ever assembled, clearly illustrate that monoplacophorans and chitons form a clade. This concept may have important implications for metazoan evolution as it allows for new interpretations of primitive segmentation in molluscs (Giribet et al. 2006).

Chitons, similarly to limpets (Gastropoda) feed on algae and other microorganisms that they take from the rocks by the scraping action of the radula, a ribbon-like organ endowed of many transverse rows of mineralized teeth. As worn teeth fall off, new teeth are advanced into place by the continuously growing radula: in chitons this occurs at the rate of one row per day. The organic framework that initially makes up the teeth, in Fig. 1.9, consists of alpha-chitin with associated proteins (Evans et al. 1990).

While some chiton species deposit only iron biominerals in these teeth, many others deposit both iron and calcium. The calcium biomineral in the teeth of one of the latter types of species, the Australian east-coast *Chiton pelliserpentis*, has been isolated and examined: the biomineral was identified as a carbonate-substituted apatite with significant fluoride content; the carbonate content was less than that of either bovine tibia cortical bone or human tooth enamel. The biomineral was poorly crystalline due to small crystal size and appreciable anionic substitution. The lattice parameters were those of a fluorapatite material (Evans and Alvarez 1999).

In the core of the major lateral teeth of the chiton *Acanthopleura echinata* calcium mineralization takes place as an ordered process, with crystalline carbonated apatite being the first mineral deposited. Deposition begins at the top of the tooth

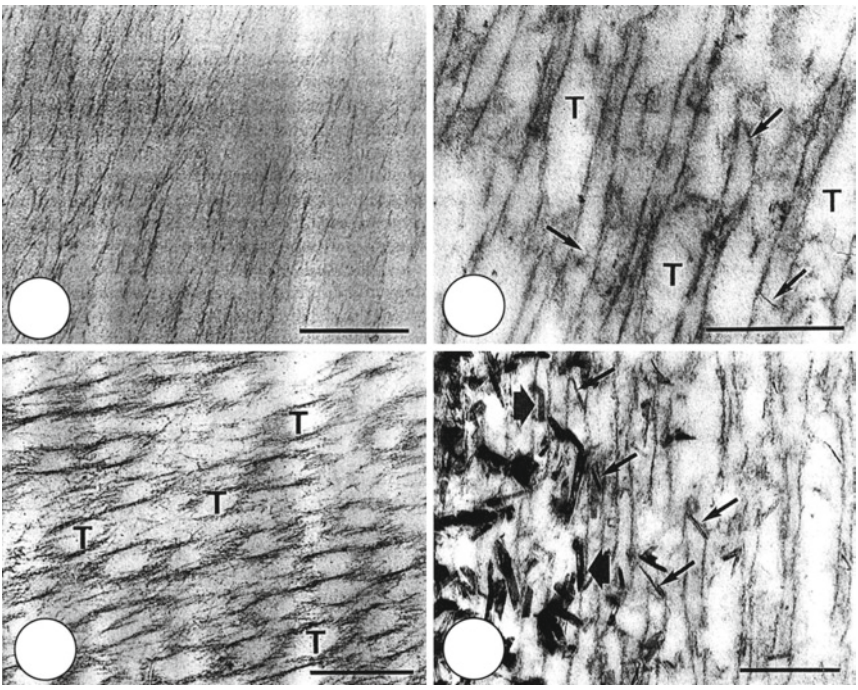

Fig. 1.9 TEM of stained sections of the acid-treated radula teeth of the chiton *Acanthopleura hirtosa*; scale bars 500 nm. (*Upper left*) Organic matrix in the posterior region of a cusp containing sparse fibers. (*Upper right*) Longitudinal section of the anterior region of a cusp containing highly organized fibers arranged as tubules. *Arrows* indicate cross-links between the tubules (T). (*Lower left*) Transverse section, as in preceding frame: the tubules (T) are apparent as interconnected open rings (note difference in fiber density between anterior and posterior regions). (*Lower right*) Longitudinal section of the anterior region near the tooth surface. Some inorganic crystals still remain oriented parallel to the long axis of the tubules (*broad arrows*) and along the interconnecting fibrous bridges (*fine arrows*) (Evans et al. 1990)

core, progresses down the interior surface of the tab and lepidocrocite layer, and then extends outwards to the anterior surface (Lee et al. 2000; Webb et al. 2001). During the mineralisation of iron in the major lateral teeth of the chiton *Acanthopleura echinata* the junction zone plays a vital role in the overall biomineralization process, contributing large amounts of iron at critical stages of development (Brooker et al. 2003). The chemical status of iron is that of limonite, hydrated iron(III) oxide, reported as a biomineral in the cores of mature *Plaxiphora albida* teeth. A narrow band of limonite separates the magnetite of the tooth surface from the central core. Other chiton species display high levels of iron and phosphorus in the cores of their mature lateral teeth (Lee et al. 2003).

In limpet, *Patella caerulea*, the radula contains teeth at various stages of maturity and thus lends itself to the study of the mineralization processes including mineral deposition and growth of inorganic crystals. By using cryo-techniques, in which unstained sections of the teeth are examined in a frozen-hydrated state in a

transmission electron microscope, the mineralization process was studied without introducing artifacts associated with staining, dehydration and embedding. The unmineralized matrix consists of relatively well ordered, densely packed arrays of chitin fibers, with only a few nanometers between adjacent fibers. There are clearly no pre-formed compartments that control goethite (alpha-FeO.OH) crystal size and shape; rather, crystals must push aside or engulf the fibers as they grow. The linear deposits of goethite nucleate on the chitin fibers, which thus control the orientation of the crystals: they are linear objects aligned with the chitin fibers with widths similar to the fibers themselves. No evidence of mineral other than goethite was found. Crystal growth in *P. caerulea* is not influenced by the matrix, on the other hand, in contrast to many other biomineralization systems (Sone et al. 2007).

An indisputable demonstration of the chitinous nature of the chiton body comes from the fact that the extremely thermophilic archaeon *Thermococcus chitonophagus,* known to feed on chitons (and therefore digesting conspicuous amounts of chitin) secretes 1,4-beta-D-N-acetyl-glucosaminidase, EC 3.2.1.14, an enzyme classified as an endochitinase due to its ability to release chitobiose from colloidal chitin: moreover, it presented considerable cellulolytic activity. Analysis of the NH_2-terminus aminoacid sequence showed no detectable homology with other known sequences. The enzyme is a monomer with an apparent molecular weight of 70 kDa and pI of 5.9; it is hydrophobic and appears to be associated with the outer side of the cell membrane; it is optimally active at 70°C and pH 7.0 and exhibits remarkable thermostability, maintaining 50% activity even after 1 h at 120°C, and therefore the enzyme is a quite thermostable chitinase. Surprisingly, the enzyme was not inhibited by allosamidin, the natural inhibitor of chitinolytic activity, and was also resistant to denaturation by urea. On the other hand, guanidine hydrochloride significantly reduced enzymatic activity, indicating that, apart from the hydrophobic interactions, ion pairs located on the surface of the protein could be playing an important role in maintaining the protein's fold and enzyme activity. The hydrolysis pattern was similar for oligomers and polymers, with N,N'-diacetylchitobiose being the final major hydrolysis product (Andronopoulou and Vorgias 2003). In fact, the low, basal and constitutive levels of chitinase gene expression may be sufficient to initiate chitin degradation and to release soluble oligomers, which in turn induce chitinase synthesis (Andronopoulou and Vorgias 2004a, b).

1.6 Chitin in Sponges and Corals

Chitin is crystalline and constitutes a network of organized fibres: this structure confers rigidity and resistance to organisms that contain it, including monocellular organisms (yeast, amoeba, diatoms) and multicellular organisms (higher fungi, arthropods, nematodes, molluscs. Whilst the skeletons of demosponges are made of spongin, glass sponges (hexactinellids) possess silica-organic composites as the main material for their skeletal fibres. Both demosponges (*Verongula gigantea, Aplysina* sp.) and glass sponges (*Farrea occa, Euplectella aspergillum*) possess

chitin as a component of their skeletons. The main practical approach used for chitin isolation was based on alkali treatment of corresponding external layers of spicules sponge material. The Morgan-Elson assay was used to quantify the N-acetylglucosamine released after chitinase treatment. The structural similarity of chitin derived from spicules of the glass sponge *Rossella fibulata* to invertebrate alpha-chitin has been confirmed unambiguously (Ehrlich et al. 2008).

According to paleontological and molecular data, the sponge class Hexactinellida may be the oldest metazoan taxon in earth's history (Reitner and Mehl 1995; Botting and Butterfield 2005). Silica-chitin scaffolds may be key templates for skeleton formation also in ancestral unicellular organisms, rather than silica-protein composites (Ehrlich et al. 2007a,b). Chitin is probably part of very old organic template system involved in a biosilicification phenomenon, which was established a long time before the origin of glass sponges and collagen as structural protein with respect to high templating activity for biomineralization. Nano-mechanical properties, hardness and elastic modulus of the closely related sponge *Rossella racovitzea* were also determined: the *Rossella* spicules, known to have optical wave conduction properties, are 10–20 cm long with a circular cross-section of diameter 200–600 μm. The spicules are layered with 2–10 μm thick siliceous material deprived of crystallinity.

Because sponges are often regarded as the most ancient metazoans (630 to 542 My) (Brasier et al. 1997; Aizenberg et al. 2004, 2005; Weaver et al. 2007; Cuttaneo-Vietti et al. 1996; Schroeder et al. 2007), the finding of chitin within skeletal formations of these organisms is of major scientific significance. As chitin also serves as a template for calcium carbonate deposition in sponges (Ehrlich et al. 2007), the evolution of mineralized skeletons in early metazoans share a common origin with respect to chitin as an unified template for biomineralization, similar to collagen as common structural protein (Ehrlich and Worch 2007). This feature may be considered a basic metazoan character and thus also has implications for the question of establishing the monophyletic status of the taxon Metazoa. Chitin as a template for biomineralization probably belongs to the basic pattern of the Metazoa.

Chitin was found to occur in the corals *Antipathes furcata* and *A. rhipidion* by x-ray diffraction by Ellis et al. (1980). In the Hawaiian reef-forming coral *Pocillopora damicornis*, chitin forms the organic matrix upon which calcification takes place, and makes up 0.01% to 0.10% of the dry coral skeleton: chitin was identified by x-ray diffraction, infrared spectrometry and biochemical tests (Dunn and Liberman 1983); the chitin of *P. damicornis* was observed to be a spongework of fibrils of average diameter 20 μm (Wainwright 1963). The UV–VIS spectra of both coral species from the Western Caribbean Sea, *Antipathes caribbeana* and *Antipathes pennacea* indicated strong absorbance around 350 nm due to iron and manganese. FTIR spectra showed the presence of a complex material similar to chitin for both species. The crystallite size in *A. caribbeana* was larger than in *A. pennacea* (Juarez-de la Rosa et al. 2007). In the New Zealand black coral *A. fiordensis*, Holl et al. (1992) studied the presence of diphenols that, once oxidised to quinones, provide mechanical stabilization of the coral skeleton by cross-linking of proteins and chitin.

1.7 Isolation of Chitin Microfibrils from Diatoms

A particularly pure form of beta-chitin is found in the monocrystalline spines of the marine diatom *Thalassiosira fluviatilis* Hustedt (McLahlan et al. 1965) as confirmed by susceptibility to chitinase (Walsby and Xypolyta 1977). The spines increase the cell's surface area, and hence its form resistance, thus decreasing the sinking rate. They are currently exploited in the biomedical field: an interesting application of chitin is the Syvek Patch® wound dressing made of chitin microfibrils from the centric diatom *Thalassiosira fluviatilis* grown under aseptic conditions (Vournakis et al. 1996). It is claimed to be seven times faster in achieving hemostasis than fibrin glue, because it agglutinates red blood cells; activates platelets whose pseudopodia make a robust contact with chitin; promotes fibrin gel formation within the patch; platelets generate force through the clot retraction process and vasoconstriction takes place very soon; and a platelet + chitin + red cells + fibrin plug is formed, due to enzyme and platelets adsorbed on the chitin surface.

The mechanism of hemostasis induction by chitin microfibrils is redundant insofar various biochemical reactions are involved simultaneously (Fischer et al. 2005) and therefore the *T. fluviatilis* microfibrils have been tested under the most demanding and crucial conditions requiring hemostasis, such as splenic hemorrage, cardiac catheterization, and bleeding esophageal varices, and found superior to all competing products. According to Vournakis et al. (2008), in an animal model the treatment of cutaneous wounds causes marked increase in angiogenesis, of endothelial cell proliferation and of Ets1 which is the pro-angiogenetic transcription factor, besides the expression of endothelial growth factor VEGF and interleukin-1.

The microcrystals were prepared in the form of porous scaffolds by lyophilization of the chitin slurry and seeded with chondrocytes for hyaline-like cartilage formation with high glycosaminoglycan content after 6 weeks (Hill et al. 2005). The repair of osteochondral defects in rabbit femoral trochlea were repaired with chondrocyte-seeded sulfate chitin microcrystals by Kang et al. (2005).

While the *T. fluviatilis* microfibrils (60 × 0.1 μm) are obviously longer than crustacean nanofibrils (typically 350 × 18 nm), both chitins used in these instances have the same molecular weight (2 MDa) and acetylation degree (>0.90) (Chan et al. 2000; Kulling et al. 1999).

The specific surface area for isolated crustacean nanofibrils is as high as 300 m^2/g, depending on the treatment techniques. For this reason, molecular recognition phenomena take place on the chitin nanofibril surface, as demonstrated by gas adsorption and with the aid of fluorescent lectins, therefore various proteins can be retained by chitin nanofibrils. Thus, a recent biomedical application of nanofibrils has been made by suspending them in gels, including chitosan gels, that dry soon after delivery to a wounded tissue thus making a flexible hydrated film (Muzzarelli et al. 2007).

Films were cast from chitosan solutions containing dispersed alpha-chitin nanofibrils. The addition of alpha-chitin nanofibrils did not affect much the thermal stability and the apparent degree of crystallinity of the chitosan matrix. The tensile strength of

chitin nanofibril-reinforced chitosan films increased from that of the pure chitosan film to reach a maximum at the nanofibril content of 3% (Sriupayo et al. 2005).

beta-Chitin microcrystals were obtained by Morin and Dufresne (2002) from tubes secreted by the vestimentiferan worm *Riftia* collected on the East Pacific ridge at the depth of 2,500 m: they were isolated by a chemical treatment leading to a colloidal suspension of pure chitin microcrystals consisting in slender parallelepiped rods with diameter of 18 nm and average length of 2 μm (minor percentages of longer crystals up to 6 μm were also present). Composite poly(caprolactone) films were produced upon mixing said colloidal suspension with the synthetic polymer: a significant reinforcing effect was observed.

1.8 Conclusion

The structural characteristics in vivo indicate that chitins are among the most resistant organic materials as exemplified by the squid beak, the diatom spines and the insect wings. This is due to the molecular structures of both alpha and beta polymorphs and to their capacity to combine with proteins and other compounds since their biosynthesis, and to form hybrid materials soon afterwards. The concerted action of chitin synthases and chitinases permits constant rebuilding of a number of essential chitinous structures. The versatility of chitins in playing different roles (perception, protection, aggression, feeding, reproduction and fertilization, locomotion and flight), with exceptionally good performances, explains their presence in living organisms since the Cambrian life explosion.

It is demonstrated that certain descendants of Cambrian animals are still living such as the onychophorans that derive from *Aysheaia* and currently live in the pluvial forests, as well as the brachiopods that prevailed in the ancient marine environment. Chitin has been documented in Cambrian fossils such as *Marrella splendens* and *Wiwaxia corrugata*; the brachiopod *Halkieria evangelista* possessed chitinous setae that are fortunately evident in some perfectly preserved fossils.

The study of the chitinous nanostructures provides inspiration for artificial chemical and biochemical devices useful in the medical and veterinary fields. It is today easy to understand the meaning of chitobiose (structural unit of chitin) in mammalian glycoproteins, as well as the activity of the newly discovered chitotriosidases in the defense armamentarium of the human body.

References

Abdullah J, Ahmad M, Heng LY, Karuppiah N, Sidek H (2006) Chitosan-based tyrosinase optical phenol biosensor employing hybrid nafion/sol-gel silicate for MBTH immobilization. Talanta 70(3):527–532

Aizenberg J, Sundar VC, Yablon AD, Weaver JC, Chen G (2004) Biological glass fibers: correlation between optical and structural properties. Proc Natl Acad Sci USA 101(10):3358–3363

Aizenberg J, Weaver JC, Thanawala MS, Sundar VC, Morse DE, Fratzl P (2005) Skeleton of Euplectella sp.: structural hierarchy from the nanoscale to the macroscale. Science 309(5732):275–278

Andronopoulou E, Vorgias CE (2003) Purification and characterization of a new hyperthermostable, allosamidin-insensitive and denaturation-resistant chitinase from the hyperthermophilic archaeon Thermococcus chitonophagus. Extremophiles 7(1):43–53

Andronopoulou E, Vorgias CE (2004a) Isolation, cloning, and over-expression of a chitinase gene fragment from the hyperthermophilic archaeon Thermococcus chitonophagus: semi-denaturing purification of the recombinant peptide and investigation of its relation with other chitinases. Protein Expr Purif 35(2):264–271

Andronopoulou E, Vorgias CE (2004b) Multiple components and induction mechanism of the chitinolytic system of the hyperthermophilic archaeon Thermococcus chitonophagus. Appl Microbiol Biot 65(6):694–702

Atkins EDT (ed) (1985) Polysaccharides: topics in structure and morphology. VCH, Weinstein

Bartnicki-Garcia S (2006) Chitosomes: past, present and future. FEMS Yeast Res 6(7):957–965

Belamie E, Davidson P, Giraud-Guille MM (2004) Structure and chirality of the nematic phase in α-chitin suspensions. J Phys Chem B-108:14991–15000

Binnington KC (1985) Ultrastructural changes in the cuticle of the sheep blowfly, Lucilia, induced by certain insecticides and biological inhibitors. Tissue Cell 17:131–140

Blackwell J, Weih MA (1980) Structure of chitin protein complexes: ovipositor of the ichneumon fly Megarrhyssa. J Mol Biol 137:49–60

Bone Q, Ryan K, Pulsford AL (1983) The structure and the composition of the teeth and grasping spines of Chaetognaths. J Mar Biol Assoc UK 63:929–939

Botting JP, Butterfield NJ (2005) Reconstructing early sponge relationships by using the Burgess Shale fossil Eiffelia globosa, Walcott, Proc Natl Acad Sci USA 102(5):1554–1559

Bracker CE, Ruiz-Herrera J, Bartnicki-Garcia S (1976) Structure and transformation of chitin synthetase particles (chitosomes) during microfibril synthesis in vitro. Proc Natl Acad Sci USA 73:4570–4574

Brasier M, Green O, Shields G (1997) Edicarian sponge spicule clusters from southwestern Mongolia and the origins of the Cambrian fauna. Geology 25(4):303–306

Brooker LR, Lee AP, Macey DJ, van Bronswijk W, Webb J (2003) Multiple-front iron-mineralisation in chiton teeth (Acanthopleura echinata: Mollusca: Polyplacophora). Mar Biol 142(3):447–454

Brown CH (1975) Structural materials in animals. Pitman, London

Chan MW, Schwaitzberg SD, Demcheva M, Vournakis J, Finkielsztein S, Connolly RJ (2000) Comparison of poly-Nacetyl glucosamine with absorbable collagen (Actifoam), and fibrin sealant (Bolheal) for achieving hemostasis in a swine model of splenic hemorrhage. J Trauma 48:454–457

Chandumpai A, Singhpibulporn N, Faroongsarng D, Sornprasit P (2004) Preparation and physicochemical characterization of chitin and chitosan from the pens of the squid species, Loligo lessoniana and Loligo formosana. Carbohydr Polym 58(4):467–474

Chen PY, Lin AYM, McKittrick J, Meyers MA (2008) Structure and mechanical properties of crab exoskeletons. Acta Biomater 4(3):587–596

Chretiennot-Dinet MJ, Giraud-Guille MM, Vaulot D, Putaux JL, Saito Y, Chanzy H (1997) The chitinous nature of filaments ejected by Phaeocystis (Prymnesiophyceae). J Phycol 33:666–672

Chuang JS, Schekman RW (1996) Differential trafficking and timed localization of two chitin synthase proteins, Chs2p and Chs3p. J Cell Biol 135:597–610

Cohen E (1982) In vitro chitin synthesis in an insect: formation and structure of microfibrils. Eur J Cell Biol 26:289–294

Cortizo MS, Berghoff CF, Alessandrini JL (2008) Characterization of chitin from Illex argentinus squid pen. Carbohydr Polym. doi:10.1016/j.carbpol.2008.01.004

Cuttaneo-Vietti R, Bavestrello G, Cerrano C (1996) Optical fibres in an Antarctic sponge. Nature 383(6599):397–398

Dunn DF, Liberman MH (1983) Chitin in sea anemone shells. Science 221:157–159

Ehrlich H, Worch H (2007) Collagen, a huge matrix in glass sponge flexible spicules of the meter-long Hyalonema sieboldi. In: Bauerlein E (ed) The biology of biominerals structure formation, vol Vol.1, Handbook of biomineralization. Wiley-VCH, Weinheim

Ehrlich H, Krautter M, Hanke T, Simon P, Knieb C, Heinemann S, Worch H (2007a) First evidence of the presence of chitin in skeletons of marine sponges. Part II. glass sponges (Hexactinellida: porifera). J Exp Zool 308B(4):473–483

Ehrlich H, Maldonado M, Spindler KD, Eckert C, Hanke T, Born R, Goebel C, Simon P, Heinemann S, Worch H (2007b) First evidence of chitin as a component of the skeletal fibers of marine sponges. Part I. Verongidae (Demospongia: porifera). J Exp Zool 308B(4): 347–356

Ehrlich H, Janussen D, Simon P, Bazhenov VV, Shapkin NP, Erler C, Mertig MC, Born R, Heinemann S, Hanke T, Worch H, Vournakis JN (2008) Nanostructural organization of naturally occurring composites. Part II: silica-chitin-based biocomposites. J Nanomater. doi:10.1155/2008/670235

Ellis LC, Chandross R, Bear RS (1980) X-Ray diffraction evidence of chitin in the axial skeleton of antipatharian corals. Compr Biochem Physiol 66B:163–165

Evans LA, Alvarez R (1999) Characterization of the calcium biomineral in the radular teeth of Chiton pelliserpentis. J Biol Inorg Chem 4(2):166–170

Evans LA, Macey DJ, Webb J (1990) Characterization and structural organization of the organic matrix of the radula teeth of the chiton Acanthopleura hirtosa. Philos Trans R Soc London Ser B 329:87–96

Fischer TK, Thatte HS, Nichols TC, Bender-Neal DE, Bellinger DA, Vournakis JN (2005) Synergistic platelet integrin signaling and factor XII activation in poly-N-acetyl glucosamine fiber-mediated hemostasis. Biomaterials 27:5433–5443

Freddi G, Anghileri A, Sampaio S, Buchert J, Monti P, Taddei P (2006) Tyrosinase-catalyzed modification of Bombyx mori silk fibroin: Grafting of chitosan under heterogeneous reaction conditions. J Biotechnol 125(2):281–294

Giraud-Guille MM, Chanzy H, Vuong R (1990) Chitin crystals in arthropod cuticles revealed by diffraction contrast transmission electron microscopy. J Struct Biol 103:232–240

Giraud-Guille MM, Belamie E, Mosser G (2004) Organic and mineral networks in carapaces, bones and biomimetic materials. CR Palevol 3:503–513

Giribet G, Okusu A, Lindgren AR, Huff SW, Schrodl M, Nishiguchi MK (2006) Evidence for a clade composed of molluscs with serially repeated structures: monoplacophorans are related to chitons. Proc Natl Acad Sci USA 103(20):7723–7728

Goffinet G, Jeuniaux C (1979) Distribution et importance quantitative de la chitine dans les coquilles de mollusques. Cah Biol Mar 20:341–349

Goodrich JD, Winter WT (2007) Alpha-Chitin nanocrystals prepared from shrimp shells and their specific surface area measurement. Biomacromolecules 8:252–257

Hanseler E, Nylen LA, Rast DM (1983) Dissociation and reconstitution of chitosomes. Biochim Biophys Acta 745:121–123

Havemann J, Muller U, Berger J, Schwarz H, Gerberding M, Moussian B (2008) Cuticle differentiation in the embryo of the amphipod crustacean Parhyale hawaiensis. Cell Tissue Res 332(2): 359–370

Henry JQ, Okusu A, Martindale MQ (2004) The cell lineage of the polyplacophoran, Chaetopleura apiculata: variation in the spiralian program and implications for molluscan evolution. Dev Biol 272(1):145–160

Hepburn A (ed) (1976) The insect integument. Elsevier, Amsterdam

Hernandez J, Lopez-Romero E, Cerbon J, Ruiz-Herrera J (1981) Lipid analysis of chitosomes, chitin synthesizing microvesicles from Mucor rouxii. Exp Mycol 5:349–356

Hill CM, An YH, Kang QK, Demcheva MV, Vournakis JN (2005) Poly-N-acetylglucosamine as a scaffold for cartilage tissue engineering in nude mice. Key Eng Mater 288/289:71–74

Holl SM, Goldberg SJ, Kramer KJ, Morgan TD, Hopkins TL (1992) Comparison of black coral skeleton and insect cuticle by a combination of C-13 NMR and chemical analyses. Arch Biochem Biophys 292:107–111

Hopkins TL, Harper MS (2001) Lepidopteran peritrophic membranes and effects of dietary wheat germ agglutinin on their formation and structure. Arch Insect Biochem Physiol 47:100–109

Horisberger M, VonLanthen M (1977) Location of mannan and chitin on thin sections of budding yeasts with gold markers. Arch Microbiol 115:1–7

Horst MN (1981) The biosynthesis of crustacean chitin by a microsomal enzyme from larval brine shrimp. J Biol Chem 249:1973–1979

Imai T, Watanabe T, Yui T, Sugiyama J (2003) The directionality of chitin biosynthesis: a revisit. Biochem J 374(Pt 3):755–760

Jeuniaux C (1958) Recherches sur les chitinases. I. Méthode néphélometrique. Archives Internationaux de Physiologie et Biochimie 66:408–427

Jeuniaux C (1959) Recherches sur les chitinases. II. Purification de la chitinase. Archives Internationaux de Physiologie et Biochimie 67:597–617

Jeuniaux C (1963) Chitine et chitinolyse. Masson, Paris

Jeuniaux C (1965) Chitine et philogénie: application d'une méthode enzymatique de dosage de la chitine. Société de Chimie et Biologie Bulletin 47:2267–2278

Jollès P, Muzzarelli RAA (eds) (1999) Chitin and Chitinases. Birkhauser, Basel

Juarez-de la Rosa BA, Ardisson PL, Azamar-Barrios JA, Quintana P, Alvarado-Gil JJ (2007) Optical, thermal, and structural characterization of the sclerotized skeleton of two antipatharian coral species. Mater Sci Eng, C 27(4):880–885

Kang QK, Hill CM, Demcheva MV, Vournakis JN, An YH (2005) Poly-N-acetylglucosamine for repairing ostochondral defects in rabbits. Key Eng Mater 288/289:83–86

Kelly RP, Eernisse DJ (2008) Reconstructing a radiation: the chiton genus Mopalia in the north Pacific. Invertebr Syst 22(1):17–28

Kulling D, Vournakis JN, Woo S, Demcheva MV, Tagge DU, Rios G (1999) Endoscopic injection of bleeding esophageal varices with a poly-N-acetyl glucosamine gel formulation in the canine portal hypertension model. Gastrointest Endosc 49:764–771

Kumar RHMN, Muzzarelli RAA, Muzzarelli C, Sashiwa H, Domb AJ (2004) Chitosan chemistry and pharmaceutical perspectives. Chem Rev 104:6017–6084

Kurita K (2006) Chitin and chitosan: Functional biopolymers from marine crustaceans. Mar Biotechnol 8(3):203–226

Landers SC (1991) The fine structure of secretion in Hyalophysa chattoni: formation of the attachment peduncle and the chitinous phoretic cyst wall. J Eukaryot Microbiol 38(2):148–152

Lavall RL, Assis OBG, Campana SP (2007) Beta-Chitin from the pens of Loligo sp.: Extraction and characterization. Bioresour Technol 98:2465–2472

Leal-Morales CA, Bracker CE, Bartnicki-Garcia S (1988) Localization of chitin synthetase in cell-free homogenates of Saccharomyces cerevisiae: chitosomes and plasma membrane. Proc Natl Acad Sci USA 85:8516–8520

Leal-Morales CA, Bracker CE, Bartnicki-Garcia S (1994) Subcellular localization, abundance and stability of chitin synthetases 1 and 2 from Saccharomyces cerevisiae. Microbiology 140:2207–2216

Lee AP, Brooker LR, Macey DJ, van Bronswijk W, Webb J (2000) Apatite mineralization in teeth of the chiton Acanthopleura echinata. Calcif Tissue Int 67(5):408–415

Lee AP, Brooker LR, Macey DJ, Webb J, van Bronswijk W (2003) A new biomineral identified in the cores of teeth from the chiton Plaxiphora albida. J Biol Inorg Chem 8(3):256–262

Lehane MJ (1997) Peritrophic matrix structure and function. Annu Rev Entomol 42:525–550

Leise EM, Cloney RA (1982) Chiton integument: ultrastructure of the sensory hairs of Mopalia muscosa (Mollusca: Polyplacophora). Cell Tissue Res 223:43–59

Li J, Revol JF, Naranjo E, Marchessault RH (1996) Effect of the electrostatic interaction on phase separation behaviour of chitin crystallite suspensions International. J Biol Macromol 18:177–187

Li J, Revol JF, Marchessault RH (1997) Effect of N-sulfation on the colloidal and liquid crystal behaviour of chitin crystallites. J Colloid Interface Sci 192:447–457

Locke M (1991) Insect epidermal cells. In: Binnington K, Retnakaran A (eds) Physiology of the insect epidermis. Melbourne, CRISCO, pp 1–22

Lotmar W, Picken LER (1950) A new crystallographic modification of chitin and its distribution. Experientia 6:58–59

Lu XB, Zhang Q, Zhang L, Li JH (2006) Direct electron transfer of horseradish peroxidase and its biosensor based on chitosan and room temperature ionic liquid. Electrochem Commun 8(5):874–878
Martin R, Walther P (2003) Protective mechanisms against the action of nematocysts in the epidermis of Cratena peregrina and Flabellina affinis (Gastropoda, Nudibranchia). Zoomorphology 122:25–35
Martin R, Hild S, Walther P, Ploss K, Boland W, Tomaschko KH (2007) Granular chitin in the epidermis of nudibranch molluscs. Biol Bull 213:307–315
McLahlan J, McInnes AG, Falk M (1965) Studies on the chitin fibres of the diatom. I. Production and isolation of chitin fibers of Thalassiosira fluviatilis Hustedt. Can J Botany 43:707–713
Merz RA, Horsch M, Nyhlen LE, Rast DM (1999) Biochemistry of chitin synthase. EXS 87:9–37
Merzendorfer H (2006) Insect chitin synthases: a review. J Comp Physiol B 176(1):1–15
Merzendorfer H, Zimoch L (2003) Chitin metabolism in insects: structure, function and regulation of chitin synthases and chitinases. J Exp Biol 206:4393–4412
Meyer WT (1913) Tintenfische mit besonderer Berucksictigung von Sepia und Octopus. Monographien Einheimischer Tiere. W. Klinkhardt, Leipzig
Meyer KH (1942) Natural and synthetic high polymers. Interscience, New York
Minke R, Blackwell J (1978) The structure of alpha chitin. J Mol Biol 120:167–181
Miscoria SA, Desbrieres J, Barrera GD, Labbe P, Rivas GA (2006) Glucose biosensor based on the layer-by-layer self-assembling of glucose oxidase and chitosan derivatives on a thiolated gold surface. Anal Chim Acta 578(2):137–144
Miserez A, Li YL, Waite JH, Zok F (2007) Jumbo squid beaks: inspiration for design of robust organic composites. Acta Biomater 3:139–149
Morin A, Dufresne A (2002) Nanocomposites of chitin whiskers from *Riftia* tubes and poly(caprolactone). Macromolecules 35:2190–2199
Mulisch M, Herth W, Zugenmaier P, Hausmann K (1983) Chitin fibrils in the lorica of the ciliate Eufolliculina uhligi: ultrastructure, extracellular assembly and experimental inhibition. Biol Cell 49:169–178
Mulish M, Hausmann K (1989) Localization of chitin in cysts of two ciliated protozoa, Blepharisma undulans and Pseudomicrothorax dubius. Protoplasma 152(2–3):77–86. doi:10.1007/BF01323065
Murray SB, Neville AC (1998) The role of pH, temperature and nucleation in the formation of cholesteric liquid crystal spherulites from chitin and chitosan. Int J Biol Macromol 22:137–144
Muzzarelli RAA (1977) Chitin. Pergamon, Oxford
Muzzarelli RAA (ed) (1993) Chitin enzymology. Atec Grottammare, Italy
Muzzarelli RAA (ed) (1996) Chitin enzymology. Atec Grottammare, Italy
Muzzarelli RAA (ed) (2001) Chitin enzymology 2001. Atec Grottammare, Italy
Muzzarelli C, Muzzarelli RAA (2002a) Reactivity of quinones towards chitosans. Trends Glycosci Glyc 14(78):229–235
Muzzarelli RAA, Muzzarelli C (2002b) Natural and artificial chitosan-inorganic composites. J Inorg Biochem 92:89–94
Muzzarelli RAA, Muzzarelli C (2005) Chitin nanofibrils. In: Dutta PK (ed) Chitin and chitosan: research opportunities and challenges. New Age, New Delhi, India
Muzzarelli RAA, Tubertini O (1969) Chitin and chitosan as chromatographic adsorbents and supports for collection of trace metals from aqueous and organic solutions and sea water. Talanta 16:1571–1579
Muzzarelli RAA, Jeuniaux C, Gooday GW (eds) (1986) Chitin in nature and technology. Plenum, New York
Muzzarelli RAA, Ilari P, Xia W, Pinotti M, Tomasetti M (1994) Tyrosinase-mediated quinone tanning of chitinous materials. Carbohydr Polym 24:294–300
Muzzarelli RAA, Littarru GP, Muzzarelli C, Tosi G (2003) Selective reactivity of biochemically relevant quinones towards chitosans. Carbohydr Polym 53:109–115
Muzzarelli RAA, Morganti P, Morganti G, Palombo P, Palombo M, Biagini G, Mattioli-Belmonte M, Giantomassi F, Orlandi F, Muzzarelli C (2007) Chitin nanofibrils/chitosan glycolate composites as wound medicaments. Carbohydr Polym 70(3):274–284

Nair KG, Dufresne A (2003) Crab shell chitin whisker reinforced natural rubber nanocomposites. 1. Processing and swelling behavior. Biomacromolecules 4:657–665

Neville AC (1975) Biology of the arthropod cuticle. Springer, Berlin

Neville AC (1993) Biology of fibrous composites: development beyond the cell membrane. Cambridge University Press, New York

Noishiki Y, Nishiyama Y, Wada M, Okada S, Kuga S (2003) Inclusion complex of beta-chitin and aliphatic amines. Biomacromolecules 4:944–949

Pont Lezica R, Quesada-Allue L (1990) Chitin. Method Plant Biochem 2:443–481

Pryor MGM (1940) On the hardening of the ootheca of Blatta orientalis. Proc Roy Soc-B 128:378–398

Quicke DLJ, Wyeth P, Fawke JD, Basibuyuk HH, Vincent JFV (1998) Manganese and zinc in the ovipositors and mandibles of hymenopterous insects. Zool J Linn Soc 124(4):387–396

Raabe D, Al-Sawalmih A, Romano P, Sachs C, Brokmeier HG, Yi SB, Servos G, Hartwig HG (2005a) Structure and crystallographic texture of arthropod bio-composites. Icotom 14: Texture of Materials, Pts 1 and 2: 495–497 and 1665–1674

Raabe D, Romano P, Sachs C (2005b) The crustacean exoskeleton as an example of a structurally and mechanically graded biological nanocomposite material. Acta Mater 53:4281–4292

Raabe D, Romano P, Sachs C, Al-Sawalmih A, Brokmeier HG, Yi SB, Servos G, Hartwig HG (2005c) Discovery of a honeycomb structure in the twisted plywood patterns of fibrous biological nanocomposite tissue. J Cryst Growth 283:1–7

Raabe D, Romano P, Sachs C, Fabritius H, Al-Sawalmih A, Yi SB, Servos G, Hartwig HG (2006) Microstructure and crystallographic texture of the chitin-protein network in the biological composite material of the exoskeleton of the lobster Homarus americanus. Mat Sci Eng A-421:143–153

Raabe D, Al-Sawalmih A, Yi SB, Fabritius H (2007) Preferred crystallographic texture of alpha-chitin as a microscopic and macroscopic design principle of the exoskeleton of the lobster Homarus americanus. Acta Biomater 3:882–895

Reitner J, Mehl D (1995) Early Paleozoic diversification of sponges: new data and evidences. *Geologisch Palaontologische Mitteilungen Innsbruck* 20:335–347

Revol JF, Marchessault RH (1993) In vitro chiral nematic ordering of chitin crystallites. Int J Biol Macromol 15:329–335

Revol JF, Li J, Godbout L, Orts WJ, Marchessault RH (1996) Chitin crystallite suspension in water: phase separation and chiral nematic ordering. In: Domard A, Jeuniaux C, Muzzarelli RAA, Roberts G (eds) Advances in Chitin Sciences. Jacques André, Lyon, pp 355–360

Reynolds SE (1975) The mechanical properties of the abdominal cuticle of Rhodnius larvae. J Exp Biol 62:69–80

Richards AG (ed) (1951) The integument of arthropods. University of Minnesota Press, Minneapolis

Rinaudo M (2006) Chitin and chitosan: properties and applications. Prog Polym Sci 31:603–632

Rudall KM (1955) The distribution of collagen and chitin. In Fibrous proteins and their biological significance. Sym Soc Exp Biol 9:49–71

Rudall KM, Kenchington W (1973) The chitin system. Biol Rev 48:597–636

Ruiz-Herrera J, Bartnicki-Garcia S (1974) Synthesis of chitin microfibrils in vitro with a “soluble” chitin synthetase from Mucor rouxii. Science 186:357–359

Runham NW (1961) Investigations into the histochemistry of chitin. J Histochem Cytochem 9:87–92

Saito Y, Okano T, Chanzy H, Sugiyama J (1995) Structural study of alpha-chitin from the grasping spines of the arrow worm Sagitta spp. J Struct Biol 114:218–228

Sakamoto J, Sugiyama J, Kimura S, Imai T, Itoh T, Watanabe T, Kobayashi S (2000) Artificial chitin spherulites composed of single crystalline ribbons of alpha-chitin via enzymatic polymerization. Macromolecules 33:4155–4160

Sampaio S, Taddei P, Monti P, Buchert J, Freddi G (2005) Enzymatic grafting of chitosan onto Bombyx mori silk fibroin: kinetic and IR vibrational studies. J Biotechnol 116(1):21–33

Schermuly G, Markmann-Mulish U, Mulisch M (1996) In vitro studies of the pathway of chitin synthesis in the ciliated protozoon Eufolliculina uhligi. In: Domard A, Jeuniaux C, Muzzarelli RAA, Roberts G (eds) Advances in Chitin Science. Jacques André, Lyon, pp 10–17

Schofield RM, Nesson MH, Richardson KA (2002) Tooth hardness increases with zinc-content in mandibles of young adult leaf-cutter ants. Naturwissenschaften 89:579–583
Schofield RM, Nesson MH, Richardson KA, Wyeth P (2003) Zinc is incorporated into cuticular tools after ecdysis: the time course of the zinc distribution in tools and whole bodies of an ant and a scorpion. J Insect Physiol 49:31–44
Schroeder HC, Brandt D, Schlossmacher U (2007) Enzymatic production of biosilica glass using enzymes from sponges: basic aspects and application in nanobiotechnology (material sciences and medicine). Naturwissenschaften 94(5):339–359
Sone ED, Weiner S, Addadi L (2007) Biomineralization of limpet teeth: a cryo-TEM study of the organic matrix and the onset of mineral deposition. J Struct Biol 158(3):428–444
Sriupayo J, Supaphol P, Blackwell J, Rujiravanit R (2005) Preparation and characterization of alpha-chitin whisker-reinforced chitosan nanocomposite films with or without heat treatment. Carbohydr Polym 62:130–136
Stankiewicz BA, VanBergen P (eds) (1998) Nitrogen-containing macromolecules in the bio- and geosphere. American Chemical Society, Washington
Sugumaran and Lipke (1983) Sclerotization of insect cuticle: a new method for studying the ratio of quinone and beta-sclerotization. Insect Biochem 13:307–312
Surholt B (1975) Formation of glucose-6-phosphate in chitin synthesis during ecdysis of the migratory locust Locusta migratoria. Insect Biochem 5:585–593
Tate LG, Wimer LT (1974) Incorporation of ^{14}C from glucose into chitin, lipid, protein and soluble carbohydrate during metamorphosis of the blowfly Phormia regina. Insect Biochem 4:89–98
Terbojevich M, Cosani A, Conio G, Marsano E, Bianchi E (1991) Chitosan chain rigidity and mesophase formation. Carbohydr Res 209:251–260
Thompson PR, Hepburn HR (1978) Changes in chemical and mechanical properties of honeybee (Apis mellifera Adamsonii) cuticle during development. J Comp Physiol 126:257–262
Toth G, Zechmeister L (1939) Chitin in Helix pomatia mandible. Nature 144:1049
Turek A (1933) Chemisch-analytische untersuchungen an Mollusken schalen. Archives Naturgeschaften Neue Folge 2(2):291–302
Uyama H, Kobayashi S (2006) Enzymatic synthesis and properties of polymers from polyphenols. Enzyme-Catalyzed Syn Polym 194:51–67
Varki A (1996) Does DG42 synthesize hyaluronan or chitin? Proc Natl Acad Sci 93:4523–4525
Vendrasco MJ, Wood TE, Runnegar BN (2004) Articulated Palaeozoic fossil with 17 plates greatly expands disparity of early chitons. Nature 429(6989):288–291
Vincent JFV (1980) Insect cuticle: a paradigm for natural composites. In: Vincent JFV, Currey JD (eds) The mechanical properties of biological materials. Cambridge University Press, Cambridge, pp 183–210
Vincent JFV (1990) Structural biomaterials. University Press, Princeton, NJ
Vincent JFV, Wegst UGK (2004) Design and mechanical properties of insect cuticle. Arthropod Struct Devel 33(3):187–199
Vournakis JN, Finkielsztein S, Pariser ER, Helton M (1996) Poly-beta-1-4-N-acetyl glucosamine. PTC WO 96/39122
Vournakis JN, Eldridge J, Demcheva M, Muise-Helmericks RC (2008) Poly-N-acetyl glucosamine nanofibers regulate endothelial cell movement and angiogenesis: dependence on integrin activation of Ets1. J Vasc Res 45:222–232
Wainwright SA (1963) Skeletal organization in the coral Pocillophora damicornis. Q J Microsc Sci 3:169–183
Walsby AE, Xypolyta A (1977) The form resistance of chitin fibres attached to the cells of Thalassiosira fluviatilis Hustedt. Brit Phycol 11:201–209
Weaver JC, Aizenberg J, Fantner GE (2007) Hierarchical assembly of the siliceous skeletal lattice of the hexactinellid sponge Euplectella aspergillum. J Struct Biol 158(1):93–106
Webb J, Brooker LR, Lee AP, Hockridge JG, Liddiard KJ, Macey DJ, van Bronswijk W (2001) Biomineralization-controlled microarchitecture in the radula teeth of chitons and limpets. Aust J Chem 54(9–10):611–613

Yamada K, Inoue T, Akiba Y, Kashiwada A, Matsuda K, Hirata M (2006) Removal of p-alkylphenols from aqueous solutions by combined use of mushroom tyrosinase and chitosan beads. Biosci Biotechnol Biochem 70(10):2467–2475

Yi HM, Wu LQ, Bentley WE, Ghodssi R, Rubloff GW, Culver JN, Payne GF (2005) Biofabrication with chitosan. Biomacromolecules 6(6):2881–2894

Yoon JH (2005) Enzymatic synthesis of chitooligosaccharides in organic cosolvents. Enzyme Microb Technol 37:663–668

Yui T, Taki N, Sugiyama J, Hayashi S (2007) Exhaustive crystal structure search and crystal modeling of beta-chitin. Int J Biol Macromol 40(4):336–344

Ziman M, Chuang JS, Schekman RW (1996) Chs1p and Chs3p, two proteins involved in chitin synthesis, populate a compartment of the Saccharomyces cerevisiae endocytic pathway. Mol Biol Cell 7:1909–1919

Zimoch L, Merzendorfer H (2002) Immunolocalization of chitin synthase in the tobacco hornworm. Cell Tissue Res 308:287–297

Chapter 2
Chitin in the Exoskeletons of Arthropoda: From Ancient Design to Novel Materials Science

H. Fabritius, C. Sachs, D. Raabe, S. Nikolov, M. Friák, and J. Neugebauer

Contents

Abstract The Arthropoda use chitin and various proteins as basic materials of their cuticle which is forming their exoskeletons. The exoskeleton is composed of skeletal elements with physical properties that are adapted to their function and the eco-physiological strains of the animal. These properties are achieved by forming elaborate microstructures that are organized in several hierarchical levels like the so-called twisted plywood structure, which is built by stacks of planar arrays of complex chitin-protein fibres. Additionally, the properties are influenced by variations in the

H. Fabritius (✉) and D. Raabe
Department Microstructure Physics and Metal Forming, Max-Planck-Institut für Eisenforschung, Max-Planck-Str. 1, 40237 Düsseldorf, Germany
e-mail: h.fabritius@mpie.de; d.raabe@mpie.de

C. Sachs
Department of Mechanical Engineering, MIT, 77 Massachusetts Ave., Cambridge MA 02139–4307, USA
e-mail: csachs@mit.edu

S. Nikolov
Institute of Mechanics, Bulgarian Academy of Sciences, Acad. G. Bontchev Str. Bl. 4, 1113 Sofia, Bulgaria
e-mail: sv.nikolov@imbm.bas.bg

M. Friák and J. Neugebauer
Department Computational Materials Design, Max-Planck-Institut für Eisenforschung, Düsseldorf, Germany
e-mail: m.friak@mpie; neugebauer@mpie.de

N.S. Gupta (ed.), *Chitin*, Topics in Geobiology 34,
DOI 10.1007/978-90-481-9684-5_2, © Springer Science+Business Media B.V. 2011

chemical composition of the cuticle, for instance by combining the organic material with inorganic nano-particles. From a materials science point of view, this makes the cuticle to a hierarchical composite material of high functional versatility. The detailed investigation of microstructure, chemical composition and mechanical properties of cuticle from different skeletal elements of the crustacean *Homarus americanus* shows that cuticle can combine different design principles to create a high-performance anisotropic material. Numerical modelling of the cuticle using ab initio and multi-scale approaches even enables the study of mechanical properties on hierarchical levels where experimental methods can no longer be applied. Understanding and eventually applying the underlying design principles of cuticle bears the potential for realization of a completely new generation of man-made structural materials.

Keywords Chitin • Biological materials • Multi-scale model • Mechanical properties

2.1 Introduction

Chitin is one of the, if not the most abundant structural biomolecule found in nature. It occurs in a multitude of organisms from bacteria and fungi to molluscs and others, but is certainly most prominent in the largest and most diverse group of the animal kingdom, the Arthropoda (Muzzarelli 1977; Khor 2001). In arthropods, chitin is used together with various proteins to form the exoskeleton which they all have in common. The Arthropoda are a very old group of organisms and appear about 550 million years ago very early in the fossil record. Their evolution has started in early Cambrian and has seen several explosive radiations since then, first in the sea where they developed many forms which were adapted to a multitude of ecological niches (Edgecombe 1998; Brusca 2000). These forms range from very small planctonic organisms which were partially preserved in three-dimensional fossils of the so-called Orsten-fauna to large and partially bizarre organisms known from the Burgess-Shale and Chengjiang formations (Müller and Walossek 1985; Chen et al. 1994). With the appearance of the trilobites the Arthropoda became even more diverse and are the "Leitfossilien" for many geological formations, as their exoskeletons were not only ideal for the protection of the organisms themselves but also ideally suited for fossil preservation. During this period of earth's history the arthropods evolved, with the Eurypterids forming some top-of-the-food-chain predators with some species reaching body lengths of more than two meters. Arthropoda, namely the ancestors of the insects, are also considered to be one of the first animal groups to take the step from water to land and switch from aquatic to terrestrial life. They certainly can be regarded to be the first animals that conquered the air by developing wings and the necessary sensory and motor organs. Later in history, the extinction of the trilobites and changing environmental and concurrence situations slowed the success story of the arthropods slightly down until the evolution of the Gymnosperms or flowering plants, which led to an enormous radiation and diversification of the flying insects which became pollinators of plants.

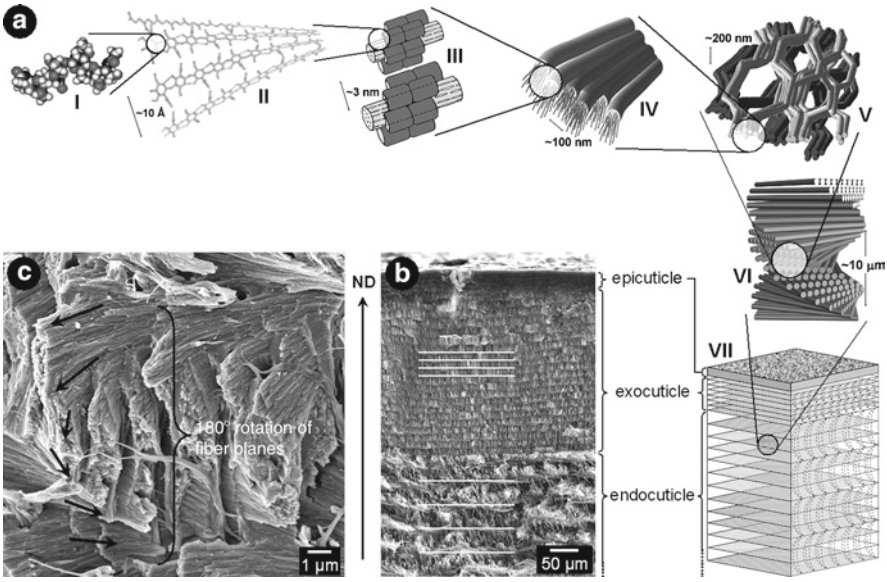

Fig. 2.1 Microstructure of arthropod cuticle using the American lobster *Homarus americanus* as model. (**a**) Hierarchical organization starting with the acetylglucosamine molecules (**I**) forming anti-parallel chains of α-chitin (**II**). Eighteen to 25 chitin molecules wrapped with proteins form nanofibrils (**III**) which aggregate forming chitin protein fibres (**IV**) that are arranged in horizontal planes where the long axes of the fibres are all oriented in the same direction around the cavities of the pore canal system (**V**). The chitin protein fibres form the typical twisted plywood structure (**VI**) of the three-layered cuticle (**VII**). (**b**) SEM micrograph of a cross section through the cuticle showing epicuticle and the organization of exo- and endocuticle with different stacking heights of the chitin protein fibres (*white lines*). (**c**) SEM micrograph of cross-fractured lobster cuticle showing the gradual rotation of the fibre planes around the normal axis (ND) of the cuticle and the interspersed pore canals (Modified from Romano et al. 2007 (a, b) and Sachs et al. 2006 (a). Copyright 2006/2007 Elsevier)

One of the reasons for Arthropoda to become one of the most successful and diverse groups of organisms is certainly their exoskeleton. Members like insects, crustaceans and chelicerates have adapted to virtually every habitat on earth. One common feature of all arthropods is that the integument forms a cuticle. From the material science point of view, this cuticle is a hierarchically structured fibre-based composite material based on chitin (Fig. 2.1). The polysaccharide macromolecule chitin is the linear polymer of ß-1,4-linked N-acetylglucosamine. The presence of the amino groups is highly advantageous for conducting modification reactions. Thus, chitin can be expected to have a high potential as a functional material. Nevertheless, apart from its chemical properties, only limited attention has been paid to chitin and its potential as a structural material.

Learning and understanding how nature achieves to produce such a light, resistant, and at the same time poly-functional material is crucial to design novel bio-inspired materials. The hydrogen-bond network plays a key role in the physical properties of the material such as its elemental solubility, elasticity (structural stiffness), or its

remarkable resistance to crack expansion. A deeper understanding of chitin's unique properties has been long hindered by the lack of detailed ground-state structure information. A structural model of the atomic structure of α-chitin was first established by Carlström (1957) and Minke and Blackwell (1978) by X-ray techniques. However, since X-ray experiments are not sensitive to the hydrogen atoms, only the atomic positions of 56 out of the 108 atoms in the unit cell of the crystalline α-chitin could be determined. The structure and arrangement of hydrogen bond patterns that are to a large extent responsible for physical (e.g. elastic) and chemical properties (e.g. solubility) could only be roughly estimated.

In arthropod cuticle the acetyl glucosamine monomer represents the lowest level of structural hierarchy (Fig. 2.1a, I). Crystalline chitin is the second level of hierarchy (Fig. 2.1a, II). Here, three polymorphic forms have been found that differ in the arrangement of the molecular chains. In α-chitin the chains are arranged in an anti-parallel fashion exhibiting the most crystalline orthorhombic form. The highly ordered crystalline structure of α-chitin originates from hydrogen bonds of four hydroxyl groups and two amide groups in the repeating unit. Because of its densely packed structure α-chitin shows a low solubility in most of the common organic solvents. In β-chitin the chains are aligned parallel to each other having monoclinic crystal symmetry. This form can be swollen in water and dissolved in formic acid. γ-chitin is a mixture of both, α- and β-chitin, with two parallel chains in one direction and the third one in the opposite direction. All three forms can be found in parts of the same organism but in arthropod cuticle the crystalline α-chitin predominates (Andersen 1979; Giraud-Guille 1984). Typically, 18–25 chitin molecules wrapped by proteins form nanofibrils with diameters between 2 and 5 nm and lengths of about 300 nm (Fig. 2.1a, III) which aggregate to form 50–250 nm thick chitin-protein fibres (Fig. 2.1a, IV) representing the next two levels of hierarchy. On the fifth level of hierarchy chitin-protein fibres are organized in parallel forming planar arrays (Fig. 2.1a, V). These fibrous sheets form stacks in which the long axis of the fibres gradually rotate around the normal axis of the cuticle from one sheet to the next, thereby creating a twisted plywood structure (Fig. 2.1a, VI) (Bouligand 1970; Giraud-Guille 1998; Weiner and Addadi 1997). The distance in which the superimposed fibre sheets complete a 180° rotation is defined as the stacking height of the twisted plywood. This helicoidally arranged structure forms the three main layers of the cuticle, where the chitin-protein fibre twisted plywood can vary in stacking height (Fig. 2.1a, VII). The three layers are called from distal to proximal sequence the exocuticle, endocuticle and membranous layer. These and the external epicuticle which is thin and waxy and consists mainly of long chain hydrocarbons, esters of fatty acids, and alcohols form the whole cuticle (Fig. 2.1b, c) (Hadley 1986).

Exo-, endocuticle and the membranous layer deviate in the density of chitin-protein fibres, the number of planes within a 180° helical twist and the shape and density of pore canals that pervade the cuticle from the proximal to the distal side. In the cuticle of Crustacea the organic material within the exo- and endocuticle is combined with inorganic nano-particles arranged according to the hierarchical organisation of the chitin-protein fibres. The inorganic phase consists mainly of amorphous calcium carbonate (ACC), amorphous calcium phosphate (ACP) or

Mg-calcite (Raabe et al. 2006; Boßelmann et al. 2007). Thus, the crustacean cuticle is a hierarchical composite material that combines high mechanical strength with a high functional versatility.

The cuticle surrounds the entire organism and forms skeletal elements that are interconnected by arthrodial membranes. These skeletal elements serve a large variety of different functions (Roer and Dillaman 1984) that are of interest for a biomimetic approach. The shells of the main body segments for instance provide support and serve as a protective shield against predation. Besides, the cuticle forms a number of other interesting skeletal elements like the mandibles and other mouthparts that function in holding, cutting and grinding of food items, others form joints to assist controlled relative movements between skeletal elements. The cuticle also provides optical lenses in the compound eyes of Arthropoda and in some stridulating species even cuticular structures for the generation of sonic waves. These examples represent only a minor fraction of specific structures and functions of cuticular elements in arthropods. An interesting aspect is that these skeletal elements perform similar functions in a wide range of length scales. The body size of arthropods varies between tens of centimeters to less than 1 mm. This raises the question of how miniaturization of skeletal elements affects the physical properties and thus functional morphology at the various levels of hierarchical organisation.

The general architecture of the cuticle is well understood (Bouligand 1970; Giraud-Guille 1984, 1998; Hadley 1986; Weiner and Addadi 1997). However, for many specialized cuticular elements the internal organisation that depends on specific physical requirements is unknown. Structure and characteristics of chitin-protein fibres are not yet fully understood and the nature of the interface between organic and inorganic components in mineralized cuticles is still unknown. Furthermore the distribution of the inorganic phase and its impact on specific functions needs to be clarified.

Several of their inherent properties have brought biological structural materials into the focus of material science in the last years. Most of these materials are composites based on a matrix made of relatively simple structural biomolecules like collagen, cellulose, chitin and others, which have usually relatively poor mechanical properties compared to the final material like bone, wood or cuticle. In combination with additional organic components like various proteins but also inorganic components like crystalline or amorphous biominerals the fibrous matrices undergo structural modifications which can occur on multiple hierarchical levels and bridge all length scales from the nano- to the macro level. The type of compositional modifications and the final size of the material then determine the final mechanical properties of the material. Within the boundary conditions of the organisms, these properties have been optimized during evolution for the specific functions of the materials. Due to the multitude of different functions the chitinous arthropod cuticle has to perform as exoskeleton, one can find chemical and structural modifications of the matrix resulting in a wide variety of mechanical properties. Therefore, Arthropod cuticle can be regarded as a true multifunctional material and studying its construction principles bears high potential for the development of more sophisticated man-made structural materials.

2.2 Microstructure Analysis of Arthropod Cuticle

The cuticle of the American lobster *Homarus americanus* has proven to be an ideal model material for studying mechanical properties of hierarchically organized biological composites due to its suitable dimensions and it is compared to other materials such as bone less complex with a better defined microstructure. The microstructure of cuticle from different body parts of the large decapod *H. americanus* has been studied extensively using scanning electron microscopy (SEM) (Fig. 2.2a, c) and transmission electron microscopy (TEM) (Raabe et al. 2006). The microstructure of the organic cuticle fraction corresponds largely to the general arthropod cuticle model (Fig. 2.1). However, besides the twisted plywood structure a second design

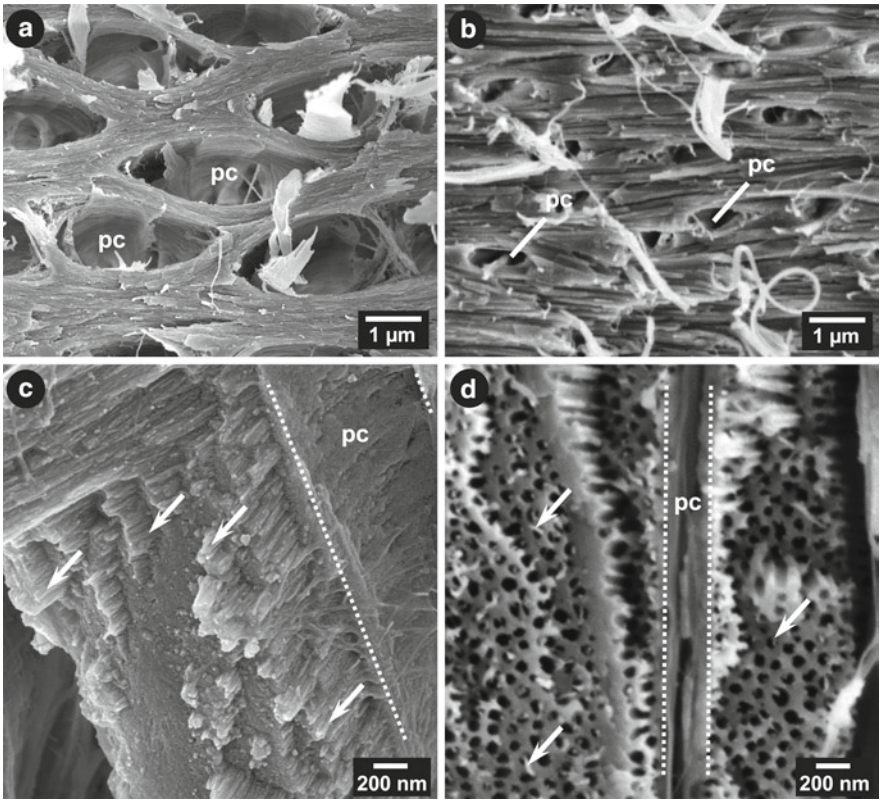

Fig. 2.2 (**a**, **c**) SEM micrographs showing the microstructure of mineralized chitin protein fibres in *H. americanus* endocuticle fractured horizontally (**a**) and sagittally (**c**). The fibres have diameters between 25 and 50 nm (*arrows*) and are not very well defined, the mineral particles cannot easily be distinguished. The pore canals (pc) are large and take up a high volume fraction of the material. (**b**, **d**) SEM micrographs showing chitin protein fibres and mineral in cuticle of *C. pagurus* fractured horizontally (**b**) and sagittally (**d**). Fibers with very small diameters (*arrows*) are surrounded by solid mineral tubes which are fused, creating a block of mineral penetrated by long holes organized in twisted plywood fashion. The pore canals are rather small and dispersed within the structure (Modified from Raabe et al. 2006 (a, b). Copyright 2006 Elsevier)

principle can be found in the mineralized, load bearing parts of lobster cuticle (Fig. 2.2a). Due to a well-developed pore canal system a honeycomb-like structure is generated as numerous canals penetrate the cuticle perpendicular to its surface (Raabe et al. 2005, 2006; Romano et al. 2007). Each pore canal contains a long, soft and probably flexible tube which has an elliptical-like cross section. In each plane the long axis of this ellipse is parallel to the fibre orientation. Thus, due to the rotation of the twisted plywood structure the outer shape of each tube resembles a twisted ribbon. Similar pore canals also occur in the cuticles of other Crustacea and serve as transport system for minerals during the molt cycle. In lobster cuticle, the combination of a honeycomb-like structure and a twisted plywood structure with tightly connected lamellae leads to remarkable mechanical properties and an anisotropic deformation behaviour (Sachs et al. 2008). TEM investigations of conventionally prepared samples (Raabe et al. 2006) have shown that in mineralized lobster cuticle the mineral is present in the form of nanoparticles with diameters between 10 and 30 nm. These particles are interspersed densely along and between the chitin-protein nanofibrils. This organization makes it difficult to distinguish the fourth hierarchical level, the chitin protein-fibres (Fig. 2.2a, c). Interestingly, in fully calcified cuticle of the edible crab *Cancer pagurus* single chitin protein fibers are surrounded by minerals forming a solid tube (Fig. 2.2b, d). The tubes of neighboring fibers are fused, which results in a structure which resembles a block of solid mineral containing long straight canals arranged in the same twisted plywood fashion as the chitin-protein fibers located inside the cavities. This implies that the way minerals are incorporated not only heavily influences the overall structure of the composite and thus its mechanical properties but also the organization of the organic cuticle fraction above the nanofibril level. It is of interest that despite having a higher volume fraction of mineral than *H. americanus* (Boßelmann et al. 2007) the pore canal system of *C. pagurus* is far less well developed than that of the lobster. It is therefore possible that in lobster cuticle the pore canals are not only a transport system but also help to reduce weight and energy consumption for the animals.

Unmineralized structures of the lobster exoskeleton like joint membranes have a similar structural hierarchy with the chitin-protein fiber twisted plywood as basic construction principle but they lack all mineral components (Fig. 2.3). Additionally the pore canal system is less developed and pore canals are rarely detected.

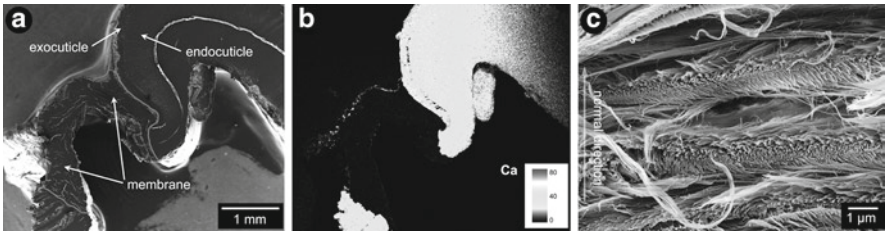

Fig. 2.3 Qualitative EDX mapping of calcium at the interface between mineralized cuticle and a joint membrane. (**a**) SEM micrograph of the interface. (**b**) Calcium is only present in the mineralized cuticle and shows a gradient from exo- to endocuticle, the membrane shows no indication of mineralization. (**c**) Cross section through an unmineralized joint membrane showing only smooth fibres and no pore canals

2.3 Mechanical Analysis of Arthropod Cuticles

2.3.1 Macroscopic Mechanical Properties

In materials like arthropod cuticle the mechanical properties are not just determined by the internal material composition including its structure on all levels of organization. The physiological state of the sample including factors like the actual stage of the molting cycle, nutrition state or diseases and its artificial or preparation state including factors like storage conditions and the grade of hydration of the investigated samples also play an important role (Fabritius et al. 2009). Therefore, it is crucial to examine test specimens in a state as close as possible to the natural state in order to obtain authentic values for the material in its incipient functional state. By taking these aspects into account the macromechanical properties of mineralized and non-mineralized cuticle from the American lobster were examined. Identical tests were performed on dry and wet claws endocuticle and arthrodial membranes, since it is particularly the water content which strongly affects the properties of biological composites.

Tensile tests show the influences of mineralization and hydration on the deformation and fracture behaviour of cuticle from the lobster *Homarus americanus* (Sachs et al. 2006a; Fabritius et al. 2009). The global stress strain behavior of endocuticle and joint membrane cuticle which was investigated using uniaxial tensile tests (Fig. 2.4; Table 2.1) shows the difference in the material response between the wet and the dry state. In the dry state the claw cuticle displays a linear elastic behaviour typical for a brittle response whereas the wet specimens show an onset of plastic

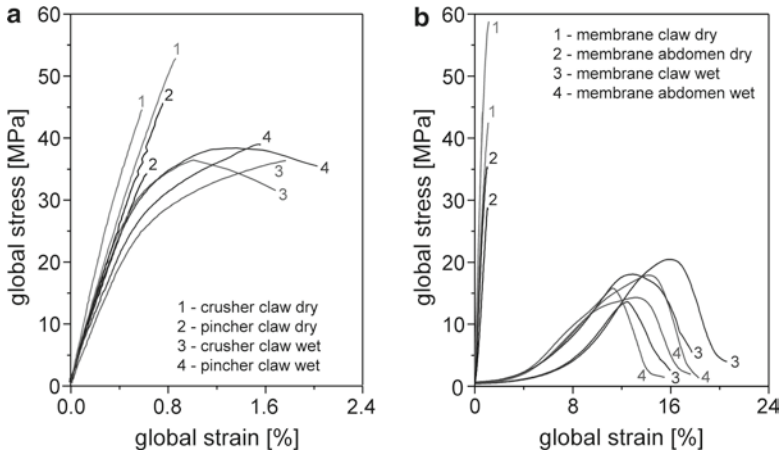

Fig. 2.4 Global stress–strain behavior of lobster endocuticle from the pincher and crusher claw (**a**) and membranes (**b**) taken from the joints of the claw (membrane c) and the abdomen (membrane a) both in the dry and in the wet state (Modified from Sachs et al. 2006a. Copyright 2006 Elsevier)

Table 2.1 Mechanical properties derived from the global stress–strain curves. The properties determined are the average values of the samples from each location and testing condition including their standard deviation: structural stiffness s_{st}, Poisson's ratio ν, yield strain ε_y, yield stress σ_y, strain to fracture ε_f and stress to fracture σ_f. The standard deviation is given in *brackets*

Sample	s_{st} (GPa)	ν (-)	ε_y (%)	σ_y (MPa)	ε_f (%)	σ_f (MPa)
Pincher claw dry	5.8 (0.4)	0.43 (0.00)	–	–	0.7 (0.09)	40.1 (7.9)
Crusher claw dry	7.0 (0.8)	0.34 (0.01)	–	–	0.7 (0.19)	48.8 (5.8)
Pincher claw wet	4.9 (0.6)	0.33 (0.03)	0.5 (0.04)	26.6 (3.2)	1.8 (0.33)	37.2 (2.5)
Crusher claw wet	4.8 (0.6)	0.34 (0.06)	0.5 (0.05)	25.8 (5.9)	1.7 (0.06)	34.1 (3.6)
Membrane c dry	5.9 (1.03)	0.28 (0.02)	–	–	1.0 (0.22)	48.5 (8.9)
Membrane a dry	3.6 (0.80)	0.28 (0.02)	–	–	0.9 (0.27)	32.1 (7.1)
Membrane c wet	0.19 (0.02)	0.5 (0.0)	11.9 (1.5)	13.4 (2.7)	14.5 (1.5)	17.4 (3.5)
Membrane a wet	0.24 (0.04)	0.5 (0.0)	9.6 (1.2)	11.3 (2.2)	13.7 (2.2)	15.9 (1.8)

deformation which begins relatively early and extends to a strain to fracture of about 1.8% (Fig. 2.4a). The lower strain to fracture achieved by dry cuticle shows the absence of irreversible deformation and stress reduction mechanisms in dehydrated endocuticle. In wet mineralized cuticle, significant necking does not seem to occur in the tensile test specimens at the end of deformation, which is rather untypical for more ductile materials such as the wet samples. Similar deformation behaviour was observed for untreated dry and wet cuticle from the walking legs of the crab *Scylla serrata* and the carapace of the prawn *Penaeus mondon* (Hepburn et al. 1975; Joffe et al. 1975). While the difference in structural stiffness between the two morphologically distinct claws is negligible, it is more pronounced between the dry and the wet state (Table 2.1). Nevertheless, it is comparably small which can probably be explained with the relatively high content of minerals in the claws whose elastic properties are less affected by the water content than the organic constituents (Vincent 2002). This becomes evident in the global stress strain behaviour of the membranous cuticle which is proven to be non-mineralized by qualitative EDX analysis (Fig. 2.3). The dry membrane samples from the claws and the abdomen show a linear elastic stress-strain response before brittle failure (Fig. 2.4b). Remarkably, both the mineralized and the non-mineralized samples reach similar values for the stress to fracture in the dry state (Table 2.1). Furthermore, the structural stiffness of the membranes is only slightly lower compared to the mineralized samples reaching approximately 4.8 GPa in the dry state. The hydration of the membrane changes the stress–strain response dramatically. The structural stiffness decreases by one order of magnitude and the strain to fracture increases from about 1% to about 14% while the stress to fracture is reduced to about 16 MPa.

The effect of water acting as a plastifier is reflected in the fracture surfaces of the samples tested in the dry and in the wet state (Vincent and Wegst 2004). In dry mineralized cuticle failure is caused by cracks propagating through the twisted plywood structure. They cause either cleavage of the fibers oriented parallel to the fracture surface along their junctions or cutting of the fibers oriented perpendicularly to the fracture surface along their cross-sections (Fig. 2.5a, b). The fracture surfaces show subsequent alternation of these two types of fracture modes. The residual overlapping platelets display smooth facets typical for a brittle failure. Features that would be characteristic for plastic deformation or gradual delamination effects which impede crack growth could not be observed. Cleaved cuticular pores which recur on the fracture surfaces probably act as natural defects in the material. Additional sources for defects are microcracks generated during the drying process by internal stresses. Natural defects and microcracks together can lead to a critical crack size resulting in a brittle failure as also known from various ceramic materials (Suresh 2004). The combination of these effects leaves the original microstructure below the fracture surface almost unaltered. In contrast, in the fracture surface of the dry membranes indications of a periodic twisted plywood structure are not visible but layers in a lamellar fashion are exposed which might comprise several planes of non-mineralized chitin-protein fibers (Fig. 2.5e, f).

Fracture surfaces of wet mineralized cuticle representing the natural state reveal a different type of fracture mechanism when compared to the artificial dry state (Fig. 2.5c, d). In wet samples the twisted plywood structure is strongly distorted and split up with its fibrous components aligned in tensile direction. Fiber bundles which were originally oriented perpendicular to the fracture surface slide and are torn apart, indicating delamination inside the twisted plywood layers. Additionally, the junctions between the fibers at the torn ends of the bundles are separated by flexible pore canal tubes which are stabilized by the parallel oriented parts of adjacent twisted plywood layers and remain located in their original position. Those pore canal tubes which are pushed out of the honeycomb structure protrude out of the fracture surface. Delamination, rotation and deflection causes the obliquely oriented parts of the honeycomb structure to become arranged along the tensile direction during elongation, and the honeycomb structure is divided into bundles in which the pore canals appear compressed and elongated. The fibers oriented parallel to the fracture plane delaminate in a similar way as in the dry samples. These fracture mechanisms indicate the occurrence of crack deflection and bridging of cracks which both lead to stepwise crack propagation before the actual fracture. In the wet state the fracture surfaces of the membranes reveal their ability to undergo large

Fig. 2.5 (continued) (**d**) Detail image showing the distorted twisted plywood structure with drawn-out pore canals (pc) and irregularly protruding pore canal tubes (pct). (**e**) Overview of the dry sample showing the relatively smooth surface. (**f**) Detail image displaying layers presumably consisting of several planes of non-mineralized chitin-protein fibers. (**g**) Overview of the wet sample showing the disrupted surface. (**h**) Detail image showing delaminated and torn stacked planes of non-mineralized chitin-protein fibers (Modified from Sachs et al. 2006a. Copyright 2006 Elsevier)

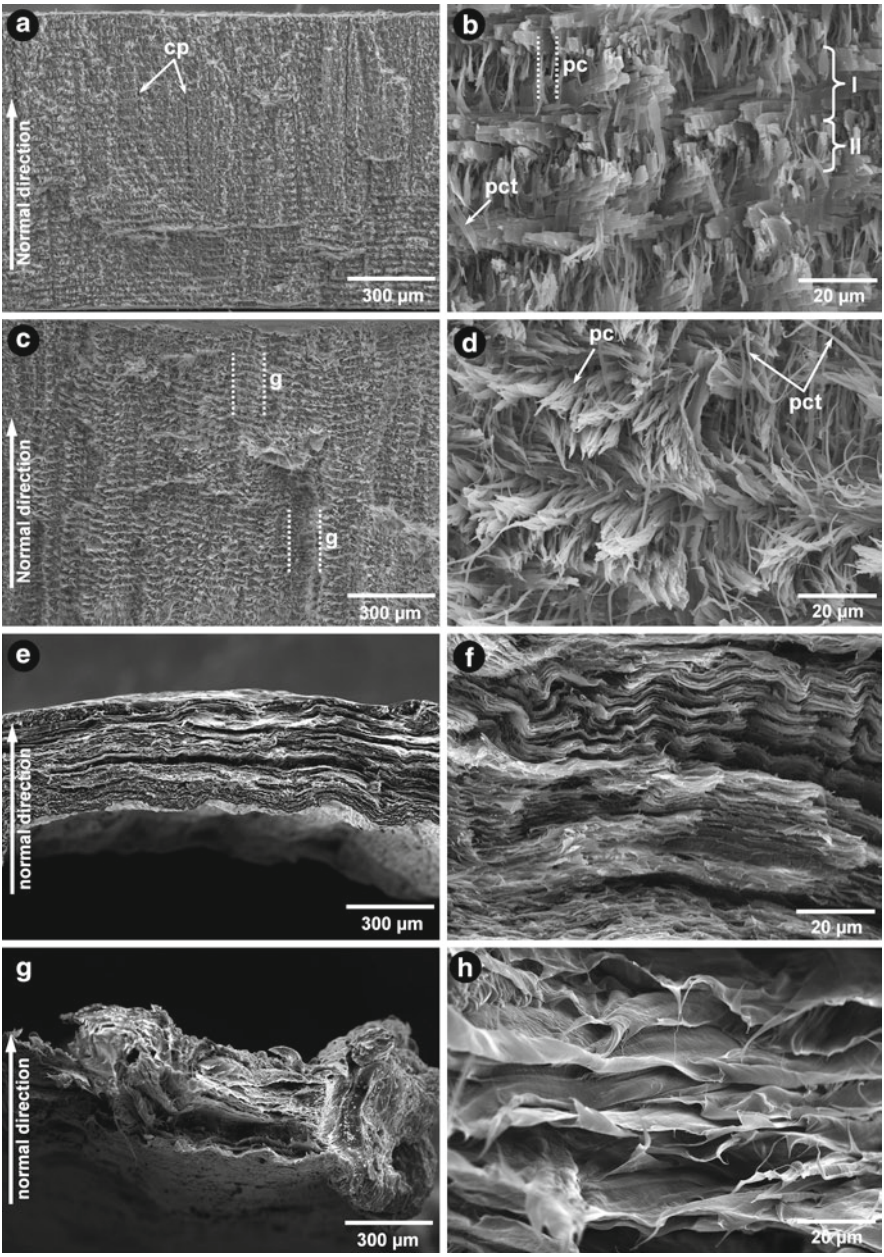

Fig. 2.5 Fracture surfaces of the crusher claw tested in dry (**a, b**) and in wet (**c, d**) state and of joint membranes taken from the claws and tested in dry (**e, f**) and in wet (**g, h**) state. (**a**) Overview of the dry crusher claw showing the smooth surface and numerous cleaved cuticular pores (cp). (**b**) Detail image displaying the fracture modes of fibers oriented more parallel (I) and fibers oriented closer to perpendicular (II) to the fracture surface. (**c**) The corrugated and uneven surface of the wet crusher claw with numerous deep irregular grooves (g, indicated by *dashed lines*).

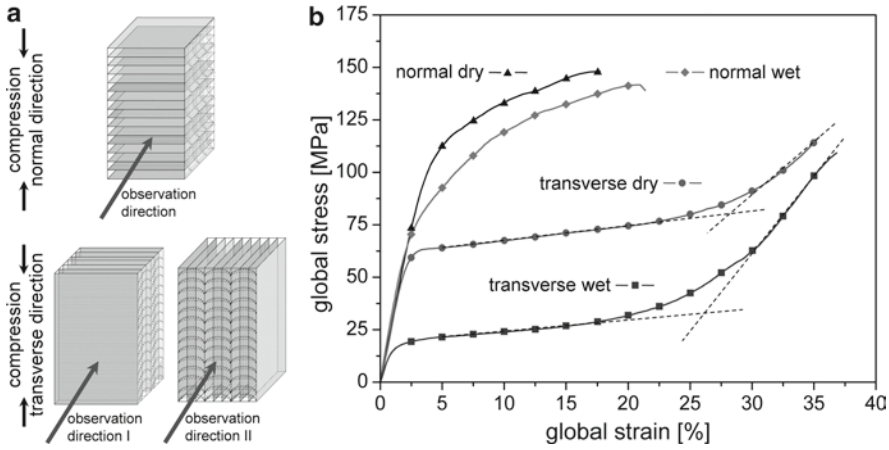

Fig. 2.6 Compression tests of mineralized lobster endocuticle. (**a**) For compression in normal direction of the cuticle, the cross section is observed. For compression in transverse direction of the cuticle, the two possible observation directions are parallel to the surface (observation direction I) and the cross section (observation direction II). (**b**) The global averaged stress–strain behaviour under compression of endocuticle in normal and transverse direction both in dry and in wet state. The *interception points* of the *dashed straights* fitted to the curves obtained for compression in transverse direction give the values for strain (ε_d) and stress (σ_d) at densification. The *vertical dotted line* indicates the strain range used for determining Poisson's ratio (ν) and structural stiffness (s_{st}) (Modified from Sachs et al. (2008). Copyright 2008 Elsevier)

deformations (Fig. 2.5g, h). Thin and smooth layers of non-mineralized chitin-protein fiber planes which protrude from the fracture surface indicate their delamination and slipping which occurred between the adjacent layers. In the hydrated state protein chains are bonded via water molecules forming hydrogen bonds between them which facilitate slip during deformation. Dehydration or incorporation of mineral particles is likely to hinder this process.

Compression tests of lobster endocuticle display a strong structural anisotropy in the global stress–strain behaviour (Sachs et al. 2008; Fabritius et al. 2009). While cuticle tested in normal direction shows a large linear elastic region and an onset of plasticity, samples tested in transverse direction show an extended plateau region after a relatively small elastic region and at the end a steeply rising portion of the stress–strain curve (Fig. 2.6). In dry state the structural stiffness in the normal direction and in transverse direction are almost equal (Table 2.2). In wet state the structural stiffness in normal direction is higher than in transverse direction and only slightly lower than the value obtained for the dry samples. Apparently, dehydration shows only little effect on the structural stiffness in normal direction, while in transverse direction the structural stiffness slightly increases from wet to dry state. The effect of dehydration on Poisson's ratio is about equal as its value is increased by a factor of about 1.3 in normal direction and nearly the same for the observation direction I in transverse direction. The difference in Poisson's ratio is remarkable when comparing observation directions I and II (see Fig. 2.6). Poisson's ratio is about a factor 3.6 times higher for observation direction I than for observation direction II

Table 2.2 Average mechanical properties of mineralized endocuticle from two different lobsters derived from compression tests. s_{st} structural stiffness; ν Poisson's ratio; ε_y yield strain; σ_y yield stress; ε_d strain at densification; σ_d stress at densification; ε_f strain to fracture; σ_f stress to fracture. The standard deviations are given in brackets. A set of six samples was tested in the normal and 12 samples in the transverse direction both in the dry and in the wet state

Direction	s_{st} (GPa)	ν (-)	ε_y (%)	σ_y (MPa)	ε_d (%)	σ_d (MPa)	ε_f (%)	σ_f (MPa)
Normal dry	4.7 (1.6)	0.13 (0.01)	2.4 (0.7)	96.8 (16.0)	–	–	18.7 (5.5)	147.5 (39.3)
Normal wet	4.1 (1.4)	0.10 (0.03)	1.8 (0.6)	56.4 (25.6)	–	–	19.4 (3.5)	124.7 (53.8)
Transverse dry observation direction I/II	4.6 (1.6)	0.29/0.08 (0.02/0.03)	1.6 (0.7)	54.9 (12.3)	30.2 (3.4)	87.0 (12.3)	42.3 (2.6)	163.4 (14.7)
transverse wet observation direction I/II	3.0 (1.3)	0.28/0.08 (0.08/0.02)	0.7 (0.3)	14.0 (4.0)	24.6 (2.6)	35.1 (6.7)	35.6 (3.7)	93.4 (5.4)

both in dry and in wet state. Compared to Poisson's ratios obtained in tensile tests (Table 2.1), the values for observation direction I are slightly lower. When compressed in transverse direction, the elastic deformation in the normal direction of the cuticle is much smaller than in the transverse direction of the cuticle. This behaviour is a result of the honeycomb-like structure of the pore canal system and the direction of the applied stress. When lobster cuticle is loaded in transverse direction, the pore canals are compressed and broaden in transverse direction, which corresponds to the cross section of the pore canals. In normal direction, which corresponds to the long axis of the pore canals, the increase in length during compression is negligible (Fig. 2.7).

The beginning of plastic deformation is defined by the yield strain and yield stress. The yield strain amounts to higher values in the normal direction than in the transverse direction and increases from the wet to the dry state (Fig. 2.6; Table 2.2). The same trends can be observed for the yield stress which is in both the dry and the wet state higher in normal direction than in transverse direction. The difference in the yield strain and stress in normal direction is less pronounced between the dry and the wet state while in transverse direction dehydration affects the values of the yield strain and yield stress. In the transverse direction the yield point marks the beginning of the plateau region. After reaching a critical stress level the structure deforms continuously without a strong increase in stress. This deformation behaviour is similar in dry and wet state but the stress is shifted to much higher values in the dry state. Considering the honeycomb-like structure, the observed stress values are the threshold at which the pore canals probably start collapsing. A similar behaviour has been described for polycarbonate honeycombs (Papka and Kyriakides 1998). At a strain of about 30% and a stress of 87 MPa in the dry state and of 25% and 35 MPa in the wet state, densification is reached and the stress increases, in the dry state more than in the wet state. The final strain to fracture and stress to fracture values are higher for dry cuticle than for wet cuticle. In normal direction the strains to fracture are much lower compared to the transverse direction, whereas the corresponding

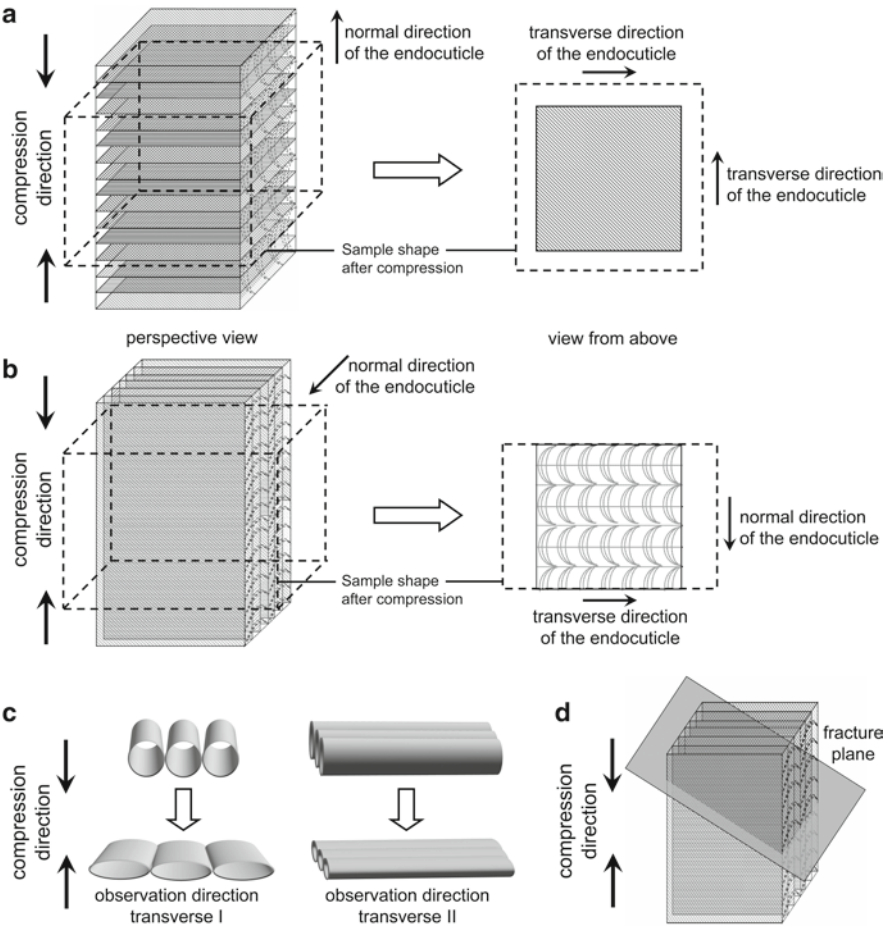

Fig. 2.7 Schematic illustration of the elastic–plastic deformation of the endocuticle under compression in the normal direction (**a**) and in the transverse direction (**b**). The *dashed lines* mark the shape of the specimens after deformation. (**c**) Schematic figure of the deformation of pore canals compressed in transverse direction. When observing the cuticle surface (transverse I), lateral broadening caused by collapsing pore canals is visible. During observation of the cuticle's cross section (transverse II) this broadening is also occurring, but does not become visible. (**d**) Schematic sketch showing the orientation of the fracture plane in samples tested in transverse direction (Reproduced from Sachs et al. 2008. Copyright 2008 Elsevier)

stresses to fracture are higher for wet but lower for dry cuticle. A fundamental difference was observed in the failure of the samples. While samples tested in normal direction failed by cleavage in compression direction, the samples tested in transverse direction showed a distinct fracture plane oriented perpendicular to the cuticle surface and 45° to the compression direction (Fig. 2.7d), which corresponds to the direction of the maximum shear stress. This can be explained by failure of the structure along the long axes of the pore canals, resulting in the propagation of

the crack from one pore canal to the next. To investigate the origin of these phenomena shear tests were performed on dry cuticle to evaluate the fracture energy which is needed to create distinct fracture planes. In the twisted plywood structure of the cuticle there are two different shear planes which are oriented either parallel to the cuticle surface (mode I) or perpendicular to the cuticle surface (modes II and III) (Fig. 2.8). Mode II and III differ in the shear direction which is either the normal or the transverse direction of the cuticle. Fractures of mode II have the highest fracture energy because the planes of mineralized fibers are displaced against each other in normal direction of the cuticle geometry and the fibers have to be fractured (Fig. 2.8). In mode I the superimposed mineralized fiber planes have to be delaminated and displaced laterally. Additionally, the pore canal tubes have to be sheared off. Here, the fracture energy amounts to a slightly lower value. In mode III, neither the pore canals nor the mineralized fiber planes have to be sheared off and the fracture energy is reduced about 40%. In a unidirectional fiber reinforced composite the fracture plane is also oriented 45° to the compression direction and parallel to the fiber axis if the composite is loaded perpendicular to the fiber orientation (Piggott 1980). The numerous pore canal tubes may play an important role as they act like the unidirectional fibers in this load case and likely stitch the mineralized fiber planes together improving the resistance against delamination (Dow and Dexter 1997). In crustaceans the original function of the pore canal system is the transport of minerals used for hardening the new exoskeleton after the molt (Dillaman et al. 2005). The obtained mechanical properties of *H. americanus* cuticle suggest that the pore canal system also performs structural functions in the lobster's exoskeleton.

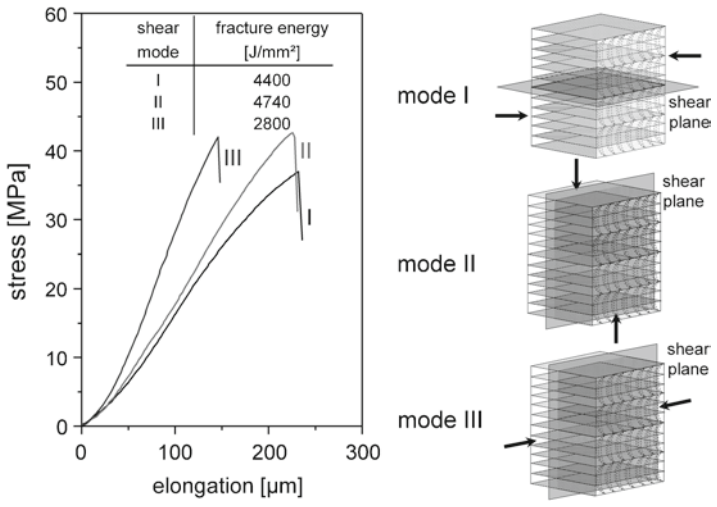

Fig. 2.8 Averaged displacement-stress curves for the three different shear modes I, II and III. In mode I the shear plane is parallel to the cuticle surface. In mode II and III the shear plane is perpendicular to the cuticle surface but the shear direction is either in normal direction (mode II) or in transverse direction (mode III) (Modified from Sachs et al. 2008. Copyright 2008 Elsevier)

Previous studies have shown that the pore canals also contain chitin-protein fibers, which are probably reinforcing them (Raabe et al. 2006; Romano et al. 2007).

By performing the compression tests combined with a detailed local strain analysis via digital image correlation, the elastic–plastic deformation of the endocuticle at the microscopic scale can be observed with high resolution (Sachs et al. 2008; Fabritius et al. 2009). The local strain analysis revealed significant differences in the plastic deformation behaviour between samples which were compressed in normal and in transverse direction. By comparing the two observation directions in the transversally compressed cuticle, a strong anisotropy in the plastic deformation can be found. While in the samples tested in normal direction a relatively homogeneous strain distribution was observed in longitudinal direction, the samples tested in transverse direction developed band-like regions of high strain which expanded into the adjacent areas. Their evolution corresponds to the plateau region in the global stress-stain curve indicating that in these zones the honeycomb-like structure of the pore canal system is already collapsed while the adjacent areas are still intact. During compression in transverse direction the samples become shorter in longitudinal direction due to collapsing pore canals which are responsible for the honeycomb-like structure, analogous to the elastic behaviour of the samples described above (Fig. 2.7). In lateral direction two deformation modes are observed depending whether one looks at the surface of the sample (observation direction I) or at the cross section of the sample (observation direction II). In the first case the collapsing pore canals lead to a broadening of the sample. This broadening of the sample cannot be seen in the observation direction II because the pore canals are parallel to the observation direction. Distinct differences of the local deformation cannot be observed between the dry and the wet state. The underlying deformation mechanisms become visible by examining the microstructure of test specimens after compression. Since the dry and wet cuticle tested in normal direction was only deformed about 10%, significant deformation of the complex microstructure was not observed. In the transverse testing direction two forms of deformation mechanisms were observed (Fig. 2.9). In layers where the fibers are oriented perpendicular to the compression direction the pore canals are collapsed (Fig. 2.9a, c) and in layers where the fibers are oriented parallel to the compression direction the fiber bundles buckle into the cavities of the pore canals (Fig. 2.9b, d). The pore canal tubes appear hardly damaged and are obviously able to prevent delamination of the layers when they are distorted against each other. Consequently, the samples do not expand in this direction. The buckling of fibers demonstrates their ability to undergo large plastic deformation in the wet but also in the dry state. However, in the dry state microcracks are visible which do not lead to a brittle failure due to the compression loading (Fig. 2.9a). This deformation is likely to take place in the plateau region of the stress–strain curve. When a critical stress level is reached in transverse direction, the honeycomb-like structure starts to collapse followed by progressive failure of the adjacent structure. While the deformation behaviour in transverse direction is similar in dry and wet state the stress threshold in the dry state is much higher than in the wet state. Hydration seems to affect the deformation and fracture behavior of lobster cuticle during compression much less than during tension. This is due to the

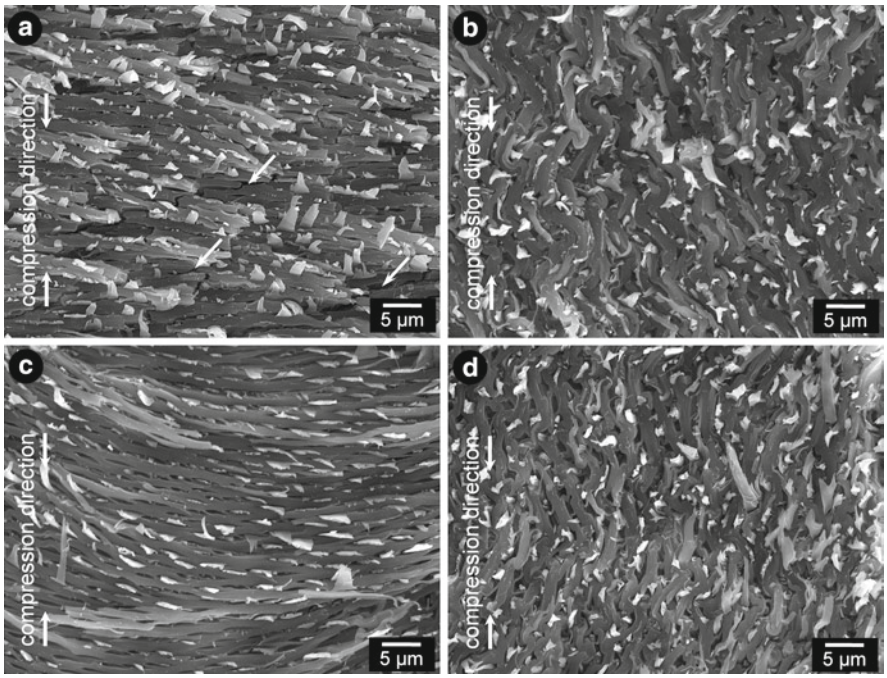

Fig. 2.9 SEM micrographs of compression test specimens fractured after being tested in transverse direction in the dry state (**a**, **b**) and in the wet state (**c**, **d**). In layers where the fibers are oriented perpendicular to the compression direction the pore canals are collapsed and microcracks (*arrows*) have formed in the dry state (**a**) but not in the wet state (**c**). In layers where the fibers are oriented parallel to the compression direction the fiber bundles have buckled irregularly into the cavities of the pore canals (**b, d**) (Reproduced from Sachs et al. 2008. Copyright 2008 Elsevier)

fact that beyond the yield point the endocuticle undergoes a densification instead of a separation of fibers which hinders crack opening and propagation and thus delays the failure of the test specimens. Nevertheless, hydrated samples are more ductile and support higher strains to fracture than dry samples. Additionally, hydration seems to impede the formation of microcracks in the structure during compression, supporting the role of water as a plastifier (Vincent and Wegst 2004). Generally, the observed deformation characteristics are typical for honeycomb structures. The observed and measured properties of lobster endocuticle in transverse and in normal direction resemble the mechanical response of a classical honeycomb in its in-plane and out-of-plane direction (Gibson and Ashby 1997).

2.3.2 Microscopic Mechanical Properties

In contrast to the highly anisotropic elastic–plastic deformation behavior, the elastic properties of the endocuticle such as the elastic moduli are relatively isotropic which

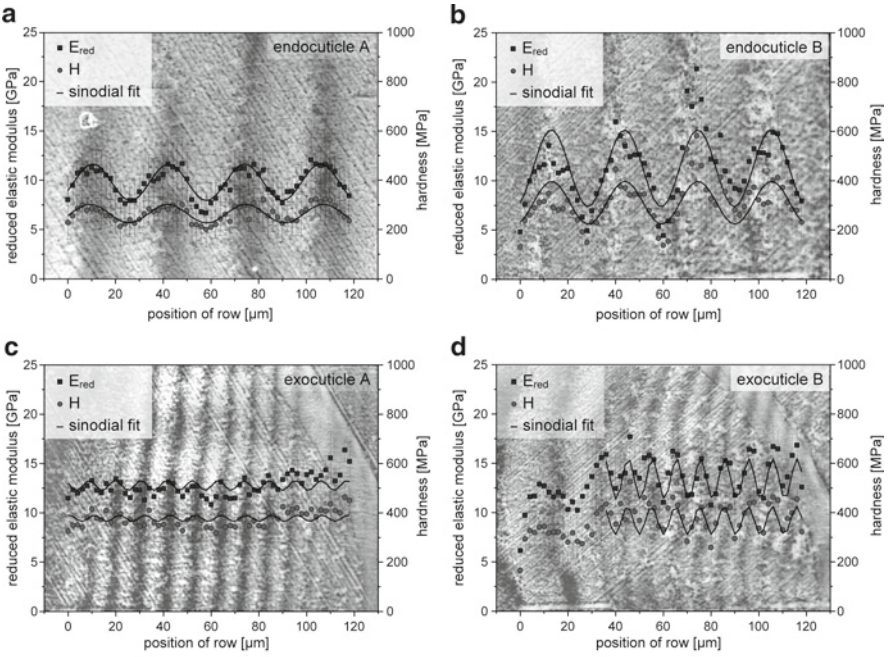

Fig. 2.10 Profiles of the reduced elastic modulus E_{red} and the hardness H shown on top of optical micrographs of the probed lobster cuticle areas. *Curves* obtained for endocuticle (**a, b**), exocuticle (**c**) and transition zone between exo- and endocuticle (**d**). Alternating *bright* and *dark areas* correspond to the change in orientation of exposed fibers with respect to the probed surface. Each data point represents the average of 20 indents which are included in each row of the indentation pattern. The standard deviation is indicated by the *scatter bars*

is rather atypical for honeycomb-like structures. In order to investigate this finding, we performed nanoindentation tests on the next lower level of the hierarchical organization to examine the orientation dependence of elastic properties and hardness and the influence of the grade of mineralization of fibers by probing cross-sectional areas of the endocuticle and the exocuticle. In the investigated samples the stacking height which amounts to about 10 µm in the exocuticle and about 30 µm in the endocuticle is consistent with the wavelengths observed in the profiles of the reduced elastic modulus and the hardness (Fig. 2.10; Table 2.3). In the light micrographs of the microtome polished microstructure alternating dark and bright areas indicate where the fibers change their orientation with respect to the probed surface. A comparison of the profiles of the reduced elastic modulus and the hardness with the fiber orientation shows that their maxima and minima correspond to this change in fiber orientation. The wide scatter bands in the measured values of both reduced elastic modulus and hardness can originate from deviations between fiber planes and the line of indents in the pattern, differences in the surface roughness of the cross-section or surface artifacts like pore canals exposed by sample preparation. In the exocuticle the relatively lower spatial resolution is likely to further increase the scatter in

Table 2.3 Characteristic data derived from the profiles of the reduced elastic modulus E_{red} and the hardness H. M is the height of a 180° rotated fiber stack

Sample		E_{red} wavelength (μm)	E_{red} amplitude (GPa)	E_{red} mean value (GPa)	H wavelength (μm)	H amplitude (MPa)	H mean value (MPa)	M wavelength (μm)
A	exo	10.8±0.2	0.5±0.2	12.8±1.1	10.6±0.2	12.6±5.6	378.0±31.8	10.5
	endo	31.8±0.3	1.9±0.1	9.8±1.4	32.7±0.4	37.4±3.7	264.5±32.7	32.2
B	exo	10.1±0.1	2.1±0.3	13.4±2.2	10.1±0.1	57.4±10.3	368.1±65.1	9.7
	endo	30.7±0.4	3.9±0.4	11.3±3.4	30.7±0.6	86.9±11.7	310.6±87.1	31.7

the profile of the reduced elastic modulus and the hardness. Nevertheless, the fit of the data matches the stacking height of the microstructure accurately but less precisely. The volume which the indenter interacts with at the maximum indentation depth comprises fibers with different twist angles of 7° in the endocuticle and 14° in the exocuticle. The observed correlation between the rotation angles of the fibers and the reduced elastic modulus clearly shows a difference in the mechanical response depending on the orientation in which the fibers are loaded. At the present state it is not yet clear whether the high elastic modulus and hardness values correspond to fibers indented in axial direction or perpendicular to their long axis. Due to the high volume fraction of exposed pore canals in polished cross sections (see Fig. 2.2a) which are probed by the indenter it is possible that the high values correspond to the areas where the fibers are oriented parallel to the probed sample surface. The other possibility is supported by the fact the direction of the fiber axis is the direction along the covalent backbone of the chitin crystallites (Raabe et al. 2006), which is their stiffest axis (Nikolov et al. 2009, accepted). In this case, with changing orientation towards the indenter, the response becomes less stiff. A possible reason for this could be that this direction is softer due to directional anisotropy in the bonding between the molecules forming the fibers. It is also likely that partial bending occurs as deformation mode under this loading condition.

The comparison of the reduced elastic modulus and the hardness between the endocuticle and the exocuticle for the same rotation angles allows investigating the effect of mineralization on the mechanical properties depending on the fiber orientation. An increase in mineral content would particularly affect the properties parallel to the fiber axis whereas the effect in the fiber axis is less pronounced. This behavior could be explained by the already higher stiffness in this direction so that the enhancement is less strong. The elastic properties seem to be mainly affected by the grade of mineralization (Sachs et al. 2006b). Variations in the stacking height have little to no effect on the elastic properties but might improve fracture toughness, for instance.

Nanoindentation experiments on human and bovine osteonal bone on a similar length scale have shown similar heterogeneous responses of the probed microstructure, although a direct correlation to the orientation of the mineralized collagen fibers could also not be shown due to the much thinner plywood lamellae and periodic variations in the mineralization occurring in these materials (Gupta et al. 2006; Tai et al. 2007).

2.4 Multi-scale Modeling of the Hierarchical Structure of Arthropod Cuticles

Numerical multi-scale modeling allows for a more detailed analysis of experimental results as has been shown recently for the elastic properties of bone at submicron scales (Nikolov and Raabe 2008). The advantage of using multi-scale models for the analysis of hierarchically structured biological materials is that models are unaffected by methodological problems such as associated with sample preparation or scatter in the test data. Also, they allow the user to apply such models to the respective scale and region of interest. Finally, through sensitivity and error propagation analysis multi-scale models can tell us which of the ingredients and structural sub-units of natural materials produce or influence specific properties.

Our model developed for the cuticle of the lobster *Homarus americanus* allows us to calculate the anisotropic properties of the bulk mineralized tissue in terms of the orientation of the chitin-protein fibers and the mineralization grade (Nikolov et al. 2010). The model is based on ab initio and atomistic simulations on the lower scales and continuum micromechanics where the overall properties are obtained via step-by-step homogenization from lower to higher levels of structural hierarchy at the larger scales (see Figs. 2.1a and 2.11).

At the lowest level of hierarchy (~1 nm), the orthotropic elastic tensor of α-chitin is obtained via ab initio calculations. The major challenge of such a structural analysis

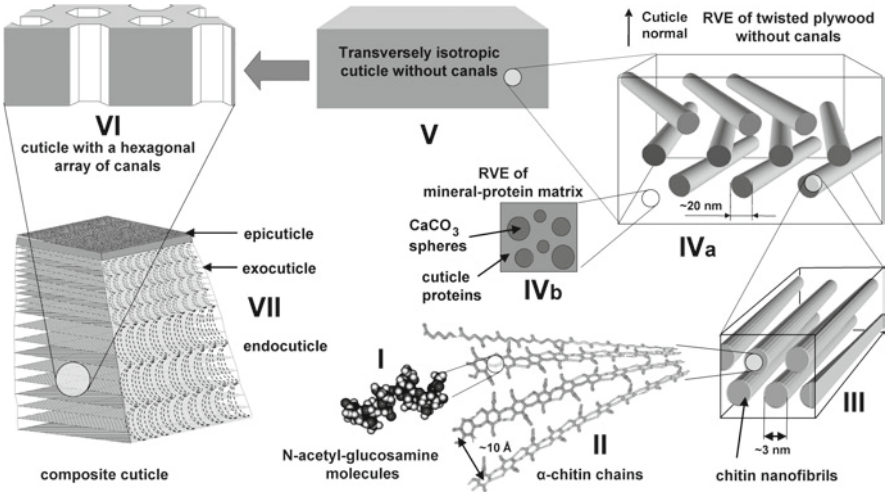

Fig. 2.11 Hierarchical model for lobster cuticle: (**I**), (**II**) – α-chitin properties via ab initio calculations; (**III**) representative volume element (RVE) for a single chitin-protein fiber; (**IVa**) RVE for chitin-protein fibers arranged in twisted plywood and embedded in mineral-protein matrix; (**IVb**) RVE for the mineral-protein matrix; (**V**) homogenized twisted plywood without canals; (**VI**) homogenized plywood pierced with hexagonal array of canals; (**VII**) 3-layer cuticle (Modified from Nikolov et al. 2010. Copyright Wiley-VCH Verlag GmbH & Co. KGaA. Reproduced with permission)

is the multi-dimensionality of the relevant configurational space of possible geometries that exists close to the true ground state. Not only the exact positions of the hydrogen atoms in the unit cell but also the number of the hydrogen bonds were at first unknown. In order to explore possible atomic geometries, a hierarchical approach that combines (i) empirical force field molecular dynamics (EFFMD), (ii) tight binding (TB), and (iii) density functional theory (DFT) calculations was used.

In a first step, starting from a quite arbitrary atomic geometry which reproduces the chemical formula of α-chitin, an extended EFFMD molecular-dynamics run (EFFMD: Extended force field molecular dynamics; Materials Studio software package) resulted in 10^5 most promising structures that possessed (i) low energy and (ii) maximum number of hydrogen bonds. In a second step, the properties of the pre-selected configurations have been refined and calculated again by employing a self-consistent *ab-initio*-based tight-binding scheme (SC-DFT-TB, see e.g. Jalkanen et al. 2004). Thirdly, about 10 structures with the lowest energy and reasonable hydrogen-bond network that emerged from the SC-DFT-TB calculations served as input to the subsequent parameter-free (*ab initio*) calculations (SC-DFT-TB: self consistent density functional based Tight Binding). The calculations have been performed within the density-functional-theory (DFT) (Hohenberg and Kohn 1964; Kohn and Sham 1965) to determine a complete set of the single-crystalline α-chitin lattice and elastic constants (Ravindran et al. 1998) (Fig. 2.12). As shown in the right diagram in Fig. 2.12, the principal elastic constants along the crystallographic directions exhibit a strong elastic anisotropy. While the crystal response to deformations along the

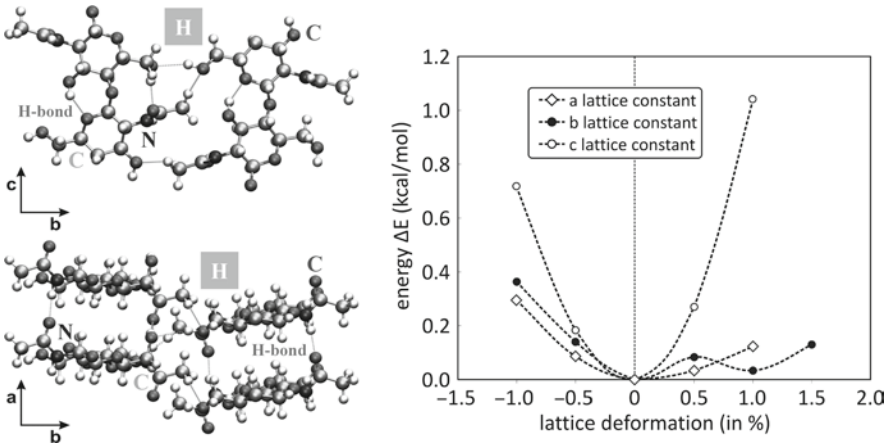

Fig. 2.12 **Left**: theoretically determined ground state structure of single-crystalline α-chitin: a, b and c (chain direction) denote the orthorhombic unit cell vectors. Different atoms are coloured in different shades of grey. **Right**: total unit cell energy vs. uniaxial strain profiles for deformations along a, b, and c. Positive (negative) values along the x-axis denote tensile (compressive) strain. The shallow minimum which appears at ~1% tensile strain in the lattice deformation profile along b denotes a metastable configuration and depicts the complex and flexible character of the hydrogen bond pattern (Modified from Nikolov et al. 2010. Copyright Wiley-VCH Verlag GmbH & Co. KGaA. Reproduced with permission)

a, and *b* directions is rather soft, the material is nearly one order of magnitude stiffer along the *c*-axis. This can be explained in terms of the different nature of chemical bonds dominating the different axis: Along the molecule axis stiff covalent bonds dominate the mechanical behaviour. On the other hand softer and structurally flexible hydrogen bonds are responsible for the cohesion of the adjacent α-chitin strings.

The effective elastic properties at higher hierarchy levels can now be derived by using homogenization methods (Benveniste 1987; Benveniste et al. 1991; Torquato 1998) which require as an input the elastic properties of each phase within the composite as well as their volume fractions, shapes, and orientations. Regarding the chitin as one of the components, the ab initio determined elastic data have been used.

In the Representative Volume Element (RVE) for chitin-protein fibers, the chitin-protein nanofibrils (~3 nm) are modeled as aligned, needle-like chitin crystallites with infinite aspect ratio and volume fraction of 0.16, embedded in a nearly incompressible protein matrix (Giraud-Guille 1990). The elastic modulus of the nano-fibril proteins has been identified to be about 5 MPa, a typical value for soft proteins. Given the relatively small volume fraction of the chitin crystallites, the homogenized properties of the chitin-protein fibers are obtained via the well-known Mori-Tanaka method (Mori and Tanaka 1973). In parallel, the mineral-protein matrix containing the chitin-protein fibers is represented as an assembly of isotropic space-filling amorphous calcium carbonate (ACC) spheres with different diameters and with properties assumed to be equal to those of calcite, i.e. elastic modulus 78 GPa and Poisson's ratio 0.34. The spherical shape of the biominerals is assumed since ACC particles are known to grow spherically. The spheres are embedded in a nearly incompressible matrix of cuticle proteins with elastic modulus identified as 1 GPa. The RVE of the mineral-protein matrix is homogenized with the 3-point Torquato method taking into account not only the shape of the inclusions and their volume fraction but also the spatial correlations between the spheres and their arrangement (Torquato 1998). Remarkably, our modeling results show that the microstructure of the calcium carbonate spheres assembly must have optimal properties (i.e. to be as stiff as possible for a given volume fraction of mineral) in order to match the experimental results. In our case, such a microstructure is the so called symmetrical cell material where the local probability for a given spherical cell with random diameter to be "made" of calcium carbonate is equal to the overall volume fraction of the mineral. The local RVE of the bulk cuticle is taken to be small enough so that the chitin-protein fibers can be considered as being locally aligned in a first approximation. Thus, the gradual rotation of the chitin fibers within the plywood is represented as a sequence of many RVEs with aligned fibers rotated at a fixed small angle and stacked over each other. The RVE with aligned chitin-protein fibers is homogenized again with the Mori-Tanaka mean-field method given that their volume fraction is less than 20%. The anisotropy of this representative volume is the same as the local anisotropy of the cuticle evaluated by nanoindentation and can be compared to the experiment for different fiber orientations and different mineral contents. The simulation results for the endocuticle containing 70 wt% calcium carbonate and for the exocuticle containing 73 wt% calcium carbonate are shown in Fig. 2.13 and compared to the experimental data. Provided that all

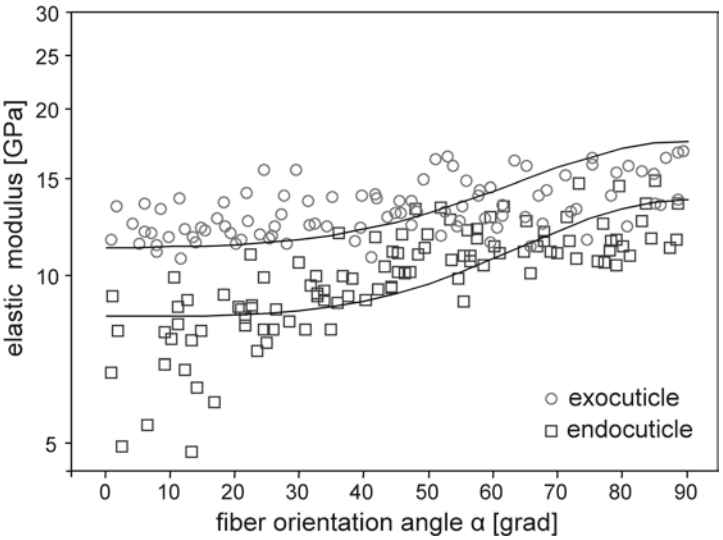

Fig. 2.13 Comparison between simulation results and experiment. *Symbols*: experimental data, open circles – exocuticle, squares – endocuticle. *Solid lines* – model predictions

cuticle components except the α-chitin are assumed to be isotropic, the local variations of the elastic modulus are likely due to the different orientation of the chitin fibers and their higher elastic modulus along the chitin chains. However, the elastic properties of the cuticle are determined to a large degree by the mineral content. The experimentally observed sinusoidal variation of the elastic modulus through the cuticle (Fig. 2.10) is only partly predicted by the model which may be due to uncertainty in the evaluation of some of the elastic constants of chitin or to the assumption that the fibers are perfectly aligned.

2.5 Conclusions

The crustacean exoskeleton, the cuticle, consists of chitin and protein molecules that are organized in at least seven hierarchical levels. It forms skeletal elements with physical properties that are adapted to their function and the eco-physiological strains of the organism. All skeletal elements have in common the so-called twisted plywood structure, which is built by stacks of planar arrays of complex chitin-protein fibres. In most parts of the cuticle the organic material is combined with inorganic nano-particles. These particles are arranged according to the organisation of the chitin-protein fibres making the cuticle a hierarchical composite material of high functional versatility. The diversity of the physical properties of the cuticle must be caused by structural and chemical alterations at one or several hierarchical levels. The cuticle of the American lobster is an ideal model material for studying

mechanical properties of such hierarchically organized fiber-based biological composites. In biological structural materials like arthropod cuticle the mechanical properties vary on different length scales due to the hierarchical organization of these materials. Tensile tests show the influences of mineralization and hydration on the deformation and fracture behaviour of the cuticle. While unmineralized hydrated cuticle deforms plastically, a higher grade of mineralization leads to an increase in stiffness and reduces plasticity. Dehydration of the organic matrix leads to an increase in stiffness and to a complete loss of plasticity. Due to the well developed pore canal system, the mineralized material deforms like a honeycomb structure under compression. However, the twisted plywood arrangement of the fibers makes the in-plane direction stiffer than the normal direction. The flexible tubes in the pore canals increase fracture resistance in transverse direction as shown by shear testing. The macroscopic mechanical properties demonstrate that the combination of twisted plywood and honeycomb structure results in a material with better properties at lower weight and also economization of material and energy for the organism. This interaction of different construction principles can be used as a template for the design of novel high performance materials. On the microscopic level, the elastic properties and the hardness of the fibers depend on their spatial orientation and grade of mineralization. The increase of the average stiffness and hardness from the endocuticle to the exocuticle is caused by a higher grade of mineralization. A higher volume fraction of incorporated mineral crystallites effects the perpendicular direction of the fibers to a greater extent than the inherently stiffer and harder long axis. Numerical multi-scale modeling of the cuticle via step-by-step homogenization allows predicting the mechanical properties at all levels of structural hierarchy. The model is validated by comparing the experimentally obtained mechanical properties with the numerical predictions and can be used to derive mechanical data for the lowest hierarchical levels where experimental investigation becomes difficult.

References

Andersen SO (1979) Biochemistry of insect cuticle. Annu Rev Entomol 24:29–61

Benveniste Y (1987) A new approach to the application of Mori-Tanaka's theory in composite materials. Mech Mater 6:147–157

Benveniste Y, Dvorak GJ, Chen T (1991) On diagonal and elastic symmetry of the approximate effective stiffness tensor of heterogeneous media. J Mech Phys Solids 39:927–946

Boßelmann F, Romano P, Fabritius H, Raabe D, Epple M (2007) The composition of the exoskeleton of two crustacea: the american lobster *Homarus americanus* and the edible crab *Cancer pagurus*. Thermochim Acta 463:65–68

Bouligand Y (1970) Aspects ultrastructuraux de la calcification chez les Crabes, in: 7e Congrès int. Microsc. Électr., Grenoble, France, t. 3, 105–106

Brusca RC (2000) Unraveling the history of arthropod diversification. Ann Mo Bot Gard 87:13–25

Carlström D (1957) The crystal structure of α-chitin (Poly-N-Acetyl-D-Glucosamine). J Biophys Biochem Cytol 3:669–683

Chen JC, Ramsköld L, Zhou G (1994) Evidence for monophyly and arthropod affinity of cambrian giant predators. Science 263:1304–1308

Dillaman RM, Hequembourg S, Gay M (2005) Early pattern of calcification in the dorsal carapace of the blue crab, *Callinectes sapidus*. J Morphol 263:356–374

Dow MB, Dexter HB (1997) Development of stitched, braided and woven composite structures in the ACT program and at Langley research center (1985 to 1997) summary and bibliography. NASA CASI 301:621–0390

Edgecombe GD (ed) (1998) Arthropod fossils and phylogeny. Columbia University Press, New York, USA

Fabritius H, Sachs C, Romano P, Raabe D (2009) Influence of structural principles on the mechanics of a biological fiber-based composite material with hierarchical organization: the exoskeleton of the lobster *Homarus americanus*. Adv Mater 21:391–400

Gibson LJ, Ashby MF (1997) Cellular solids – structure and properties, 2nd edn. Cambridge University Press, Cambridge, UK

Giraud-Guille M-M (1984) Fine structure of the chitin-protein system in the crab cuticle. Tissue Cell 16:75–92

Giraud-Guille M-M (1990) Chitin crystals in arthropod cuticles revealed by diffraction contrast transmission electron microscopy. J Struct Biol 103:232–240

Giraud-Guille M-M (1998) Plywood structures in nature. Curr Opin Solid State Mater Sci 3:221–228

Gupta HS, Stachewicz U, Wagermaier W (2006) Mechanical modulation at the lamellar level in osteonal bone. J Mater Res 21:1913–1921

Hadley NF (1986) The arthropod cuticle. Sci Am 255:98–106

Hepburn HR, Joffe I, Green N, Nelson KJ (1975) Mechanical properties of a crab shell. Comp Biochem Physiol 50A:55l–554

Hohenberg P, Kohn W (1964) Inhomogeneous electron gas. Phys Rev 136:B864–B871

Jalkanen KJ, Elstner M, Suhai S (2004) Amino acids and small peptides as building blocks for proteins: comparative theoretical and spectroscopic studies. J Mol Struct THEOCHEM 675:61–77

Joffe I, Hepburn HR, Nelson KJ, Green N (1975) Mechanical properties of a crustacean exoskeleton. Comp Biochem Physiol 50A:545–549

Khor E (2001) Chitin: fulfilling a biomaterials promise. Elsevier Science, Amsterdam, The Nederlands

Kohn W, Sham LJ (1965) Self-consistent equations including exchange and correlation effects. Phys Rev 140:A1133–A1138

Materials Studio. http://accelrys.com/products/materials-studio/modules/forcite.html

Minke R, Blackwell J (1978) The structure of α-chitin. Mol Biol 120:167–181

Mori T, Tanaka K (1973) Average stress in matrx and average elastic energy of materials with misfitting inclusions. Acta Metall 21(5):571–574

Müller KJ, Walossek D (1985) A remarkable arthropod fauna from the Upper Cambrian "Orsten" of Sweden. Trans R Soc Edin Earth Sci 76:161–172

Muzzarelli RAA (1977) Chitin. Pergamon, Oxford, UK

Nikolov S, Raabe D (2008) Hierarchical modeling of the elastic properties of bone at submicron scales: the role of extrafibrillar mineralization. Biophys J 94:4220–4232

Nikolov S, Petrov M, Lymperakis L, Friák M, Sachs C, Fabritius H, Raabe D, Neugebauer J (2010) Revealing the design principles of high-performance biological composites using ab initio multiscale simulations. Adv Mater 22:519–526

Papka DS, Kyriakides S (1998) In-plane crushing of a polycarbonate honeycomb. Int J Solids Struct 35:239–267

Piggott MR (1980) Load bearing fibre composites, 2nd edn. Kluwer, Norwell, USA

Raabe D, Romano P, Sachs C, Al-Sawalmih A, Brokmeier H-G, Yi S-B, Servos G, Hartwig HG (2005) Discovery of a honeycomb structure in the twisted plywood patterns of fibrous biological nanocomposite tissue. J Cryst Growth 283:1–7

Raabe D, Romano P, Sachs C, Fabritius H, Al-Sawalmih A, Yi S-B, Servos G, Hartwig HG (2006) Microstructure and crystallographic texture of the chitin-protein network in the biological composite material of the exoskeleton of the lobster *Homarus americanus*. Mater Sci Eng, A 421:143–153

Ravindran P, Fast L, Korzhavyi PA, Johansson B, Wills J, Eriksson J (1998) Density functional theory for calculation of elastic properties of orthorhombic crystals: application to $TiSi_2$. J Appl Phys 84:4891–4904

Roer RD, Dillaman RM (1984) The structure and calcification of the crustacean cuticle. Am Zool 24:893–909

Romano P, Fabritius H, Raabe D (2007) The exoskeleton of the lobster *Homarus americanus* as an example of a smart anisotropic biological material. Acta Biomater 3:301–309

Sachs C, Fabritius H, Raabe D (2006a) Experimental investigation of the elastic-plastic deformation behavior of mineralized cuticle by digital image correlation. J Struct Biol 155:409–425

Sachs C, Fabritius H, Raabe D (2006b) Hardness and elastic properties of dehydrated cuticle from the lobster *Homarus americanus* obtained by nanoindentation. J Mater Res 21:1987–1995

Sachs C, Fabritius H, Raabe D (2008) Influence of microstructure on deformation anisotropy of mineralized cuticle from the lobster *Homarus americanus*. J Struct Biol 161:120–132

Suresh S (2004) Fatigue of materials, 2nd edn. Cambridge University Press, Cambridge

Tai K, Dao M, Suresh S, Palazoglu A, Ortiz C (2007) Nanoscale heterogeneity promotes energy dissipation in bone. Nat Mater 6:454–462

Torquato S (1998) Effective stiffness tensor of composite media: II. Applications to isotropic dispersions. J Mech Phys Solids 46:1411–1440

Vincent JFV (2002) Arthropod cuticle: a natural composite shell system. Compos A 33:1311–1315

Vincent JFV, Wegst UGK (2004) Design and mechanical properties of insect cuticle. Arthropod Struct Dev 33:187–199

Weiner S, Addadi L (1997) Design strategies in mineralized biological materials. J Mater Chem 7:689–702

Chapter 3
Radiocarbon Dating of Chitin

Jennifer A. Tripp and Thomas F.G. Higham

Contents

Abstract Remains of insects are often found in an archaeological context, and because insects are sometimes temperature sensitive, their presence in archaeological and environmental contexts gives them climatic significance. The use of accelerator mass spectrometry (AMS) to date small samples has allowed for the direct analysis of insect remains, and these studies have given a deeper understanding of Quaternary climate change and its effects on human activity during this time. In addition, the presence of certain insects can indicate particular types of human activity (i.e. animal husbandry or the existence of timber structures or open fields), and direct dating of insects provides chronological constraints on these activities throughout the range of the radiocarbon timescale.

This chapter covers recent advances in pretreatment chemistry for AMS radiocarbon dating of insects, including isolation of polymeric chitin or chitin monomers. The uses of chitin dates, in particular the archaeological and palaeoenvironmental applications, are also discussed. Problems with the radiocarbon dating of insects, including contamination, degradation, and the often observed offset between dates of insect remains and surrounding organic material, are addressed along with potential solutions.

J.A. Tripp (✉)
Department of Chemistry and Biochemistry, San Francisco State University,
San Francisco, CA 94132, USA
e-mail: tripp@sfsu.edu

T.F.G. Higham
Oxford Radiocarbon Accelerator Unit, Research Laboratory for Archaeology
and the History of Art, University of Oxford, Oxford OX1 3QY, UK
e-mail: thomas.higham@rlaha.ox.ac.uk

N.S. Gupta (ed.), *Chitin*, Topics in Geobiology 34,
DOI 10.1007/978-90-481-9684-5_3, © Springer Science+Business Media B.V. 2011

3.1 Introduction

Remains of chitin-containing organisms are found in archaeological contexts throughout the world. Insects, in particular, are often recovered from archaeological deposits and analyzed to provide a range of information about palaeoclimate and human activities in the past (Elias 1994). Robinson (2001) notes that insect remains have provided information about abrupt climate change that cannot be gleaned from the pollen record. In addition, some species indicate specific human activities and are only present in the archaeological record in densely populated settlements or in areas where particular industries, such as animal husbandry, are being practiced. Because insects throughout the Quaternary are morphologically consistent (archaeological finds can be identified as extant species) and are almost certainly ecologically consistent (an ancient insect of a particular species would have behaved in the environment in a similar fashion to its modern counterpart), insect remains have been successfully used to study environmental conditions and human economies in a number of areas around the world (Robinson 2001).

Besides insects, chitin is present in molluscan shells (Peters 1972) and the cell walls of several species of fungus (Blumenthal and Roseman 1957). Isolation of chitin from archaeological shells for radiocarbon dating is without precedent, mainly because the bulk of the shell material, calcium carbonate, is present in much larger amounts and is itself suitable for radiocarbon dating. Several issues with shell dating, including diagenetic recrystallization, the presence of marine carbon, and hard water effects (Schmidt 2000) make shell dating challenging, and isolation of chitin from shells may present a reasonable route to the radiocarbon dating of shells in the future; however, no such work has been reported. Likewise, archaeological applications for fungal chitin do not yet exist, most likely due to problems with preservation and contamination. This chapter will therefore focus on the radiocarbon dating of insect chitin, since a number of examples of the radiocarbon dating of insect remains have been published. Studies have focused primarily on Coleoptera and chironomidae (order: Diptera) which have been used for palaeoenvironmental analysis. Well-preserved chitin has been detected in ancient samples, and its chemical purification for isotopic analysis, including radiocarbon, is an active area of research at the Oxford Radiocarbon Accelerator Unit.

Insect remains can sometimes be directly related to human activities. For example, the carcasses of termites, grasshoppers, beetles and ants have been found preserved in human coprolites in a number of locales, and provide a significant source of information about dietary and subsistence practices (Elias 1994, pp. 127–129). Insects that occupy specific ecological niches, such as wood beetles that infest timber structures or flies that thrive in conditions found in latrines, reflect living conditions in the past (Robinson 2001). Although the ecology of temperature-sensitive insects is not directly related to human activities, these insects can offer insight into palaeoclimatic conditions that may have impacted human agricultural activities or migration.

Insects can complement other temperature-sensitive proxies that have been used in palaeoecological studies, such as stable oxygen isotope measurements of annually layered ice (Grootes et al. 1993; Meese et al. 1997, Svensson et al. 2006),

palynological reconstructions of peat bogs and lake sediments (e.g. Barber et al. 2000), tree-ring inferred palaeotemperature records (e.g. Palmer and Xiong 2004), and stable isotope analysis of stalagmites and corals (Wang et al. 2001). Often, studies use a variety of data to draw conclusions about ancient climate.

The utility of insects, as with other archaeological and palaeological finds, depends upon their placement within a dependable and accurate chronological scale. Building a relative chronology of insect remains relies upon the site having a reliable stratigraphy, allowing changes through time to be documented. Absolute chronology further requires the judicious application of radiometric dating techniques that anchor the archaeological objects on a calendrical time scale. Radiocarbon dating, in which the concentration of a radioactive isotope of carbon (^{14}C) within an object is measured, is the dating method of choice for organic objects less than about 50,000 years old. Typically, objects associated with the insects, such as charcoal or other plant remains, have been thought to give more reliable dates than the insects themselves and these have been preferentially analyzed.

Radiocarbon dating of insect chitin is made possible through the use of accelerator mass spectrometry (AMS). This technique requires approximately 1 mg of carbon for a measurement; in the case of chitin, which is about 45% carbon by weight, over 2 mg of sample is needed. AMS can, however, also provide results on smaller amounts of carbon, ranging between 30 and 100 μg, and it is these smaller sample sizes that open up the possibilities for dating very small insect remains. A precision of approximately ±0.3% (about ±25–30 years) is now attainable in routine AMS dating of samples containing 0.7–1.0 mg of carbon (Bronk Ramsey et al. 2004b); however, increasing capabilities promise to extend this precision to smaller samples. Direct dating of insects is desirable because it removes any uncertainty of association between the insects and other dated objects, providing a more accurate placement of the insects upon a chronological scale.

3.2 Compound-Specific Radiocarbon Dating

Accurate radiocarbon dating of an archaeological object depends upon the removal of any carbonaceous contamination. Often the best method for purifying the object is to isolate in pure form a compound or substance known to be autochthonous to the object (Tripp and Hedges 2004). Libby and coworkers were the first to suggest that the isolation of protein components of bone and shell would allow for the measurement of more accurate radiocarbon dates (Berger et al. 1964). Because this work was reported prior to the AMS era, tens of grams of bones or kilograms of shell were required for the measurements. The dating of single compounds has become increasingly feasible because of the small sample size requirements of AMS (Currie et al. 1989; Stafford et al. 1991; Hedges 1995; Eglinton et al. 1996; van Klinken and Hedges 1998). Compound-specific radiocarbon dating has been applied to a number of ancient materials, such as amino acids from bone (van Klinken et al. 1994; Tripp et al. 2006), sterols from marine sediments (Smittenerg et al. 2002), and fatty acid residues from potsherds (Stott et al. 2001, 2003).

The radiocarbon dating of bone is undertaken effectively on a routine basis by isolating the high-molecular weight collagen, and this process removes any mineral or low-molecular weight protein contamination that has incorporated into the bone from the environment (Brown et al. 1988; Bronk Ramsey et al. 2004a). Isolation of single amino acids (Tripp et al. 2006) and tripeptides (van Klinken et al. 1994) has proved to be a useful pretreatment methodology for contaminated bone. 4-Hydroxyproline, in particular, has been proposed as a reliable proxy for radiocarbon dating of contaminated bone (Stafford et al. 1982). Because insect remains contain protein this approach could in theory lead to accurate radiocarbon dating, but no dates of purified insect protein have been reported.

Single compounds are typically isolated using preparative chromatography, either gas chromatography (GC) for the isolation of volatile compounds such as methylated fatty acids (Stott et al. 2001, 2003) or high performance liquid chromatography (HPLC) for nonvolatile components of archaeological materials (van Klinken et al. 1994; Smittenerg et al. 2002; Tripp et al. 2006). Preparative chromatography requires intensive sample handling procedures in order to prepare the samples for injection onto the column, isolate the desired compounds from the mobile phase after separation, and further prepare and transfer the compounds to the AMS for analysis. One approach to reduce sample handling is the direct connection of the separation system to the AMS, similar to the "hyphenated" techniques used for stable isotope analyses that connect a GC (Meier-Augenstein 1999) or HPLC (Thermo Electron Finnegan LC IsoLink – www.thermo.com/lcisolink) to an isotope ratio mass spectrometer. Bronk Ramsey and coworkers have reported the connection of analytical-scale gas chromatography to the gas ion source of the AMS at Oxford, with the result that separated compounds can be directly injected into the AMS (Bronk Ramsey and Hedges 1995; Bronk Ramsey et al. 2004c). This hyphenated GC-AMS approach allows for the analysis of further reduced sample sizes, though reported measurement errors become significantly higher at the sample sizes reported.

Sclerotized insect cuticles are composed of chitin covalently bound to proteins. Diagenetic processes can alter the structure of the proteins and introduce minerals into the insect exoskeleton altering the isotopic composition; hence, chitin, which is resistant to decay, is a likely candidate for compound-specific radiocarbon dating of insects. Chitin itself offers a number of other substances that could be isolated for radiocarbon dating: purified chitosan, D-glucosamine, or the *N*-acetyl group in the form of acetic acid. Tripp et al. (2004) have reported the isolation of chitosan (deacetylated chitin) for radiocarbon dating, and showed that this produced accurate radiocarbon dating results. D-glucosamine and the *N*-acetyl group has been purified and used for stable isotope analysis (Hodgins et al. 2001; Schimmelmann and DeNiro 1986), but not for radiocarbon dating. We discuss the specifics of pretreatment chemistry protocols in more detail below.

The main disadvantage of most compound-specific techniques is low yield of the desired compounds after pretreatment chemistry and separation procedures. Increased sample handling often leads to loss of products, meaning that an increased amount of the original artifact is needed in order to obtain the required mass of

carbon for AMS measurements. In addition, laboratory contamination can be introduced, particularly from chromatographic mobile phases if they contain organic components. Considerable care must be taken to deal with these issues during pretreatment method development. However, if a sample is highly contaminated then single-compound methods offer an important approach to obtaining accurate dates of insect chitin and a host of other materials.

3.3 Chitin Preservation and Sample Requirements

For accurate radiocarbon dating, both the chemical and isotopic integrity of the chitin must be preserved over the timescale being analyzed. Any diagenetic processes that occur must not alter the radiocarbon content of the chitin, and contamination that introduces carbon of a different age than the object could also alter the date. If chitin is to be used as a substrate for molecular measurements in archaeological and palaeoenvironmental studies, it must be able to withstand the chemical assault of the environment and still be isolated in large enough quantities for the required measurements.

Another issue to consider is the inherent radiocarbon concentration in the insect, which is dependent not just on the age but on the environment. Radiocarbon concentrations can be significantly affected by the presence of a large concentration of limestone-derived carbonate in the local water; geological limestone is considered to be radiocarbon "dead" because it contains no ^{14}C. The hard water effect, as this is called, is usually the result of water drainage over limestone formations into a body of water (Shotton 1972; Marchenko et al. 1989). The hard water effect leads to the dilution of the ^{14}C concentration in the water, and therefore dates on organisms such as mollusks that incorporate the carbonate into their exoskeletons, or aquatic plants that use dissolved CO_2 for photosynthesis, can appear older than their actual age. Bulk sediment from lake bottoms can also sometimes exhibit a hard water effect. Insect dietary habits have been reported to produce additional observed dating errors (Fallu et al. 2004). While each species of insect tends to have a fairly restricted diet, insects as a class consume a wide array of food. Particular patterns of consumption, including ingestion of detritus, old wood, or other food that contains older carbon has the potential to alter the measured radiocarbon age. These effects have yet to be systematically evaluated; however, for some aquatic environments, it may be wise to carefully consider the food-web and the origin of carbon within the water catchment. Unfortunately, pretreatment chemistry can do nothing to correct the environmental effects, and these have been blamed for dating inaccuracies at a number of sites.

The preservation of chitin seems to depend less on the time since the death of the organism and more on the burial environment (Stankiewicz et al. 1997b). Preservation of insect cuticle is promoted by rapid burial in anaerobic conditions such as those found in fine, silty sediments, lake beds, or peat bogs; or in cold or arid environments (Miller et al. 1993; Robinson 2001). Chitin has been detected in arthropod fossils as old as 25 million years (Stankiewicz et al. 1997b), though its

quantification is more challenging (Flannery et al. 2001). Intact insect chitin has been observed in insects preserved in amber (Stankiewicz et al. 1998) and in tar deposits (Stankiewicz et al. 1997a); however, biomolecular preservation even in these conditions is not universal. It has been noted (Stankiewicz et al. 1997a) that even in cases where the cuticle appears to be well-preserved, significant chemical alteration of the chitin may have occurred.

3.4 Pretreatment Methods

The purpose of the pretreatment protocol for radiocarbon dating of insect chitin is to remove any allochthonous carbon from the sample. The presence of carbon older or younger than the object to be dated can considerably alter the measured radiocarbon date, rendering questionable any site interpretation based upon those dates. Sources of contaminating carbon include substances from the burial environment as well as any organic compounds introduced during the isolation, recovery, cleaning and purification of the archaeological object. Insects in reference collections are often glued to cards or stored in alcohol, introducing additional sources of contamination. Care must be taken to remove contaminating environmental carbon without introducing significant amounts of modern carbon into the sample in the laboratory.

The standard procedure for the recovery of macroscopic insect remains such as Coleoptera from archaeological contexts involves sieving the sediment, followed by flotation of the insect fragments in paraffin (Coope and Osborne 1967). The insects are then washed in water and alcohol to remove the paraffin. Complete removal of the paraffin prior to taxonomic identification is not necessary, but it is essential that all of the paraffin be removed prior to radiocarbon dating since paraffin contains carbon. Because paraffin is derived from petroleum it contains "dead" carbon and therefore a date measured on a contaminated insect sample would appear older than it should.

Contamination from the environment typically consists of soil carbonates, which are removed by washing with mineral acid such as HCl, and proteinaceous substances, which are hydrolyzed in hydroxide base and washed away with water. Any suspected contamination by lipids or other nonpolar substances is removed by extracting the object with organic solvents, which must then be removed by thorough drying. Paraffin contamination from the flotation process can be removed by careful repeated washing with volatile organic solvents, and indeed many reported pretreatment procedures for the radiocarbon dating of insects include solvent extraction steps.

Unfortunately, only a handful of papers have been published that report radiocarbon dates of chitinous organisms (Table 3.1, References), and not all of these explain in detail the pretreatment chemistry that was used on the remains. Table 3.1 outlines the pretreatment methods described in the literature for Coleopteran remains. Assumptions about pretreatment protocol were made when experimental details were lacking, and these assumptions are explained in the footnotes of the table.

The first four papers listed in Table 3.1 (Elias et al. 1991; Törnqvist et al. 1992; Cong et al. 1996; Walker et al. 2001) use a combination of standard pretreatment

Table 3.1 Radiocarbon dating pretreatment protocols on subfossil Coleoptera

Study	Purified material	Protocol
Elias et al. (1991)	Bulk insect	• Standard treatment[a] • Pentane wash • Hot water wash
Törnqvist et al. (1992)	Bulk insect	• 4% HCl (50°C)[b] • 0.5% NaOH (20°C) • 4% HCl (20°C)
Cong et al. (1996)	Bulk insect	• Standard treatment[c]
Walker et al. (2001)	Bulk insect	• 2 M HCl • Water wash
Hodgins et al. (2001)	Glucosamine•HCl	• Water wash • Extraction with methanol, 2:1 • Methanol:chloroform, then chloroform • 1 N HCl (rt, 3 h), followed by water wash • Protein digestion with 1 N NaOH (100°C, 3–12 h), and in some cases Proteinase K, followed by water wash • 7 N HCl (100°C, 4 h) • Anion exchange chromatography
Tripp et al. (2004)	Chitosan•HCl	• Extraction with acetone, methylene chloride, then acetone • 0.5 M HCl (rt, 3 days), then water wash • Deacetylation with 50% NaOH (120°C, 30 min) • Acidified to pH 5, filtered • Filtrate acidified to pH < 1, solids filtered and collected

[a] The paper specified "standard chemical treatments", which can be assumed to be an acid wash or acid-alkali-acid treatment

[b] No reaction times were specified

[c] No pretreatment protocol was reported, but a standard acid wash or acid-alkali-acid treatment can probably be assumed

chemistry to purify the insects. Organic solvents wash any lipids, paraffin, or other nonpolar contaminants from the insect remains. Acid washes remove carbonate contaminants, while treatment with base removes protein. Basic treatment will also deacetylate the chitin to chitosan, though under the conditions used by Törnqvist et al. the extent of this reaction is probably quite low.

Hodgins et al. (2001) and Tripp et al. (2004) took a more rigorous approach to purification of chitin, attempting to isolate a well-defined single compound for analysis. Hodgins et al. (2001) treated Coleoptera remains with organic solvents and dilute acid, and then digested the protein with either 1 N NaOH at high temperature or with Proteinase K, an enzyme that promotes protein degradation. The basic treatment would also have the effect of deacetylating the chitin to form chitosan. After washing the recovered residue, the chitin was depolymerized by treatment with 7 N HCl at high temperature. High-pH anion exchange chromatography

using 200 mM NaOH as the mobile phase was used to purify glucosamine•HCl. Figure 3.1 shows the series of reactions leading to isolation of the monomer. This study highlighted one of the main problems often noted with compound-specific isotopic analysis: low yield. Only 5% of the glucosamine could be recovered using this procedure, and not enough of the monomer could be reliably isolated for

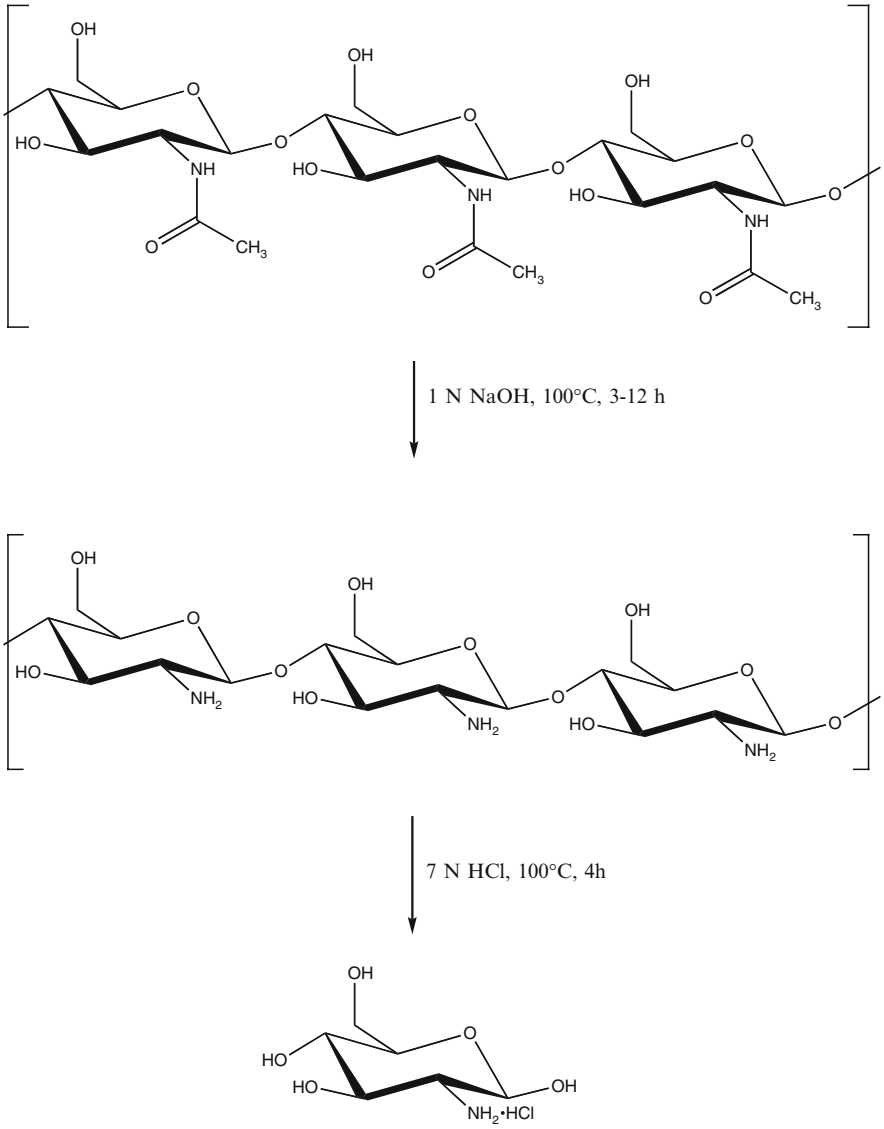

Fig. 3.1 Isolation of glucosamine•HCl. Treatment of the sample with sodium hydroxide hydrolyzes the amide groups (along with any protein that is present) to form chitosan. Strong acid cleaves the glycosidic linkages to form glucosamine•HCl (Hodgins et al. 2001)

radiocarbon dating. The authors suggested that the main fault in the procedure lay in the hydrolysis step, and proposed that further work ought to focus on refining this step, perhaps through the use of chitinase enzymolysis in place of acidic hydrolysis.

Tripp et al. (2004) isolated chitosan•HCl from Coleoptera remains via the reactions outlined in Fig. 3.2; this protocol mirrors the industrial purification of chitin

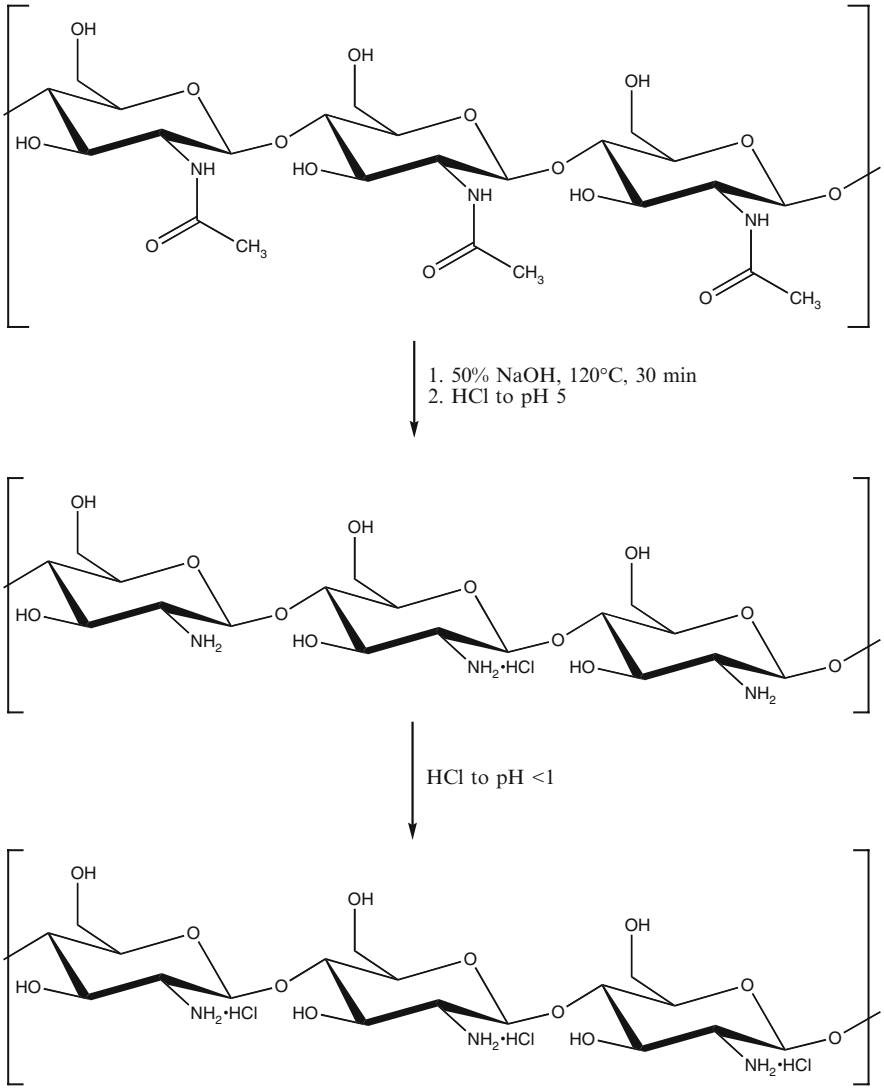

Fig. 3.2 Deacetylation of chitin and isolation of chitosan•HCl. Strong base hydrolyzes the amide bonds and the weakly acidic conditions enable solution of the deacetylated chain in water. Further acidification of the solution results in multiple charges forming along the chitosan backbone and precipitation of the polymer from aqueous solution (Tripp et al. 2004)

as described by Roberts (1992). Because the carbohydrate backbone is highly stable in alkaline conditions, a rigorous deproteinization/dealkylation step using strong base produces chitosan. Making the solution weakly acidic promotes its aqueous solubility, and once the chitosan is in solution any residual material can be removed by filtration. Addition of strong acid creates multiple charges along the chitosan chain, precipitating it from solution and facilitating its collection by filtration. The purified chitosan•HCl was then subjected to radiocarbon dating. Again, the main problem with this procedure is the yield; only 15% of the original mass could be recovered, meaning that a substantial number of insect exoskeletons must be collected in order to utilize this pretreatment protocol. Future development of pretreatment chemistry should focus on the improved yield of these well-characterized compounds. Only then can these procedures be reliably and routinely applied to insect samples at sites with lower abundance of insect remains.

Because of the low yield, compound-specific dating has not yet been practical for microscopic insect remains such as chironomids. Most published examples of the AMS dating of chironomid head capsules (Jones et al. 1993; Snyder et al. 1994; Child and Werner 1999) use the following pretreatment protocol: dried lake sediment containing the chironomid remains is heated in 10% NaOH solution, sieved and rinsed in distilled water; the head capsules are then picked individually from the sediment under a microscope and subjected to acidic treatment to remove any carbonate contamination. Fallu et al. (2004) altered this only in their choice of base, using 5% KOH instead of 10% NaOH. Each head capsule was squeezed with tweezers to maximize removal of organic residue trapped inside. The hundreds, or in some cases several thousand, head capsules isolated in this manner provide barely enough carbon for a single AMS measurement, and therefore any pretreatment protocol that results in a significant loss of mass cannot be applied to these precious samples. Protocols with improved yield may make compound-specific dating of these samples feasible in the future.

3.5 Radiocarbon Dating Using Accelerator Mass Spectrometry

A perusal of the literature shows that there is some debate regarding the reliability of insect chitin as a substrate for AMS dating, primarily related to an often-observed offset between AMS dates on bulk sediments compared to the directly-dated insects contained within them. Typically, insect remains appear younger than the surrounding sediment, an observation ascribed alternately to insect ecology, laboratory contamination during pretreatment, or the presence of “old” carbon in the bulk sediment in the form of carbonate or coal. Occasionally the insects and sediment provide comparable dates, though even in these cases an alternate material, such as plant macrofossils, may be deemed more reliable (Jones et al. 1993; Walker et al. 2001).

Elias et al. (1991) dated a series of moss, wood and Coleoptera macrofossils from a core drilled at Lake Emma in southwest Colorado using both AMS and conventional dating techniques (Table 3.2). The wood and insect samples dated

Table 3.2 Radiocarbon dates from Lake Emma, Colorado (Elias et al. 1991)

Stratigraphic depth (cm)	Material dated	Radiocarbon age (y BP)
81	Wood	5,440 ± 100
96	Wood	6,670 ± 70
160	Wood	8,625 ± 90[a]
175	Wood	9,220 ± 120
170–180	Wood	9,400 ± 70[a]
	Moss	12,900 ± 200
195–205	Insect	8,200 ± 160[a]
	Moss	13,580 ± 200
225–235	Insect	8,940 ± 85[a]
	Insect	9,020 ± 80[a]
	Moss	14,130 ± 150
	Moss	14,900 ± 250
	Moss	14,940 ± 140

[a] AMS dates. Others are conventional

consistently younger than the moss, though no level contained a date from both wood and insect samples, making a direct comparison between these two materials impossible. However, insect exoskeletons at lower stratigraphic levels dated younger than wood at higher levels. The authors discount a hard water effect to explain the unusually old dates for the moss, and indicate that no other proposed explanation seemed plausible. The older wood dates may be influenced by the fact that krummholz trees, such as those used for the dates in this study, can live for hundreds of years and therefore wood derived from the center of the timber may be several hundred years old at the time of the death of the tree. Also, the woody fragments can last for an extended time in the landscape, so their deposition in the lake may have occurred centuries after the death of the tree. Thus, the authors conclude, the insect dates are probably the most accurate for this site because insects live for only a short time and would have rapidly decayed had they not been deposited in the lake sediment shortly after death.

Törnqvist et al. (1992) included one AMS date of Coleoptera fragments and two dates of samples that combined Coleoptera with plant macrofossils in their study of cores from the Leerdam-Gorkum area in the Rhine-Meuse delta of the Netherlands (Table 3.3). In addition, bulk sediment, sediment with modern roots removed, and various plant macrofossils were also dated. The insect samples were considerably smaller than the bulk sediment samples, but even so, the measured radiocarbon ages were identical within statistical errors within the same sediment sample, and calibrated dates show significant overlap (Fig. 3.3). The authors conclude that macrofossil dating can be highly accurate compared to bulk sediment dates, because it can eliminate hard water effects and other bulk contamination. Along the same lines, Cong et al. (1996) used AMS dates on Coleoptera and wood to date a 40,000-year-old climatic change observed in their study of fossil beetle assemblages from Titusville, Pennsylvania. Only two insect dates were measured, and they fit well into the overall chronology of the site.

Table 3.3 AMS radiocarbon dates of bulk sediment samples and insect macrofossils from Leerdam-Gorkum area, The Netherlands (Törnqvist et al. 1992)

Sample no.[a]	Dated material	Mass (mg C)	Radiocarbon age (y BP)
8a	*Phragmites* peat	2.84	5,090 ± 50
8b	*Phragmites* peat with living roots removed	2.99	4,940 ± 70
8c	Fragments of Coleoptera and plant macrofossils	0.39	4,990 ± 70
12a	Clayey *Phragmites* peat	1.04	5,320 ± 60
12b	Fragments of Coleoptera and plant macrofossils	0.87	5,230 ± 50
13a	Clayey *Phragmites* peat	3.09	5,440 ± 50
13b	*Scirpus lacustris* nuts	1.15	5,240 ± 70
13c	Fragments of Coleoptera	0.59	5,330 ± 70

[a] Sample numbers assigned by Törnqvist et al.

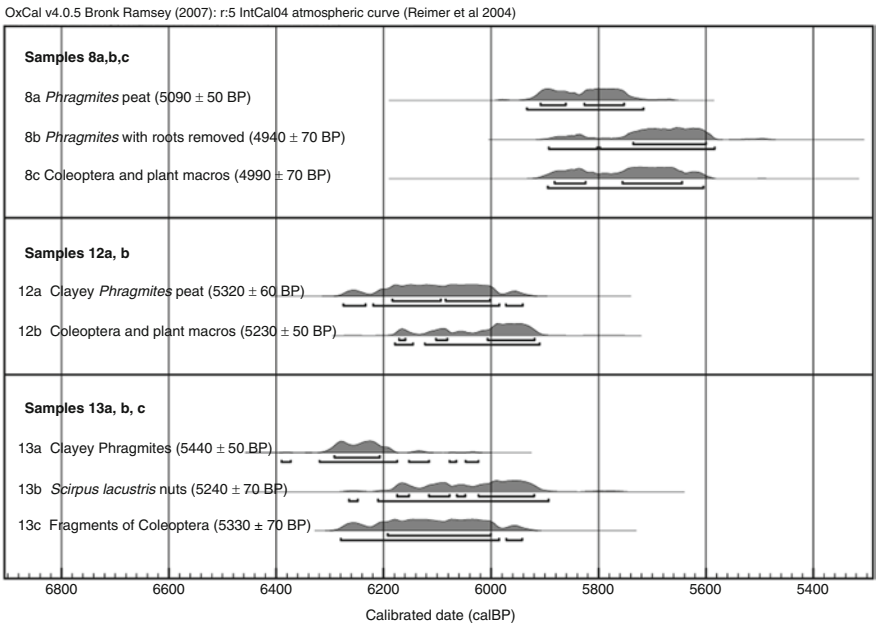

Fig. 3.3 Calibrated (using OxCal, Bronk Ramsey 2001) AMS radiocarbon dates of bulk sediment samples and macrofossils from Leerdam-Gorkum area, The Netherlands (Törnqvist et al. 1992)

Walker et al. (2001) measured a number of species-specific Coleoptera dates and compared them to plant macrofossils along with humic (base-soluble) and humin (base-insoluble) fractions of late Glacial sediments from Britain. Not only did the insect dates consistently measure younger than the other materials, the dates failed to follow a regular stratigraphic pattern whereby insects from deeper sediments should produce older dates. Figure 3.4 compares dates of plant macrofossils from

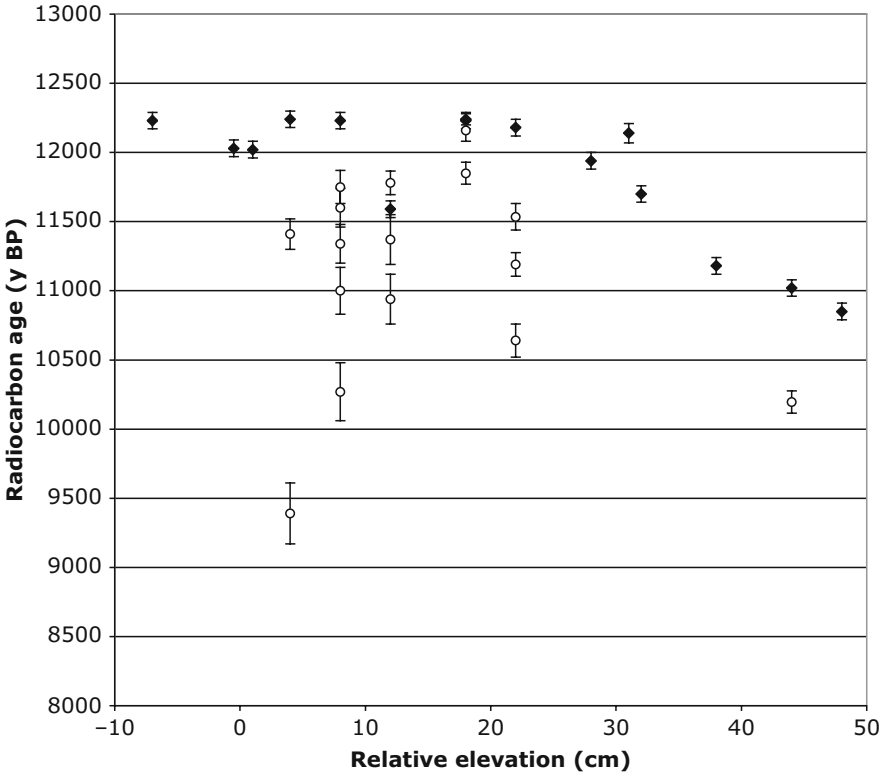

Fig. 3.4 AMS radiocarbon ages of plant microfossils (◆) and insect remains (O) from St. Bees, Britain (data from Walker et al. 2001). The error bars show 1σ errors

St. Bees in northwest England with stratigraphically correlated Coleoptera remains from the same site. Clearly, the plant macrofossils follow a general trend toward younger dates at shallower deposits while the insect dates are significantly scattered and generally younger than the plants. The humic and humin materials tended to follow a similar trend to the plant macrofossils. The error in the insect dates could be due in part to sample size; while both macrofossil materials had high carbon recovery (ranging from 40% to 54% by weight), plant macrofossils were regularly available in sufficient quantity to prepare graphite targets containing over 1 mg of carbon, while the insects provided only 0.15–0.5 mg per target. The authors note that a similar offset in dating was seen by Elias et al. (1991), but in this case Walker et al. conclude that the plant macrofossils are more accurate, given that they follow stratigraphic trends, while the insect dates are problematic. Another explanation for the offset, besides the sample size issue, is the possible occurrence of post-depositional chemical changes to the chitin or associated proteins that allow the incorporation of younger carbon.

These observations were further reinforced by dates on whole insects from the St. Bees site in England, measured by Hodgins et al. (2001). They reported a similar

offset between plant macrofossils and various species of insects, though in this case the insect dates did follow a stratigraphic trend. Attempts to solve this problem by isolating glucosamine•HCl for compound-specific radiocarbon dating proved unsuccessful due to the low yield of the hydrolysis reaction and chromatographic purification (Fig. 3.1). However, a comparison of pretreatment methods demonstrated that the offset could be partially removed by subjecting the insects to standard pretreatment protocols (Table 3.4). Untreated insects gave a date 300 years younger than associated peat, while all attempted pretreatment protocols gave dates identical to the peat within errors. The authors suggest that in many cases further purification of the chitin should provide complete resolution of the offset, implying that the problem lies with the chemistry of the chitin and/or the pretreatment protocol and is not an unresolvable issue inherent to the dating of insect remains.

Tripp et al. (2004) further explored the pretreatment of the insect remains with attempts to isolate chitosan•HCl from Coleoptera obtained from Roman-era settlements in Britain. A comparison of two pretreatment methods, the first a simple solvent wash followed by acid treatment, and the second the base-promoted deacetylation of chitin followed by isolation of chitosan•HCl (Fig. 3.2), provided statistically identical dates of 1851 ± 23 and 1830 ± 50 y BP, respectively, for Coleoptera remains from the Priors Gate site in Cambridgeshire, England. These dates are fully in line with archaeological expectations for this site. Additional dates from the site of Godmanchester compared Coleoptera treated only with a solvent wash and aqueous acid to waterlogged and carbonized seeds found in the same deposit. These dates (Table 3.5) are statistically indistinguishable from each other, indicating that the offset seen in a number of sites is not universal and that simple pretreatment protocols may be sufficient in many cases to obtain accurate dates.

AMS dates on chironomid remains tend to follow the same patterns as those measured for Coleoptera in which the insects routinely date younger than the

Table 3.4 Oxford AMS dates on *Otiorhynchus nodosus* from Redkirk Point, UK showing differences between standard insect pretreatment protocols (Hodgins et al. 2001)

Pretreatment protocol	Radiocarbon date (y BP)
Untreated	11,390 ± 70
Solvent wash	11,670 ± 65
Solvent wash, then acid	11,665 ± 65
Solvent wash, then acid/alkali/acid	11,645 ± 119
Redkirk point peat[a]	11,690 ± 65

[a] Measured for comparison with insect dates

Table 3.5 AMS dates for macrofossil samples from Godmanchester, UK (Tripp et al. 2004)

Sample type	AMS date (y BP)
Coleoptera	1,764 ± 29
Waterlogged seeds	1,690 ± 32
Carbonized seeds	1,650 ± 45

surrounding sediment. Jones et al. (1993) observed an offset of 400 to 1,300 years between chironomid dates and bulk sediment from a Scottish site, as well as an inversion in the chironomid dates relative to stratigraphy. Due to this offset, the authors conclude that AMS dating of chironomid remains is not recommended. Nevertheless, the following year Snyder et al. (1994) reported an even larger offset of nearly 9,000 years between their one chironomid date and surrounding lake sediment (Table 3.6). Associated plant macrofossils in the same sediment provided a date similar to that measured for the insects, and at other depths in the core the plant samples dated consistently younger than bulk sediment. The authors concluded that due to the presence of coal in the sediment the insect and plant macrofossil dates were more accurate than those measured for bulk sediment. Coal, which contains "dead" carbon, would cause the sediment to date older than its actual age. The process of isolating the chironomid remains would remove the coal and therefore the insects would provide a better estimate of the true age.

Child and Werner (1999) observed no offset between the chironomid and bulk sediment dates from the Wonder Lake site in Alaska, but both provided older dates than the plant macrofossils. The bulk sediment and chironomid dates did not correlate with dates for felsic tephras present in the sediment, while the plant terrestrial dates agreed well. They concluded that the dates of plant macrofossils from terrestrial species were the most accurate due to hard water conditions in the lake that would affect both the bulk sediment and the aquatic chironomids. In contrast to Snyder et al. (1994) they observed no coal in the sediment that could affect the dates of the bulk sediment. The terrestrial plant remains that they measured by AMS would not be affected by carbonates from the lake. Fallu et al. (2004) explained their observed offset (Table 3.7) with a series of arguments about chironomid feeding habits. They supposed that the chironomids would not feed on lake detritus

Table 3.6 AMS dates of insect remains and associated materials from Linnévatnet, Spitsbergen, Svalbard (Snyder et al. 1994)

Depth (cm)	Sample type	AMS date (y BP)
230	Terrestrial plant macrofossils	3,990 ± 55
227–233	Aquatic insects (chironomidae)	5,100 ± 125
223–233	Bulk sediment	13,900 ± 95

Table 3.7 Selected AMS radiocarbon dates from chironomids and bulk sediments, Lake K2, northern Quebec (Fallu et al. 2004)

Depth (cm)	Material	Number of head capsules	AMS date (y BP)
19–20	Bulk sediment		3,960 ± 60
19–21	Chironomids	1,309	1,230 ± 53
46–47	Bulk sediment		4,790 ± 54
46–48	Chironomids	2,445	3,390 ± 61
60–61	Bulk sediment		5,470 ± 60
59–60	Chironomids	1,900	4,820 ± 68
83–34	Bulk sediment		6,140 ± 60
84–85	Chironomids	2,020	5,880 ± 170

if higher-quality, fresh terrestrial food was available, and therefore the insects would not be affected by the hard water effect that was seen in the sediment. They thus concluded that the insect dates were the most accurate for the Lake K2 site in Québec. Currently, data sets at each site require individual explanations and no general rule for interpreting insect dates can be stated.

Taken together, then, an offset between radiocarbon ages of insects and the associated sediment and other materials has often been reported at sites worldwide and dating to different periods. The cause of this offset, in which the insect remains tend to give younger dates, has been explained in a number of means, but tends to vary on site-specific grounds; in some cases the offset is due to hard water effects or the presence of coal in the sediment and in others due to contamination in the insects. For this reason, insects are still routinely dated in conjunction with other materials, and further developments will be required before reliable dating of insects can be demonstrated. Correct selection of pretreatment protocols can sometimes reduce or eliminate the observed offset.

3.6 Future Perspectives

High quality chronological sequences are vital for Quaternary scientists to assess rates of change within ecosystems and understand associated feedbacks caused by environmental forcing. Lake sediments are often used for producing detailed records of past environmental and ecosystem changes, but the principal limitation of interpreting these sedimentary archives is in developing reliable chronological frameworks. Dating lake sediments, swamps and peats can sometimes be difficult because one is often unsure of how the material one is dating arrived within the site. McGlone and Wilmshurst (1999), for example, have shown that there are often significant contaminating influences within palaeoenvironmental sites that influence accurate dating, with old carbon from burnt forest trees, humic sources and dissolved carbonate rocks entering lakes and bogs, and material derived from younger carbon sources, such as roots, the main culprits. Developing a reliable method for dating insect chitin (e.g. Tripp et al. 2004), is therefore an attractive addition to the range of potential dateable materials in such sites.

A direct radiocarbon measurement, as opposed to an indirect correlation with a dated item, is always to be preferred in archaeology, or indeed any discipline. The direct radiocarbon dating of insect chitin offers the most significant potential benefits over bulk sediments or plant materials. The presence and absence of temperature-dependent insects is clearly of interest in climatic and environmental reconstruction, and if the insect chitin itself can be directly dated it is possible to fix an age range. One example of the type of work that could be undertaken with profit would be to examine the rise in temperatures at the end of the Last Glacial, and its timing (Walker et al. 2001). This warming, which initiated the Late Glacial Interstadial, is important for understanding the time scale and extent of rapid climate change and its global impacts in ancient human activities. The recolonization

of Europe and the British Isles by people and animals, for example, is thought likely to have been influenced by climatic factors. Local proxy climatic data, in the form of fossil beetles within peat bogs, suggest that in north-west Europe warming may have begun earlier than the time when it is first registered in the Greenland deep ice-cores (Walker et al. 2003; Blockley et al. 2004), with implications for animal communities and recolonization of increasingly northerly locales. The chronologies developed for these peat and swamp sequences are problematic, however, for the reasons described above, and so it has been difficult to reach firm conclusions without a strong framework. Direct dates of temperature-dependent insect samples could contribute to a more refined chronology for such sequences. In tandem with other methods, such as tephra-based studies, correlations with other proxies like ice and marine cores, as well as other climate records, an improved chronology could result. Further work is required to bring this type of application to fruition. This chapter has shown that considerable progress towards direct chitin dating has already been made.

References

Barber KE, Maddy D, Rose N, Stevenson AC, Stoneman R, Thompson R (2000) Replicated proxy-climate signals over the last 2000 yr from two distant UK peat bogs: new evidence for regional palaeoclimate teleconnections. Quatern Sci Rev 19:481–487

Berger R, Horney AG, Libby WF (1964) Radiocarbon dating of bone and shell from their organic components. Science 144:999–1001

Blockley SPE, Lowe JJ, Walker JJ, Asioli A, Trincardi F, Coope GR, Donahue RE, Pollard AM (2004) Bayesian analysis of radiocarbon chronologies: examples from the European Lateglacial. J Quatern Sci 19:159–175

Blumenthal HJ, Roseman S (1957) Quantitative estimation of chitin in fungi. J Bacteriol 74:222–224

Bronk Ramsey C (2001) Development of the radiocarbon calibration program OxCal. Radiocarbon 43:355–363

Bronk Ramsey C, Hedges REM (1995) Radiocarbon with gas chromatography. Radiocarbon 37:711–716

Bronk Ramsey C, Higham TFG, Bowles A, Hedges R (2004a) Improvements to the pretreatment of bone at Oxford. Radiocarbon 46:155–163

Bronk Ramsey C, Higham TFG, Leach P (2004b) Towards high precision AMS: progress and limitations. Radiocarbon 46:17–24

Bronk Ramsey C, Ditchfield P, Humm M, Leach P (2004c) Using a gas ion source for radiocarbon AMS and GC-AMS. Radiocarbon 46:25–32

Brown TA, Nelson DE, Vogel JS, Southon JR (1988) Improved collagen extraction by modified Longin method. Radiocarbon 30:171–177

Child JK, Werner A (1999) Evidence for a hardwater radiocarbon dating effect, Wonder Lake, Denali National Park and Preserve, Alaska, U.S.A. Géogr Phys Quatern 53:407–411

Cong S, Ashworth AC, Schwert DP (1996) Fossil beetle evidence for a short warm interval near 40,000 yr B.P. at Titusville, Pennsylvania. Quatern Res 45:216–225

Coope GR, Osborne PJ (1967) Report on the Coleopterous fauna of the Roman well at Barnsley Park, Glocestershire. Trans Bristol Gloucestershire Archaeol Soc 86:84–87

Currie LA, Stafford TW, Sheffield AE, Klouda GA, Wise SA, Fletcher RA (1989) Microchemical and molecular dating. Radiocarbon 31:448–463

Eglinton TI, Aluwihare LI, Bauer JE, Druffel ERM, McNichol AP (1996) Gas chromatographic isolation of individual compounds from complex matrices for radiocarbon dating. Anal Chem 68:904–912

Elias SA (1994) Quaternary insects and their environments. Smithsonian Institution Press, Washington

Elias SA, Carrara PE, Toolin LJ, Jull AJT (1991) Revised age of deglaciation of Lake Emma based on new radiocarbon and macrofossil analyses. Quatern Res 36:307–321

Fallu MA, Pienitz R, Walker IR, Overpeck J (2004) AMS ^{14}C dating of tundra lake sediments using chironomid head capsules. J Paleolimnol 31:11–22

Flannery MB, Stott AW, Briggs DEG, Evershed RP (2001) Chitin in the fossil record: identification and quantification of D-glucosamine. Org Geochem 32:745–754

Grootes PM, Stuiver M, White JWC, Johnsen SJ, Jouzel J (1993) Comparison of oxygen isotope records from the GISP2 and GRIP Greenland ice cores. Nature 366:552–554

Hedges REM (1995) Radiocarbon dating by accelerator mass spectrometry. In: McGovern PE (ed) Science in archaeology: a review. Amer J Archaeol 99:105–108

Hodgins GWL, Thorpe JL, Coope GR, Hedges REM (2001) Protocol development for purification and characterization of sub-fossil insect chitin for stable isotopic analysis and radiocarbon dating. Radiocarbon 43:199–208

Jones VJ, Battarbee RW, Hedges REM (1993) The use of chironomid remains for AMS ^{14}C dating of lake sediments. Holocene 3:161–163

Marchenko E, Srdoc D, Golubic S, Pezdic J, Head MJ (1989) Carbon uptake in aquatic plants deduced from their natural 13C and 14C content. Radiocarbon 31:785–794

McGlone MS, Wilmshurst JM (1999) Dating initial Maori environmental impact in New Zealand. Quatern Int 59:5–16

Meese DA, Gow AJ, Alley RB, Zielinski GA, Grootes PM, Ram M, Taylor KC, Mayewski PA, Bolzan JF (1997) The Greenland Ice Sheet Project 2 depth-age scales: methods and results. J Geophys Res 102:26411–26423

Meier-Augenstein W (1999) Applied gas chromatography coupled to isotope ratio mass spectrometry. J Chromatogr A 842:351–371

Miller RF, Voss-Foucart MF, Toussaint C, Jeuniaux C (1993) Chitin preservation in Quaternary Coleoptera: preliminary results. Palaeogeogr Palaeoclimatol Palaeoecol 103:133–140

Palmer JG, Xiong L (2004) New Zealand climate over the last 500 years reconstructed from *Libocedrus bidwillii* Hook. f. tree-ring chronologies. Holocene 14:282–289

Peters W (1972) Occurrence of chitin in Mollusca. Comp Biochem Physiol 41B:541–550

Roberts GAF (1992) Chitin chemistry. Macmillan, Hong Kong, Chapter 2

Robinson M (2001) Insects as palaeoenvironmental indicators. In: Brothwell DR, Pollard AM (eds) Handbook of archaeological sciences. Wiley, Chichester

Schimmelmann A, DeNiro MJ (1986) Stable isotopic studies on chitin, measurements on chitin/chitosan isolates and D-glucosamine hydrochloride from chitin. In: Muzzarelli R, Jeuniaux C, Goody GW (eds) Chitin in nature and technology. Plenum, New York

Schmidt M (2000) Radiocarbon dating New Zealand prehistory using marine shell. Hadrian Books, Oxford

Shotton FW (1972) An example of hard-water error in radiocarbon dating of vegetable matter. Nature 240:460–461

Smittenerg RH, Hopmans EC, Schouten S, Sinninghe Damsté JS (2002) Rapid isolation of biomarkers for compound specific radiocarbon dating using high-performance liquid chromatography and flow injection analysis–atmospheric pressure chemical ionisation mass spectrometry. J Chromatogr A 978:129–140

Snyder JA, Miller GH, Werner A, Jull AJT, Stafford TW Jr (1994) AMS-radiocarbon dating of organic-poor lake sediment, an example form Linnévatnet, Spitsbergen, Svalbard. Holocene 4:413–421

Stafford TW Jr, Duhamel RC, Haynes CV Jr, Brendel K (1982) Isolation of proline and hydroxyproline from fossil bone. Life Sci 31:931–938

Stafford TW Jr, Hare PE, Currie L, Jull AJT, Donahue DJ (1991) Accelerator Radiocarbon Dating at the Molecular Level. J Archaeol Sci 18:35–72

Stankiewicz BA, Briggs DEG, Evershed RP, Duncan IJ (1997a) Chemical preservation of insect cuticle from the Pleistocene asphalt deposits of California, USA. Geochim Cosmochim Acta 61:2247–2252

Stankiewicz BA, Briggs DEG, Evershed RP, Flannery MB, Wuttke M (1997b) Preservation of chitin in 25-million-year-old fossils. Science 276:1541–1543

Stankiewicz BA, Poinar HN, Briggs DEG, Evershed RP, Poinar GO Jr (1998) Chemical preservation of plants and insects in natural resins. Proc R Soc Lond B 265:641–647

Stott AW, Berstan R, Evershed P, Hedges REM, Bronk Ramsey C, Humm MJ (2001) Radiocarbon dating of single compounds isolated from pottery cooking vessel residues. Radiocarbon 43:191–197

Stott AW, Berstan R, Evershed RP, Bronk-Ramsey C, Hedges REM, Humm MJ (2003) Direct dating of archaeological pottery by compound-specific ^{14}C analysis of preserved lipids. J Archaeol Sci 75:5037–5045

Svensson A, Andersen KK, Bigler M, Clausen HB, Dahl-Jensen D, Davies SM, Johnsen SJ, Muscheler R, Rasmussen SO, Rothlisberger R, Steffensen JP, Vinther BM (2006) The Greenland Ice core chronology 2005, 15–42 ka. Part 2: comparison to other records. Quatern Sci Rev 25:3258–3267

Törnqvist TE, de Jong AFM, Oosterbaan WA, van der Borg K (1992) Accurate dating of organic deposits by AMS ^{14}C measurement of macrofossils. Radiocarbon 34:566–577

Tripp JA, Hedges REM (2004) Single-compound isotopic analysis of organic materials in archaeology. LC GC Eur 17:358–364

Tripp JA, Higham TFG, Hedges REM (2004) A pretreatment procedure for the AMS radiocarbon dating of subfossil insect remains. Radiocarbon 46:147–154

Tripp JA, McCullagh JSO, Hedges REM (2006) Preparative separation of underivatized amino acids for compound-specific stable isotope analysis and radiocarbon dating of hydrolyzed bone collagen. J Sep Sci 29:41–48

van Klinken GJ, Hedges REM (1998) Chemistry strategies for organic ^{14}C samples. Radiocarbon 40:51–56

van Klinken GJ, Bowles AD, Hedges REM (1994) Radiocarbon dating of peptides isolated from contaminated fossil bone collagen by collagenase digestion and reversed-phase chromatography. Geochim Cosmochim Acta 58:2543–2551

Walker MJC, Bryant C, Coope GR, Harkness DD, Lowe JJ, Scott EM (2001) Towards a radiocarbon chronology of the late-glacial: sample selection strategies. Radiocarbon 43:1007–1019

Walker MJC, Coope GR, Sheldrick C, Turney CSM, Low JJ, Blockley SPE, Harkness DD (2003) Devensian Lateglacial environmental changes in Britain: a multi-proxy environmental record from Llanilid, South Wales, UK. Quatern Sci Rev 22:475–520

Wang YJ, Cheng H, Edwards RL, An ZS, Wu JY, Shen C-C, Dorale JA (2001) A high-resolution absolute-dated Late Pleistocene monsoon record from Hulu Cave, China. Science 294:2345–48

Chapter 4
Carbon, Nitrogen and Oxygen Stable Isotope Ratios in Chitin

Arndt Schimmelmann

Contents

Abstract Stable isotope ratios in chitin are firmly imprinted during biopolymer biosynthesis and reflect dietary, metabolic, and environmental influences. Chitin is a chemically complex amino sugar biopolymer that also includes non-amino-sugar moieties with contrasting isotopic compositions. Reproducible N, C, O-stable isotope determinations should rely on a chemically purified chitin substrate with limited non-amino-sugar contributions. Insecta, Crustacea and Merostomata are not distinguished by systematic isotopic differences. δ^{13}C, δ^{15}N and δ^{18}O values of arthropod chitins show a few ‰ variance within a single individual (lobster), among individuals within a population, along ecdysis (i.e., molting), and age, as long as growth is not accompanied by strong dietary or behavioral changes. Marine arthropod chitin averages 9.1‰ more ^{13}C-enriched than terrestrial chitin. δ^{15}N values of chitin become more positive with increasing trophic level. Although $\delta^{18}O_{chitin}$ from a large array of aquatic crustacean species across many ecosystems expresses only weak overall correlation with $\delta^{18}O_{water}$ and no clear dependence on temperature,

A. Schimmelmann (✉)
Department of Geological Sciences, Indiana University, 1001 East 10th Street, Bloomington, IN 47405-1405, USA
e-mail: aschimme@indiana.edu

N.S. Gupta (ed.), *Chitin*, Topics in Geobiology 34,
DOI 10.1007/978-90-481-9684-5_4, © Springer Science+Business Media B.V. 2011

a more careful selection of specific modern insect fauna or preserved insect chitin from sediments yields $\delta^{18}O_{chitin}$ values that are useful for reconstructing the isotopic composition of paleoenvironmental water, and for constraining paleohumidity and paleotemperatures. Experimental oxic and anoxic heating and partial biodegradation of chitin in marine anoxic mud and in terrestrial oxic soils did not result in any significant C, N, O-isotopic shifts in the preserved amino sugar. Chemically preserved archeological chitin was found to be isotopically compatible with modern chitin from comparable environments. New analytical stable isotope techniques with reduced sample size requirements open opportunities to utilize geologically preserved chitin in paleoenvironmental studies.

Keywords Carbon stable isotopes • Chitin • Exoskeleton • Nitrogen stable isotopes • Oxygen stable isotopes

4.1 Introduction: Sources of Carbon, Nitrogen and Oxygen in Chitin

Chitin is best known as an important structural amino sugar biopolymer adding strength to exoskeletons of arthropods, but it is also biosynthesized by fungi and some microbiota (Muzzarelli 1977; Muzzarelli et al. 1985). Biosynthesis of chitin utilizes carbon, nitrogen, and oxygen atoms with dietary and environmental isotopic signals and embeds them into a large organic macromolecule where isotopic exchange of carbon, nitrogen and oxygen is negligible or impossible as long as amino sugar remains chemically preserved. Although chitin's high organic nitrogen content makes it a prized target for rapid biodegradation, some sedimentary chitin can become fossilized and used for archeological, paleoecological, paleoenvironmental, and paleoclimatic studies. The biosynthesis of chitin in heterotrophic organisms relies exclusively on dietary organic carbon and nitrogen (DeNiro and Epstein 1978, 1981a). Nitrogen in exoskeletal chitin is derived from excretory ammonia of dietary origin, which is known to be ^{15}N-depleted compared with dietary organic nitrogen (Webb et al. 1998, and refs. therein). The origin of organic oxygen in chitin is more complicated due to its multiple chemical sources and major differences in water availability among habitats. During biosynthesis of chitin, oxygen from water can partially exchange with biochemical precursors of chitin. In contrast, the oxygen in macromolecular chitin is strongly bonded to carbon and isotopically conservative. Like all fauna, arthropods metabolize dietary organic oxygen and utilize oxygen in drinking or body water. They also convert elemental atmospheric oxygen or aquatically dissolved oxygen to body water (Ayliffe and Chivas 1990), from where the oxygen can exchange isotopically with biochemicals that form chitin. The isotopic influence of elemental oxygen on newly synthesized chitin may be partially responsible for the limited correlation between oxygen and hydrogen stable isotope ratios among chitins of widely different faunal origin (Schimmelmann and DeNiro 1986c). Regardless of

the complexity of isotopic sourcing of chitin, chemically preserved chitin isotopically 'remembers' its biogeochemical heritage from the time of biosynthesis.

This chapter first outlines preparative and analytical caveats of C, N, O-stable isotopic characterizations, followed by a review of the relationships between the C, N, O-isotopic compositions of chitin to diet and water available to chitin-producing organisms. The last part of the chapter gives an overview on C, N, O-isotopic results from studies that utilized chemically preserved fossil and archeological chitin in paleoenvironmental and paleoclimatic research.

4.2 Preparation of Chitin Substrates and C, N, O-isotopic Measurements

Chitin is a chemically complex biopolymer consisting mostly of polycondensated N-acetyl-glucosamine units where some amino sugar units are deacetylated. Chitin also contains various amounts of covalently bonded proteinaceous, carbohydrate, and lipidic components, and in the case of crustacean chitin may be closely linked with biologically deposited minerals containing inorganic carbon and oxygen (Muzzarelli 1977). Due to different biosynthetic pathways, organic compound classes may exhibit systematically different isotopic compositions. For example, lipid carbon tends to be more ^{13}C-depleted than carbon in carbohydrates and chitin (e.g., Miller et al. 1985; Hayes 1993). Biochemical pathways leading to the biosynthesis of amino sugars for chitin discriminate strongly against ^{15}N and cause amino sugars to become up to 12‰ more depleted in ^{15}N than proteinaceous muscle biomass in the same organism (Schimmelmann and DeNiro 1986b). Chitin's hygroscopicity causes the adsorption of a few weight % water (Muzzarelli 1977) adding inorganic oxygen to the organic oxygen in chitin if no rigorous drying is employed. In order to measure meaningful stable isotope ratios in chitin that can be compared with data from different organisms, ecosystems and among studies, the chemical preparation of chitin-derived analytes for C, N, O-isotopic studies should therefore limit the abundance of non-amino-sugar components.

The isotopic influence of residual non-amino-sugar components cannot be completely eliminated from macromolecular chitin, although a sequence of extractions can yield an amino-sugar-rich residual chitin isolate. Nevertheless, different wet-chemical preparation procedures for 'purification' of macromolecular chitin yield significantly different isotopic and atomic N/C results (Fig. 4.1; Schimmelmann and DeNiro 1986a). Chemically aggressive methods can increase deacetylation and yield a substrate more similar to chitosan (Muzzarelli 1977; Muzzarelli et al. 1985). Each study should employ an internally standardized procedure to limit preparative and analytical noise. Schimmelmann's C, N, O-isotopic studies preferred acid depolymerization of chitin and preparation of pure, crystalline D-glucosamine hydrochloride as a reliable substrate for generating reproducible data (Schimmelmann and DeNiro 1986a). In brief, mineral components were first removed in dilute hydrochloric acid, then bulk proteinaceous

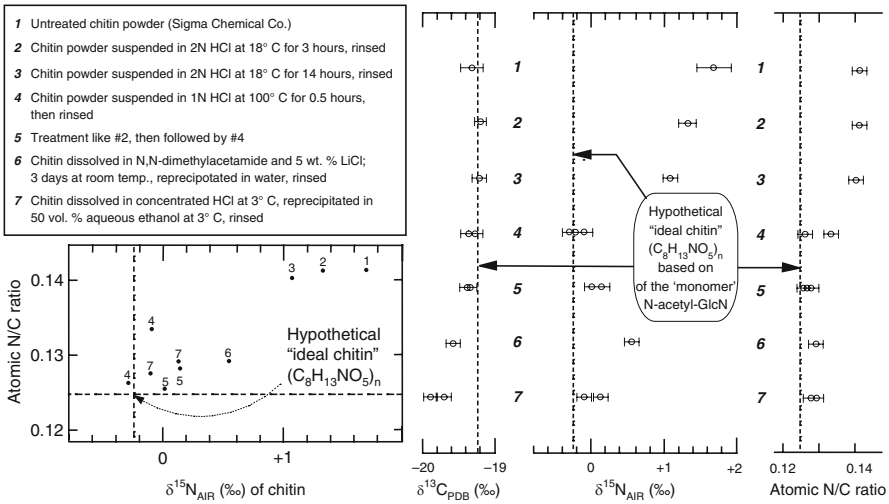

Fig. 4.1 $\delta^{13}C$ values, $\delta^{15}N$ values and atomic N/C ratios of chitin isolates prepared from chitin powder (Sigma Chemical Co.). Different wet-chemical preparation procedures for 'purification' of macromolecular chitin yield significantly different isotopic and atomic N/C results. The $\delta^{13}C$ and $\delta^{15}N$ values for 'ideal chitin' (i.e., hypothetical pure polymer of N-acetyl glucosamine) are based on measured $\delta^{13}C$ and $\delta^{15}N$ values of D-glucosamine hydrochloride and the $\delta^{13}C$ of acetyl carbon prepared from the same commercial chitin. The *lower left cross-plot* shows that the chemical removal of nitrogen-rich, ^{15}N-enriched proteinaceous matter from chitin tends to lower the atomic N/C ratio and the $\delta^{15}N$ value in the direction towards the N/C ratio and the $\delta^{15}N$ value of 'ideal chitin' (adapted from Schimmelmann and DeNiro 1986a)

material was hydrolyzed in hot aqueous 1N sodium hydroxide and rinsed away. Following hydrolysis of remaining chitin in hot hydrochloric acid, the resulting D-glucosamine hydrochloride was purified from neutral and amino acid contaminants by ion-exchange chromatography, freeze-dried, and used for determination of stable isotope ratios.

C, N-stable isotope ratios expressed as $\delta^{13}C$ and $\delta^{15}N$ values can be determined off-line or on-line using the combustion products CO_2 and N_2 of chitin or D-glucosamine hydrochloride. Before the introduction of the TC/EA on-line method for the determination of organic oxygen stable isotope ratios in pyrolytically produced CO, labor-intensive off-line procedures were employed for preparation of CO_2 analyte gas from chitin. The first published method converted all oxygen in D-glucosamine hydrochloride from chitin to carbon dioxide for off-line determination of $\delta^{18}O$ values (Schimmelmann and DeNiro 1985, 1986c). Acid hydrolysis of chitin to form D-glucosamine hydrochloride adds one oxygen atom from water to each D-glucosamine hydrochloride molecule. The preparation of D-glucosamine hydrochloride from all chitins followed a standard protocol and utilized isotopically equivalent reagents and procedures in order to yield mutually comparable $\delta^{18}O$ values. Motz (2000) developed an alternate chemical route to generate CO_2 from organic matter, by pyrolyzing chitin or cellulose at 1050°C in nickel tubes (Motz et al. 1997). He collected and purified the

resulting CO_2 on a vacuum line and determined $\delta^{18}O$ values off-line. Modern on-line TC/EA techniques of macromolecular chitin are faster, more economic, safer, and unaffected by many of the analytical shortcomings of earlier methods (Wang et al. 2008). However, TC/EA-based determination of $\delta^{18}O$ values remains sensitive to chitin's hygroscopicity and partial deacetylation during preparation of chitin.

Unless noted otherwise, all following C, N, O-isotope data in this chapter relating to chitin were determined using D-glucosamine hydrochloride from chitin. Isotopic data from different techniques and chemically different chitin isolates are mutually comparable only within a few ‰ uncertainty. It is important to remember that macromolecular chitin isolates contain some chemical moieties other than amino sugars, and thus stable isotope ratios of a chitin isolate may slightly deviate from the isotope ratios of the isolated pure amino sugar fraction. The calibration of older data prior to modern international stable isotope calibration methods and standards relied on SMOW and PDB, but is approximately compatible with modern VSMOW-SLAP and VPDB scales.

4.3 Factors Controlling Natural C, N, O-isotopic Variability in Chitin

4.3.1 Variability Due To Controlled Diet

Several studies examined the isotopic relationship between diet and chitin. Populations of five different arthropod species were raised on controlled diets (DeNiro and Epstein 1978, 1981a; Schimmelmann and DeNiro 1986b), followed by a comparison of the $\delta^{13}C$ and $\delta^{15}N$ values of diets against the corresponding isotopic compositions of D-glucosamine hydrochloride from chitins (Fig. 4.2). Differences in $\delta^{13}C$ values between diet and D-glucosamine hydrochloride are due to metabolic and biosynthetic fractionation, range narrowly between −2.2‰ and +2.1‰, and average 0.0 ± 1.5‰ for all eight animal-diet combinations. The $\delta^{13}C$ value of an arthropod's chitin tends to be similar to the $\delta^{13}C$ value of the animal's diet. The same conclusion was reached by Miller et al. (1985) who raised American cockroaches *Periplaneta americana* on two isotopically different diets and found that chitin $\delta^{13}C$ was tightly coupled to $\delta^{13}C$ of their diet. Moreover, chitin $\delta^{13}C$ was similar to that of the whole body biomass.

Miller (1984) raised a colony of flour beetles *Tenebrio molitor* on a diet of whole wheat flour with $\delta^{13}C = -24.4‰$. Some specimens of the non-feeding pupae stage were kept in whole wheat flour, whereas others were removed from the colony and introduced either to icing sugar with $\delta^{13}C = -12.7‰$, or to corn meal with $\delta^{13}C = -11.5‰$. The diet-switch experiment started immediately after molting. Actively feeding specimens from the three populations were removed 24, 48, 96 and 240 h after molting and $\delta^{13}C_{chitin}$ values were determined. $\delta^{13}C_{chitin}$ data across the first 2 to 3 days after molting expressed isotopic variance, but clear trends toward ^{13}C-enrichment

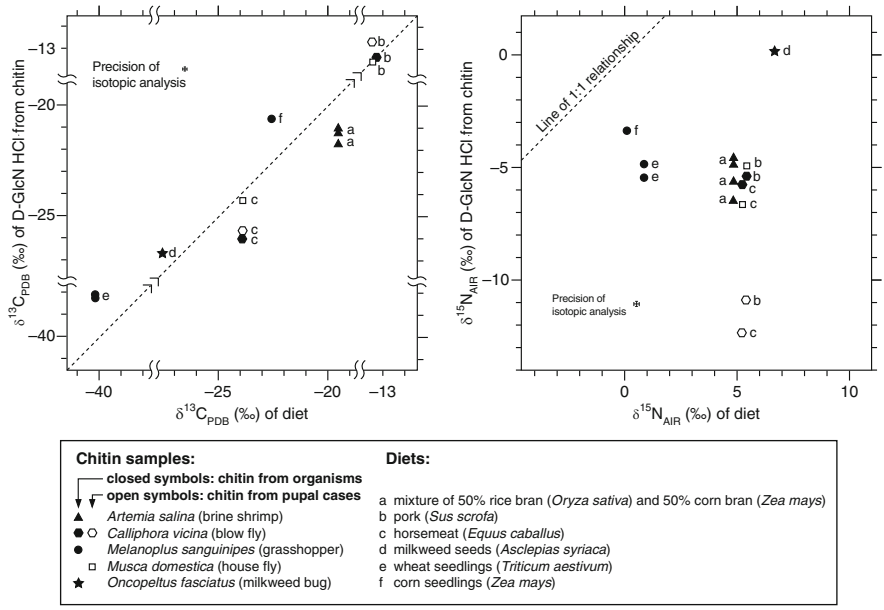

Fig. 4.2 $\delta^{13}C$ and $\delta^{15}N$ values of D-glucosamine hydrochloride from chitin versus $\delta^{13}C$ and $\delta^{15}N$ values of diet. The analytical precision is indicated (adapted from Schimmelmann and DeNiro 1986b. Reproduced with permission from *Contrib. Mar. Sci.* 1986, *29*, 113–130. Copyright 1986 University of Texas at Austin, Marine Science Institute)

were observed over the next 4 to 10 days reaching $\delta^{13}C_{chitin}$ values of −21.7‰ and −20.8‰ for larvae feeding on icing sugar and corn meal, respectively.

In contrast to carbon, $\delta^{15}N$ values of D-glucosamine hydrochloride prepared from chitin are always far lower than $\delta^{15}N$ values of corresponding diets (Fig. 4.2). $\delta^{15}N$ differences between D-glucosamine hydrochloride and diet range from −17.5‰ to −3.3‰ and average −9.5 ± 3.6‰, thus comparing well with similar differences between chitin and muscle biomass in individuals (Schimmelmann and DeNiro 1986b). Interestingly, DeNiro and Epstein (1981a) observed little isotopic difference between $\delta^{15}N$ values of diet and macromolecular chitin isolates from the same populations. It is unclear how much nitrogen in non-amino sugar was present in their macromolecular chitin isolates. Data in Fig. 4.2 further indicate that D-glucosamine hydrochloride from the chitin of pupal cases of the dypterid fly *Calliphora vicina* is about 6‰ more negative than that of the exoskeletons of the adult flies that emerged from the pupal cases, suggesting ongoing metabolic fractionation during stages of maturation. Montoya (1994) determined a $\Delta\delta^{15}N_{chitin-diet}$ offset of 0.7‰ between marine amphipods' bulk chitin and their algal diet.

Webb et al. (1998) switched between C, N-isotopically controlled diets when raising locusts *Locusta migratoria*. Monitoring of $\delta^{13}C_{chitin}$ along dietary isotopic changes demonstrated that chitin was the most rapidly changing biochemical component of immature locusts. Insect chitin is continuously enzymatically depolymerized and reassembled over the course of repeated molts. Carbon turnover in chitin

was estimated to be approximately 8 days for locusts fed on maize and 5 days on wheat diet, making chitin a good indicator of recent dietary source carbon for growing insects. Relative to diet, the chitin of wheat-fed adult locusts was ^{13}C-enriched with $\Delta\delta^{13}C_{diet-chitin} = 2.2 \pm 0.2‰$, whereas chitin of maize-fed adults showed a contrasting $\Delta\delta^{13}C_{diet-chitin} = -0.2 \pm 0.1‰$. The respective isotopic differences for nitrogen were $\Delta\delta^{15}N_{diet-chitin} = 3.7 \pm 0.3‰$ for wheat-fed and $\Delta\delta^{15}N_{diet-chitin} = 4.2 \pm 0.2‰$ for maize-fed locusts.

Tibbets et al. (2008) determined N-isotopic differences between diet, larvae, pupal exuviae (i.e., chitin-rich empty pupal cases) and adults from six different species of insects that were raised on isotopically distinct diets. Their study confirmed a strong dietary influence on $\delta^{15}N$ values in resulting insect biomass but warned that (i) the isotopic responses are species-specific, and (ii) different life stages of metamorphosing insects may differ in tissue-to-diet isotopic ^{15}N discrimination. The need for caution was confirmed by Overmyer et al.'s (2008) observation that chitin-rich, shed head capsules of molting larvae of laboratory-reared black flies *Simulium vittatum* were enriched in ^{15}N by 1.2–7.1‰ relative to bulk larval biomass.

Only circumstantial evidence is available to constrain oxygen isotopic fractionation between diet and chitin. Motz (2000) determined $\delta^{18}O$ values of chitin from tree-feeding insects and of cellulose in the beetles' dietary wood (Fig. 4.3). Most insects

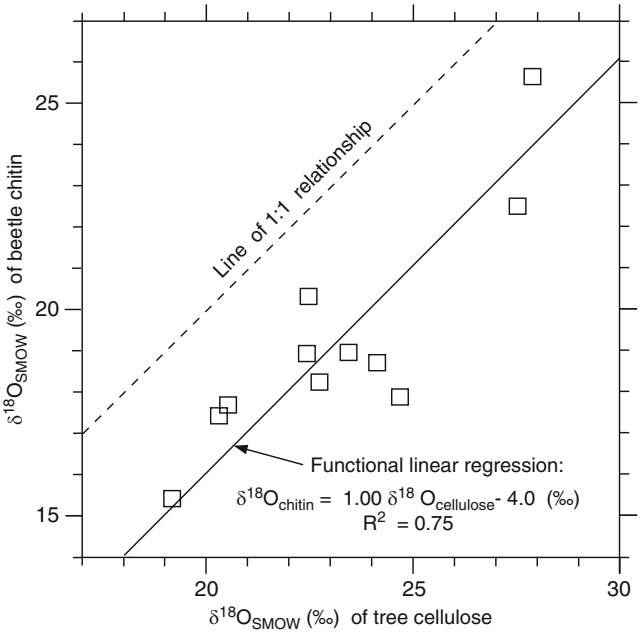

Fig. 4.3 $\delta^{18}O$ values of chitin from tree-feeding insects versus $\delta^{18}O$ values of cellulose in the beetles' dietary wood along a Canadian geographic transect (adapted from the dissertation of Motz 2000. The functional linear regression was calculated according to Ricker 1973. Reproduced with permission from John E. Motz)

were bark-beetles collected along a climatic transect in Canada. Chitin is ^{18}O-enriched over environmental water by ~37‰ while cellulose is enriched over environmental water by ~41‰ (the relationship between δ^{18}O of water and tree ring cellulose was reviewed by McCarroll and Loader 2004). Some of the ^{18}O-enrichment in cellulose is due to evapotranspirative loss of water from leaves before water circulates back into the trunk to support the biosynthesis of cellulose, and ultimately the biosynthesis of bark beetle chitin. Unfortunately, the isotopic difference of ~4‰ between chitin and its partial dietary precursor cellulose is insufficient evidence to constrain the metabolic/trophic oxygen isotopic fractionation in chitin biosynthesis, because a diet of wood and bark also includes water, oxygen-containing lignin, tannin, lipids, etc.

The comparison of δ^{18}O values of ocean water, marine chitin, and marine cellulose qualitatively corroborates Motz's (2000) observations. δ^{18}O values of D-glucosamine hydrochloride from 42 fully aquatic marine chitin samples average 26.3‰ more positive than δ^{18}O values of ocean water that ranges close to 0‰ (Schimmelmann and DeNiro 1986c). The δ^{18}O values of fully aquatic marine chitins overlap with δ^{18}O values of marine celluloses (DeNiro and Epstein 1981b). Wooller et al. (2004) observed a similar isotopic offset in a survey of chitin from modern chironomid head capsules.

4.3.2 Variability Within an Individual Exoskeleton and Along Molting

Different body parts of arthropods contain variable quantities of chitinous exoskeletal armor that is biosynthesized at different times and rates and may exhibit isotopic inhomogeneity within an individual animal. Isotopic variability within exoskeletons must be considered when it is not possible or practical to process and homogenize an entire chitinous exoskeleton. Chitin samples from five body sections of a Northern lobster *Homarus americanus* were measured to evaluate the variability of C, N, O-isotope ratios (Fig. 4.4; Schimmelmann and DeNiro 1986b, c). D-glucosamine hydrochloride from chitin yielded the following mean δ-values, standard deviations, and ranges:

$$\delta^{13}\mathrm{C} = -17.5 \pm 0.2‰, \text{ range } 0.5‰$$
$$\delta^{15}\mathrm{N} = +0.5 \pm 0.5‰, \text{ range } 1.3‰$$
$$\delta^{18}\mathrm{O} = +25.4 \pm 0.4‰, \text{ range } 0.9‰$$

The growth of an arthropod can only occur after the old exoskeleton is shed and the new, still soft exoskeleton is rapidly expanded before hardening. Exoskeletal construction during molting (ecdysis) involves substantial body reworking. In order to conserve valuable amino sugars, most of the old exoskeleton is enzymatically depolymerized and a new exoskeleton is formed initially using old amino sugar, with the remainder of the new exoskeleton being formed using newly biosynthesized amino

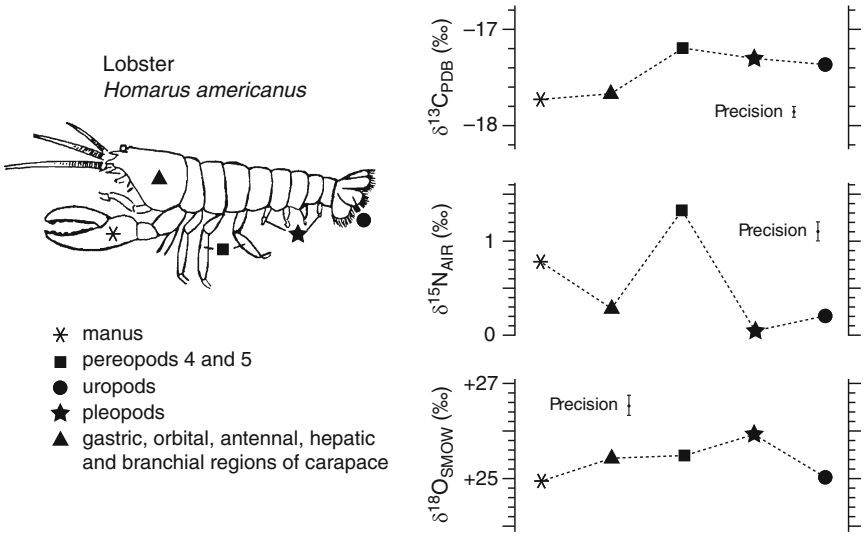

Fig. 4.4 $\delta^{13}C$, $\delta^{15}N$ and $\delta^{18}O$ values of D-glucosamine hydrochloride from the chitin of five different body sections of a Northern lobster *Homarus americanus.* The analytical precision is indicated (data from Schimmelmann and DeNiro 1986b, c)

sugars (Webb et al. 1998, and refs. therein). After ecdysis, the new carapace will gradually accumulate chitin (Vigh and Dendinger 1982; Kulkarni 1983), giving an opportunity for isotope fractionation to occur between old, remaining chitin in the shed carapace and newly depositing chitin in the new carapace. Old and new carapaces were collected from crayfish *Oronectes limosus*, a shore crab *Grapsus tenuicrustatus*, and three green crabs *Carcinus maenas*. The comparison of D-glucosamine hydrochloride from the chitins of old versus new carapaces showed non-systematic but significant isotopic differences, with the following mean isotopic differences, standard deviations, and ranges (Fig. 4.5; Schimmelmann and DeNiro 1986b, c):

$$\Delta\delta^{13}C_{old-new} = +0.4 \pm 0.6‰; \text{ range } 1.5‰$$
$$\Delta\delta^{15}N_{old-new} = -1.0 \pm 1.9‰; \text{ range } 4.8‰$$
$$\Delta\delta^{18}O_{old-new} = +1.2 \pm 1.7‰; \text{ range } 4.3‰$$

The relatively small $\Delta\delta^{13}C$ and relatively larger $\Delta\delta^{15}N$ differences between old and new crustacean carapaces are qualitatively matched by observed isotopic differences between insect pupal cases and adults of the blow fly *Calliphora vicina* (Fig. 4.2). Scatter in $\Delta\delta^{15}N_{old-new}$ values is also suggested by data from larvae and chitin-rich pupal exuviae from six species of insects along metamorphosis. Exuviae were mostly, but not always ^{15}N-depleted relative to larval biomass (Tibbets et al. 2008).

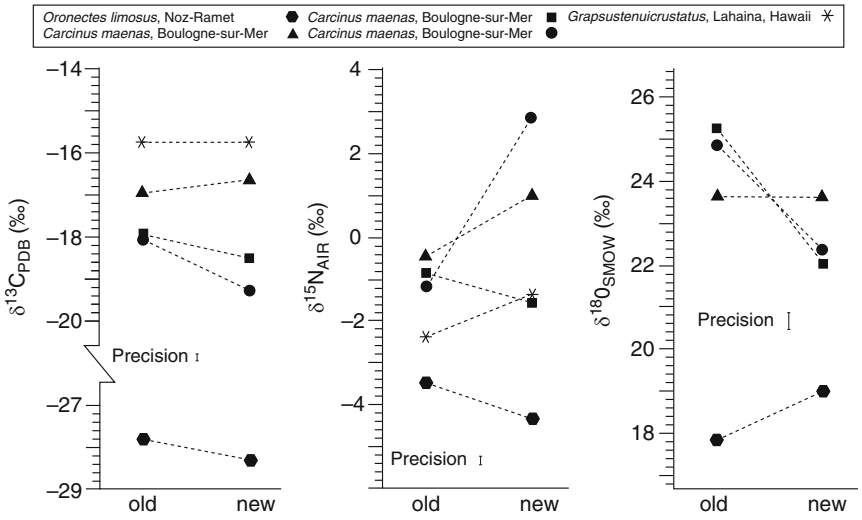

Fig. 4.5 $\delta^{13}C$, $\delta^{15}N$ and $\delta^{18}O$ values of D-glucosamine hydrochloride from the chitin of the old (i.e., recently shed via molting) and new carapaces of crustaceans. The analytical precision is indicated (data from Schimmelmann and DeNiro 1986b, c)

4.3.3 Variability Within Crustacean Populations

Isotopic differences among individuals were evaluated within several populations of crustaceans. The data matrix also tested for isotopic differences due to age and sex (Schimmelmann and DeNiro 1986b, c). D-glucosamine hydrochloride was measured from the chitin of the right claws of ten adult male red swamp crayfish *Procambarus clarkii* whose carapace widths were within ±10% of each other. Mean δ-values, standard deviations, and ranges were as follows:

$$\delta^{13}C = -19.2 \pm 0.4‰, \text{ range } 1.5‰$$

$$\delta^{15}N = +0.6 \pm 0.6‰, \text{ range } 1.9‰$$

$$\delta^{18}O = +20.2 \pm 0.4‰, \text{ range } 1.2‰$$

Populations of ghost crabs *Ocypode ceratophtalmus*, wharf crabs *Sesarma* sp., and striped shore crabs *Pachygrapsus crassipes*, including different ages and sexes, did not express any systematic trends in $\delta^{15}N$ that were related to either age or sex (Fig. 4.6; Schimmelmann and DeNiro 1986b, c). The only significant trend for $\delta^{13}C$ was apparent in ghost crabs where older individuals tended to have chitin with lower $\delta^{13}C$ values. Field observations indicated that older and larger ghost crabs locate their burrows further inland and higher above the water table (Cott 1929; Crane 1941), thus possibly prompting a gradual dietary shift from marine to more terrigenous biomass.

Ghost crabs and wharf crabs are both essentially supralittoral and were caught on the same Hawaiian island along beaches at a short distance from each other, at

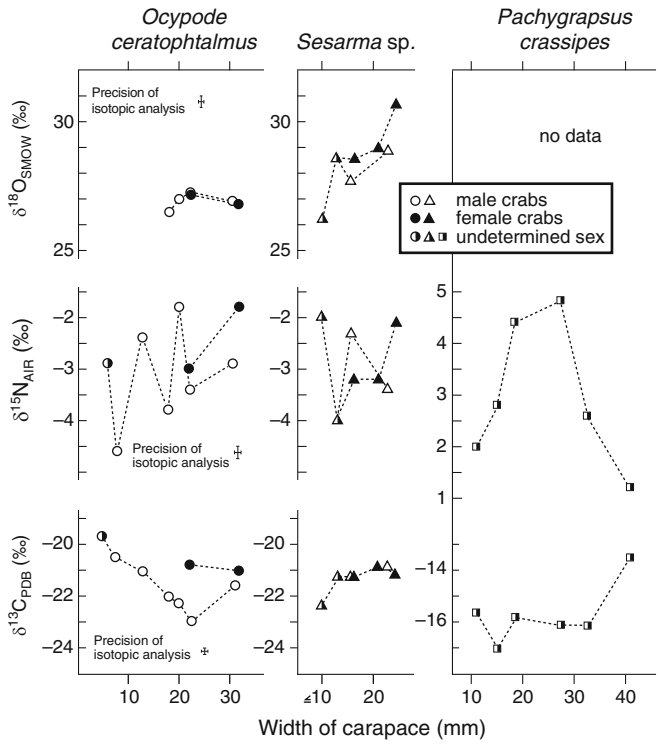

Fig. 4.6 $\delta^{13}C$, $\delta^{15}N$ and $\delta^{18}O$ isotopic variation among individuals of crustacean populations of ghost crabs *Ocypode ceratophtalmus*, wharf crabs *Sesarma* sp., and striped shore crabs *Pachygrapsus crassipes*. *Open symbols* represent male crabs, *filled symbols* female crabs, and *half-filled symbols* specimens of undetermined sex (data from Schimmelmann and DeNiro 1986b, c). The analytical precision is indicated. *Dashed lines* guide the eye (adapted and reproduced with permission from *Contrib. Mar. Sci.* 1986, *29*, 113–130. Copyright 1986 University of Texas at Austin, Marine Science Institute)

locations with identical isotopic compositions of seawater. $\delta^{18}O$ values of wharf crabs were more scattered and displayed a trend towards ^{18}O-enrichment with increasing crab size, whereas ghost crabs' $\delta^{18}O$ values clustered more tightly and did not exhibit an isotopic trend with size. Carbon and nitrogen isotope data from the wharf crab population ruled out large dietary shifts with increasing age. The contrasting behavior of both crab species may explain their oxygen isotopic differences. Ghost crabs are essentially nocturnal and avoid evaporative loss of moisture during daytime while hiding in their moist burrows (Cott 1929). Consequently their $\delta^{18}O$ values approach those of fully aquatic marine Hawaiian crustaceans averaging +25.3 ± 0.7‰ (n=6) (Schimmelmann and DeNiro 1986c). In contrast, wharf crabs live among and partly under boulders and pebbles in the intertidal zone where they are frequently exposed to evaporative loss of water, especially during daytime. The resulting ^{18}O-enrichment of their body liquid may translate into relative ^{18}O-enrichment of biosynthesized chitin.

The sex of a crustacean did not cause any systematic influence on stable isotopic compositions of chitin (Schimmelmann and DeNiro 1986b, c).

4.3.4 *^{15}N-enrichment with Increasing Trophic Level in Ecosystems*

A comparison among several arthropod species representing different trophic levels at four geographic locations yields a general trend towards more positive $\delta^{15}N$ values in D-glucosamine hydrochloride from chitin with increasing trophic level (Fig. 4.7; Schimmelmann and DeNiro 1986b). This qualitative observation is in agreement with the well-known fact that organic $\delta^{15}N$ increases by several ‰ with each trophic level, and therefore can serve as trophic indicator in the study of ecosystems (e.g., Schoeninger and DeNiro 1984; Minagawa and Wada 1984; Post 2002; Tibbets et al. 2008). The isotopic enrichment of chitin in ^{15}N along the food chain is balanced by the excretion of ^{15}N-depleted nitrogen waste. An increase in trophic level is not accompanied by systematic carbon (Fig. 4.7) or oxygen isotopic trends (Schimmelmann and DeNiro 1986c). Recent studies indicate that (i) lower trophic levels express the largest isotopic variability in biomass, (ii) the trophic isotopic enrichment from primary to secondary consumers can be quite variable for nitrogen, and to a lesser degree for carbon, and (iii) the diet's nutritional composition and food quality as well as the stoichiometric needs of consumers affect the trophic isotopic enrichment in biomass (Aberle and Malzahn 2007).

4.3.5 *Variability Among Environments*

Environmental and climatic influences on C, N, O-isotopic compositions of chitin from arthropods were evaluated using 56 arthropod species sampled at 50 locations in the Hawaiian Islands, the Caribbean, North and South America, and Europe (Schimmelmann and DeNiro 1986b, c). In addition, several species of crustaceans were grown in the lab at controlled conditions. Several brine shrimp species *Artemia* sp. grown in different waters and different geographic locations could be unambiguously distinguished from each other based on environmentally specific isotopic fingerprints (Schimmelmann et al. 1987). Marine chitin with a mean $\delta^{15}N$ value of -1.1 ± 2.8‰ (range 13.8‰; n = 43) is similar to terrestrial and freshwater chitins with a mean $\delta^{15}N$ value of -1.7 ± 2.7‰ (range 11.7‰; n = 16), although marine invertebrate bulk organic matter is generally enriched in ^{15}N relative to terrestrial and freshwater invertebrate bulk organic matter (France 1994). Categorizing the chitin samples on the basis of various types of marine and terrestrial environments demonstrates that the range of marine $\delta^{15}N$ values is smaller than the more variable terrestrial $\delta^{15}N$ record (Fig. 4.8). A separation between marine and

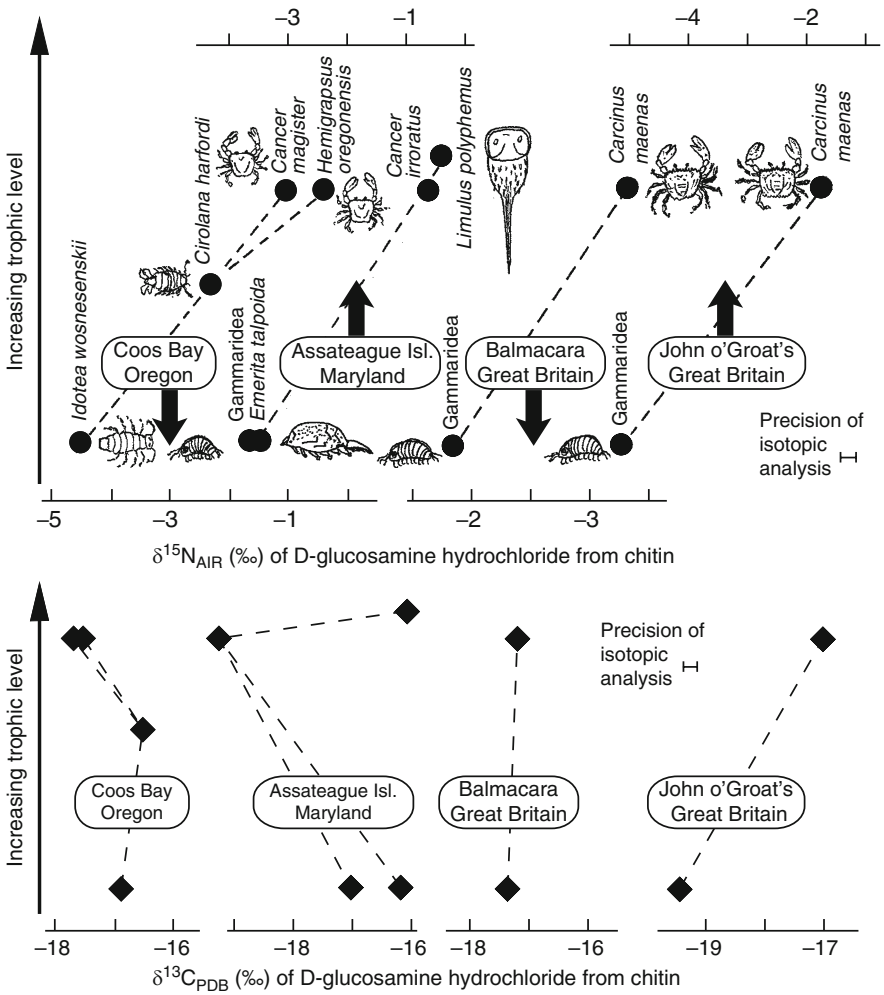

Fig. 4.7 $\delta^{15}N$ and $\delta^{13}C$ values of D-glucosamine hydrochloride from the chitin of different arthropods feeding at different approximate trophic levels in four marine environments. For example, $\delta^{15}N$ increases from the filterfeeding *Emerita talpoida* (Atlantic mole crab) and Gammaridea (scud), to the omnivore *Cancer irroratus* (Atlantic rock crab), and to the carnivore *Limulus polyphemus* (horseshoe crab), whereas no systematic trend is expressed by $\delta^{13}C$ values. Each location has its own isotopic scales. *Dashed lines* guide the eye. The analytical precision is indicated (data from Schimmelmann and DeNiro 1986b)

terrestrial chitin samples is possible, however, based on $\delta^{13}C$ values of chitin (Fig. 4.9; Schimmelmann and DeNiro 1986b):

$$\text{Marine chitin}: \delta^{13}C = -16.5 \pm 2.2‰;\ \text{range } 9.1‰;\ n = 43$$

$$\text{Terrestrial chitin}: \delta^{13}C = -25.6 \pm 3.9‰;\ \text{range } 17.6‰;\ n = 16$$

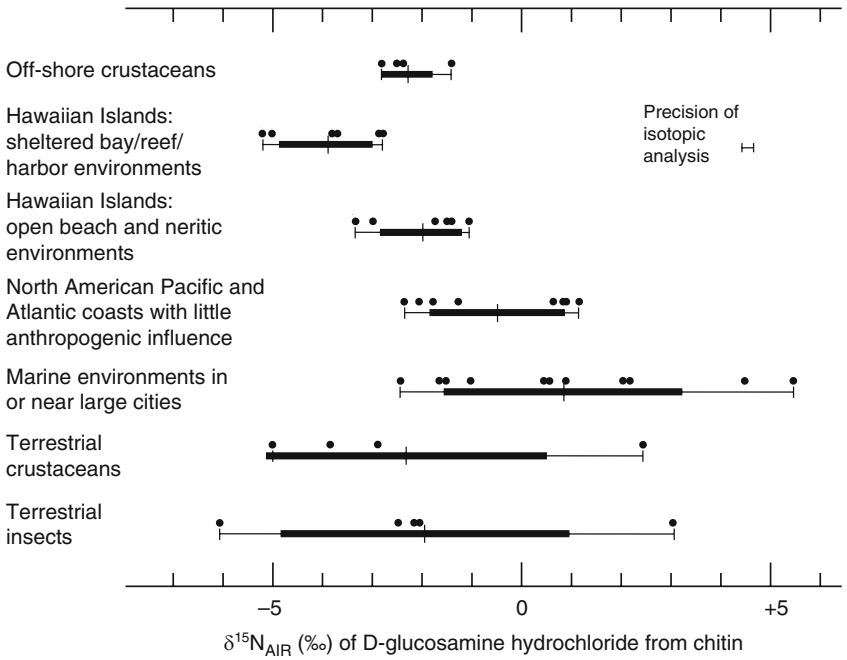

Fig. 4.8 Distribution of $\delta^{15}N$ values of arthropod chitin from various marine and terrestrial environments. Each data point represents the mean $\delta^{15}N$ value of D-glucosamine hydrochloride from chitin for all species at a single location. Range, mean, and standard deviation are indicated by *bars* and *brackets*. The analytical precision is indicated. Additional information on locations is given by Schimmelmann and DeNiro (1986b) (adapted and reproduced with permission from *Contrib. Mar. Sci.* 1986, *29*, 113–130. Copyright 1986 University of Texas at Austin, Marine Science Institute)

Although marine chitin samples outnumber terrestrial samples almost 3:1, marine chitin spans a more narrow carbon isotopic range than terrestrial chitin. The marine realm is better mixed and less variable than terrestrial ecosystems. The systematic $\delta^{13}C$ difference between many terrestrial plant materials averaging −26‰ and typical phytoplanktonic organic matter of marine origin averaging about −21‰ has been used to trace the influence of land-derived organic matter in the marine environment (e.g., Fry and Sherr 1984) and explains the carbon isotopic distinction between marine and terrestrial chitin.

Severe pollution by sewage fallout at a near-coastal site off San Pedro near Los Angeles caused a significant shift in the chitin of four marine crustacean species towards more negative $\delta^{13}C$ and $\delta^{15}N$ values (Fig. 4.10; Schimmelmann and DeNiro 1986b), in agreement with comparable nitrogen isotopic data on muscle tissue of ridgeback prawn *Sicyonia* sp. from the same polluted area (Rau et al. 1981). Oxygen stable isotope ratios in chitin did not exhibit a response to pollution. The nitrogen isotopic shift in food webs due to sewage influx into marine ecosystems is not directly comparable to the effect in sewage-affected non-marine environments, for example in estuaries (Hadwen and Arthington 2007).

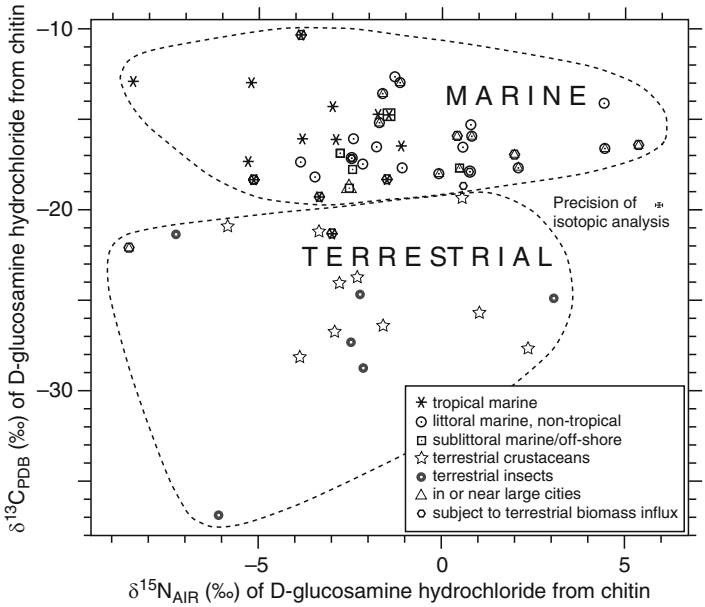

Fig. 4.9 Carbon and nitrogen isotopic distribution among arthropod chitins from different environments, as measured in D-glucosamine hydrochloride. Each *data point* represents the mean $\delta^{13}C$ and $\delta^{15}N$ value for all species at one location, calculated using an average value for each species. The analytical precision is indicated. Further details on individual locations are given in Schimmelmann and DeNiro (1986b) (adapted and reproduced with permission from *Contrib. Mar. Sci.* 1986, *29*, 113–130. Copyright 1986 University of Texas at Austin, Marine Science Institute)

The distribution of $\delta^{18}O$ values in D-glucosamine hydrochloride from chitin is plotted in Fig. 4.11 against $\delta^{18}O$ of environmental water for many species of aquatic, semi-aquatic, and non-aquatic arthropods (Schimmelmann and DeNiro 1986c). Linear regression analyses yielded R^2 values close to zero for the correlation between water and chitin from non-aquatic and semi-aquatic arthropods, whereas an R^2 of 0.64 was obtained for $\delta^{18}O_{water}$ versus $\delta^{18}O_{chitin}$ from aquatic arthropods:

$$\delta^{18}O_{chitin} = 1.14\delta^{18}O_{water} \pm 30.6‰ \ (n = 74).$$

Chitins from marine aquatic arthropods cluster most tightly with a $\delta^{18}O$ range of only 4.2‰ because ocean waters and water-derived marine organic oxygen express limited isotopic variability. In contrast, the larger isotopic variability of meteoric waters and the influence of evapotranspiration cause the chitins of semi-aquatic and non-aquatic animals to widely range across 13.0‰ (Fig. 4.11).

Motz (2000) developed transfer functions and models with predictive capabilities to reconstruct the H, O-isotopic composition of environmental water and relative humidity from H, O-isotopic values of terrestrial insect chitin. The model also considers the influence of annual mean temperature. Data were first normalized to

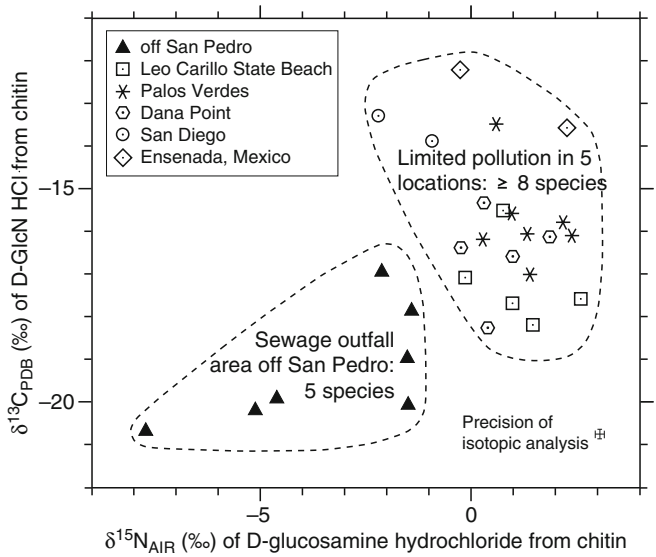

Fig. 4.10 The $\delta^{15}N$ and $\delta^{13}C$ values of D-glucosamine hydrochloride (D-GlcN·HCl) from marine arthropod chitins from a sewage outfall area off San Pedro near Los Angeles. No overlap is observed with values from less contaminated marine environments in Southern California and northern Baja California. Each *data point* represents one marine crustacean sample. The analytical precision is indicated (adapted and reproduced with permission from *Contrib. Mar. Sci.* 1986, *29*, 113–130. Copyright 1986 University of Texas at Austin, Marine Science Institute)

100% relative humidity to correct for the isotopic effects of partial evaporation. The signal transfer from $\delta^{18}O_{\text{environmental water}}$ via $\delta^{18}O_{\text{leaf water}}$ to $\delta^{18}O_{\text{chitin}}$ is expressed by the highly significant empirical relationship

$$\delta^{18}O_{chitin} = 1.12\,\delta^{18}O_{\text{environmental water}} + 28.95‰;\ R^2 = 0.94 \text{ (Fig. 4.12)}.$$

Motz (2000) further extracted a moderately strong temperature signal from a set of insect chitins along a Canadian transect. Higher annual mean temperatures cause ^{18}O-enrichment in terrigenous insect chitin:

$$\delta^{18}O_{\text{chitin}} = 0.96\ T\ (°C) + 8.16‰.$$

The underlying data had been normalized for 100% relative humidity. Further work is needed to establish a temperature effect for aquatic chitin where increased evapotranspirative ^{18}O-enrichment in body fluid can be ruled out as a contributing factor. However, the presence of strong trophic and other isotopic influences tends to overwhelm the possible effect of relatively small temperature ranges encountered in most aquatic habitats. Schimmelmann and DeNiro's (1986c) extensive data set on marine and freshwater chitins fails to identify a temperature signal.

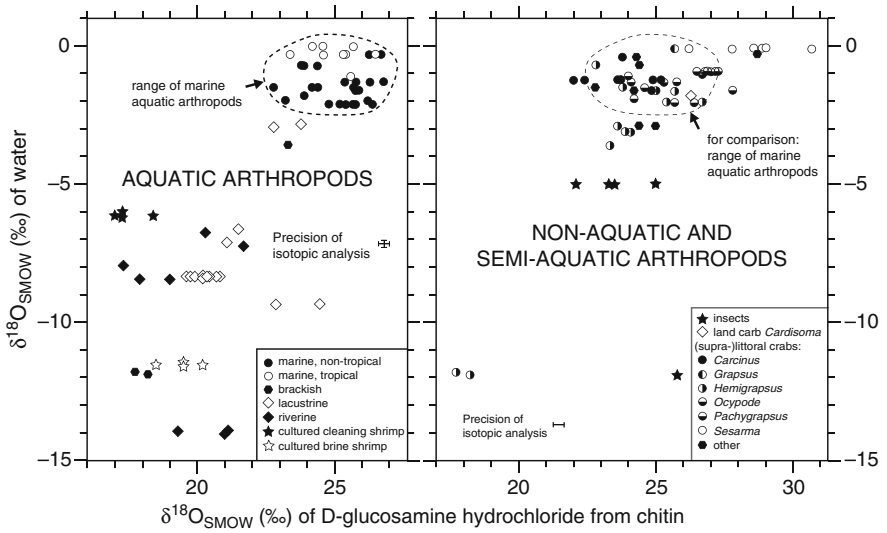

Fig. 4.11 $\delta^{18}O$ values of aquatic, semi-aquatic, and non-aquatic arthropod chitins show moderate correlation with $\delta^{18}O$ values of ambient and available waters. Marine data in the left graph are encircled by a dashed line. $\delta^{18}O$ values of waters were measured for aquatic arthropod environments, whereas $\delta^{18}O$ values for waters available to semi-aquatic and non-aquatic arthropods were estimated according to reported isotope data for regional precipitation. Each data point represents one arthropod sample. The analytical precision is indicated (data from Schimmelmann and DeNiro 1986c)

4.4 Effects of Biodegradation, Fossilization, and Roasting on Stable Isotope Ratios in Chitin

Following the death of an arthropod, its chitinous exoskeleton is typically subject to rapid biodegradation, although certain sedimentary environments may partially preserve chitin (e.g., Stankiewicz et al. 1998a). Archeological arthropod remains may include chitin that has been cooked or roasted. To test for isotopic shifts, aliquots of isotopically characterized ground chitin samples from several arthropod species were partially biodegraded in marine mud for ten weeks under anoxic conditions, or in garden soil for eight weeks. Other aliquots of chitin were roasted in air for three hours at 275°C, or were heated in an anoxic water vapor atmosphere for three hours at temperatures from 200°C to 325°C (Schimmelmann et al. 1986). D-glucosamine hydrochloride was prepared from the recovered chitin and quantified to determine the extent of amino sugar degradation. Isotope ratios were measured in D-glucosamine hydrochloride.

Although biodegradation occurred for less than three months, microbes in mud and soil caused losses of up to 75% of the original chitin. This finding is in excellent agreement with results from many chitin biodegradation experiments in marine oxic, estuarine, limnic, and lotic suburban waters, and in the rhizosphere (see references in Schimmelmann et al. 1986; Poulicek and Jeuniaux 1991; Stankiewicz et al. 1998b).

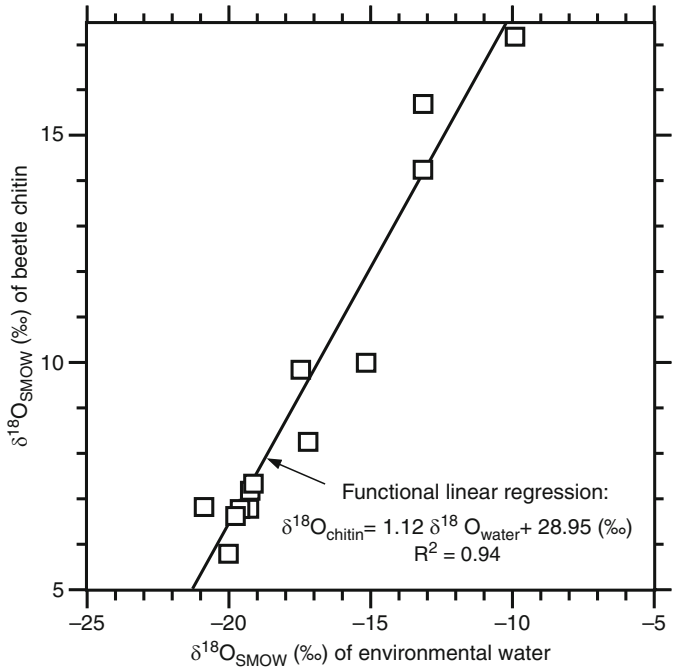

Fig. 4.12 $\delta^{18}O$ values of insect chitin from beetles versus $\delta^{18}O$ values of environmental water along a Canadian geographic transect (adapted from the dissertation of Motz 2000). Data were first normalized to 100% relative humidity to correct for the isotopic effects of partial evaporation. The functional linear regression was calculated according to Ricker (1973) (adapted and reproduced with permission from John E. Motz)

The key for isotopically conservative behavior of chitin is the preservation of intact D-glucosamine units within a biomacromolecular chitin structure that protects interior sections of the macromolecule from external chemical agents. Heating and roasting also reduced the amount of recoverable D-glucosamine hydrochloride. The observed mean C, N, O-isotopic shifts in all degradation experiments from original chitin to residual amino sugar in partially degraded chitin were $\Delta\delta^{13}C = +0.1 \pm 0.3‰$ (n = 19), $\Delta\delta^{15}N = -0.2 \pm 0.6‰$ (n = 18), and $\Delta\delta^{18}O = -0.3 \pm 0.9‰$ (n = 12). These isotopic shifts are relatively small and cannot significantly impact paleoenvironmental assessments. Schimmelmann et al. (1986) also demonstrated the use of scanning electron microscopy to assess the presence of fungal neo-formed chitin that may contaminate fossil or archeological chitin.

Extensive isotopic exchange or reaction with chemical N- and O-containing species percolating through a burial assemblage would require thermal or pH conditions that exceed those usually encountered in shallow depositional environments. However, extreme thermal and pH conditions preclude the chemical preservation of chitin (Schimmelmann et al. 1998).

4.5 C, N, O-isotope Research Using Fossil Chitin

Biodegradation of arthropod chitin in aquatic environments causes the eventual loss of most amino sugar biomass due to fungi, bacteria, and scavengers (e.g., Poulicek and Jeuniaux 1991; Hillman et al. 1989; Simon et al. 1994; Boetius and Lochte 1994; Baas et al. 1995; Stankiewicz et al. 1998a, b). Some soil environments seem to better preserve chitin, especially beetle chitin (Miller 1984, 1991; Miller et al. 1993), which may be due to the relatively high degree of sclerotization of insect chitin (Muzzarelli 1977).

Chitin samples from a variety of arthropods from Peruvian archeological excavations with ages up to 1,400 years were measured C, N, O-isotopically and found to be isotopically similar to modern chitin in comparable environments (Schimmelmann et al. 1986). Bulk fossil chitinous exuviae of cladoceran *Bosmina longispina maritima* (planktonic crustaceans) from dated sediment cores from the Gotland Basin of the central Baltic Sea yielded a paleoceanographic time-series of $\delta^{15}N$ values that was used to reconstruct the onset of enhanced nitrogen fixation around AD 1965 (Struck et al. 1998). The study relied on Montoya's (1994) empirical determination of the $\Delta\delta^{15}N_{chitin-diet}$ offset of 0.7‰ between amphipods' chitin and their algal diet.

Motz (2000) measured $\delta^{18}O_{chitin}$ values in identified fossil insect fragments from ~18,000 year old sedimentary till in Illinois, along with $\delta^{18}O_{cellulose}$ values from the same sediment samples and matching hydrogen isotope ratios in chitin and cellulose. A mathematical model based on modern isotopic calibration data from chitin and cellulose was used to reconstruct Pleistocene paleoenvironmental water isotopic composition and paleohumidity. Relative depletion of Pleistocene waters in heavy isotopes implied a colder Pleistocene climate. A synopsis of chitin and cellulose isotope data suggested a gradient in relative paleohumidity from lower humidity in the understorey to higher humidity in the canopy.

The paleoclimatic evaluation of Late Quaternary lake and bog sediments increasingly relies on the abundance and isotopic composition of subfossil chitinous head capsules of chironomid insect larvae. Biosynthesis of chitin during the aquatic stage of insect development records a $\delta^{18}O_{chitin}$ that is related to $\delta^{18}O$ of lake water, which in suitable lakes is related to $\delta^{18}O$ of local precipitation and mean annual air temperature. Stratigraphic time-series of chironomid $\delta^{18}O$ can be used in paleothermometry to examine past changes in mean annual temperature, as demonstrated in two arctic lakes with strong early Holocene paleoclimatic gradients (Wooller et al. 2004). A systematic study by Wang et al. (2008) offered a greatly improved method of C, N, O, H-isotopic determination in chironomids using as few as 120 head capsules, or less than 100 μg of chitin. Wooller et al. (2008) used this new approach to analyze C, N and O isotope ratios of chironomid fossil heads from a Northern Icelandic lake core. Downcore shifts in $\delta^{18}O$ did not correlate with $\delta^{13}C$ and $\delta^{15}N$ of chironomid head capsules, implying that $\delta^{18}O$ variance was not primarily driven by changes in chironomid diet during the Holocene.

Two C, N-isotopic studies on bulk chironomid biomass suggest potential caveats for carbon and nitrogen stable isotope studies on chironomid chitin. Grey et al. (2004)

studied chironomid populations in deep, partially anoxic lakes where values from individual chironomid larvae had a range of 35‰ for $\delta^{13}C$ and a range of 16‰ for $\delta^{15}N$, which is equivalent to five trophic levels. The authors suspected the influence of methanotrophy along the food chain. Doi et al. (2007) observed that C, N-isotopic ratios in bulk chironomid larvae and hatched adults changed mostly during growth and pupation. A significant increase in $\delta^{13}C$ during starvation suggested metabolization of ^{13}C-depleted lipid energy reserves. Isotopic C, N-relationships between diet and chironomid larval biomass from laboratory-raised chironomids were described by Doi et al. (2006).

Morphological preservation of 'chitinous structures' in older sediments does not necessarily imply chemical preservation of chitin (e.g., Stankiewicz et al. 1997). The chemical stabilization of chitin in some old sediments via complexation with protein makes acid hydrolysis necessary to liberate D-glucosamine hydrochloride as an unambiguous witness to partial chitin preservation (Flannery et al. 2001). The same deacetylated chitin monomer has proven its value as an isotopic proxy for paleoenvironmental conditions because partial chitin degradation does not significantly impact its isotopic composition (Schimmelmann et al. 1987).

4.6 Conclusions

C, N, O-stable isotope ratios in chitin reflect trophic and environmental conditions of chitin biosynthesis. Chitin's abundance in most ecosystems make it an almost universally available organic substrate of choice for ecological and environmental investigations. Chitin can also become archeologically and geologically preserved in some sedimentary environments where its isotopic properties can serve as proxy for paleoenvironmental and paleoclimatic conditions. The insolubility of chitin in water and organic solvents and its chemical resistance to many acids facilitate its preparation and purification from arthropod biomass. The limited isotopic variability and heterogeneity within exoskeletons of individual arthropods, along molting, with increasing age, and within populations is dwarfed by the much larger isotopic variance due to different environmental and climatic conditions. Neither biological nor thermal partial degradation of chitin produces significant isotopic changes when the deacetylated monomer of chitin (i.e., D-glucosamine) is extracted from preserved chitin, purified, and used for analysis.

Acknowledgements Expert advice and contributions were provided by Drs. Hideyuki Doi, Randy F. Miller, John E. Motz, Teresa M. Tibbets, and Matthew Wooller. I gratefully acknowledge support from the U.S. Department of Energy, Basic Energy Sciences Research Grant number DEFG02-00ER15032, and from National Science Foundation grant OCE-0550295. Several figures were adapted and re-drawn, and accompanying text was reproduced from earlier publications, with permission from (1) American Chemical Society Symposium Series 1998, 707, 226–242 (© 1998 American Chemical Society), (2) Contributions in Marine Science 1986, 29, 113–130 (© 1986 Marine Science Institute of the University of Texas at Austin), and from (3) the dissertation of John E. Motz 2000 (© 2000 John E. Motz).

References

Aberle N, Malzahn AM (2007) Interspecific and nutrient-dependent variations in stable isotope fractionation: experimental studies simulating pelagic multitrophic systems. Oecologia 154:291–303

Ayliffe LK, Chivas AR (1990) Oxygen isotope composition of the bone phosphate of Australian kangaroos: potential as a palaeoenvironmental recorder. Geochim Cosmochim Acta 54:2603–2609

Baas M, Briggs DEG, van Heemst JDH, Kear AJ, de Leeuw JW (1995) Selective preservation of chitin during the decay of shrimp. Geochim Cosmochim Acta 59:945–951

Boetius A, Lochte K (1994) Regulation of microbial enzymatic degradation of organic-matter in deep-sea sediments. Mar Ecol Prog Ser 104:299–307

Cott HB (1929) The Zoological Society's expedition to the Zambesi, 1927: No. 3 Observations on the natural history of the racing crab *Ocypode ceratophtalma*, from Beira. Proc Zool Soc Lond 1929:755–765

Crane J (1941) Eastern Pacific expeditions of the New York Zoological Society. XXIX. On the growth and ecology of brachyuran crabs of the genus *Ocypode*. Zoologica 26:297–310

DeNiro MJ, Epstein S (1978) Influence of diet on the distribution of carbon isotopes in animals. Geochim Cosmochim Acta 42:495–506

DeNiro MJ, Epstein S (1981a) Influence of diet on the distribution of nitrogen isotopes in animals. Geochim Cosmochim Acta 45:341–351

DeNiro MJ, Epstein S (1981b) Isotopic composition of cellulose from aquatic organisms. Geochim Cosmochim Acta 45:1885–1894

Doi H, Kikuchi E, Takagi S, Shikano S (2006) Selective assimilation by deposit feeders: experimental evidence using stable isotope ratios. Basic Appl Ecol 7:159–166

Doi H, Kikuchi E, Takagi S, Shikano S (2007) Changes in carbon and nitrogen stable isotopes of chironomid larvae during growth, starvation and metamorphosis. Rapid Commun Mass Spectrom 21:997–1002

Flannery MB, Stott AW, Briggs DEG, Evershed RP (2001) Chitin in the fossil record: identification and quantification of D-glucosamine. Org Geochem 32:745–754

France RL (1994) Nitrogen isotopic composition of marine and freshwater invertebrates. Mar Ecol Prog Ser 115:205–207

Fry B, Sherr EB (1984) $\delta^{13}C$ measurements as indicators of carbon flow in marine and freshwater systems. Contrib Mar Sci 27:13–47

Grey J, Kelly A, Jones RI (2004) High intraspecific variability in carbon and nitrogen stable isotope ratios of lake chironomid larvae. Limnol Oceanogr 49(1):239–244

Hadwen WL, Arthington AH (2007) Food webs of two intermittently open estuaries receiving ^{15}N-enriched sewage effluent. Estuar Coast Shelf Sci 71:347–358

Hayes JM (1993) Factors controlling ^{13}C contents of sedimentary organic compounds: principles and evidence. Mar Geol 113:111–125

Hillman K, Gooday GW, Prosser JI (1989) The mineralization of chitin in the sediments of the Ythan Estuary, Aberdeenshire, Scotland. Estuar Coast Shelf Sci 29:601–612

Kulkarni KM (1983) Some changes in the biochemical composition of the sand crab, *Emerita holthuisi*, during molt cycle. Comp Physiol Ecol 8:202–204

McCarroll D, Loader NJ (2004) Stable isotopes in tree rings. Quat Sci Rev 23:771–801

Miller RF (1984) Stable isotopes of carbon and hydrogen in the exoskeleton of insects: developing a tool for paleoclimatic research. University of Waterloo, Dissertation

Miller RF (1991) Chitin paleoecology. Biochem Syst Ecol 19:401–411

Miller RF, Orr GL, Fritz P, Downer RGH, Morgan AV (1985) Stable carbon isotope ratios in *Periplaneta americana* L., the American cockroach. Can J Zool 63:584–589

Miller RF, Voss-Foucart MF, Toussaint C, Jeuniaux C (1993) Chitin preservation in Quaternary Coleoptera: preliminary results. Palaeogeogr Palaeocl 103:133–140

Minagawa M, Wada E (1984) Stepwise enrichment of ^{15}N along food chains: further evidence and the relation between $\delta^{15}N$ and animal age. Geochim Cosmochim Acta 48:1135–1140

Montoya JP (1994) Nitrogen isotope fractionation in the modern ocean: implications for the sedimentary record. In: Zahn R, Pedersen TF, Kaminski MA, Labeyrie L (eds) Carbon cycling in the glacial ocean: constraints on the ocean's role in global change. NATO ASI Series I: Global Environmental Change, vol 17, pp 259–279

Motz JE (2000) Oxygen and hydrogen isotopes in fossil insect chitin as paleoenvironmental indicators. Dissertation, University of Waterloo

Motz JE, Edwards TWD, Buhay WM (1997) Use of nickel-tube pyrolysis for hydrogen-isotope analysis of water and other compounds. Chem Geol 140:145–149

Muzzarelli RAA (1977) Chitin. Pergamon, Oxford

Muzzarelli RAA, Jeuniaux C, Gooday GW (eds) (1985) Chitin in nature and technology. Plenum, New York

Overmyer JP, MacNeil MA, Fisk AT (2008) Fractionation and metabolic turnover of carbon and nitrogen stable isotopes in black fly larvae. Rapid Commun Mass Spectrom 22:694–700

Post DM (2002) Using stable isotopes to estimate trophic level position: models, methods, and assumptions. Ecology 83:703–718

Poulicek M, Jeuniaux C (1991) Chitin biodegradation in marine environments – an experimental approach. Biochem Syst Ecol 19:385–394

Rau GH, Sweeney RE, Kaplan IR, Mearns AJ, Young DR (1981) Differences in animal ^{13}C, ^{15}N and D abundance between a polluted and an unpolluted coastal site: likely indicators of sewage uptake by a marine food web. Estuar Coast Shelf Sci 13:701–707

Ricker WE (1973) Linear regressions in fishery research. J Fish Res Board Can 30:409–434

Schimmelmann A, DeNiro MJ (1985) Determination of oxygen stable isotope ratios in organic matter containing carbon, oxygen, hydrogen, and nitrogen. Anal Chem 57:2644–2646

Schimmelmann A, DeNiro MJ (1986a) Stable isotopic studies on chitin. Measurements on chitin/chitosan isolates and D-glucosamine hydrochloride from chitin. In: Muzzarelli RAA, Jeuniaux C, Gooday GW (eds) Chitin in nature and technology. Plenum, New York, pp 357–364

Schimmelmann A, DeNiro MJ (1986b) Stable isotopic studies on chitin II. The $^{13}C/^{12}C$ and $^{15}N/^{14}N$ ratios in arthropod chitin. Contrib Mar Sci 29:113–130

Schimmelmann A, DeNiro MJ (1986c) Stable isotopic studies on chitin III. The $^{18}O/^{16}O$ and D/H ratios in arthropod chitin. Geochim Cosmochim Acta 50:1485–1496

Schimmelmann A, DeNiro MJ, Poulicek M, Voss-Foucart MF, Goffinet G, Jeuniaux C (1986) Isotopic composition of chitin from arthropods recovered in archaeological contexts as palaeoenvironmental indicators. J Archaeol Sci 13:553–566

Schimmelmann A, Lavens P, Sorgeloos P (1987) Carbon, nitrogen, oxygen and hydrogen stable isotope ratios in *Artemia* from different geographical origin. In: Sorgeloos P, Bengtson DA, Decleir W, Jaspers E (eds) Morphology, genetics, strain characterization, toxicology. *Artemia* research and its applications, vol 1. Universal, Wetteren, Belgium, pp 167–172

Schimmelmann A, Wintsch RP, Lewan MD, DeNiro MJ (1998) From modern chitin to thermally mature kerogen: lessons from nitrogen isotope ratios. In: Stankiewicz BA, van Bergen PF (eds) Nitrogen-containing macromolecules in the biosphere and geosphere, vol 707, American Chemical Society Symposium Series. American Chemical Society, Washington DC, pp 226–242

Schoeninger M, DeNiro MJ (1984) Nitrogen and carbon isotopic composition of bone collagen from marine and terrestrial animals. Geochim Cosmochim Acta 48:625–639

Simon A, Poulicek M, Velimirov B, Mackenzie FT (1994) Comparison of anaerobic and aerobic biodegradation of mineralized skeletal structures in marine and estuarine conditions. Biogeochemistry 25:167–195

Stankiewicz BA, Briggs DEG, Evershed RP (1997) Chemical composition of Paleozoic and Mesozoic fossil invertebrate cuticles as revealed by pyrolysis-gas chromatography/mass spectrometry. Energy Fuels 11:515–521

Stankiewicz BA, Briggs DEG, Evershed RP, Miller RF, Bierstedt A (1998a) The fate of chitin in Quaternary and Tertiary strata. In: Stankiewicz BA, van Bergen PF (eds) Nitrogen-containing

macromolecules in the biosphere and geosphere, vol 707, American Chemical Society Symposium Series. American Chemical Society, Washington DC, pp 211–224

Stankiewicz BA, Mastalerz M, Hof CHJ, Bierstedt A, Flannery MB, Briggs DEG, Evershed RP (1998b) Biodegradation of the chitin-protein complex in crustacean cuticle. Org Geochem 28:67–76

Struck U, Voss M, von Bodungen B (1998) Stable isotopes of nitrogen in fossil cladoceran exoskeletons: Implications for nitrogen sources in the central Baltic Sea during the past Century. Naturwissenschaften 85:597–603

Tibbets TM, Wheeless LA, Martinez del Rio C (2008) Isotopic enrichment without change in diet: an ontogenetic shift in $\delta^{15}N$ during insect metamorphosis. Funct Ecol 22:109–113

Vigh DA, Dendinger JE (1982) Temporal relationships of postmolt deposition of calcium, magnesium, chitin and protein in the cuticle of the Atlantic blue crab, *Callinectes sapidus* Rathbun. Comp Biochem Physiol 72A:365–369

Wang Y, Francis DR, O'Brien DM, Wooller MJ (2008) A protocol for preparing subfossil chironomid head capsules (Diptera: Chironomidae) for stable isotope analysis in paleoclimate reconstruction and considerations of contamination sources. J Paleolimnol 40:771–781

Webb SC, Hedges REM, Simpson SJ (1998) Diet quality influences the $\delta^{13}C$ and $\delta^{15}N$ of locusts and their biochemical components. J Exp Biol 201:2903–2911

Wooller MJ, Francis D, Fogel ML, Walker MGH, IR WAP (2004) Quantitative paleotemperature estimates from $\delta^{18}O$ of chironomid head capsules preserved in arctic lake sediments. J Paleolimnol 31:267–274

Wooller MJ, Wang Y, Axford Y (2008) A multiple stable isotope record of Late Quaternary limnological changes and chironomid paleoecology from northeastern Iceland. J Paleolimnol 40:63–77

Chapter 5
Hydrogen Isotopes in Beetle Chitin

Darren R. Gröcke, Maarten van Hardenbroek, Peter E. Sauer, and Scott A. Elias

Contents

Abstract Beetles, one of the most diverse and long-lived animal groups, provide a trove of ecological and palaeoenvironmental information largely because their exoskeletons contain chitin, a highly resistant biopolymer which preserves well in the geological record. In addition to palaeoenvironmental inferences that can be derived from presence or absence of particular taxa, beetle chitin records the hydrogen stable isotope ratios (D/H) of environmental water, which is related to temperature and other environmental variables. Because the vast majority of beetle fossils consists of incomplete body parts, the H isotopic variability within and between beetle specimens must be quantified. We provide data that show intra- and inter-specimen D/H variation in modern water beetles that may relate to systematic variations in chitin biosynthesis during exoskeleton development. A discussion of existing hydrogen-isotope studies of chitin are presented, including recent advances in hydrogen-isotope analysis that can enhance sample throughput.

D.R. Gröcke (✉)
Department of Earth Sciences, Durham University, Science Labs, Durham, DH1 3LE, UK
e-mail: d.r.grocke@durham.ac.uk

M. van Hardenbroek
Institute of Environmental Biology, Palaeoecology, Laboratory of Palaeobotany and Palynology, Utrecht University, Budapestlaan 4, 3584 CD Utrecht, The Netherlands
e-mail: m.r.vanhardenbroek@uu.nl

P.E. Sauer
Department of Geological Sciences, Indiana University, Bloomington, IN 47405-1405, USA
e-mail: pesauer@indiana.edu

S.A. Elias
Department of Geography, Royal Holloway University of London, Egham, Surrey TW20 0EX, UK
e-mail: s.elias@rhul.ac.uk

N.S. Gupta (ed.), *Chitin,* Topics in Geobiology 34,
DOI 10.1007/978-90-481-9684-5_5,

5.1 Introduction

Until a decade ago, the analytical arsenal of Quaternary palaeoclimate reconstruction in the terrestrial realm was almost exclusively dependent upon palynology with some contribution based on other proxy indicators of climate, such as plant macrofossils, chironomids, and tree rings. In addition, isotope-derived palaeotemperature estimates have become relatively common in recent years, mainly from deep-sea sediments, polar ice cores, and lake sediments. For instance, the analysis of oxygen-isotope ratios from fossil foraminifera has been an essential part of the reconstruction of sea-surface temperatures (e.g., Shackleton and Opdyke 1973; Bauch and Erlenkeuser 2003). Likewise, hydrogen- and oxygen-isotope analyses have played a pivotal role in the palaeoclimatic interpretation of Greenland and Antarctic ice-core records (e.g., Dansgaard et al. 1989; Grootes et al. 2002).

A lack of quantitative palaeoclimatological reconstructions is apparent for mid- to high-latitude terrestrial environments, although stable-isotope ratios in ostracods, peat cores, groundwaters, speleothems, vertebrate fossils, and even freshwater diatoms have occasionally been utilized. For example, lake sediments containing calcium carbonate have yielded oxygen-isotope reconstructions of palaeoenvironmental water (e.g., Oeggl and Eicher 1989; Talbot 1990), but suitable limnic sediments are not available in every region. Even than aquatic proxies are speleothems, vertebrate fossils, and pre-Holocene dendrochronological records.

Stable-isotope ratios of biologically important elements such as C, H, N, and O have widespread application in earth science and biology, with proven utility in addressing questions of palaeoclimate, animal origin and migration, trophic level status, and nutrient availability. Despite problems posed by diagenesis and low preservation potential for organic materials, analysis of fossil organic material has been emphasized because it is a primary record of the life conditions for an organism. Of the most abundant elemental constituents of organic matter (C, H, N, O, and S), hydrogen has received the least attention due to several factors (primarily, exchangeable hydrogen) that have, until recently, complicated the analysis and interpretation of H isotope data derived from organic materials. Recent advances in analytical techniques (Bowen et al. 2005b; Filot et al. 2006; Sauer et al. 2009) for organic H have facilitated the analysis of large numbers of samples, and the scientific community is just beginning to explore fundamental controls on the variability in H isotope ratios (D/H) from organic matter preserved in the fossil record.

The concept of "you are what you eat" applies to animals. The large climatic fluctuations that occurred during the Quaternary inevitably forced animals to contend with vastly shifting diets through time. Fossil beetles and other insects thus carry palaeoclimatic information in their chitinous exoskeletons, where isotopic signatures in chitin relate to isotope ratios of their palaeodiet, which in turn is linked to palaeoenvironmental conditions. Previous research on H isotope ratios in organic materials (Cormie et al. 1994; Leyden et al. 2006) has revealed a strong climatic control in parallel to the strong D/H gradients in precipitation (Dansgaard 1964; Rozanski et al. 1993). Because many migratory bird (and some butterfly) species cross climatic gradients, D/H ratios of non-exchangeable H of feather keratin and

insect chitin has been used to document migration patterns (Hobson et al. 1999; Gröcke et al. 2006; Hobson and Wassenaar 2008). D/H ratios in collagen from large herbivores (North American bison) have been shown to vary through the Holocene and track changes in moisture availability and temperature (Leyden et al. 2006). Trophic levels influence N-isotope ratios due to well-understood mechanisms (e.g., Robbins et al. 2005), and preliminary studies indicate similar trophic level controls may affect H isotope ratios (Birchall et al. 2005; Reynard and Hedges 2008). Due to metabolic effects and inefficiencies in nutrient transfer up food chains, higher-level consumers exhibit higher N-isotope ratios than their prey. Similarly, a study of several European archaeological sites showed a progressive enrichment of D in bone collagen from herbivores (deer, sheep, cow, horse) to omnivores (pigs) to carnivores (humans), with a total enrichment of 20–50‰ (Reynard and Hedges 2009). A similar trophic-level effect in beetle chitin may be expected and requires investigation.

The relationship between the D/H ratio of chitin, or at least of insect biomass containing chitin, and the D/H of meteoric water in the organism's habitat has been demonstrated by several studies, using ladybird beetles (Coccinellidae) (Ostrom et al. 1997), Monarch butterflies (*Danaus plexippus*) (Wassenaar and Hobson 1998; Hobson et al. 1999) and beetles belonging to various families (Miller et al. 1988). Additional hydrogen-isotope data for modern arthropod chitin samples (Schimmelmann and DeNiro 1986a,b) and a few archaeological chitin samples (Schimmelmann et al. 1986) focused on marine non-exchangeable hydrogen in chitin, making these D/H data incompatible with data from other studies (reviewed by Schimmelmann and Miller 2002). Schimmelmann et al. (1993) demonstrated that exchangeable hydrogen in chitin could be equilibrated with isotopically controlled water vapour, thus reducing isotopic noise in the determination of D/H in bulk chitin and avoiding chemical derivatization. The same study applied the equilibration method to a set of ca. 11 kyr old beetle chitins from Nova Scotia, with D/H data representing mixtures of more than one beetle species. The aim was to focus on ground beetles (Carabidae), because they are carnivores and therefore their diet (other invertebrates) averages across a broad spectrum of isotopically divergent sources. Herbivorous beetles rely on specific host plants that may reflect a particular enrichment or depletion of deuterium (or other isotopes) in their tissues, thus potentially affecting the D/H value of the chitin that forms in these beetles.

The hydrogen isotope composition of environmental water varies widely and systematically across the globe, and strong and well-understood correlation exists between D/H ratios in precipitation and temperature (Dansgaard 1964; Rozansky et al. 1993). Because water is a key constituent of many biosynthesis reactions, the isotope signature present in local environmental water is transferred to organisms that live in it (Estep and Dabrowski 1980; Hobson et al. 1999). Aquatic insects such as water beetles 'lock' this isotope signature in their exoskeletons, as chitin is a compound that is chemically very stable. In lakes where evaporation is limited and water is in isotopic equilibrium with precipitation, water beetles thus record the isotopic signature of precipitation at the time of chitin synthesis (Schimmelmann et al. 1993; Gröcke et al. 2006), which makes water beetle chitin a valuable source

of climatic information. Because chitin can preserve up to 25 million years in the fossil record (Stankiewicz et al. 1997; Flannery et al. 2001) it provides scientists with an extremely proxy for reconstructing the terrestrial palaeoclimatic well into the deep geologic past.

In order to interpret lacustrine isotope records it is vital to understand them in the context of lake hydrology. In most large, open-basin lakes, lake water is isotopically representative of mean annual precipitation. In lakes where evaporation is an important factor in the water balance (e.g., lakes that are small, closed or in arid regions) isotopic ratios (D/H and $^{18}O/^{16}O$) increase through the preferential removal of the lighter isotope (Gonfiantini 1986). Using records of past lake isotopic composition, it is possible to interpret records of either past temperature or hydrologic conditions, depending on the hydrologic status of the lake in question (e.g., Wolfe et al. 1996; Leng 2003).

Lake water is the main source of hydrogen for aquatic plants and animals as the food chain is based on plant matter that grows in situ. Good correlations have been observed between isotope ratios in meteoric water and animal tissue that is biochemically inert after synthesis such as feathers, hair and nails (Bowen et al. 2005). A similarly good correlation is to be expected between meteoric water and aquatic animal tissue since fractionation effects in lacustrine environments are similar in size or smaller than fractionation effects in terrestrial environments (Sauer et al. 2001a, b). This is especially true for regions with high precipitation, where evaporation does not have a major effect on the isotopic composition of lake water (Leng 2003; Leng et al. 2006). However, high latitude sites must be treated with caution since they have low precipitation levels and with evaporation that might cause a drop in water level, this could lead to highly enriched hydrogen and oxygen isotope values. Additionally, where the stable isotope ratios of meteoric inputs to a lake can be inferred from groundwater proxies or other means, the degree of D or ^{18}O enrichment in small, shallow ponds can be used to infer aridity, particularly when evaporation dominates for the summer months.

Lakes offer many different proxies for isotopic analysis where calcareous elements, biogenic silica, or organic material are inferred to represent past lake water isotopic composition (e.g., Stuiver 1970; Duthie et al. 1996; Von Grafenstein et al. 1999; Wolfe et al. 2001; Leng et al. 2006). However, some lakes are acidic and carbonate records are not present. In these cases, lacustrine organic matter is useful to obtain palaeo-isotope records (Edwards 1993). A common source of lacustrine organic matter that is used for palaeo-isotope analysis is cellulose (Sauer et al. 2001b; Wolfe et al. 2001), however cellulose of unequivocal aquatic origin is rarely continuously present (Sauer et al. 2001a).

Chitin is an under-utilised source of palaeo-isotope records from lakes, even though it contains a high amount of oxygen and hydrogen (Miller 1991). It was found that the amount of beetle chitin that was preserved in late-glacial and last interglacial deposits comprised 10–30% of the dry weight of fossil beetle fragments, which is half to three-quarters of the amount of chitin found in modern insects (Miller et al. 1993). This makes chitin preserved in lake sediments a very suitable proxy for palaeoenvironmental reconstructions (Schimmelmann et al. 1986, 2006).

More recently, Wang et al. (2009) demonstrate that 31% of hydrogen in chironomid larvae is derived from habitat water in culturing experiments. Comparable culturing studies will need to be undertaken to test this dependency in water beetles.

A number of chitin producing organisms such as chironomids (the larvae of non-biting midges) and aquatic beetles have been used for palaeoenvironmental reconstructions because of the ecological significance of their occurrences (e.g., Brooks 2006; Elias 2006). Combining climatic, environmental and isotopic information from these proxies has only been adopted in a few studies to date (Miller et al. 1988; Schimmelmann et al. 1993; Wooller et al. 2004, 2008; Gröcke et al. 2006).

The stable isotope 'signal' of lake water is locked into the chitin at the moment of chitin synthesis, which happens in a relatively short period when the exoskeleton is formed during metamorphosis into the adult stage in a period of hours to days (Candy and Kilby 1962; Surholt 1975). It has been assumed that chitin is homogenous and represents the lake water at the time of chitin synthesis and hardening, although systematic biochemical fractionations will take place because of vital effects (Urey et al. 1951; Wooller et al. 2004; Wang et al. 2009). In this manner, the isotopic ratio in beetle chitin provides a source of climatic and environmental information (Schimmelmann et al. 1986; Gröcke et al. 2006). Although the biochemical processes involved in chitin synthesis are well understood (Merzendorfer 2005), there is virtually no information about isotopic fractionation processes during chitin synthesis. Therefore, we present here some preliminary data on D/H in modern beetle chitin to test the relation between lake water and beetle chitin as well as the variability within a single specimen and between specimens from the same location (discussed below).

We anticipate that there will be greater interest in beetle chitin D/H investigations with the improved grid of geographic D/H distribution from precipitation (IAEA 2001; Bowen and Wilkinson 2002; Fig. 5.1) and advances in mass-spectrometry and Mutual Climatic Range analysis of fossil Coleoptera (Miller and Elias 2000; Bray et al. 2006; Elias 2006) warrant revisiting stable isotope analysis of chitin from fossil beetles as a palaeoclimate tool. It is not apparent how trophic levels, water loss, food-derived water, isolated waters on the microscale (i.e., small ponds) influence D/H values of beetle chitin, although a detailed study parallel to one performed on lab-raised quail (Hobson et al. 1999) and chironomids (Wang et al. 2009) should be undertaken on beetles.

5.2 Analytical Advances in Hydrogen-Isotope Measurements

Hydrogen in organic matter can occupy many different positions in organic molecules, and the different environmental and biological factors thus influence the D/H ratio. Since H is only loosely bound to O and N, the H in these positions exchanges readily with ambient water. The amount of exchangeable hydrogen is expressed as percentage of the total amount of hydrogen and is 15.3 ± 2.9% in chitin

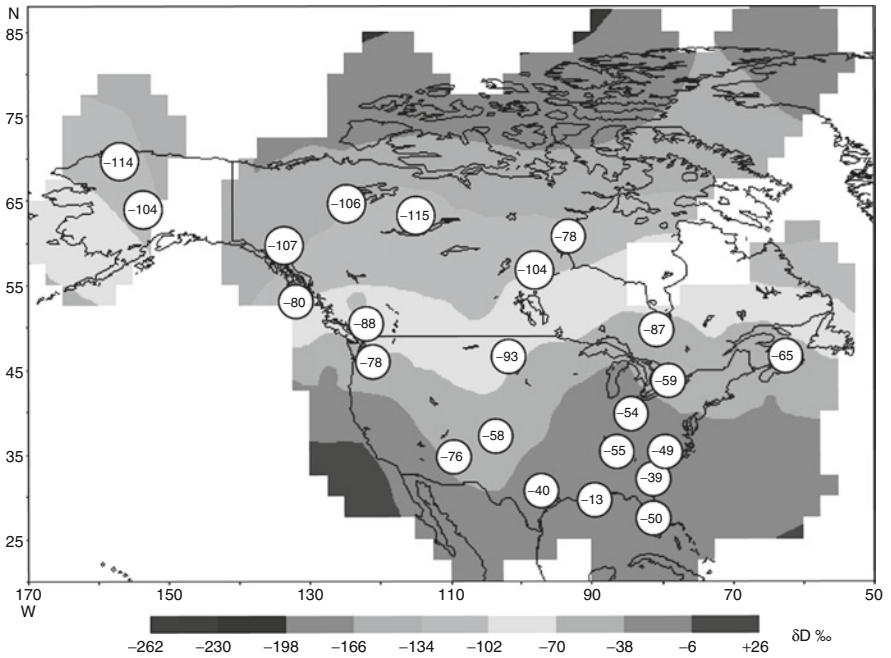

Fig. 5.1 Precipitation map for June (IAEA 2001) against D/H values from "nitrated" beetles in North America (data from Miller et al. 1988). D/H values within the *white circles* are either single isotopic results or averages from a single location

(Schimmelmann et al. 1993). For this reason, the D/H ratio of these H pools provide both information about the recent exposure to water vapour (e.g., in laboratory air) and information about primary environmental or biological conditions.

Schimmelmann and Miller (2002) reviewed different analytical strategies to eliminate or isotopically control the exchangeable hydrogen from chitin in order to arrive at reproducible D/H ratios characterizing only non-exchangeable organic hydrogen in chitin. Different analytical approaches targeted different pools of non-exchangeable hydrogen, eliminated some exchangeable hydrogen, or chose to isotopically account for exchangeable hydrogen. As a result, D/H values from different methods are typically not quantitatively comparable, although each method provides internally meaningful information about relative D/H differences among chitins. Thus, within each study, comparability of data mandates that all chitin samples (including internal standards), both modern and fossil, must be processed in the same fashion following the so-called "Principle of Identical Treatment" (Werner and Brand 2001). It was concluded that an equilibration of exchangeable hydrogen in chitin with H_2O with a known D/H value, followed by drying and high-temperature pyrolytic liberation of H_2 from chitin in presence of excess carbon, provides the most economical analytical approach while requiring the least amount of sample.

In order to remove the effect of H on the analysis of organic material, the O- and N- bound H must be either removed. Chemical removal can be performed on certain materials (e.g., nitration of cellulose; Epstein et al. 1976), but is labour-intensive, requires a larger initial sample. Moreover, this is possible only with certain materials with well-defined chemical structures. The "nitration" method removes a significant portion of exchangeable organic hydrogen in hydroxyl groups (–OH) via esterification (i.e., formation of $–ONO_2$ groups). Some hydroxyl groups in chitin are sterically hindered and thus not accessible by nitric acid, whereas the smaller water molecules can still cause hydrogen isotopic exchange (Miller et al. 1988). A simpler and more general approach is to control the D/H ratio of the exchangeable H by means of exposure to a vapour of known isotopic composition and controlled temperature (Schimmelmann 1991; Sauer et al. 2009). By exposing aliquots of each sample to two or more isotopically distinct water vapours, it is possible to calculate both the D/H of non-exchangeable H and the fraction of organic H that exchanges, which is a useful proxy of chemical alteration during diagenesis. Equilibration is performed either at room temperature for several days (e.g., Bowen et al. 2005) or in a heated chamber supplied with vapour of known D/H ratio for several hours (Schimmelman 1991; Filot et al. 2006; Sauer et al. 2009). Current methods allow the simultaneous processing of 40 samples or more, enhancing sample throughput. By coupling this equilibration technique with the automated H isotopic analysis of modern instrumentation (such as a ThermoFinnigan mass spectrometer configured with a TC/EA inlet), it is possible to analyze hundreds of samples per month.

5.3 Inter- and Intra-Isotopic Variability in D/H Beetle Chitin

Another factor that must be taken into consideration is variation in isotopic composition of chitin from various parts of the exoskeleton of arthropods. In order to test the variability within and between specimen of the same species we dissected three large predaceous diving beetles (*Dytiscus harrisii)* from a museum collection. One specimen was collected in 1978 and two specimens in 1981 from Houghton Pond, Ithaca, New York State, USA. Soft tissue was chemically removed by boiling for 24 h in 1N NaOH and carbonates were removed by washing with 10% HCl. Subsequently, the samples were rinsed repeatedly with deionized water before freeze-drying. The specimens were sub-sampled and analysed on a TCEA connected to a ThermoFinnigan Delta Plus XP isotope-ratio mass-spectrometer, as described by van Hardenbroek et al. (in prep.)

The D/H values of the samples from the two specimens from 1981 are similar: 2 ± 9‰ (n = 50) and 0 ± 7‰ (n = 33), as shown in Fig. 5.2, which indicates that specimens collected in the same place and in the same year do not vary greatly between one another. The 1978 specimen has D/H values that are approximately 15‰ higher (15 ± 8‰; n = 33) than the 1981 specimens, which indicates that the isotopic values can vary between years (see Table 5.1). As all specimens are from

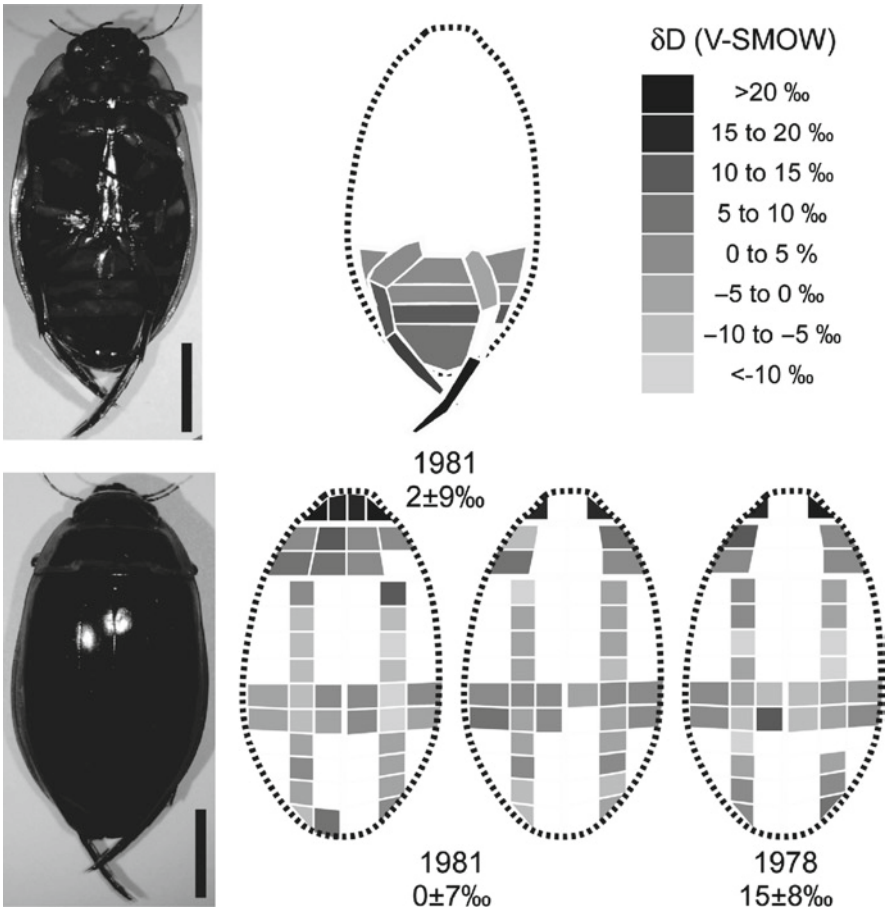

Fig. 5.2 Internal variability of D/H in head, pronotum and elytra of one specimen collected in 1978 (*right*) and two specimens collected in 1981 (*middle* and *left*). For one 1981 specimen (*left*) the abdomen and hind legs were analysed as well. All values are corrected to VSMOW. Note that15‰ should be added to values in the legend to interpret the 1978 specimen. Scale bar represents 1 cm

Table 5.1 Variability between different body parts of three specimens of *Dytiscus harrisii* from Houghton Pond, Ithaca, NY State, USA (van Hardenbroek 2006)

Specimen	Body part	n	Variation in D/H (‰)
1978	Head	2	34
	Pronotum	4	21 ± 5
	Elytra	27	13 ± 5
1981	Head	2	15
	Pronotum	4	3 ± 7
	Elytra	27	–2 ± 6
1981	Head	4	20 ± 3
	Pronotum	8	4 ± 4
	Elytra	29	–3 ± 6
	Hind legs	5	11 ± 11
	Abdomen	4	7 ± 5

the same location and species, this variation is not caused by differences in feeding strategy, but must be attributed to different D/H values of their hydrogen source, be it lake water or food.

Furthermore, the δD values of heads and the outermost part of legs are 10–15‰ higher than the other parts of the exoskeleton (Table 5.1; Fig. 5.2). This difference is significant ($p < 0.01$ for each of the three specimens). Schimmelmann and DeNiro (1986) measured variance in five body sections from a Northern lobster (*Homarus americanus*) and recorded much lower variance in D/H (~5‰). Miller et al. (1988) performed repeated analyses of D/H ratios from one to four beetles each from six different taxa from locations in Canada. They found standard deviation values between specimens on the order of 2–6‰ for repeated measurements of these same specimens. Similar to this pilot study, Wassenaar and Hobson (2006) showed a variance in D/H of 3–13‰ in keratin from single feathers from different species of wild birds.

In this pilot study, a variance of 10–15‰ in D/H "deviation values between specimens on the order" values was observed between different parts of the same specimen of the water beetle, *D. harrisii*. These different variances could indicate two things. First, it could indicate that proteinaceous material, which has high amounts of exchangeable hydrogen, may not have been completely removed in sample pre-treatments. Since legs and head are hollow 'chambers' these body parts are more likely to still contain protein-rich tissue. If the variation in D/H values is not caused by the removal of all the exchangeable hydrogen, then it could be that there is an additional fractionation effect that influences D/H during chitin synthesis of these parts of the body. Although this aspect requires further detailed investigation, the upside to this pilot study result is that sediment records typically only contain elytra and pronota, which can be identified, and they have less D/H variability (Fig. 5.2 and Table 5.1).

Acknowledgements The museum specimens were kindly provided (i.e. sacrificed) by Dr. P. Bouchard and Mr. A.E. Davies at the Canadian National Collection of Insects, Agriculture and Agri-Food Canada.

References

Bauch HA, Erlenkeuser H (2003) Implications of subarctic deepwater foraminiferal $\delta^{18}O$ for interpreting glacial-interglacial changes in sea level/ice volume and climate. In: Droxler AW, Poore RZ, Burckle LH (eds) Earth's climate and orbital eccentricity: The Marine Isotope Stage 11 question, American Geophysical Union Geophys Monogr 137:87–102

Birchall J, O'Connell TC, Heaton THE, Hedges REM (2005) Hydrogen isotope ratios in animal body protein reflect trophic level. J Animal Ecol 74:877–881

Bowen GJ, Wilkinson B (2002) Spatial distribution of $\delta^{18}O$ in meteoric precipitation. Geology 30:315–318

Bowen GJ, Wassenaar LI, Hobson KA (2005a) Global application of stable hydrogen and oxygen isotopes to wildlife forensics. Oecologia 143:337–348

Bowen GJ, Chesson L, Nielson K, Cerling TE, Ehleringer JR (2005b) Treatment methods for the determination of $\delta^{2}H$ and $\delta^{18}O$ of hair keratin by continuous-flow isotope-ratio mass spectrometry. Rapid Commun Mass Spectrom 19:2371–2378

Bray PJ, Blockley SPE, Coope GR, Dadswell LF, Elias SA, Lowe JJ, Pollard AM (2006) Refining mutual climatic range (MCR) quantitative estimates of palaeotemperature using ubiquity analysis. Quatern Sci Rev 25:1865–1876

Brooks SJ (2006) Fossil midges (Diptera: Chironomidae) as palaeoclimatic indicators for the Eurasian region. Quatern Sci Rev 25:1894–1910

Candy DJ, Kilby BA (1962) Studies on Chitin Synthesis in the Desert Locust. J Exp Biol 39:129–140

Cormie AB, Schwarcz HP, Gray J (1994) Relation between hydrogen isotopic ratios of bone collagen and rain. Geochim Cosmochim Acta 58:377–391

Dansgaard W, White JWC, Johnsen J (1989) The abrupt termination of the Younger Dryas climate event. Nature 339:532–534

Duthie HC, Yang J-R, Edwards TWD, Wolfe BB, Warner BG (1996) Hamilton Harbour, Ontario: 8,300 years of limnological and environmental change inferred from microfossil and isotopic analyses. J Paleolimnol 15:79–97

Edwards TWD (1993) Interpreting past climate from stable isotopes in continental organic matter. In: Swart PK, Lohmann KC, McKenzie J, Savin S (eds), Climatic change in continental isotopic records. American Geophysical Union, Geophys Monogr 78:333–341

Elias SA (2006) Quaternary beetle research: the state of the art. Quatern Sci Rev 25:1731–1737

Epstein S, Yapp CJ, Hall JH (1976) The determination of the D/H ratio of non-exchangeable hydrogen in cellulose extracted from aquatic and land plants. Earth Planet Sci Lett 30:241–251

Estep MF, Dabrowski H (1980) Tracing foodwebs with stable hydrogen isotopes. Science 209:1537–1538

Filot MS, Leuenberger M, Pazdur A, Boettger T (2006) Rapid online equilibration method to determine the D/H ratios of non-exchangeable hydrogen in cellulose. Rapid Comm Mass Spec 20:3337–3344

Flannery MB, Stott AW, Briggs DEG, Evershed RP (2001) Chitin in the fossil record: identification and quantification of D-glucosamine. Org Geochem 32:745–754

Gonfiantini R (1986) Environmental isotopes in lake studies. In: Fritz P, Fontes JC (eds) Handbook of environmental isotope geochemistry, vol 2, The terrestrial environment. Elsevier, New York, pp. 113–168

Gröcke DR, Schimmelmann A, Elias S, Miller RF (2006) Stable hydrogen-isotope ratios in beetle chitin: preliminary European data and re-interpretation of North American data. Quat Sci Rev 25:1850–1864

Grootes PM, Steig EJ, Stuiver M, Waddington ED, Morse DL, Nadeau MJ (2002) The Taylor Dome Antarctic $\delta^{18}O$ record and globally synchronous changes in climate. Quat Res 56:289–298

Hobson KA, Wassenaar LI, Taylor OR (1999) Stable isotopes (δD and $\delta^{13}C$) are geographic indicators of natal origins of monarch butterflies in eastern North America. Oecologia 120:397–404

Hobson KA, Wassenaar LI (2008) Tracking Animal Migration with Stable Isotopes. Terrestrial Ecology Volume 2. Academic Press. pp. 160

International Atomic Energy Agency (2001) GNIP maps and animations. http://www-naweb.iaea.org/napc/ih/IHS_resources_gnip.html

Leng MJ (2003) Stable isotopes in lakes and lake sediment archives. In: Mackay A, Battarbee R, Birks J, Oldfield F (eds) Global change in the holocene. Arnold, London, pp. 124–139

Leng MJ, Lamb AA, Heaton THE, Marshall JD, Wolfe BB, Jones MD, Holmes JA, Arrowsmith C (2006) Isotopes in lake sediments. In: Leng MJ (ed) Isotopes in palaeoenvironmental research. Springer, Dordrecht, pp. 147–184

Leyden JJ, Wassenaar LI, Hobson KA, Walker EG (2006) Stable hydrogen isotopes of bison bone collagen as a proxy for Holocene climate on the Northern Great Plains. Palaeogeogr Palaeoclimatol Palaeoecol 239:87–99

Merzendorfer H (2005) Insect chitin synthases: a review. J Comp Physiol B 176:1–15

Miller RF (1991) Chitin paleoecology. Biochem Syst Ecol 19:401–411

Miller RF, Fritz P, Morgan AV (1988) Climatic implications of D/H ratios in beetle chitin. Palaeogeogr Palaeocl 66:277–288
Miller RF, Vos-Foucart M-F, Toussaint C, Jeuniaux C (1993) Chitin preservation in Quaternary Coleoptera: preliminary results. Palaeogeogr Palaeocl 103:133–140
Miller RF, Elias SA (2000) Late-glacial climate in Maritime Canada, reconstructed from Mutual Climatic Range analysis of fossil Coleoptera. Boreas 29:79–88
Oeggl K, Eicher U (1989) Pollen and oxygen isotope analyses of late- and postglacial sediments from the Schwemm raised bog near Walchsee in Tirol, Austria. Boreas 18:245–253
Ostrom PH, Colunga-Garcia M, Gage SH (1997) Establishing pathways of energy flow for insect predators using stable isotope ratios: field and laboratory evidence. Oecologia 109:108–113
Reynard LM, Hedges REM (2008) Stable hydrogen isotopes of bone collagen in palaeodietary and palaeoenvironmental reconstruction. J Archaeol Sci 35:1934–1942
Robbins CT, Felicetti LA, Sponheimer M (2005) The effect of dietary protein quality on nitrogen isotope discrimination in mammals and birds. Oecologia DOI 10.1007/s00442-005-0021–8
Rozanski K, Araguds-Araguds L, Gonfiantini R (1993) Isotopic patterns in modem global precipitation. In: Swart PK, Lohmann KC, McKenzie J, Savin S (eds) Climate change in continental isotopic records. American Geophysical Union. Geophys Monogr 78:1–36
Sauer PE, Miller GH, Overpeck GH (2001a) Oxygen isotope ratios of organic matter in arctic lakes as a paleoclimate proxy: field and laboratory investigations. J Paleolimnol 25:43–64
Sauer PE, Eglinton TI, Hayes JM, Schimmelmann A, Sessions AI (2001b) Compound-specific D/H ratios of lipid biomarkers from sediments as a proxy for environmental and climatic conditions. Geochim Cosmochim Acta 65:213–222
Sauer PE, Schimmelmann A, Sessions AL, Topalov K (2009) Simplified batch equilibration for D/H determination of non-exchangeable hydrogen in solid organic matter. Rapid Comm Mass Spec 23:949–956
Schimmelmann A, DeNiro MJ (1986a) Stable isotopic studies on chitin. Measurements on chitin/chitosan isolates and D-glucosamine hydrochloride from chitin. In: Muzzarelli RAA, Jeuniaux C, Gooday GW (eds), Chitin in Nature and Technology. Plenum Publishing Corporation, New York, pp. 357–364
Schimmelmann A, DeNiro MJ (1986b) Stable isotopic studies on chitin. III. The D/H and $^{18}O/^{16}O$ ratios in arthropod chitin. Geochim Cosmochim Acta 50:1485–1496
Schimmelmann A (1991) Determination of the concentration and stable isotopic composition of non-exchangeable hydrogen in organic matter. Anal Chem 63:2456 –2459
Schimmelmann A, Miller RF (2002) Review of methods for the determination of deuterium/hydrogen stable isotope ratios in chitin. In: Muzzarelli RAA, Muzzarelli C (eds) Chitin in Pharmacy and Chemistry. Atec: 469–474
Schimmelmann A, DeNiro MJ, Poulicek M, Voss-Foucart M, Goffinet G, Jeuniaux C (1986) Stable isotopic composition of chitin from arthropods recovered in archaeological contexts as palaeoenvironmental indicators. J Archaeol Sci 13:553–566
Schimmelmann A, Miller RF, Leavitt SW (1993) Hydrogen isotopic exchange and stable isotope ratios in cellulose, wood, chitin, and amino compounds. In: Swart PK, Lohmann KC, McKenzie J, Savin S (eds) Climate change in continental isotopic records. American Geophysical Union. Geophys Monogr 78:367–374
Schimmelmann A, Sessions AL, Mastalerz M (2006) Hydrogen isotopic (D/H) composition of organic matter during diagenesis and thermal maturation. Annu Rev Earth Planet Sci 34:501–533
Shackleton NJ, Opdyke ND (1973) Oxygen isotope and palaeomagnetic stratigraphy of equatorial Pacific core V28-238: oxygen isotope temperatures and ice volumes on a 105 and 106 year scale, Quat Res 3:39–55
Stankiewicz BA, Briggs DEG, Evershed RP, Flannery MB, Wuttke M (1997) Preservation of Chitin in 25-Million-Year-Old Fossils. Science 276:1541–1543
Stuiver M (1970) Oxygen and carbon isotope ratios of fresh-water carbonates as climatic indicators. J Geophys Res 75:5247–5257
Surholt B (1975) Studies in vivo and in vitro on chitin synthesis during the larval-aldult moulting cycle of the migratory locust, Locusta migratoria L. J Comp Physiol 102:135–147

Talbot MR (1990) A review of the paleohydrological interpretation of carbon and oxygen isotope ratios in primary lacustrine carbonates. Chem Geol 80:261–279

Urey HC, Lowenstam HA, Epstein S, McKinney CR (1951) Measurement of paleotemperatures and temperatures of the Upper Cretaceous of England, Denmark, and the southeastern United States. Geol Soc Am Bull 62:399–416

Von Grafenstein U, Erlenkeuser H, Brauer A, Jouzel J, Johnsen SJ (1999) A mid-European decadal isotope-climate record from 15,500 to 5,000 years BP. Science 284:1654–1657

Wang Y, O'brien D, Jenson J, Francis D, Wooller M (2009) The influence of diet and water on the stable oxygen and hydrogen isotope composition of Chironomidae (Diptera) with paleoecological implications. Oecologia 160:225–233

Wassenaar LI, Hobson, KA (1998) Natal origins of migratory monarch butterflies at wintering colonies in Mexico: new isotopic evidence. Proc Nat Acad Sci 95:15436–15439

Wassenaar LI, Hobson KA (2006) Stable-hydrogen isotope heterogeneity in keratinous materials: mass spectrometry and migratory wildlife tissue sub-sampling strategies. Rapid Commun Mass Spectrom 20:2505–2510

Werner RA, Brand WA (2001) Referencing strategies and techniques in stable isotope ratio analysis. Rapid Commun Mass Spectrom 15:501–519

Wolfe BB, Edwards TWD, Aravena R, MacDonald GM (1996) Rapid Holocene hydrologic change along boreal treeline revealed by $\delta^{13}C$ and $\delta^{18}O$ in organic lake sediments, Northwest Territories, Canada. J Paleolimnol 15:171–181

Wolfe BB, Edwards TWD, Elgood RJ, Beuning KRM (2001) Carbon and oxygen isotope analysis of lake sediment cellulose: methods and applications. In: Smol JP, Birks HJB, Last WM (eds) Tracking environmental change using lake sediments, volume 2: physical and geochemical methods. Kluwer, Dordrecht, pp 373–400

Wooller MJ, Francis D, Fogel ML, Miller GH, Walker IR, Wolfe AP (2004) Quantitative paleotemperature estimates from $\delta^{18}O$ of chironomid head capsules preserved in arctic lake sediments. J Paleolimnol 31:267–274

Wooller MJ, Axford Y, Wang Y (2008) A multiple stable isotope record of Late Quaternary limnological changes and chironomid paleoecology from northeastern Iceland. J Paleolimnol 40:63–77

Chapter 6
Identification and Characterization of Chitin in Organisms

Neal S. Gupta and George D. Cody

Contents

Abstract Model compound chitin and invertebrate cuticles were analysed using pyrolysis-gas chromatography-mass spectrometry, ^{13} C NMR and C-, N-, and O-Xray Absorption Near Edge Structure (XANES) spectral imaging using Scanning Transmission X-ray Microscopy (STXM) to detect spectra that are characteristic of chitin. Acetylpyridones, acetamidofuran, 3-acetamido-5-methylfuran and 3-acetamido-(2 and 4)-pyrones appear to be characteristic pyrolysis products for chitin. Pyrolysis products with ions of m/z 70, 154, 168, 194 likely derive from diketopiperazine structures and provide potential markers for proteins and peptides in which proline, alanine, valine, arginine and glycine are the dominant amino acids. The ^{13}C NMR spectra of chitin reveals that amidyl methyl group resonates at 23 ppm, amidyl linked glyocosyl carbon resonates at 56 ppm, glucosyl secondary alcohols resonate between 62 and 84 ppm, and glycosidic carbon absorption is evident at ~105 ppm. The presence of protein in the arthropod cuticles is evident by resonance intensity associated with sp^2 bonded carbon associated in unsaturated amino acids (e.g. phenyl alanine, tyrosine, and histidine) occurring at 116, 129, and 137 ppm. Additionally, the protein back bone methine carbon atoms are indicated by resonance intensity at 43 ppm. Additional broad resonance intensity in the 20–30 ppm range is derived both from

N.S. Gupta (✉)
Indian Institute of Science Education and Research, Transit Campus MGSIPAP, Complex Sector 26, Chandigarh 160 019, Mohali, India
e-mail: sngupta@iisermohali.ac.in

G.D. Cody
Geophysical Laboratory, Carnegie Institution of Washington, Washington, DC 20015, USA
e-mail: gcody@ciw.edu

N.S. Gupta (ed.), *Chitin*, Topics in Geobiology 34,
DOI 10.1007/978-90-481-9684-5_6, © Springer Science+Business Media B.V. 2011

aliphatic aminoacids (e.g. valine and leucine) as well as the fatty acids associated with the waxy cuticulin layer of the cuticle. High energy resolution C-, N-, and O-XANES spectra provide further functional group level characterization of the biomacromolecular assemblages at spatial scales on the order of 100's of nm. Combining the power of Solid state ^{13}C NMR , pyrolysis with the micro-analytical capabilities of C-, N-, and O-XANES yields a formidable analytical approach towards detecting and quantitating the presence of chitin in complex biomacromolecular assemblages.

6.1 Introduction

Chitin occurs in arthropods as one of the main components of the cuticle in association with protein component linked covalently with catechol-amine and histidine/aspartic moieties (Schaefer et al. 1987). Chitin has been studied using a wide variety of methods in order to elucidate its chemical composition. Such methods include ^{13}C and or/ ^{15}N nuclear magnetic resonance spectroscopy (NMR, Kramer et al. 1995), pyrolysis–gas chromatography–mass spectrometry (py–GC–MS, Stankiewicz et al. 1996, Gupta et al. 2009) and enzymatic methods (Flannery et al. 2001). These methods attempt to address the chemical structure of the cuticle, detect chitin moieties and identify those involved in crosslinking chitin with other components such as proteins that are a part of the cuticle (Kramer et al. 1995). Py–GC–MS is extensively applied to study insoluble organic polymers (Boon 1992). Pyrolysis allows rapid screening and detection of complex polymers making use of very little material, often in the 100-200 microgram range (Chiavari and Galletti 1992). This makes the method especially useful for study of organic fossils where very little material is available (Stankiewicz et al. 1996; Briggs 1999). The GC separates the pyrolysed compounds and the mass spectrometer allows qualitative detection of even trace amounts of the separated polymers. NMR detects bulk molecular and structural characteristics complementing data from pyrolysis, however, it requires more sample material than pyrolysis.

In this chapter we present results from analytical methods using pyrolysis, ^{13}C NMR and C-, N-, and O-Xray Absorption Near Edge Structure (XANES) spectral imaging using Scanning Transmission X-ray Microscopy (STXM) on model compound chitin and on modern shrimp, and scorpion all of which have a chitinous exoskeleton (with protein) to help identify characteristic compounds from these. This will help (1) identification of chitin in studies using mass spectrometric, XANES-STXM and NMR methods in future studies, (2) characterization of pyrolysis products derived from chitin and proteins, (3) identification of biomarkers for chitin and proteins in geobiological material.

6.2 Materials and Methods

Modern cuticles of scorpion and shrimp were isolated from the organism mechanically and then extracted with organic solvents using 2:1 dichloromethane and methanol. The model compound chitin obtained from Sigma was similarly extracted to remove any soluble component and impurities.

6.2.1 Pyrolysis

The insoluble residue remaining after lipid extraction of the modern cuticle was analysed using a CDS 5150 Pyroprobe by heating at 650°C for 20 s (py–GC–MS). Compound detection and identification were performed with on-line GC–MS in full scan mode using a Hewlett Packard HP6890 gas chromatograph interfaced to a Micromass AutoSpec Ultima magnetic sector mass spectrometer. GC was performed with a J&W Scientific DB-1MS capillary column (60 m × 0.25 mm ID, 0.25 μm film thickness) using He as carrier gas. The oven was programmed from 50°C (held 1 min) to 300°C (held 28 min) at 8°C min^{-1}. The source was operated at 250°C and 70 eV ionization energy in the electron ionization (EI) mode. The AutoSpec full scan rate was 0.80 s-decade over a mass range of 50–700 Da and a delay of 0.20 s.

6.2.2 ^{13}C NMR Analysis

Solid state ^{13}C nuclear magnetic resonance spectroscopy (^{13}C-NMR) was conducted on the modern shrimp and scorpion and model compound chitin, after crushing the solvent extracted residue in liquid nitrogen followed by freeze drying to remove excess water. All ^{13}C solid state NMR experiments were performed on a Varian-Chemagnetics Infinity spectrometer located at the W. M. Keck Solid State NMR Facility at the Geophysical Laboratory. The static field of this instrument is 7.05 T; the corresponding Larmor frequencies of ^{1}H and ^{13}C are ~300 and 75 Mhz, respectively. All experiments were performed using a 5 mm double resonance probe with zirconia rotors. ^{1}H-^{13}C cross polarization was employed utilizing a RF ramp protocol on the ^{13}C channel. The ^{1}H 90° pulse width was 4 μs and high power decoupling ($w1/2\pi$ = 75 kHz) was employed during signal acquisition. The Magic Angle spinning frequency ($wr/2\pi$) was 11.6 kHz. The contact time was determined from a standard of chitin to optimum at 6 ms. A recycle delay of 2 s was chosen to minimize longitudinal interference during signal averaging. Typically 36,000 acquisitions were obtained per sample.

6.2.3 Scanning Transmission X-ray Microscopy (STXM) and C-, N-, O-μXANES

The STXM employed in this study is located at beam line 5.3.2 at the Advanced Light Source (ALS), Lawrence Berkeley Laboratory. BL5.3.2 employs a bending magnet providing a useful photon range spanning ~250–700 eV with a photon flux of 10^7 photons/sec. Energy selection on BL5.3.2 is performed with a low dispersion spherical grating monochromator affording an energy resolution of 5,000. BL11.0.2 utilizes an elliptical polarization undulator, with gap correlated with monochromator position, that provides a wider energy range: 80–2,100 eV with a photon flux

of 10^{12}–10^{13} photons/s (10^{9} photons/s with full spatial resolution) and employs a monochromator that can provide energy resolution up to 7,500.

Beam focusing utilizes Fresnel zone plate optics providing a theoretical spot size down to 25 nm, in optimum cases smaller structures (~15 nm) can be resolved. Maximum scanning rates for BL5.3.2 12 Hz, with a scanning range of 4,000 × 2,000 pixels covering a region up to 20 × 4 mm, with a minimum step size 2.5 nm. Sample position precision during spectra acquisition is better than 50 nm (controlled by laser interferometry) (Kilcoyne et al. 2003).

C-, N-, and O-XANES spectra were acquired using a multi-spectral imaging method ("Stacks", Jacobsen et al. 2000). The "Stacks" method relies on creating a highly aligned hyper-spectral data cube of x by y pixilated images acquired over a range of energies that span a given XANES region. In the fine structure regions of the near edge, the energy step size (ΔE) employed typically was 0.1 eV; in the less featured pre-edge and post edge regions, energy steps of 1–2 eV are typically sufficient for spectral resolution.

Samples of Chitin and modern scorpion were embedded in EPOFIX histological grade epoxy. The absorption cross section for C, N, and O is very high on their respective K-edges, therefore, in order to acquire C-, N-, and O-μXANES spectra and images, samples are required to be no more than 150 nm thick. Ultramicrotomy using a diamond knife and a Leica Ultracut ultramictrome was performed to obtain ultrathin sections on the order of 100–140 nm thick.

6.3 Characteristic Products of Chitin and Protein

The moieties generated from pyrolysis of model compound chitin as well as the invertebrates reveal aromatics such as benzene derivatives, nonaromatics and other heteroatomic compounds such as furans, indoles and pyridines. Franich et al. (1984) recognised acetamide and its derivatives as characteristic chitin pyrolysis products while phenols, indoles, pyrroles and cyanobenzenes were recognized as important pyrolysis products from proteins and constituent amino acids (Stankiewicz et al. 1996). The pyrolysis products can thus be subdivided into two categories, those originating from chitin and those from the proteins (that are present in the cuticle crosslinked to chitin) that can be assigned to specific amino acids or from their sequences in polypeptide chains. The gas chromatograms generated after pyrolysis of pure chitin and those from invertebrate cuticles are presented in Fig. 6.1. The mass spectra of all important products are shown from Figs. 6.2 to 6.8.

Pyrolysis products of chitin includes acetamide and related compounds that often occur as a spread peak due to functionalized chemical nature and high relative abundance. Acetamide and other low molecular weight compounds have been actively studied as a pyrolysis product of chitin earlier and products with higher molecular weight were studied by Stankiewicz et al. (1996). Other important pyrolysis products of chitin include pyridine and related derivatives, pyrroles and pyrrolines, acetamido furans and pyrans (Stankiewicz et al. 1996). It is evident that many of the products

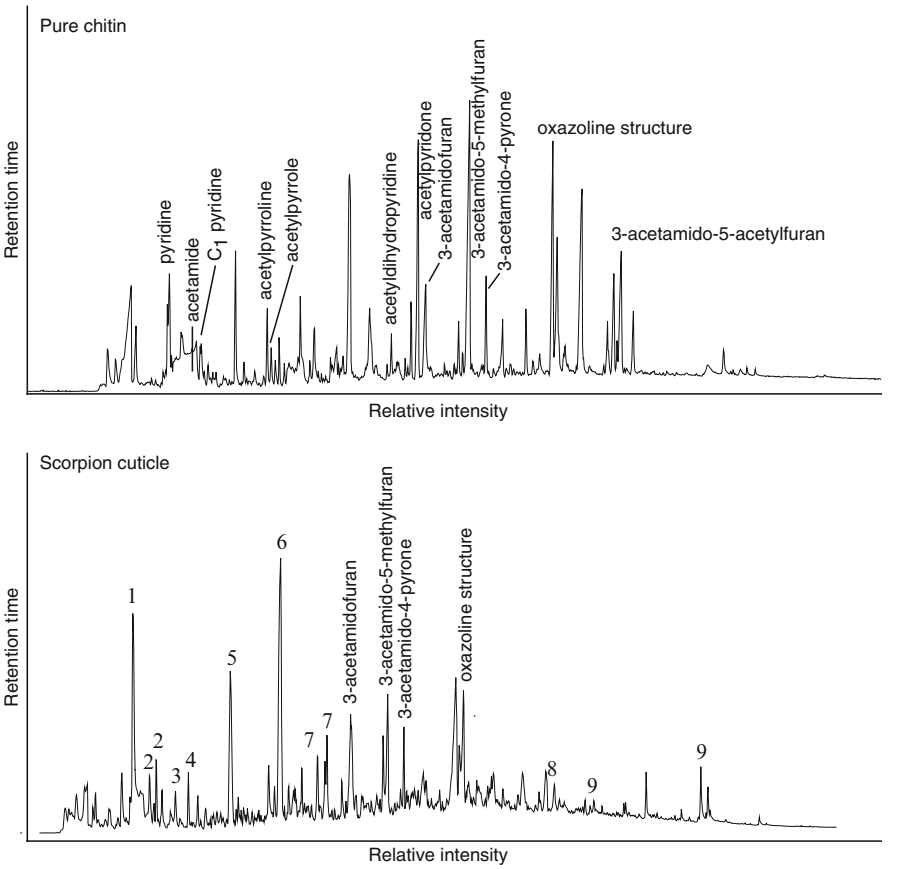

Fig. 6.1 Total ion chromatogram from py–GC–MS analysis of model compound chitin and from scorpion cuticle. *Numbers* denote pyrolysis products from protein: 1 – toluene, 2 – C_1 pyrrole, 3 – C_2 benzene, 4 – styrene, 5 – phenol, 6 – methyl phenol, 7 – C_2 phenol, 8 – diketodipyrrole, 9 – 2,5,diketopiperazine structure

detected from pure chitin are undetected in those from the invertebrate cuticles indicating that in the cuticles the originators of these compounds are associated with protein component thereby preventing their formation during pyrolysis. This indicates that the deproteinization process cleaves the chitin-protein complex resulting in moieties produced during pyrolysis that are specific to chitin. Other important pyrolysis product of chitin include acetamidofuran, 3-acetamido-5-methylfuran and 3 acetamido-(2 or 4)-pyrone. The latter two possess structures that are related to *N*-acetylglucosamine and are amongst the most important products and thus serve as markers for chitin in both modern cuticles as well as in fossil geopolymers. Other important product includes oxazoline structure present both in model compound as well as invertebrate cuticle detected by the characteristic base peak *m/z* 84.

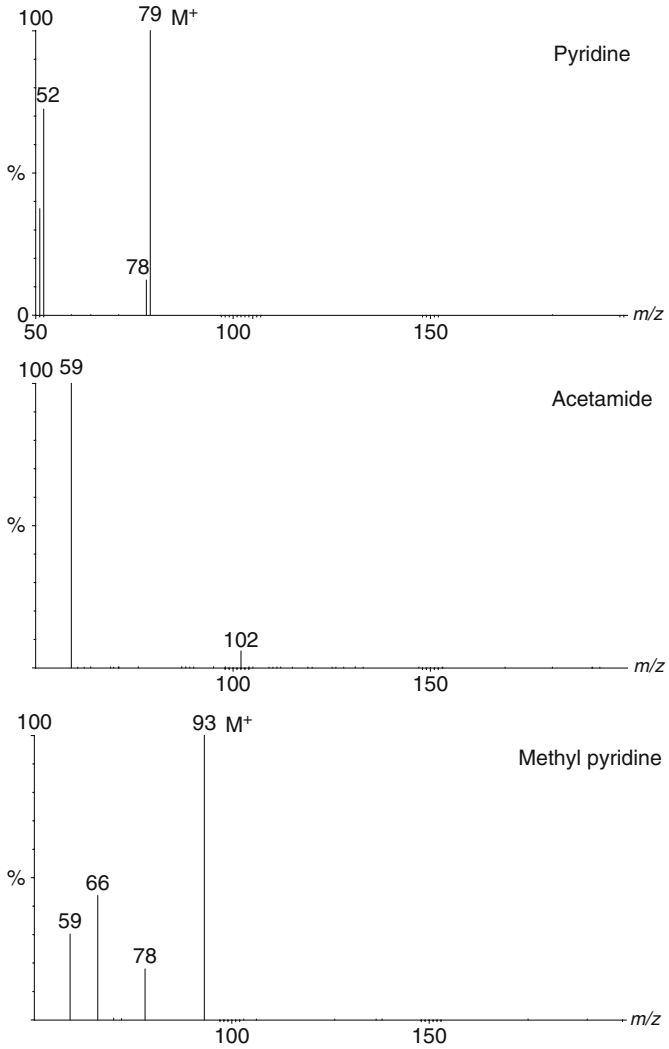

Fig. 6.2 Mass spectra of pyridine, acetamide, methyl pyridine that are chitin markers in pyrolysates of invertebrate cuticles. M^+ denotes molecular ion

Protein and amino acid products are very abundant in the pyrolyzate of arthropod cuticles. These include pyrrole and alkylated homologues derived from proline and hydroxyproline (Smith et al. 1980). Toluene, styrene and cyanobenzenes that are assumed to originate from phenylalanine. Tryptophan pyrolysis products include indole and methyl indole. Components derived from tyrosine include phenol and methyl phenol. All these amino acids are representative of the protein composition of the invertebrates. Additionally, pyrolysis products with spectra containing *m/z* 70, 154, 168, 194 derive from 2,5 Diketopiperazine derivatives and from peptides

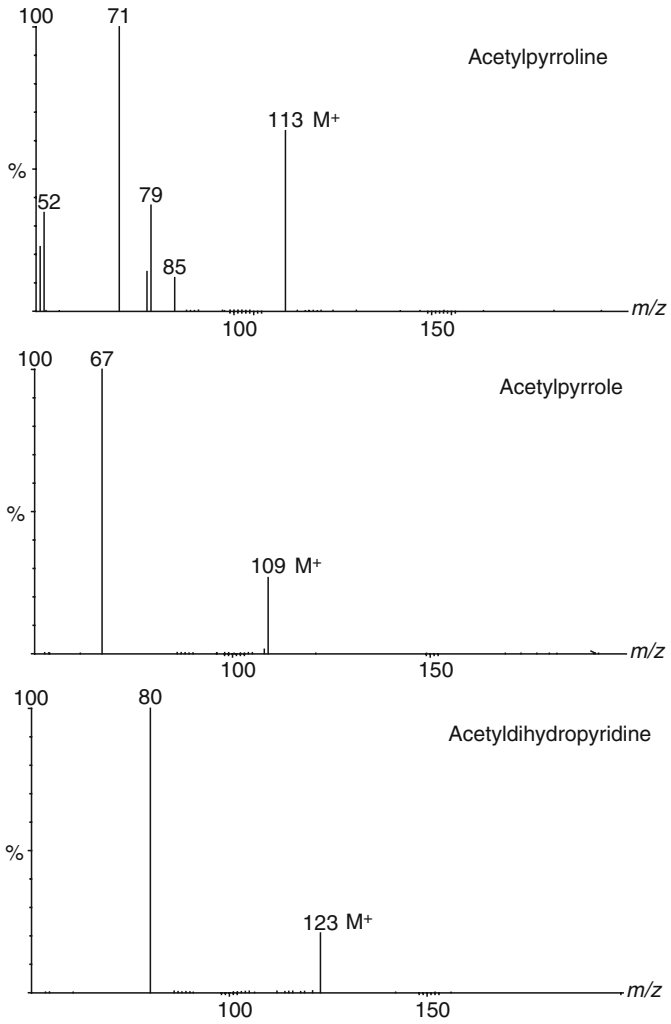

Fig. 6.3 Mass spectra of acetylpyrroline, acetylpyrrole and acetyldihydropyridine that are chitin markers in pyrolysates of invertebrate cuticles. M^+ denotes molecular ion

that have praline, alanine, arginine and glycine as the most important amino acid moieties (Stankiewicz et al. 1996). The chitin and protein are crosslinked by catecholamine and histidine or aspartic related structures, but products directly related to catechol are minor in the pyrolyzate obtained from the invertebrate cuticles. The relatively low abundance of these compounds in general is confirmed via solid state ^{13}C NMR.

Solid state ^{13}C NMR can provide a quantitative, high resolution, analysis of the functional groups present in biomacromolecules. In Fig. 6.9 we present expanded ^{13}C NMR spectra of pure chitin (top) and invertebrate (shrimp and scorpion) cuticle.

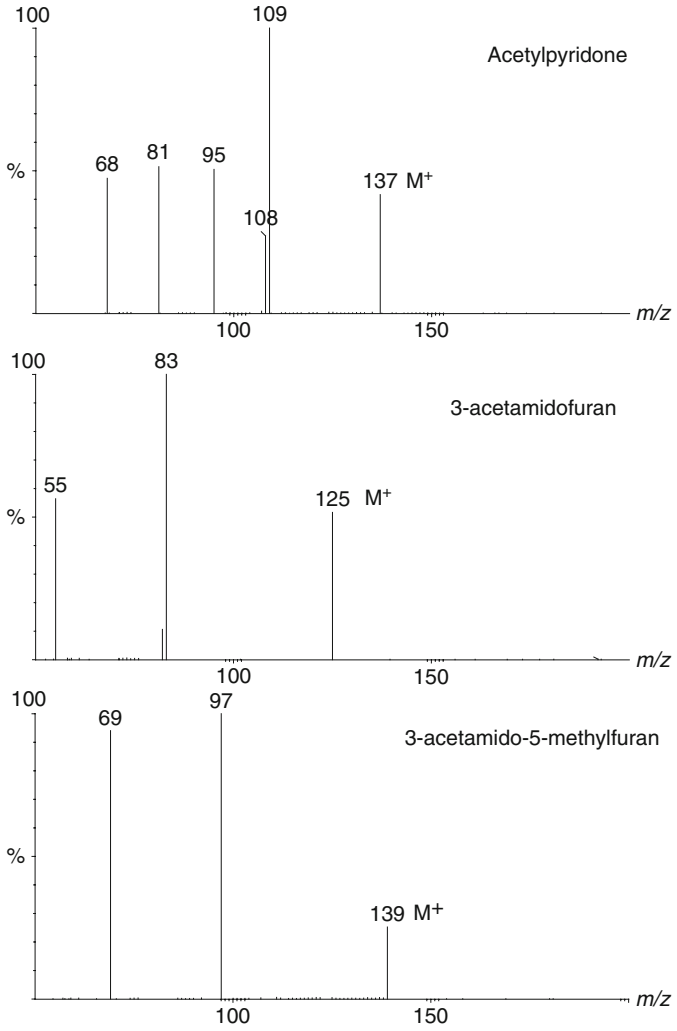

Fig. 6.4 Mass spectra of acetylpyridone, 3-acetamidofuran and 3-acetamido-5-methylfuran that are chitin markers in pyrolysates of invertebrate cuticles. M^+ denotes molecular ion

In the spectrum of chitin seven of the eight inequivalent carbons are clearly resolved, where the amidyl methyl group resonates at 23 ppm, the amidyl linked glyocosyl carbon resonates at 56 ppm, the four glucosyl secondary alcohols resonate between 62 and 84 ppm, and the glycosidic carbon absorption is evident at ~105 ppm where the relatively high frequency of this resonance signifies that the glucosyl rings are linked in the β configuration. The eight carbon in the monomer, amidyl C=O absorption resonates at 173 ppm and is not shown in these expanded spectra. The ^{13}C solid state NMR spectrum of shrimp and scorpion cuticle (Fig. 6.9, bottom) reveal the presence of highly ordered chitin (structural disorder would be manifested

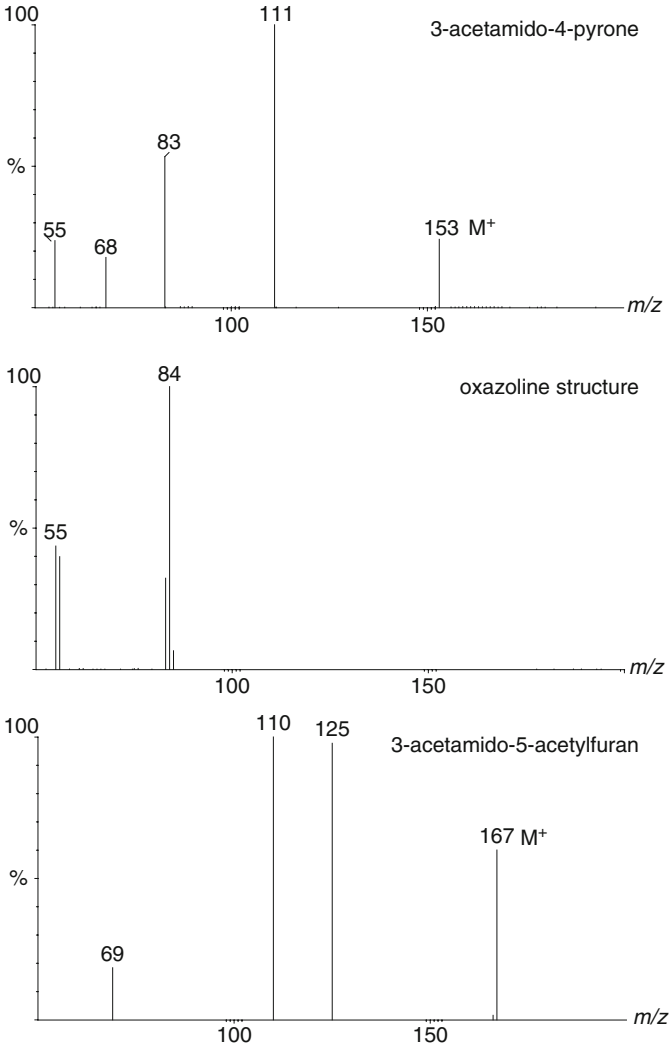

Fig. 6.5 Mass spectra of 3-acetamido-4-pyrone, ozaxoline structure and 3-acetamido-5-acetylfuran that are chitin markers in pyrolysates of invertebrate cuticles. M^+ denotes molecular ion

by considerable broadening of the characteristic resonance peaks of chitin, in particular the anomeric resonance at 105 ppm). The presence of protein in the arthropod cuticles is evident by resonance intensity associated with sp^2 bonded carbon associated in unsaturated amino acids (e.g. phenyl alanine, tyrosine, and histidine) occurring at 116, 129, and 137 ppm (note the characteristic intense resonance of tyrosine at 157 ppm is not shown). Additionally, the protein back bone methine carbon atoms are clearly indicated by resonance intensity at 43 ppm. The additional broad resonance intensity in the 20–30 ppm range is derived both from aliphatic

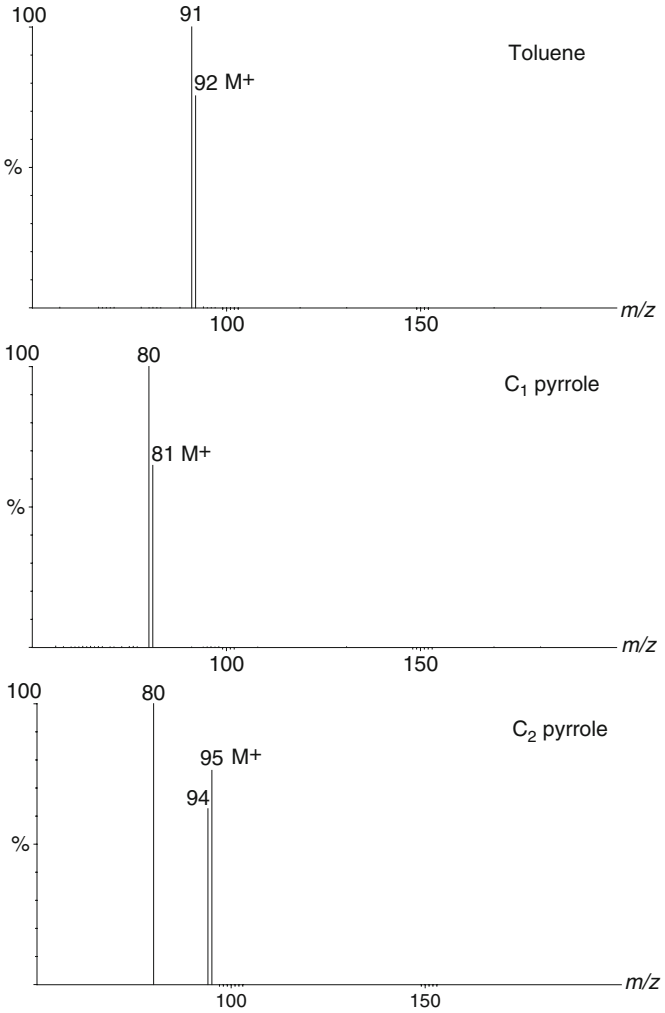

Fig. 6.6 Mass spectra of toluene, methyl pyrrole and C_2 pyrrole that are protein/amino acid markers in pyrolysates of invertebrate cuticles. M^+ denotes molecular ion

aminoacids (e.g. valine and leucine) as well as the fatty acids associated with the waxy cuticulin layer of the cuticle. Any significant presence of catechol cross-linkers would be clearly evident with an intense resonance at 149 ppm which is not observed, consistent with the conclusions derived from the pyrolysis GC–MS results above.

Solid state ^{13}C NMR is a very powerful tool for assessing the functional group distribution and biomacromolecular composition of the complex arthropod cuticle. At least directly, however, solid state ^{13}C NMR cannot reveal how biomacromolecular composition varies across the arthropod cuticle. Quantitative assessment of the biomacromolecular compositional variation within the exoskeleton at fine scale can

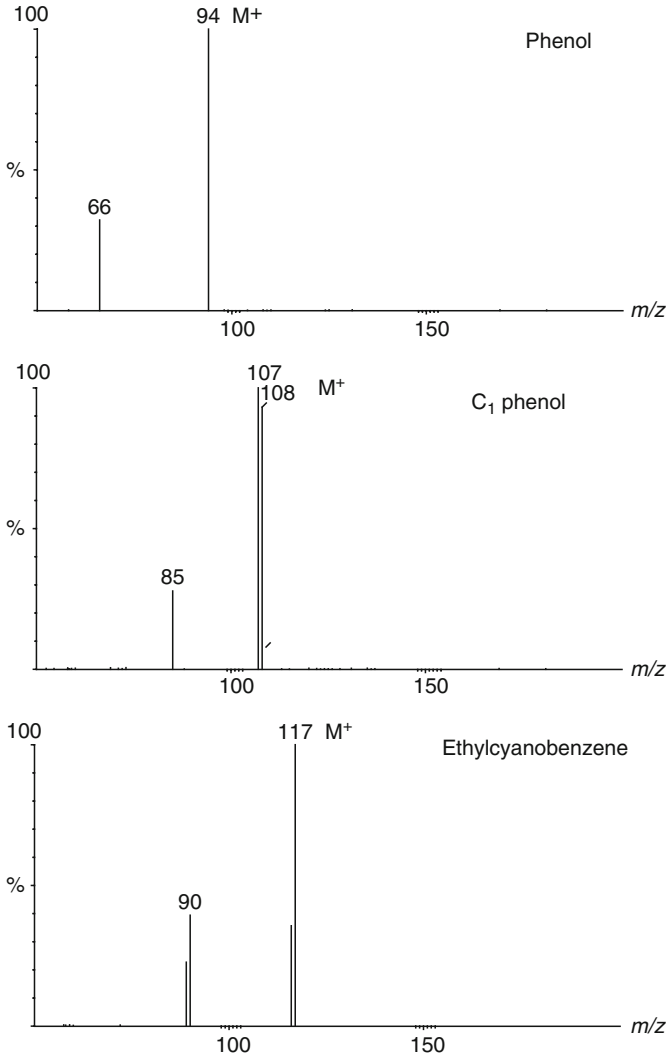

Fig. 6.7 Mass spectra of phenol, methyl phenol and ethylcyanobenzene that are protein/amino acid markers in pyrolysates of invertebrate cuticles. M^+ denotes molecular ion

be obtained via C-, N-, and O-Xray Absorption Near Edge Structure (XANES) spectral imaging using Scanning Transmission X-ray Microscopy. For example, in Fig. 6.10a high resolution cross sectional image of scorpion cuticle reveals the spatial variation in protein abundance through variation in nitrogen content. The image in Fig. 6.10 is derived by obtaining a pair of transmission images, one just below the N K edge, the other on top of the N K edge. By taking the negative logarithm of the ratio of these two images one obtains the image presented where in the intensity is directly related to absorption due to nitrogen. The dark band at the

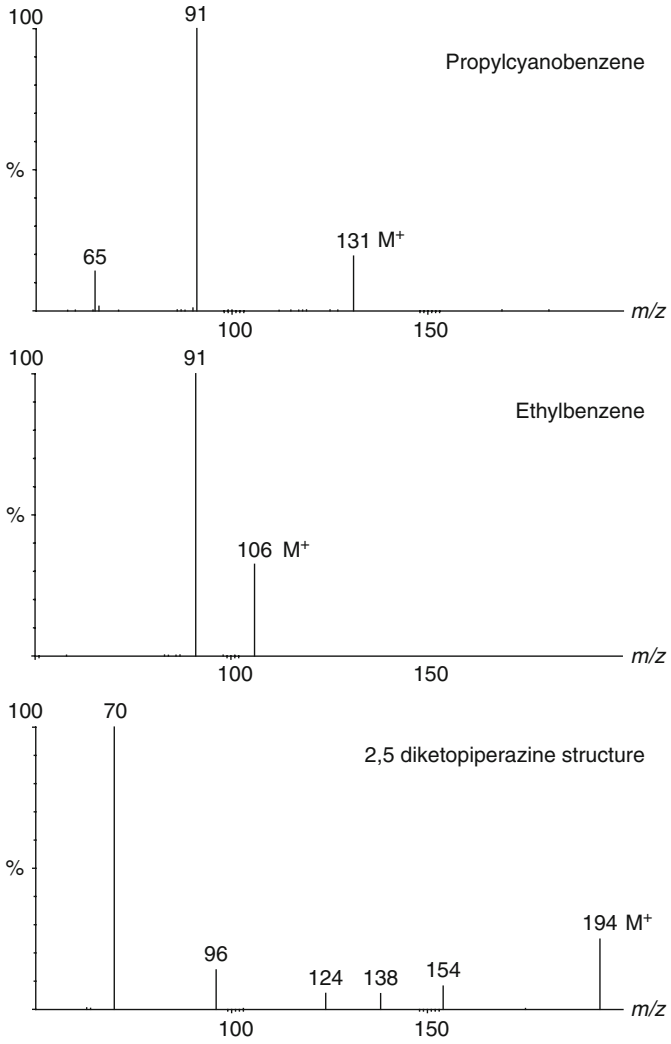

Fig. 6.8 Mass spectra of propylcyanobenzene, ethylbenzene and 2,5 diketopiperazine structure that are protein/amino acid markers in pyrolysates of invertebrate cuticles. M^+ denotes molecular ion

top of Fig. 6.10 (the outer layer of the exoskeleton) is relatively depleted in nitrogen and likely corresponds to the cuticulin layer (additional maps, not shown here, on the C Kedge reveal that this region is relatively rich in aliphatic carbon). The relatively bright regions in the inner part of the cuticle correspond to protein rich layers indicating that the distribution of chitin and protein is not homogeneous throughout the inner region of the cuticle.

High energy resolution C-, N-, and O-XANES spectra (Fig. 6.11) provide functional group level characterization of the biomacromolecular assemblages at spatial scales on the order of 100's of nm. Characteristic absorption features

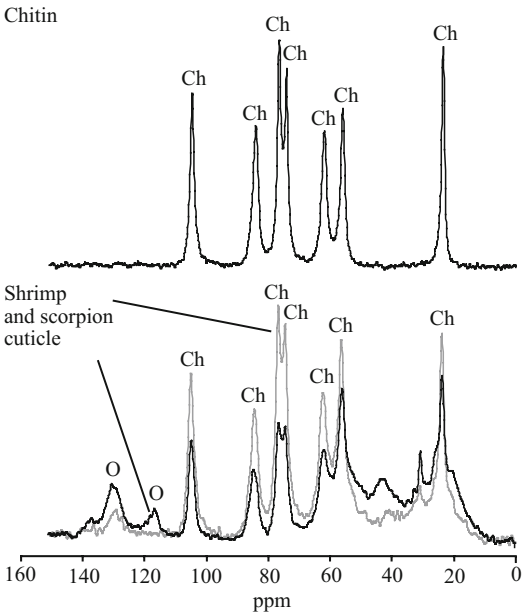

Fig. 6.9 Solid state ^{13}C Nuclear Magnetic Resonance spectra of pure chitin (*top*) and shrimp and scorpion cuticle (*bottom*). The spectra are recorded as a function of parts per million (ppm) shifts in frequency relative to the carrier frequency (~75 MHz), referenced to the methyl resonance of tetramethyl silane defined as 0 ppm. Resonance peaks corresponding to the amidyl methyl, C-N, and C-O carbons of chitin are designated here as, Ch. In the spectra of the arthropod cuticle (*bottom*), the *grey line* denotes shrimp cuticle and the solid black line denotes scorpion cuticle. In addition to resonance intensity associated with chitin, the solid state ^{13}C NMR spectra reveal the presence of functional groups associated with associated protein and waxes (see text)

associated with amide carbonyl ($1s-\pi^*$) transitions are evident in both the chitin (top) and cuticle (bottom). The weak absorption at 285 eV in the case of the scorpion cuticle corresponds to a C=C $1s-\pi^*$ transition associated with the presence of unsaturated amino acids such as phenyl alanine. In the case of chitin, however, the presence of C=C likely indicates that a slight degradation of the chitin has occurred through secondary electron induced molecular rearrangements. The presence of abundant C-OH moieties in chitin (left-top, A) is clearly revealed by the intense peak at 289.5 eV; in the scorpion cuticle C-XANES spectrum, this absorption is much weaker, due to the presence of considerable protein. In the N-XANES spectra one observes the predominance of amidyl nitrogen at 401.2 eV in both chitin and protein. The protein N-XANES spectra also exhibits intensity at ~399 eV indicative of iminic nitrogen, for example in the imidazole group of histidine. Furthermore, increased intensity at ~403 eV in the scorpion cuticle N-XANES spectrum is consistent with the presence of amines, e.g., lysine. Indirectly, the presence of multiple species of nitrogen in the scorpion cuticle and only one type of nitrogen species in the chitin is indicated by the intensity of the EXAFS oscillations exhibited above ~405 eV; photoelectron scattering waves from multiple nitrogen species with

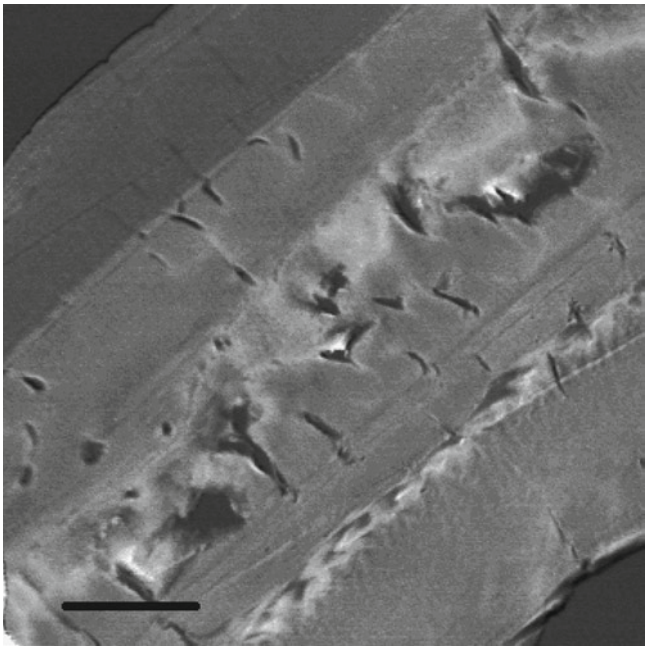

Fig. 6.10 A scanning transmission x-ray image revealing the relative concentration of nitrogen throughout an ultra-thin cross-section through a modern scorpion cuticle. The pixel size is 100 nm and the scale bar is 5 μm long. This image is produced by first acquiring a pair of images of the same region but at different energies; energy 1 = 395 eV lies just *below* the N-K edge and energy 2 = 410 eV lies on *top* of the most intense N-XANES absorption. The image above is created by taking the $-\log(I_2/I_1)$ and provides a map of local nitrogen abundance, where high abundance regions are light, low abundance regions are dark. The brightest regions are protein rich, the dark outer region corresponds to the waxy cuticulin layer

different bond lengths interfere with each other destructively, whereas a single nitrogen species with a fixed bond length exhibits an extended EXAFS oscillation. The O-XANES spectra (Fig. 6.11) of chitin and protein are dominated by a low energy C=O 1s−π* transition derived from amidyl carbonyl. Intensity at higher energies is derived from C−O* and the ionization edge of oxygen. It is clear from Fig. 6.11, that the scorpion cuticle as proportionally much more amidyl C=O, than the pure chitin consistent with the admixture of both chitin and protein. It is certainly possible to determine, quantitatively the local concentration of peptide and chitin via spectral analysis, but we shall not do so here.

It is clear from the spectra in Fig. 6.11 and the absorption based image in Fig. 6.10 that mapping of the distribution of discrete functional groups as a means of quantitatively determining the variation in biomacromolecular (i.e., chitin-protein variation) composition at 30–100 nm spatial resolution is certainly possible. Combining the power of Solid state ^{13}C NMR with the micro-analytical capabilities of C-, N-, and O-XANES yields a formidable analytical approach towards detecting and quantitating the presence of chitin in complex biomacromolecular assemblages.

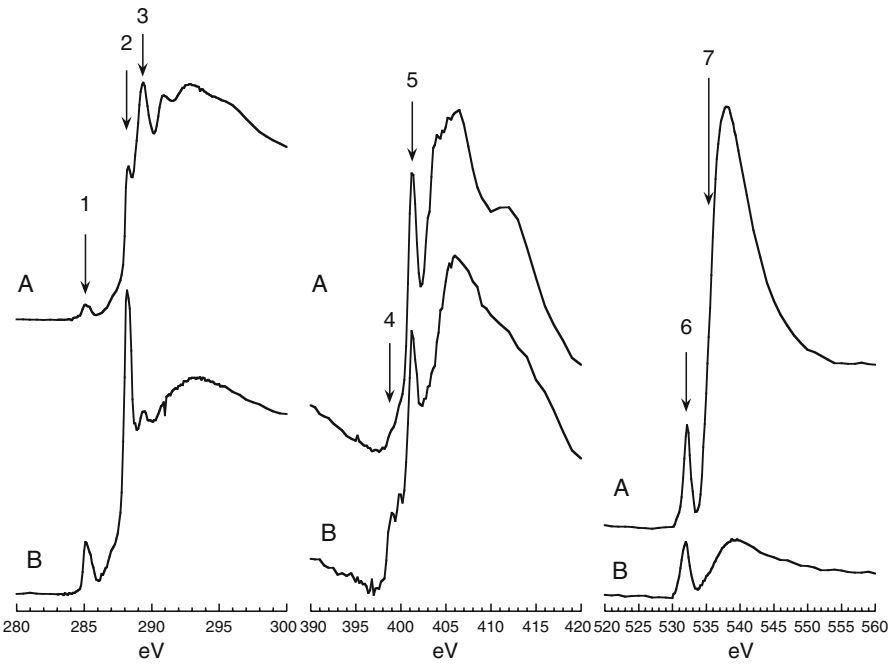

Fig. 6.11 C-, N-, and O-XANES spectra of Chitin (**A**) and modern scorpion cuticle (**B**). *Left* A & B: C-XANES spectra. Peak 1 corresponds to the olefinic/aromatic C=C 1s−π* transition, peak 2 corresponds to the amide C*=O 1s−π* transition, peak 3 corresponds to the C*-OH 1s−3p/σ* transition. *Middle* A & B: N-XANES spectra. Peak 4 corresponds to imine C=N* 1s−π* transition, peak 5 corresponds to amide N 1s−3p/σ* transition. *Right* A & B: O-XANES spectra. Peak 6 corresponds to C=O* 1s−π* transition. Peak 7 corresponds to the C-O*H 1s−3p/σ* transition and is obscured by the intense photo-electron scattering peak at ~539 eV

References

Boon JJ (1992) Analytical pyrolysis mass spectrometry: new vistas opened by temperature-resolved in-source PYMS. Int J Mass Spectrom Ion Proces 118–119:755–787

Briggs DEG (1999) Molecular taphonomy of animal and plant cuticles: selective preservation and diagenesis. Philos Trans R Soc London Ser B 354:7–16

Chiavari G, Galletti GC (1992) Pyrolysis–gas chromatography/mass spectrometry of amino acids. J Anal Appl Pyrol 24:123–137

Flannery MB, Stott AW, Briggs DEG, Evershed RP (2001) Chitin in the fossil record: identification and quantification of D-glucosamine. Org Geochem 32:745–754

Franich RA, Goodin SJ, Wilkins AL (1984) Acetamidofurans, acetamidopyrones, and acetamido-acetaldehyde from pyrolysis of chitin and n-acetylglucosamine. J Anal Appl Pyrol 7:91–100

Gupta NS, Cody GD, Tetlie OE, Briggs DEG, Summons RE (2009) Rapid incorporation of lipids into macromolecules during experimental decay of invertebrates: Initiation of geopolymer formation. Org Geochem 40:589–594

Jacobsen C, Flynn GJ, Wirick S, Zimba C (2000) Soft x-ray spectroscopy from image sequences with sub-100 nm spatial resolution. J Microsc 197:173–184

Kilcoyne ALD, Tyliszczak T, Steele WF, Fakra S, Hitchcock P, Franck K, Anderson E, Harteneck B, Rightor EG, Mitchell GE, Hitchcock AP, Yang L, Warwick T, Ade H (2003) Interferometer controlled scanning transmission microscopes at the advanced light source. J Synchrotron Radiat 10:125–136

Kramer KJ, Hopkins TL, Schaefer J (1995) Applications of solids NMR to the analysis of insect sclerotized structures. Insect Biochem Mol Biol 25:1067–1080

Schaefer J, Kramer KJ, Garbow JR, Jacob GS, Stejskal EO, Hopkins TL, Speirs RD (1987) Aromatic cross-links in insect cuticle: detection by solid-state ^{13}C and ^{15}N NMR. Science 235:1200–1204

Smith RM, Shawkat SAK, Hayes WP (1980) Pyrolysis-gas chromatography of proline, hydroxyproline and related peptides. Analyst 105:1176

Stankiewicz BA, van Bergen PF, Duncan IJ, Carter JF, Briggs DEG, Evershed RP (1996) Recognition of chitin and proteins in invertebrate cuticles using analytical pyrolysis/gas chromatography and pyrolysis/gas chromatography/mass spectrometry. Rapid Commun Mass Spectrom 10:1747–1757

Chapter 7
Fate of Chitinous Organisms in the Geosphere

Neal S. Gupta and Roger E. Summons

Contents

Abstract Organic tissues such as cuticles may survive as organic remains and account for the fossil record of a number of important groups such as graptolites, chelicerates, insects, chitinozoans, ammonite beaks and fish scales. Fossilized cuticles were assumed to be composed of chitin protein complex similar to the living relatives, however, analysis of fossils using a range of mass spectrometric and spectroscopic methods have shown that preserved cuticles include significant amounts of aliphatic hydrocarbon component at times with an aromatic component that is very different to the composition of the cuticle of the living arthropod. Analysis of successively older fossil material has revealed that this transformation to an aliphatic composition is gradual and perhaps time dependant. Taphanomic incubation experiments demonstrate that lipids such as fatty acids are incorporated into the decaying chitin protein exoskeleton as early as a few weeks contributing to the aliphatic component. This is supported by chemolytic analysis of fossils that

N.S. Gupta (✉)
Indian Institute of Science Education and Research, Transit Campus MGSIPAP,
Complex Sector 26, Chandigarh 160 019, Mohali, India
e-mail: sngupta@iisermohali.ac.in

R.E. Summons
Department of Earth Atmospheric and Planetary Sciences,
Massachusetts Institute of Technology, Cambridge, MA 02139, USA
e-mail: rsummons@mit.edu

N.S. Gupta (ed.), *Chitin*, Topics in Geobiology 34,
DOI 10.1007/978-90-481-9684-5_7, © Springer Science+Business Media B.V. 2011

reveal presence of fatty acyl moieties in the macromolecule. Thus, the aliphatic composition in the fossils is generated in-situ and not from migration from an external source. Many kerogens are similarly aliphatic and serve as a source for petroleum during thermal maturation. In such sedimentary organic matter where the contributing organism does not have a resistant aliphatic biopolymer, in situ lipid incorporation is likely an important mechanism for presence of the aliphatic component in the fossil organic matter.

7.1 Introduction

The animal fossil record is dominated by organisms with mineralized skeletons including sponges, corals, ostracods, brachiopods and vertebrates. Despite being susceptible to decay and oxidation, soft-bodied fossils also provide critical data on the history of life; decay-prone tissues, such as muscle, are sometimes preserved by replication in authigenic minerals as a result of bacterial activity (Briggs 2003) and semi-resistant organic tissues such as cuticle may survive as organic remains (see Briggs 1999 for a review). They account for the fossil record of a number of important groups including graptolites, chelicerates (that include eurypterids, horseshoe crabs, scorpions and spiders) and insects. A number of minor groups (e.g. chitinozoans) also have a non-mineralized organic cuticle. In addition, ammonite beaks and some fish scales are found as organic remains as well.

Fossilized cuticles were assumed to be composed of a chitin-protein complex like that of their living relatives until very recently. As the exoskeleton is more decay-resistant than the rest of the animal it has been argued that they can survive and be incorporated into the sedimentary rock. However, analyses of fossils, using a range of techniques, have shown that preserved cuticles include significant amounts of aliphatic hydrocarbon component and are very different in composition to the bulk of the cuticle of living arthropods. This anomaly was explained by the experimental results demonstrating that aliphatic components from the surrounding sediment replaced the original chemistry on a molecular scale (Baas et al. 1995). This chapter discusses advances in research regarding organic fossils that have an original chitinous composition and their occurrence and chemical preservation in the geologic record using modern analytical and experimental methods and general implications for understanding fate of organic molecules and their contribution to sedimentary organic matter.

7.2 Analytical Methods

Modern and fossil specimens of organisms can be analysed using a range of methods to determine their elemental, molecular and isotopic composition. Most individual techniques have defined strengths, weaknesses and biases. Thus, when different methods are used in association, the resultant information can be complementary.

Typically, organic fossil remains are not obtained in abundance. Diagenetic processes of various kinds result in loss and alteration of different structural and molecular components and sample limitation becomes a factor for consideration. Pyrolysis-gas chromatography-mass spectrometry has been routinely used for determining chemistry and is a rapid and sensitive tool for detecting the major constituents of organic matter insoluble in common organic solvents (Stankiewicz et al. 1997a, b; Gupta et al. 2007a). It involves flash heating of the material in a stream of inert gas and to thermally cleave chemical bonds, irrespective of the type of linkage (cf. chemolysis discussed later). The molecular species so generated are then separated using a gas chromatograph (GC) and identified using a mass spectrometer (MS). All the equipment is integrated and operated in concert making the process 'online'. This method, termed py–GC–MS is routinely used to track biomolecular changes of organisms from the time of its burial to fossil formation, through diagenesis at a semi-quantitative level. It requires sample amounts in the range of 150–200 μg per analysis and the fossil is destroyed in the process. Alternatively, pyrolysis can be conducted 'offline' where a standalone unit is used and the pyrolysate is collected, fractionated on a silica gel column and the fractions analysed GC–MS. One offline method that has proven particularly effective and which has been gaining popularity is high pressure catalytic hydrogen pyrolysis (Hy-Py), where high pressure hydrogen gas acts as a reducing agent and caps thermally-cleaved C-S, C-O and C-N bonds. The gas flow also flushes the product hydrocarbons from the heated zone as soon as they are formed thereby maximising recovery of the pyrolysate while minimising thermally-driven stereochemical changes (Love et al. 1995).

Organic fossils from plants and animals often record a chemical composition with a significant aliphatic (hydrocarbon rich) component that is linked within the macromolecule C-C bonds, ester and ether linkages. The ester and ether bonds can be specifically cleaved using chemical degradation. This provides insights into the overall chemical structure and is valuable for estimating the carbon chain length linked by the targeted bond thereby complementing that obtained by the less specific py–GC–MS. Methods that are useful for targeting specific aliphatic components of the macromolecule include thermally assisted methylation (THM) and ruthenium tetroxide (RuO_4) oxidation. Ruthenium tetroxide cleaves ether-linked hydrocarbon chains (Blokker et al. 2000) while THM (pyrolysis in the presence of tetramethylammonium hydroxide; de Leeuw and Baas 1993) cleaves ester linkages. The latter is useful for identifying specific fatty acids incorporated into the macromolecular structure (Gupta et al. 2007a) for and providing information on distribution of their chain lengths.

Marine organic matter that becomes buried and preserved will generally encounter a zone of sulfate reduction during transit through the lower water column or in the sediments themselves. As oxygen is excluded and nitrate and then sulfate become the dominant electron acceptors for bacterial respiration, copious amounts of reduced sulfur species can be generated. Sulfide and polysulfide acts as reductants and cross-linking agents in a (Kok et al. 2000; Adam et al. 2000; Hebting et al. 2006) a process akin to mild vulcanisation. Organically-preserved fossils such as graptolites and shrimp may have molecular components linked through C-S bonds formed during

early sulfurization. These may be assessed by subjecting the fossils to treatment with Li/NH_3 or Raney Nickel (Adam et al. 1993; Schaeffer et al. 1995a, b) that will cleave such bonds. Analysis of the released lipids, that can then be isolated and fractionated using liquid chromatography, can be completed using GC–MS.

Spectroscopic methods complement pyrolysis and chemolysis by providing an analysis that is non destructive. Spectroscopic methods routinely used for fossil study include solid state ^{13}C and ^{15}N nuclear magnetic resonance spectroscopy (NMR), Fourier transform infrared spectroscopy (FTIR) and Raman spectroscopy. NMR provides information on the immediate chemical environment of carbon and hydrogen atoms in a molecule. Application of NMR to studies of animal fossils is complicated by the fact that it requires 20–40 mg sample and this may be difficult or impossible to obtain from a single animal fossil. Fourier transform infrared spectroscopy is useful for providing insight into the functionality of the constituent oxygen atoms (carboxyl, carbonyl, ethers). These are especially important in fossils that have undergone oxidative cross-linking by reaction of chemical moieties (Gupta et al. 2008a, see discussion later). FTIR is also non-destructive and requires minimal amount amounts of sample. Raman spectroscopy provides microscale analysis of carbonaceous material and can be successfully used as a thermal maturity indicator for organic carbon (Rahl et al. 2005; Cuesta et al. 1994; Marshall et al. 2007). It has been successfully used to determine relative thermal maturity in fossil *Eurypterid* samples (Gupta et al. 2007b). X-ray absorption spectroscopy of carbon, nitrogen and oxygen (C,N,O-XANES) has been used to provide more information on the functional group chemistry in the fossils. This coupled with scanning transmission X-ray microscopy (STXM) provides means of visual and chemical mapping at a sub micron level, where other methods of chemolysis and pyrolysis are difficult to apply (Boyce et al. 2002). Application of spectroscopic methods to animal fossils is limited so far, and should be the focus of future studies.

Compound specific stable isotope analysis (CSIA), using gas chromatography-combustion-isotope ratio mass spectrometry (GC–C–IRMS), provides isotope data on individual molecular components (Hayes et al. 1990; Freeman et al 1990). Such data has been used as a geochemical tracer to analyse the transformation of biomolecules to geomolecules during diagenesis, and to determine the origin of molecular constituents in sedimentary organic matter. The application of CSIA to macromolecules has been problematic due to their insoluble and recalcitrant nature. A possible way to analyse the macromolecular component of fossils may involve chemolytic methods to generate a series of organic acids after reaction with the fossil and then measuring the isotope ratio of carbon in the chemolysate. Applying CSIA to the chemolysate has the potential to identify which lipids have been incorporated into macromolecular structures. Alternatively, isotope data for pyrolysis products of macromolecular material can be measured as well.

Transmission and scanning electron microscopy has been carried out to compare ultra-structural preservation and surface morphology. Microscopy in conjunction with rigorous chemical analysis is often the best approach for tracking changes in organic fossils though time (Mösle et al. 1998; Gupta et al. 2007a, c).

Experimental protocols have been developed to approximate organic fossilization by application of confined pyrolysis accelerated maturation techniques (Stankiewicz

et al. 2000; Gupta et al. 2006a). This involves experimental heating of modern tissues and biopolymers in a sealed gold cell (within an autoclave) at temperatures from 260°C to 350°C and 700 bars over a day (or days if temperature is lowered). The end products reveal compositions similar to that of fossils and this provides a means to track the role of different biopolymers in forming geopolymers.

7.3 Preservation of Chitinous Fossils in the Geologic Record

Chitinous macrofossils that have been studied from a biomolecular perspective include fossil arthropods (insects, scorpions, eurypterids), cephalopods and decapods. Chemical composition of the modern equivalents of these fossils have been undertaken to evaluate their molecular composition in an attempt to track the transformation of precursor biochemicals to a geochemical composition.

Arthropod cuticles consist of chitin fibers embedded in a protein matrix, cross-linked by catechol, aspartate and histidyl moieties (Schaefer et al. 1987). Calcium carbonate strengthens the cuticle of numerous crustaceans. The fossil record of arthropods, especially those found in non-marine settings, rely on the preservation potential of this material, as they lack a biomineralized exoskeleton. Fossil eurypterids, scorpions and insects, for example, are abundant as cuticular remains (see Briggs 1999 for review). The following examples below enumerate the molecular composition of chitinous fossils.

Analysis of modern beetle cuticle using py–GC–MS reveals chitin protein composition (Stankiewicz et al. 1997a). Investigation of beetles from the Cenozoic sediments of the Enspel (25Ma) lake, Germany reveal preservation of some chitin in the fossil. The bulk composition the fossils, however, is dominated by an aliphatic polymer (indicated by *n*-alkane/alkene homologues peaks) up to C_{33} in chain length (Gupta et al. 2007a) and additional aromatic compounds in pyrolysis GC–MS chromatograms (Fig. 7.1). Eurypterids (fossil relatives of living chelicerates) do not show the presence of chitin in the fossil but an aliphatic geopolymer from C_9 to C_{22} (Gupta et al. 2007b) along with alkyl phenols and benzenes (Fig. 7.2).

Analysis of a jaw of the cephalopod *Placenticeras* also revealed a dominant aliphatic character represented by series of alkane/alkene homologues (Gupta et al. 2008a), with chain length extending from $<C_9$ to C_{24} (*m/z* 83 + 85) and additional methyl ketones (*m/z* 58) extending from C_7 to C_{17} (Fig. 7.3). Aromatic compounds such as benzene and alkyl derivatives, and phenols and their alkyl derivatives, are also detected. The presence of methyl ketones indicate the presence of ether linkages and other oxygen functional groups in the fossil, indicating that oxygen may have reacted with unsaturated components in the organism during early diaganesis. The jaw of another cephalopod (Fig. 7.4), in contrast, reveals a dominant aromatic component consisting of alkyl benzenes (revealed by summing the ion chromatograms for the following ions: *m/z* 78 + 91 + 92 + 105 + 106 + 119 + 120 + 134 that selects specific molecular species from the entire analysis), alkyl phenols (*m/z* 66 + 94 + 107 + 108 + 121 + 122 + 136) and polyaromatics such as naphthalenes and phenanthrene (*m/z* 128 + 141 + 142 + 156 + 178 + 192).

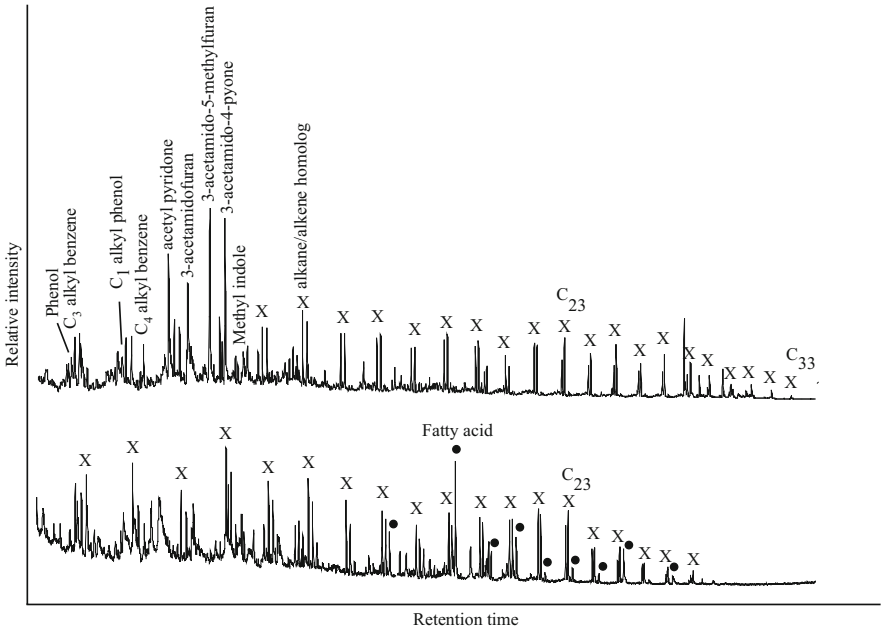

Fig. 7.1 Py–GC–MS analysis of fossil beetle from the Enspel formation showing chraracteristic chitin peaks and an aliphatic composition upto C_{33}. Thermally assisted methylation with Tetramethylammonium hydroxide (TMAH) reveals the distribution of fatty acids in the fossil macromolecule alongside the aliphatic component (Adapted from Gupta et al. 2007a)

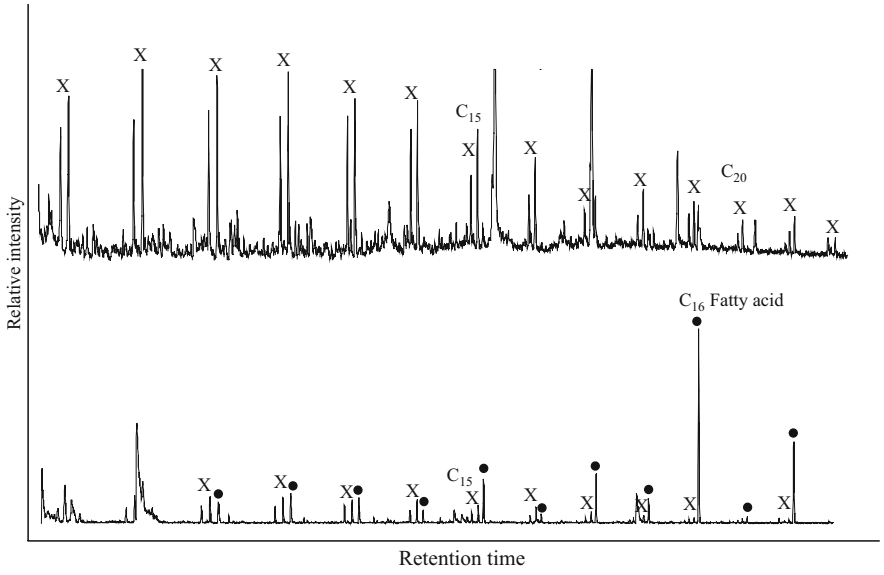

Fig. 7.2 Py–GC–MS analysis of fossil Eurypterid showing aliphatic component upto C_{22}. TMAH analysis of the fossil reveals incorporated fatty acids upto C_{18} contributing to the aliphatic composition (Adapted from Gupta et al. 2007b)

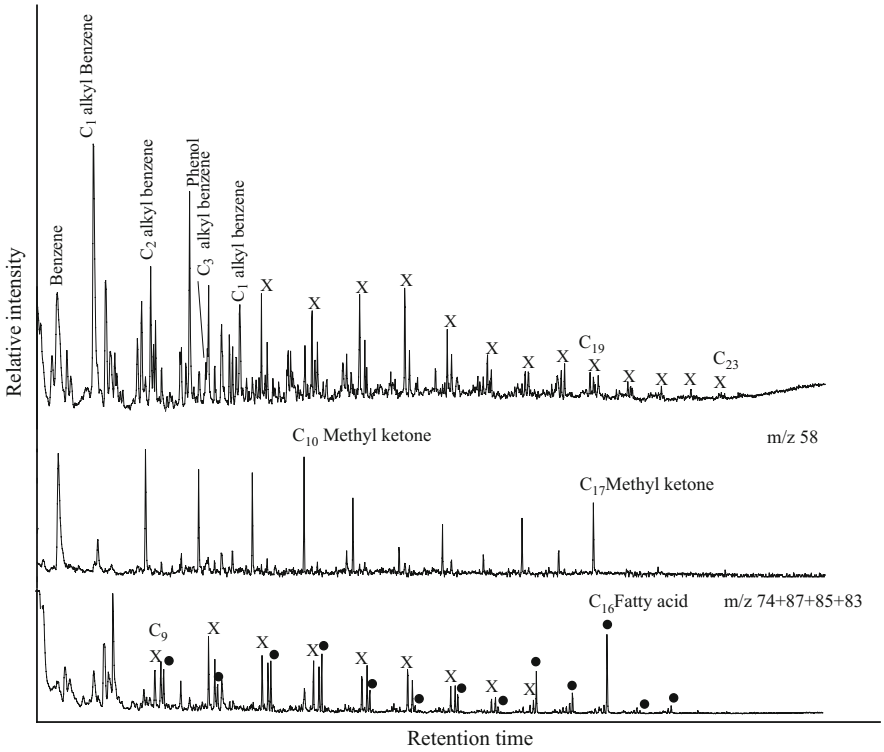

Fig. 7.3 Py–GC–MS analysis of fossil cephalopod with significant aliphatic content (as denoted by the alkane/alkene, X peaks) and some aromatic content. *m/z* 58 reveals the presence of methyl ketones that indicate oxygen crosslinking in the macromolecule. TMAH analysis reveals the distribution of fatty acids in the macromolecule contributing to the aliphatic composition (Adapted from Gupta et al. 2008a)

Thus, we see that though the initial composition is chitin/protein, the fossils are often transformed to a composition with an aliphatic macromolecular component with additional aromatics, at times with significant aromatic compounds.

7.4 Experimental Taphonomy

As discussed so far, research on the organically preserved cuticles of fossil arthropods has shown that only younger fossils retain traces of the original chitin (as determined by py–GC–MS in the fossil beetle from Enspel). Cuticles are generally transformed during diagenesis from original composition to geopolymers with a significant aliphatic component. Such molecular transformations are common to a range of organic remains with different starting compositions, including graptolites and fish scales (that have a proteinaceous composition, Gupta et al. 2006a) and leaves (consisting of lignin, polysaccharides and cutin, Gupta et al. 2006c; 2007b), similar

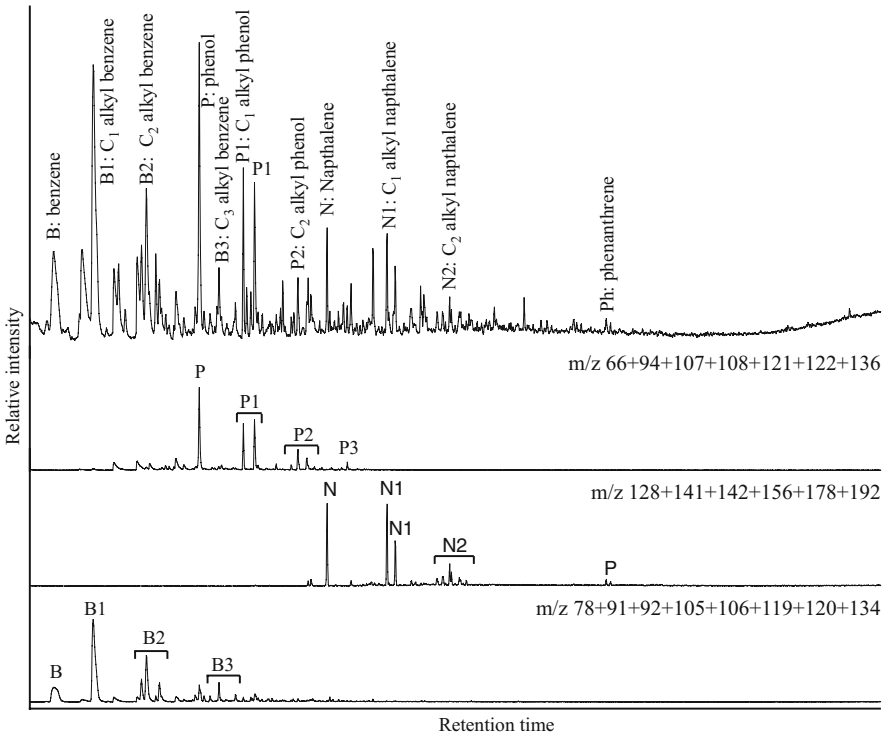

Fig. 7.4 Py–GC–MS analysis of fossil cephalopod revealing presence of polyaromatic compounds including alkyl napthalenes (*m/z* 128 + 141 + 142 + 156 + 178 + 192), phenols (*m/z* 66 + 94 + 107 + 108 + 121 + 122 + 136) and benzenes (78 + 91 + 92 + 105 + 106 + 119 + 120 + 134) and low aliphatic content (Adapted from Gupta et al. 2008a)

to kerogens with high hydrogen content (e.g. type II kerogen). Analysis of successively older fossil material has revealed that the transformation to an aliphatic component is gradual and perhaps time dependent, but it is unknown at what stage it may be initiated (Gupta et al. 2009). The constituent biopolymers and lipids are prone to degradation during decay and presumably undergo transformation prior to, and during, diagenesis (Gupta et al. 2009). Experiments can be set up to determine the fate of the lipid component and constituent biopolymers in a decaying carcass in an attempt understand early diagenetic processes.

Earlier, investigations of the molecular taphonomy of arthropods have focused on the cuticle components of crustaceans (Baas et al. 1995; Stankiewicz et al. 1998a) in experiments with a 2 month duration, primarily to monitor changes in the chitin protein composition. These revealed the loss of protein within the first 2 weeks, while chitin remained largely intact for the duration of the experiments, attesting to its greater preservation potential (Baas et al. 1995). Laboratory incubation experiments of 44 weeks duration have been employed in this study (also see Gupta et al. 2009) to determine the fate of the constituent biopolymers and associated lipids in shrimp and cockroach.

Specimens of a penaeid shrimp (~10 cm long) and the cockroach *Eublaberus posticus* (~6 cm long) were killed by asphyxiation in air (shrimp) or by drowning in deionised water (in which case the cockroach was wrapped in aluminum foil to make it sink). Six specimens of each arthropod were placed in individual 400 ml beakers with 200 ml of natural sea water obtained from Long Island Sound at West Haven. An inoculum was prepared by decaying a small piece of scorpion cuticle and associated tissue in the same sea water with anoxic sediment for a week that resulted in the development of a biofilm. A sample of this inoculum was added to the sea water in each beaker which was then covered with aluminum foil and placed in an environmental chamber maintained at 30°C and 80% relative humidity at the Briggs' experimental taphonomy laboratory in the Department of Geology and Geophysics, Yale University. A specimen each of cockroach and shrimp was removed from the incubator and processed after 1, 2, 4, 8, 12, and 24 weeks. Material remaining from the 24 week sample was returned to the incubator to monitor the effect of 44 weeks decay.

Specimens were photographed before incubation and on recovery from the experiment to record the state of decay. Tissue and cuticle samples were transferred to glass vials and frozen at −60°C for subsequent analysis. Three posterior segments of the cockroach, and two posterior segments of the shrimp were sampled for chemical analysis. For each analysis the cuticle of a single segment was cleaned of any adhering matter and internal soft tissue with a tweezer and scalpel and then subjected to ultrasonication in deionised water for 30 min. The isolated cuticle was then extracted in 2:1 dichloromethane:methanol, for 30 min three times, to remove organically soluble components or subjected to thermodesorption for thermal extraction. The remaining residue represents insoluble macromolecular material that was analysed by py–GC–MS. For scanning electron microscopy analysis, the original, 4 week- and 44 week- decayed shrimp and cockroach cuticles were analysed without any chemical treatment using a environmental scanning electron microscope (Philips XL 30).

The shrimp and cockroach showed a sequence of morphological decay similar to that recorded in previous experiments (Briggs and Kear 1994; Duncan et al. 2003; Gupta et al. 2009). The shrimp cephalothorax separated from the abdomen within 2 weeks and the cuticle was easy to remove. The muscle tissue in the abdomen, however, remained relatively solid. The cockroach remained intact, but the abdomen of the latter was visibly bloated and the soft tissue inside both had largely liquified. Within 4 weeks, the shrimp disarticulated completely on removal from the vessel; the cuticle had become very thin and brittle but some soft tissue remained in the posterior abdomen. The cockroach skeleton largely disarticulated when the specimen was removed from the vessel; some tissues remained inside but were not intact structurally. Within 24 weeks the cockroach cuticle showed some thinning on the ventral side and very little cuticle could be recovered from the shrimp. After 44 weeks, there was little major change. Figures 7.5 and 7.6 reveal changes in surface texture and thickness of cuticle in shrimp and cockroach respectively. The shrimp cuticle revealed first loss of epicuticle after 4 weeks of decay and this loss progressed over the remaining 40 week. However, the cockroach

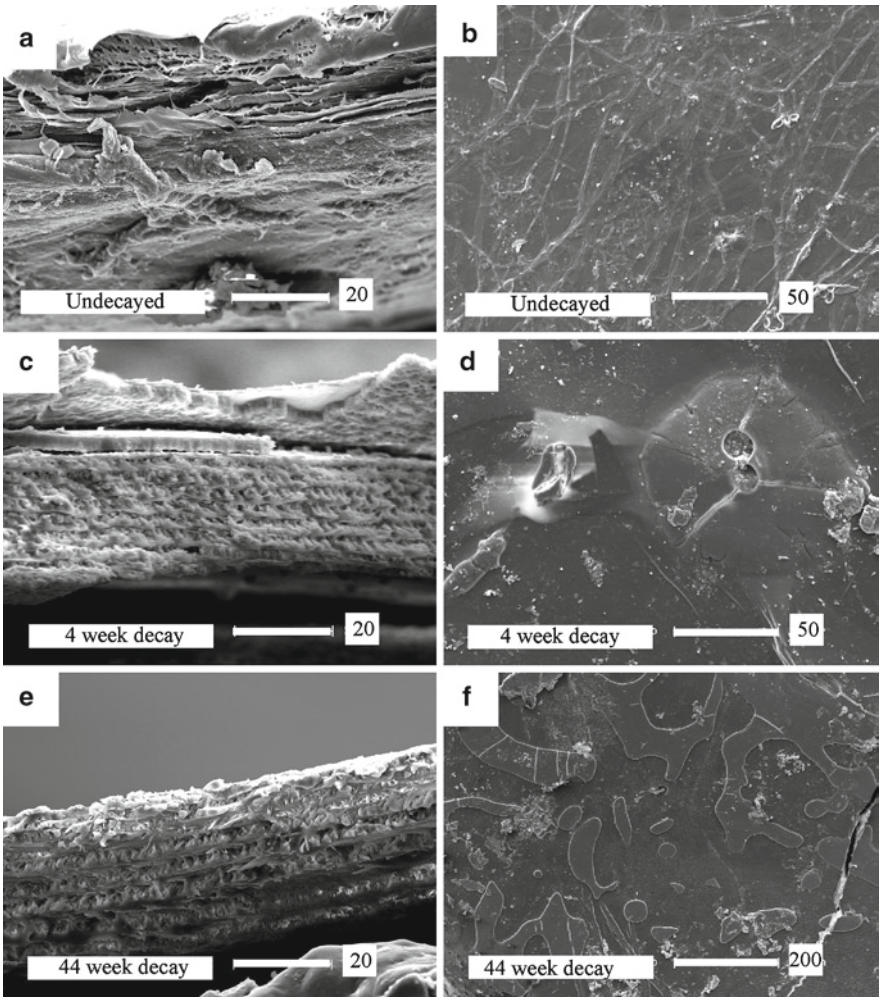

Fig. 7.5 SEM of surface texture (**b, d, f**) and cross section (**a, c, e**) of undecayed and decayed shrimp cuticles. Note loss in epicuticle after 4 weeks that continued in the 44 week decayed sample that resulted in decrease in thickness of the cuticle after 44 weeks. Scale in microns (Adapted from Gupta et al. 2009)

cuticle showed little change in surface and cross section after 44 weeks of decay (Gupta et al. 2009).

Analysis of undecayed shrimp, and cockroach using py–GC–MS revealed the presence of diagnostic chitin markers: 3-acetamidofuran, 3-methyl-5-acetamidofuran, oxazoline structures, acetylpyridone and 3-acetamido-4-pyrone together with protein-amino acid derived markers such as phenols, indoles, benzenes and diketopiperazine structures (Figs. 7.7 and 7.8). Following 4 weeks of decay, the shrimp carcass showed chitin-protein moieties after thermodesorption, but in addition, it

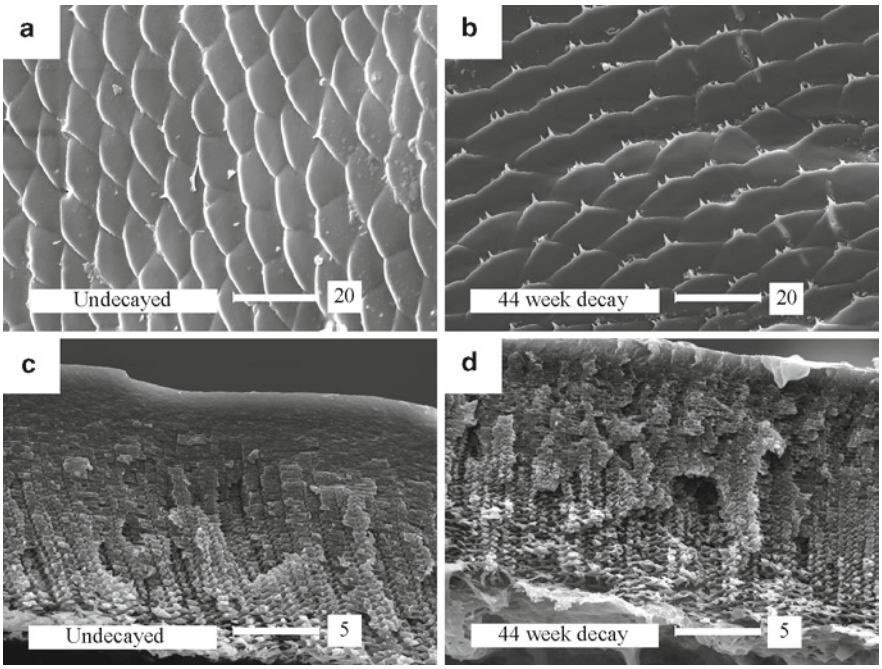

Fig. 7.6 SEM of surface and cross section of cockroach cuticle showing almost no change in surface texture (**a** and **b**) and thickness of cuticle (**c** and **d**). Scale in microns

revealed the presence of *n*-alkane/alkene homologues extending up to C_{24} derived from a macromolecular *n*-alkyl (aliphatic) component. This aliphatic component was detected in all the samples decayed for more than 4 weeks; the final sample at 44 weeks, also revealed a general reduction in the relative abundance of protein derived moieties compared to chitin (Fig. 7.7). In contrast, the cockroach (Fig. 7.8) showed little chemical change and the chitin-protein moieties were retained in relative abundances similar to those in the fresh sample and there was no evidence of the presence of *n*-alkane/alkene peaks (i.e., a macromolecular aliphatic component) in any of the decayed samples, including the one that decayed for 44 weeks.

The importance of lipids in generating an aliphatic composition during diagenesis has been demonstrated earlier by subjecting arthropods (Stankiewicz et al. 2000; Gupta et al. 2006c), leaves (Gupta et al. 2007c) and their lipids and other constituent biopolymers to experimental heating (maturation) in a gold capsule confined pyrolysis apparatus.

The living arthropods investigated here do not contain any resistant non-hydrolysable aliphatic biopolymer. Decomposition of chitin and proteins in the cuticle yields sugars and amino acids. Thus, the decay of arthropod cuticle (clearly revealed by SEM) generates a substrate to which lipids can bind to generate an aliphatic composition. Such a process was demonstrated by Larter and Douglas (1980) who synthesized melanoidins from glucose and amino acids and subsequently

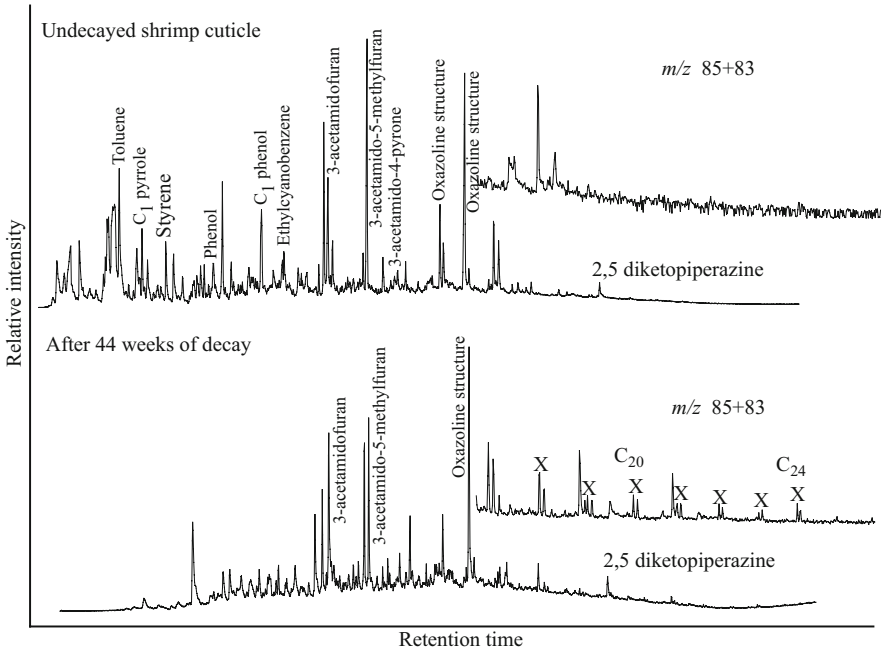

Fig. 7.7 Py–GC–MS analysis of undecayed and 44 week decayed shrimp cuticle revealing presence of incorporated lipids after 44 weeks (indicated by alkane/alkene homologs, X), that is initially absent in the undecayed sample. Note loss of proteinaceous compounds in the 44 week decayed sample (Adapted from Gupta et al. 2009)

reacted them with alcohols, fatty acids and sterols at 220°C to generate bound aliphatic components. Melanoidins can act as a 'geochemical glue' (Larter and Douglas 1980) in the formation of protokerogens and their presence, as long alkyl chains, has been demonstrated in protokerogen reaction mixtures (Shioya and Ishiwatari 1983).

The chain lengths of the aliphatic components of the decayed shrimp cuticle extend up to C_{24}. The distribution of fatty acids in modern shrimp ranges from C_{12} to C_{24} (Krzeczkowski 1970), including saturated and unsaturated fatty acids, suggesting that they may be incorporated into the macromolecule of the same fossil. Thus, it is likely that lipids that are originally functionalized (e.g. unsaturated and saturated fatty acids in this experiment, alcohols and sterols in that of Larter and Douglas 1980) are capable of reacting with the decomposing substrate. Further, the chain length of the aliphatic component in fossil shrimp does not exceed C_{24} (Baas et al. 1995; Gupta et al. 2008b), presumably reflecting the maximum chain length of the lipid available for incorporation from the organism. The lack of lipid incorporation in the cockroach cuticles (both of which are much thicker and more robust than the shrimp cuticle) during the course of the experiment presumably reflects their resistance to decay; lipids were unable to bind due to lack of decomposition substrate (Gupta et al. 2009).

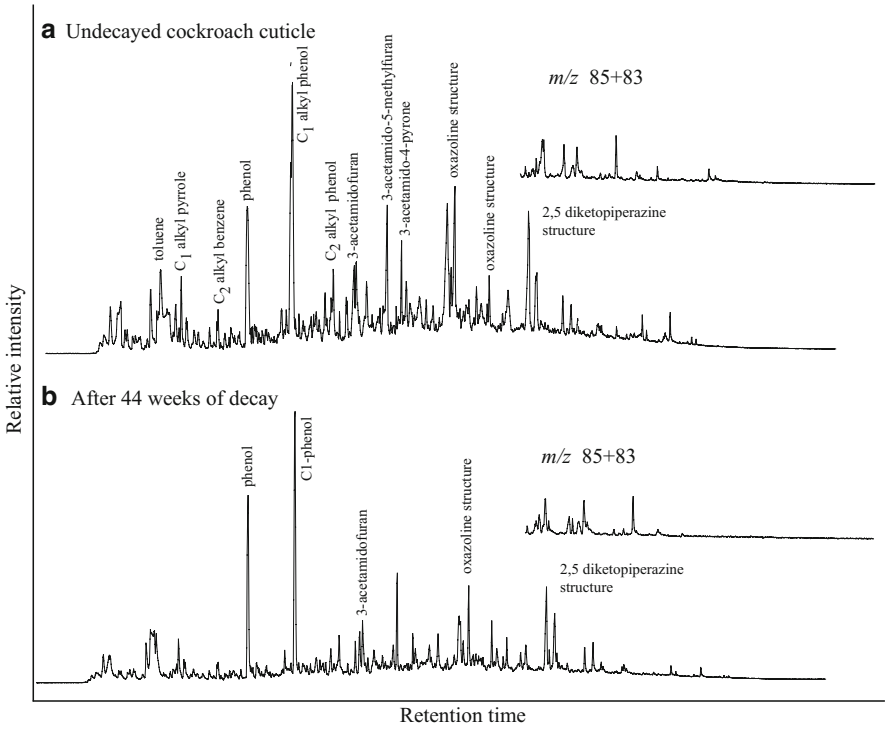

Fig. 7.8 Py–GC–MS analysis of undecayed and 44 week decayed cockroach cuticle showing little change in the chitin composition and no incorporation of lipids in the macromolecule as seen in the decayed shrimp cuticle (Adapted from Gupta et al. 2009)

7.5 Preservation of Biomolecules in Geologic Record

Laboratory simulation of decay in crustacean cuticle has shown to result in extensive loss of the protein component within the first 2 weeks of the experiment, while chitin has remained largely intact for the first 8 weeks, attesting to its greater survival potential (Baas et al. 1995). Traces of chitin have been detected in Pleistocene beetles (Stankiewicz et al. 1997c) and in beetles as old as 25 million years (Stankiewicz et al. 1997a; Gupta et al. 2007a, 2008b). However, the cuticles of fossil arthropods older than the Cenozoic, show no trace of chitin or protein, but have a dominant aliphatic component similar to bulk sedimentary organic matter (kerogen) as detected by conventional mass spectrometric methods. This contradiction has intrigued palaeontologists and chemists alike as it is difficult to explain the transformation of chitin (a carbohydrate) to a hydrocarbon polymer in the fossil. Initially, the aliphatic composition was interpreted as the result of diagenetic replacement by aliphatic organic matter from an external source (Baas et al. 1995). However, recent research has made this argument untenable (see discussion later).

Proteins are decay-prone (de Leeuw and Largeau 1993; but see Nguyen and Harvey 1998) except where they have undergone substantial cross-linking, as in the collagen that makes up the jaws of polychaetes. Protein and polysaccharide remnants have been shown to survive in 1,400 year old archaeological plant remains (Bland et al. 1998), possibly in 24.7 million years old weevil samples (Stankiewicz et al. 1997a; Gupta et al. 2007a) and even in 140 million years old sedimentary organic matter where preservation of labile moieties was facilitated by encapsulation within a resistant aliphatic matrix. While encapsulation may promote protein preservation by steric protection of labile compounds (Knicker et al. 2001; Mongenot et al. 2001; Riboulleau et al. 2001) analysis of fossil fish scale from the cretaceous failed to detect any nitrogen-bearing compounds.

7.6 Chemosystematics

The various molecular components in fossils show differences in their relative abundances. Hence, attempts have been made to see if fossils can be classified based on chemistry alone. One approach has been to understand (1) the distribution of the aliphatic component relative to the aromatic and (2) the differences in chain length of the aliphatic components. For example, in the Cretaceous Las Hoyas locality in Spain, aliphatics in fish scale range up to $C_{21/22}$, whereas the decapods show alkyl benzene and phenols (aromatics) as major components, (aliphatics ranging to C_{21} with additional sulfur compounds are less significant). Py–GC–MS of beetles from the site, on the other hand, have revealed only aliphatics, ranging from C_8 upto C_{31} likely due to the contribution of long chain waxes greater than C_{30} in insect cuticle (Lockey 1988). The diagenetic history of organic components varies with starting composition, but also with environmental setting and time (Briggs 1999; Briggs et al. 2000). Thus, differences between the fossil taxa may indicate inherent contrasts in the original components and their thermal alteration products derived from the living organism. Degree of aromaticity may also reflect thermal maturity. Similarly, differences between plants and arthropods have been reported in cuticles from the samples of Carboniferous age from North America (Stankiewicz et al. 1998a) mainly in the distribution of alkenes/alkanes rather than in the total chain length or the proportion of aromatics. Hence, to investigate fossil chemosystematics further, a comprehensive analysis of comparable material from different ages and environments is required.

7.7 Origin of Aliphatic Polymer in the Fossils

7.7.1 Migration from Sediment

Ubiquitous occurrence of aliphatic components in sediments, insect, and plant fossils, has been attributed to both diagenetic replacement and derivation of the signal from external source including the host sediment (Baas et al. 1995).

However, this argument is possibly circumstantial as revealed by several lines of evidence: (1) Macromolecular geopolymers are, by definition, insoluble in water and organic solvents, and therefore relatively immobile unless physically transported; (2) Aliphatic composition is detected in *Hymenaea* leaves and beetles, trapped in *Hymenaea* amber that are protected from external sources of chemical contamination (Stankiewicz et al. 1998b); (3) Chemical signatures in co-occurring plant and insect fossils from the Upper Carboniferous of North America are compositionally different that have altered internal morphology, indicating that they could not have been introduced solely from the sediment (Stankiewicz et al. 1998a); (4) Both experimental taphonomy and gold cell experiments prove that the organism incorporates lipids without need of any external source (5) Thermally assisted methylation (THM) analysis (providing distribution of fatty acids in fossils) of co-occurring insect and plant fossils and the associated organic rich matrix, have revealed differences in the distribution of the constituent fatty acyl components indicating that the aliphatic components of the fossil differ structurally from that in sediment (Gupta et al. 2007a). Thus, introduction from other sources such as sediment is unlikely as an explanation for the aliphatic component of macrofossils.

7.7.2 In Situ Polymerization of Labile Aliphatic Components

In the absence of resistant aliphatic biopolymer in the exoskeleton, the presence of an aliphatic component in the fossil cannot be attributed to selective preservation of such biopolymer (following decay of the more labile molecules). Derivation of aliphatics from sediment is unlikely as well. Hence, such a composition must derive *in-situ* from the organism. The fossil remains of beetles consist largely of long-chain aliphatic components. THM analysis of the beetles indicate presence of fatty acyl moieties, showing that fossilization must have involved the incorporation of lipids such as fatty acids to contribute to the aliphatic component. Such a process of in situ polymerization accounts for the fossil record of eurypterids as well as graptolites. Such a process likely accounts for the preservation of majority of organic fossils including plants.

7.8 Implications for Formation of Sedimentary Organic Matter

Ancient sedimentary organic matter is formed by diagenetic alteration of biological material that becomes progressively transformed into non-hydrolysable, polymeric substances. This recalcitrant organic matter is dispersed in sediments and is called kerogen (Tissot and Welte 1984). The composition and type of kerogen relies on the nature of the biological input, the environment of deposition and the intermediate reactions (de Leeuw and Largeau 1993). Many kerogens are highly aliphatic

(especially Type I/II, as observed in the fossils here) and serve as a feed stock for petroleum that is formed during thermal maturation (a process termed catagenesis) on deep burial. Because of its commercial and economic importance, elucidating the mechanism of kerogen formation and preservation is critical to understanding the formation of fossil fuel deposits. In turn, this helps us understand essential processes in the preservation of macroscopic and morphologically recognisable organic fossils.

Kerogen formation has been variously attributed to the following processes: (1) neogenesis (Tissot and Welte 1984) in which sedimentary organic matter is formed by random intermolecular polymerisation and polycondensation of biological residues, (2) natural vulcanisation that involves the reaction between reduced sulfur and various functional groups in organic compounds, resulting in the formation of a S-rich macromolecule, (Kok et al. 2000), (3) oxidative reticulation (Gatellier et al. 1993, Riboulleau et al. 2001) where lipids may be crosslinked with oxygen, as seen in the fossil cephalopods and finally (4) selective preservation of highly aliphatic and resistant biopolymers (e.g. algaenan or cutan present in some plants; de Leeuw and Largeau 1993). Recent analyses of a wide variety of gymnosperms and angiosperms has failed to detect cutan (a long chain resistant aliphatic biopolymer, thought to be responsible for aliphatic signal in plant fossils) in plants previously thought to contain it (Mösle et al. 1998; Collinson et al. 1998; Gupta et al. 2006c). These data raise questions about the universality of selective preservation.

Analyses reveal that, while younger fossil arthropods may preserve traces of the more resistant elements of the chitin-protein complex that make up the cuticle, older fossils have been dramatically altered and often yield an aliphatic signature similar to that of many plant fossils and kerogen. Selective preservation does not provide an adequate explanation of this observation since the aliphatic components occurring in the cuticle of modern arthropods are not decay-resistant and differ in structure from those present in fossils (Stankiewicz et al. 2000). Likewise, recent analyses of the modern leaves have indicated that they do not contain a resistant aliphatic components such as cutan, even though aliphatic signatures are dominant in the leaves of fossil taxa (Mölse et al. 1998; Gupta et al. 2006c, 2007c). Thus, the convergence in the macromolecular composition of fossilized plant cuticles, fossilized animal cuticles and kerogen cannot be explained simply on the basis of the known biochemical compositions of the living organisms.

The chemistry of fossils discussed here, cast doubt on selective preservation and simple chemical transfer as mechanisms for explaining the aliphatic composition of fossil cuticles. As clearly demonstrated by the chemical transformation of cephalopods and arthropods, more labile chemical components, such as free cuticular lipids or hydrolysable lipids (such as mon-, di- and triacyl glycerides), are transformed *in situ* and have been incorporated to form the aliphatic component of geopolymers. Indeed, such lipid incorporation has been observed to contribute significantly to kerogen formation, while the role of selective preservation has been limited (Gatellier et al. 1993; Riboulleau et al. 2001).

References

Adam P, Schmid JC, Mycke B, Strazielle C, Connan J, Huc A, Albrecht P (1993) Structural investigation of non-polar sulfur cross-linked macromolecules in petroleum. Geochim Cosmochim Acta 57:3395–3419

Adam P, Schneckenburger P, Schaeffer P, Albrecht P (2000) Clues to early diagenetic sulfurization processes from mild chemical cleavage of labile sulfur-rich geomacromolecules. Geochim Cosmochim Acta 64:3485–3503

Baas M, Briggs DEG, van Heemst JDH, Kear AJ, de Leeuw JW (1995) Selective preservation of chitin during the decay of shrimp. Geochim Cosmochim Acta 59:945–951

Bland HA, van Bergen PF, Carter JF, Evershed RP (1998) Early diagenetic transformations of Proteins and Polysaccharides in archaeological plant remains. In: Stankiewicz BA, van Bergen PF (eds) Nitrogen-containing macromolecules in the bio- and geosphere. ACS Symposium series 707, American Chemical Society

Blokker P, Schouten S, de Leeuw JW, Sinninghe Damsté JS, van den Ende H (2000) A comparative study of fossil and extant algaenans using ruthenium tetroxide degradation. Geochim Cosmochim Acta 64:2055–2065

Boyce CK, Cody GD, Feser M, Jacobsen, Knoll AH, Wirick S (2002) Preservation of cell wall chemistry and microstructure in plant fossils as old as 400 million years: detection by carbon X-ray absorption spectromicroscopy. Geology 30:1039–1042

Briggs DEG (1999) Molecular taphonomy of animal and plant cuticles: selective preservation and diagenesis. Philos Trans R Soc London Ser B 354:7–16

Briggs DEG (2003) The role of decay and mineralization in the preservation of soft-bodied fossils. Annu Rev Earth Planet Sci 31:275–301

Briggs DEG, Kear AJ (1994) Decay and mineralization of shrimps. Palaios 9:431–456

Briggs DEG, Evershed RP, Lockheart MJ (2000) The biomolecular paleontology of continental fossils. Paleobiology 26 (supplement to no. 4):169–193

Collinson ME, Mösle B, Finch P, Wilson R, Scott AC (1998) The preservation of plant cuticle in the fossil record: a chemical and microscopical investigation. Ancient Biomolecules 2:251–265

Cuesta A, Dhamelincourt P, Laureyns J, Martinez-Alonso A, Tascon JMD (1994) Raman microprobe studies on carbon materials. Carbon 32:1523–1532

de Leeuw JW, Baas J (1993) The behavior of esters in the presence of tetramethylammonium salts at elevated temperatures; flash pyrolysis or flash chemolysis? J Anal Appl Pyrol 26:175–184

de Leeuw JW, Largeau C (1993) A review of macromolecular organic compounds that comprise living organisms and their role in kerogen, coal and petroleum formation. In: Engel MH, Macko SA (eds) Organic geochemistry: principles and applications. Plenum, New York, pp 23–62

Duncan IJ, Titchener F, Briggs DEG (2003) Decay and disarticulation of the cockroach: implications for the preservation of the blattoids of Writhlington (Upper Carboniferous), UK. Palaios 18:256–265

Freeman KH, Hayes JM, Trendel J-M, Albrecht P (1990) Evidence from carbon isotope measurements for diverse origins of sedimentary hydrocarbons. Nature 343:254–256

Gatellier J-PLA, de Leeuw JW, Sinninghe Damsté JS, Derenne S, Largeau C, Metzger P (1993) A comparative study of macromolecular substances of a Coorongite and cell walls of the extant alga *Botryococcus braunii*. Geochim Cosmochim Acta 57:2053–2068

Gupta NS, Briggs DEG, Collinson ME, Evershed RP, Michels R, Pancost RD (2006a) Organic preservation of fossil arthropods: an experimental study. Proc R Soc Lond B 273:2777–2783

Gupta NS, Briggs DEG, Collinson ME, Evershed RP, Pancost RD (2006c) Re-investigation of the occurrence of cutan in plants: implications for the leaf fossil record. Paleobiology 32:432–449

Gupta NS, Briggs DEG, Collinson ME, Evershed RP, Michels R, Pancost RD (2007a) Molecular preservation of plant and insect cuticles from the Oligocene Enspel Formation, Germany: evidence against derivation of aliphatic polymer from sediment. Org Geochem 38:404–418

Gupta NS, Tetlie OE, Briggs DEG, Pancost RD (2007b) Fossilization of Eurypterids: a result of molecular transformation. Palaios 22:439–447

Gupta NS, Briggs DEG, Collinson ME, Evershed RP, Michels R, Jack KS, Pancost RD (2007c) Evidence for the in situ polymerisation of labile aliphatic organic compounds during the preservation of fossil leaves: implications for organic matter preservation. Org Geochem 38:499–522

Gupta NS, Briggs DEG, Landman NH, Tanabe K, Summons RE (2008a) Molecular structure of organic components in cephalopods: evidence for oxidative crosslinking in fossil marine inverstebrates. Org Geochem 39:1405–1414

Gupta NS, Cambra-Moo O, Briggs DEG, Love GD, Fregenal-Martinez MA, Summons RE (2008b) Molecular taphonomy of macrofossils from the Cretaceous Las Hoyas Formation, Spain. Cretaceous Res 29:1–8

Gupta NS, Cody GD, Tetlie OE, Briggs DEG, Summons RE (2009) Rapid incorporation of lipids into macromolecules during experimental decay of invertebrates: initiation of geopolymer formation. Org Geochem 40:589–594

Hayes JM, Freeman KH, Popp BN, Hoham CH (1990) Compound-specific isotopic analyses: a novel tool for reconstruction of ancient biogeochemical processes. Org Geochem 16:1115–1128

Hebting Y, Schaeffer P, Behrens A, Adam P, Schmitt G, Schneckenburger P, Bernasconi SM, Albrecht P (2006) Biomarker evidence for a major preservation pathway of sedimentary organic carbon. Science 312:1627–1631

Knicker H, del Rio JC, Hatcher PG, Minard RD (2001) Identification of protein remnants in insoluble geopolymers using TMAH thermochemolysis/GC–MS. Org Geochem 32:397–409

Kok MD, Schouten S, Sinninghe Damsté JS (2000) Formation of insoluble, nonhydrolyzable, sulfur-rich macromolecules via incorporation of inorganic sulfur species into algal carbohydrates. Geochim Cosmochim Acta 64:2689–2699

Krzeczkowski RA (1970) Fatty acids in raw and processed Alaska pink shrimp. J Am Oil Chem Soc 47:451–452

Larter SR, Douglas AG (1980) Melanoidins – kerogen precursors and geochemical lipid sinks: a study using pyrolysis gas chromatography (PGC). Geochim Cosmochim Acta 44:2087–2095

Lockey KH (1988) Lipids of the insect cuticle: origin, composition and function. Comp Biochem Physiol B Biochem Mol Biol 89:595–645

Love GD, Snape CE, Carr AD, Houghton RC (1995) Release of covalently-bound alkane biomarkers in high yields from kerogen via catalytic hydropyrolysis. Org Geochem 23:981–998

Marshall CP, Love GD, Snape CE, Hill AC, Allwood AC, Walter MR, Kranendonk MJ, Van Bowden SA, Sylva SP, Summons RE (2007) Structural characterization of kerogen in 3.4 Ga Archaean cherts from the Pilbara Craton, Western Australia. Precambrian Res 155:1–23

Mösle B, Collinson ME, Finch P, Stankiewicz BA, Scott AC, Wilson R (1998) Factors influencing the preservation of plant cuticles: a comparison of morphology and chemical comparison of modern and fossil examples. Org Geochem 29:1369–1380

Nguyen RT, Harvey HR (1998) Protein preservation during early diagenesis in marinewaters and sediments. In: Stankiewicz BA, van Bergen PF (eds) Nitrogen containing macromolecules in the bio- and geosphere. ACS Symposium Series 707, American Chemical Society

Rahl JM, Anderson KM, Brandon MT, Fassoulas C (2005) Raman spectroscopic carbonaceous material thermometry of low-grade metamorphic rocks: Calibration and application to tectonic exhumation in Crete, Grece. Earth Planet Sci Lett 240:339–354

Riboulleau A, Derenne S, Largeau C, Baudin F (2001) Origin of contrasting features and preservation pathways in kerogens from the Kashpir oil shales (Upper Jurassic, Russian Platform). Org Geochem 32:647–665

Schaefer J, Kramer KJ, Garbow JR, Jacob GS, Stejskal EO, Hopkins TL, Speirs RD (1987) Aromatic cross-links in insect cuticle: detection by solid-state ^{13}C and ^{15}N NMR. Science 235:1200–1204

Schaeffer P, Harrison BJ, Keely BJ, Maxwell JR (1995a) Product distributions from chemical degradation of kerogens from a marl from a Miocene evaporitic sequence (Vena del Gesso, N. Italy). Org Geochem 23:541–554

Schaeffer P, Reiss C, Albrecht P (1995b) Geochemical study of macromolecular organic matter from sulfur-rich sediments of evaporitic origin (Messinian of Sicily) by chemical degradations. Org Geochem 23:567–581

Shioya M, Ishiwatari R (1983) Laboratory thermal conversion of sedimentary lipids to kerogen-like matter. Org Geochem 5:7–12

Stankiewicz BA, Briggs DEG, Evershed RP, Flannery MB, Wuttke M (1997a) Preservation of chitin in 25-million-year-old fossils. Science 276:1541–1543

Stankiewicz BA, Briggs DEG, Evershed RP (1997b) Chemical composition of Paleozoic and Mesozoic fossil invertebrate cuticles as revealed by pyrolysis-gas chromatography/mass spectrometry. Energy Fuels 11:515–521

Stankiewicz BA, Briggs DEG, Evershed RP, Duncan IJ (1997c) Chemical preservation of insect cuticles from the Pleistocene asphalt deposits of California USA. Geochim Cosmochim Acta 61:2247–2252

Stankiewicz BA, Mösle B, Finch P, Collinson ME, Scott AC, Briggs DEG, Evershed RP (1998a) Molecular taphonomy of arthropod and plant cuticles from the Carboniferous of North America: implications for the origin of kerogen. J Geol Soc 155:453–462

Stankiewicz BA, Poinar HN, Briggs DEG, Evershed RP, Poinar GO Jr (1998b) Chemical preservation of plants and insects in natural resins. Proc R Soc Lond B 265:641–647

Stankiewicz BA, Briggs DEG, Michels R, Collinson ME, Evershed RP (2000) Alternative origin of aliphatic polymer in kerogen. Geology 28:559–562

Tissot B, Welte DH (1984) Petroleum formation and occurrence, 2nd edn. Springer, Berlin

Chapter 8
Transformation of Chitinous Tissues in Elevated Presssure–Temperature Conditions: Additional Insights from Experiments on Plant Tissues

Neal S. Gupta

Contents

Abstract Modern arthropod cuticles consist of chitin protein complex, but fossil arthropods older than Cenozoic, contain a significant amount of aliphatic component with or without any chitin. Such a transformation is observed in leaves of plant fossils where the bulk composition has been modified. This apparent contradiction was examined by subjecting modern animal cuticles to confined heating (350°C/700 bars/24 h) following various chemical treatments. Analysis of artificially matured untreated cuticle, yielded moieties related to phenols and alkylated substituents, pyridines, pyrroles and possibly indenes (from chitin). Components such as *n*-alkyl amides, fatty acids and alkane/alkene homologues ranging from C_9 to $<C_{20}$ were also generated, indicating the presence of an *n*-alkyl component, similar in composition to that encountered in fossil arthropods. Analysis of cuticles that had been heated after lipid extraction and hydrolysis did not yield any aliphatic polymer. This provides evidence that lipids incorporated from the cuticle were the source of aliphatic polymer. Similar heating of plant tissues generated an aliphatic macromolecule similar to that found in fossils. Comparison of the products derived from maturation of different pre-treated plant tissues demonstrates that solvent-extractable and hydrolysable lipids were precursors of the generated macromolecular

N.S. Gupta (✉)
Indian Institute of Science Education and Research, Transit Campus MGSIPAP, Complex Sector 26, Chandigarh 160 019, Mohali, India
e-mail: sngupta@iisermohali.ac.in

N.S. Gupta (ed.), *Chitin*, Topics in Geobiology 34,
DOI 10.1007/978-90-481-9684-5_8, © Springer Science+Business Media B.V. 2011

material. Thus, the experiments indicate that labile alkyl compounds can be a source of the insoluble aliphatic component of fossil organic matter in the absence of a resistant aliphatic precursor in the living organism.

8.1 Introduction

Arthropod cuticles consist of chitin fibres in a proteinaceous complex, calcium carbonate is present in crustaceans that further strengthens their cuticles.

Chitin has been shown to survive in Pliestocene beetles (Stankiewicz et al. 1997a) and in weevils as old as 25 million years (Stankiewicz et al. 1997b), as detected by mass spectrometric methods. Curiously, the cuticles of fossil arthropods invariably yield an aliphatic composition (Briggs 1999) especially in fossils older than Tertiary. Selective preservation of precursor resistant aliphatics that has been proposed to explain existence of aliphatics in plant fossils (see discussion later) is not a plausible explanation as these do not occur in the exoskeletons of modern arthropods. Initially, the aliphatic composition was thought to have been introduced by diagenetic replacement of aliphatics from an external source (Baas et al. 1995). However, it has since been suggested that in situ *polymerisation* of constituent cuticular waxes and/or tissue lipids may have resulted in an aliphatic composition in fossils (Stankiewicz et al. 2000).

Extensive taphonomic experiments have been conducted on arthropods to understand various geochemical parameters influencing their preservation in the fossil record, especially in modern shrimp (Briggs and Kear 1993; Baas et al. 1995; Hof and Briggs 1997; Sagemann et al. 1999) and cockroaches (Duncan et al. 2003). In such studies, the focus has been on controlled decay and the effect of physical disarticulation on the organism during transport. Understanding changes in the chemistry of modern arthropod cuticles to explain their composition in the fossil record (Stankiewicz et al. 2000) using experimental heating techniques has been employed to investigate the transformation of the cuticle of the emperor scorpion, *Pandinus imperator*. For example, Stankiewicz et al. (2000) generated an aliphatic composition similar to that observed in fossil scorpion.

In the present investigation a suite of gold tube confined pyrolysis studies were employed to identify the source of the aliphatic polymer encountered in the fossil record of both animals and plants (see discussion on plants later in the chapter, Fig. 8.1). In the case of animals, experiments were carried out on arthropods and model compounds following various chemical pre-treatments.

8.2 Experimental Heating of Arthropod Cuticle

The modern arthropods, *Pandinus imperator* (emperor scorpion), *Crangon crangon* (shrimp) and *Gromphadorhina portentosa* (Madagascar hissing cockroach) were chosen as they have been the subject of previous taphonomic experiments

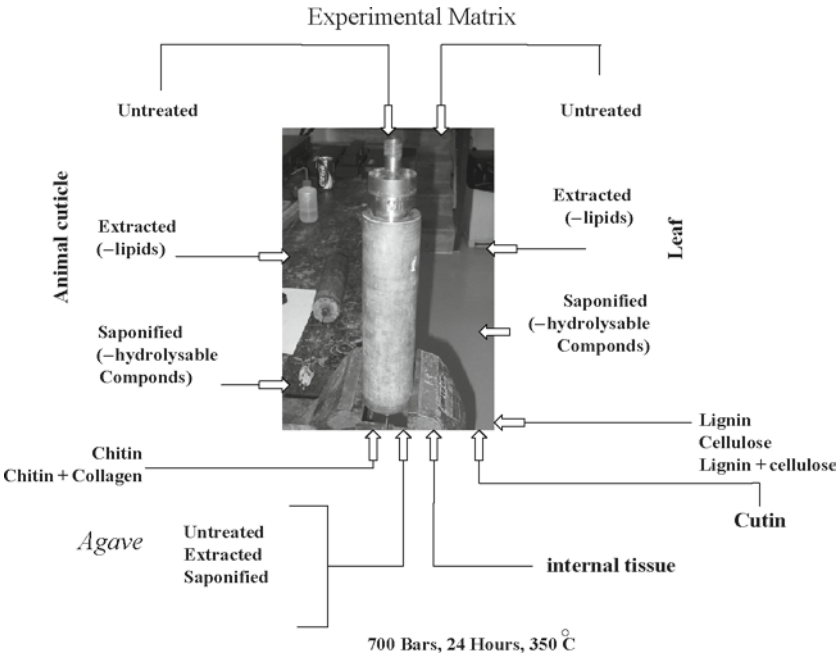

Fig. 8.1 Experimental protocol showing plant and animal tissues and the various chemical treatments they were subjected to before introducing in the confined heating apparatus

(Sagemann et al. 1999; Stankiewicz et al. 1998; Duncan et al. 2003). Body structure and ample cuticle provide additional advantages for handling and articulation with required anatomical component during the experiment. The arthropods were killed by freezing at −20°C for 24–48 h and were then dissected with a scalpel to remove the internal tissues to facilitate recovery of the cuticle from the entire organism. The cuticle was frozen in liquid nitrogen and crushed with a mortar and pestle after which the internal tissues were removed by boiling the crushed sample in distilled water at 100°C, three times for an hour each. The recovered sample was then subjected to two chemical treatments before experimental heating. Cuticle (1) was not chemically treated. Cuticle (2) was solvent extracted in 2:1 DCM/MeOH ratio, five times for 30 min each and subsequently saponified (subjected to base hydrolysis) for 24 h (Gupta et al. 2006).

The prepared arthropod cuticles were experimentally heated at 350°C and 700 bars for 24 h (Stankiewicz et al. 2000; Gupta et al. 2006) in the apparatus shown in Fig. 8.1. This technique involves subjecting samples confined in gold capsules to thermal stress at a designated pressure for a required length of time (Michels et al. 1995). Confined pyrolysis experiments have been previously undertaken in laboratory to simulate thermal maturation of organic matter (Monthioux et al. 1985) by subjecting them to elevated pressure–temperature conditions (Michels et al. 1995). The shrimp cuticle was also matured independently in two separate experiments in the presence of commercial powder $CaCO_3$ (1:1 *w/w*) and kaolinite (clay, 1:1 *w/w*)

to explore the effect of different inorganic matrix materials on transformation of the cuticle during the experiment. Commercially prepared chitin was obtained from Sigma Aldrich and was also experimentally heated under confined conditions following solvent extraction.

The matured samples were analysed using Thermodesorption–Gas Chromatography–Mass Spectrometry (TD–GC–MS) at 30°C that removes volatile non-macromolecular components followed by py–GC–MS at 610°C (see Gupta et al. 2006 for conditions).

8.3 Composition of Untreated Arthropod Cuticle

Flash pyrolysis of commercial chitin yielded 3-acetamido-4-pyrone, 3-acetamido-5-methylfuran, acetylpyridone, and 3-acetamidofuran as the main chemical moieties. Other moieties included pyridine, methyl pyridine, acetamide, acetylpyrrole, acetylpyrroline, amine derivatives, levoglucosenone, acetamide, acetyldihydropyridine and oxazoline structures (Fig. 8.2). The pyrolysates of the untreated cuticle of the cockroach (Fig. 8.2) and scorpion clearly show the presence of these chitin markers. Important pyrolysis products that are also present in the arthropod pyrolysate include benzene derivatives (e.g. derived from phenylanaline), alkyl pyrroles (possibly derived from the amino acids proline and hydroxyproline), phenol and its alkyl substituents (from tyrosine), indoles (e.g derived from tryptophan), and diketopiperazine derivatives possibly from the dipeptides proline–alanine, proline–glycine, proline–lycine, proline–arginine and proline–proline.

The fatty acids *n*-C_{16} and *n*-C_{18} were also observed in the cuticle pyrolysates, but clearly are not derived from chitin; not only are they structurally distinct from any chitin precursors, but these components were not detected in the pyrolysates of commercial chitin (Fig. 8.2). Such fatty acyl components are likely derived from lipids associated with the cuticle, the presence of these acids was reported in the pyrolysate of cuticles of modern stingless bee (Stankiewicz et al. 1997c).

8.4 Composition of the Arthropod Cuticle Heated Without Chemical Treatment

Pyrolysis of commercial chitin after experimental heating (Fig. 8.3) yielded pyridine and its alkyl derivatives, and phenol and its mono, di, tri and tetra alkyl derivatives; the phenol derivatives are amongst the most abundant. Other important compounds tentatively identified include indene and its alkyl derivatives. Furans, pyrones, pyridones, pyrroles and oxazoline structures, which are the most important pyrolysis products of unmatured chitin (Fig. 8.2) were not detected. Thus, thermal maturation has chemically transformed the composition and structure of chitin. The mass chromatogram *m/z* 83+85 does not reveal the presence of *n*-alkane/alk-1-ene

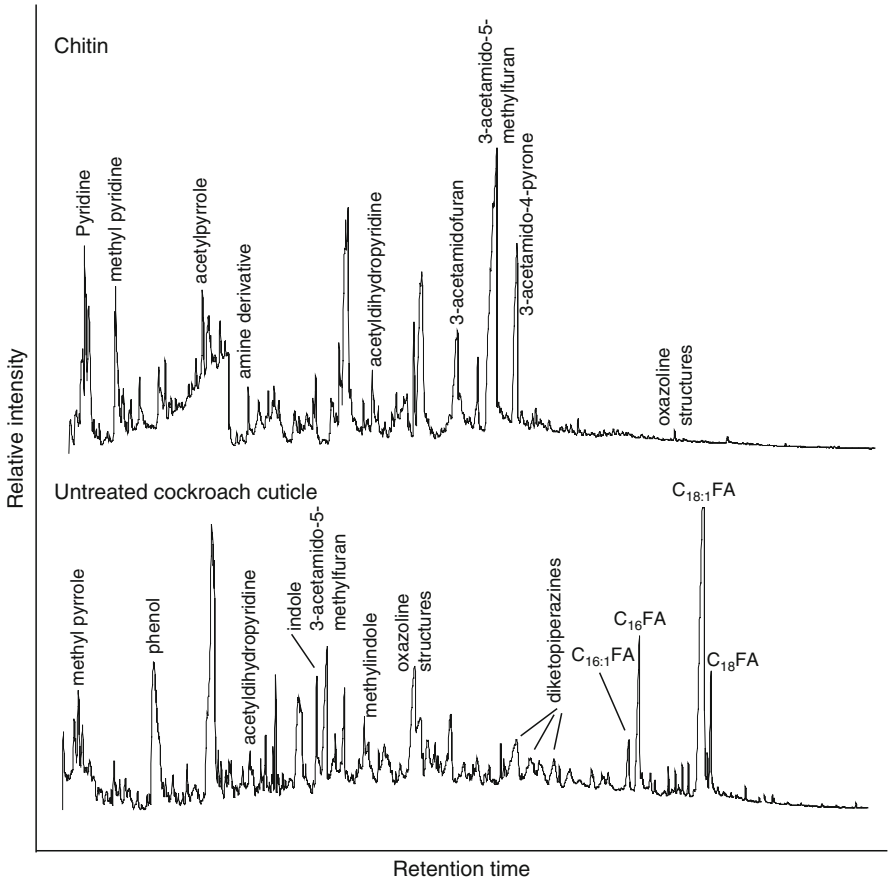

Fig. 8.2 Pyrolysis –gas chromatography–mass spectrometry analysis of chitin and modern cockroach cuticle that had not been experimentally heated. C_nFA denotes fatty acid with n carbon atoms and additional unsaturation in the carbon skeleton where present (Adapted from Gupta et al. 2006a)

homologues, indicating that chitin does not yield aliphatics under confined heating conditions.

The chitin-derived compounds are clearly evident in the pyrolysates of heated cockroach (Fig. 8.3) and scorpion cuticle. These include pyrrole and indole components, derived from proteins, pyridine and its alkyl derivatives. Phenol and its mono, di, tri and tetra alkyl derivatives and indenes were also detected, as in experimentally heated chitin model compound. The fatty acids *n*-C_{16} and *n*-C_{18} are abundant, as in fresh cuticle. The matured shrimp cuticle also shows the presence of these moieties (Fig. 8.3), but the relative abundance of fatty acids is less and *n*-C_{18} fatty acid was released in only trace abundances.

A range of compounds that are largely undetected in the pyrolysates of initially unheated cuticle and heated commercial chitin are observed. These include *n*-alkyl amides, with the C_{16} and C_{18} homologues being most abundant (Fig. 8.3). Although

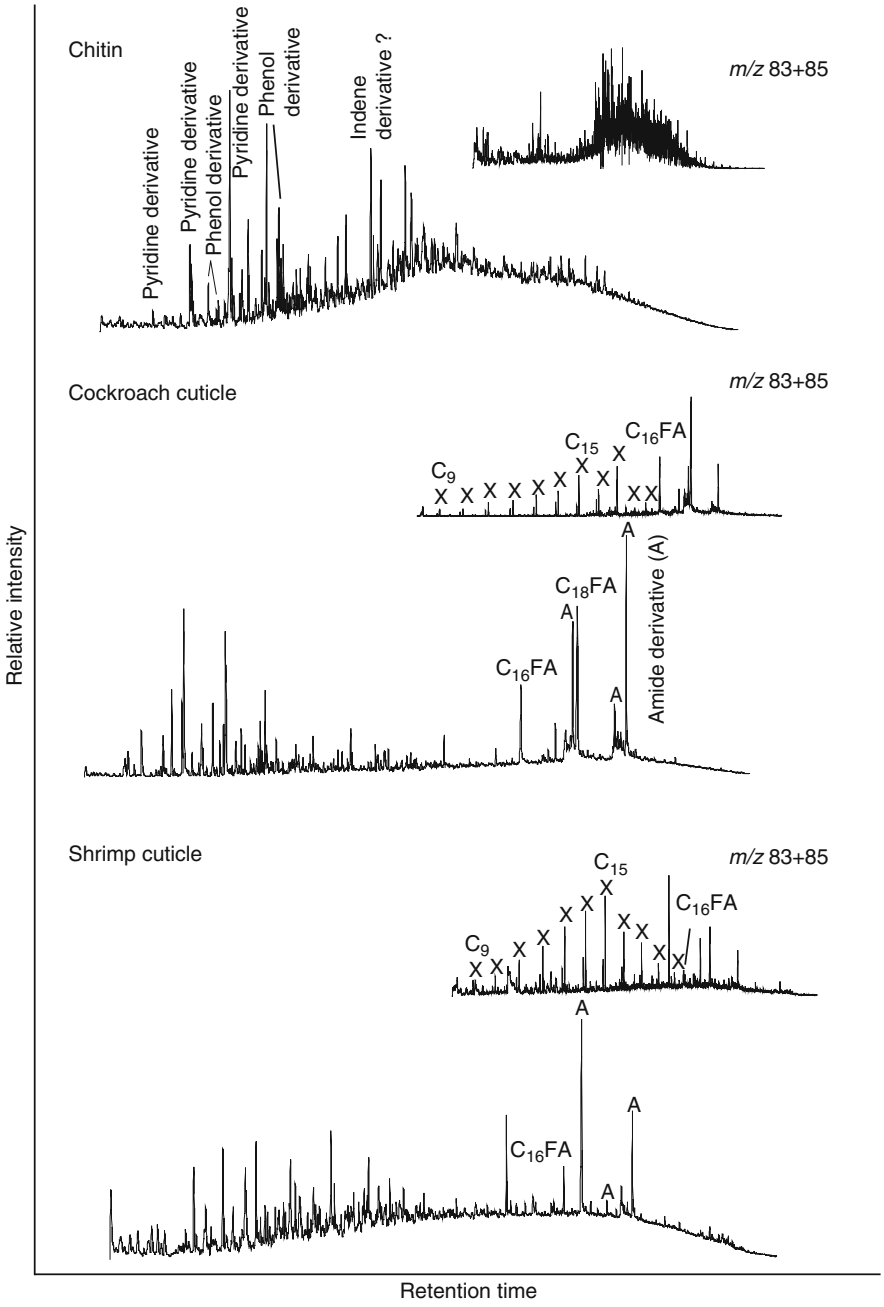

Fig. 8.3 Pyrolysis–gas chromatography–mass spectrometry analysis of chitin and modern cockroach and shrimp cuticle that has been experimentally heated. A denotes amide derivative corresponding to a certain chain length. *Inset m/z* 85+83 denotes alkane/alkene homologues (x) present in heated shrimp and cockroach cuticle but absent in heated chitin. Rest of the symbols same as in Fig. 8.2 (Adapted from Gupta et al. 2006a)

not readily apparent in the total ion current, the *m/z* 83+85 mass chromatogram reveals the presence of *n*-alkane/alk-1-ene homologues ranging from *n*-C_{10} to *n*-C_{19}. The most abundant alkanes and alkenes range from *n*-C_{14} to *n*-C_{17}. These homologues are often encountered in the pyrolysate of fossil arthropods, including scorpion (Stankiewicz et al. 2000) and shrimp (Stankiewicz et al. 1997c), and indicate the presence of an aliphatic polymer. The matured shrimp cuticle also shows the presence of these moieties (Fig. 8.3), but the relative abundance of fatty acids is less and *n*-C_{18} fatty acid was detected only in trace abundance.

8.5 Composition of Arthropod Cuticle Heated After Chemical Treatment

Shrimp cuticle matured in the presence of clay (Fig. 8.4) yielded a composition similar to untreated cuticle revealing the presence of phenols, indenes, amides, fatty acyl moieties and a distinct *n*-alkyl component. Cuticle matured in the presence of $CaCO_3$ (Fig. 8.4), in contrast, showed a considerable reduction in the relative abundance of amides and *n*-alkane/alkene homologues.

Cuticle heated following lipid extraction and saponification revealed the presence of moieties related solely to chitin and protein (with distribution of moieties comparable to that of cuticle matured without chemical treatment, Fig. 8.5) and no aliphatic components (inset, Fig. 8.5). This provides direct experimental evidence that soluble and hydrolysable lipids are necessary for the formation of the aliphatic polymer as commercial chitin failed to yield an aliphatic component on heating by itself.

8.6 Transformation of Arthropod Cuticle

Pyrolysis of modern shrimp, cockroach and scorpion cuticle reveals the presence of characteristic pyrolysis products of chitin and fatty acyl moieties derived from lipids from the cuticle. However, confined heating of the cuticle at 350°C and 700 bars resulted in significant changes in macromolecular composition. Degradation and defunctionalization of chitin and proteins are indicated by the absence of the characteristic chitin and protein markers that are present in the pyrolysate of untreated cuticle. Thermally induced changes to the chitin-protein complex (deacetylation of chitin, and aromatization of both chitin and protein) resulted in an abundance of phenol and alkyl substituted phenols in the pyrolysate. Moreover, another important change is the appearance of *n*-alk-1-enes and *n*-alkanes; as these are not thermally desorbable they provide unequivocal evidence for the presence of an aliphatic macromolecule. Additionally, *n*-alkyl amides are abundant (the most abundant being *n*-C_{16} and *n*-C_{18}) along with alkylated indenes. Cuticles are made of chitin/protein complex. Chitin has N-acetylglucosamine as the monomeric unit and proteins have

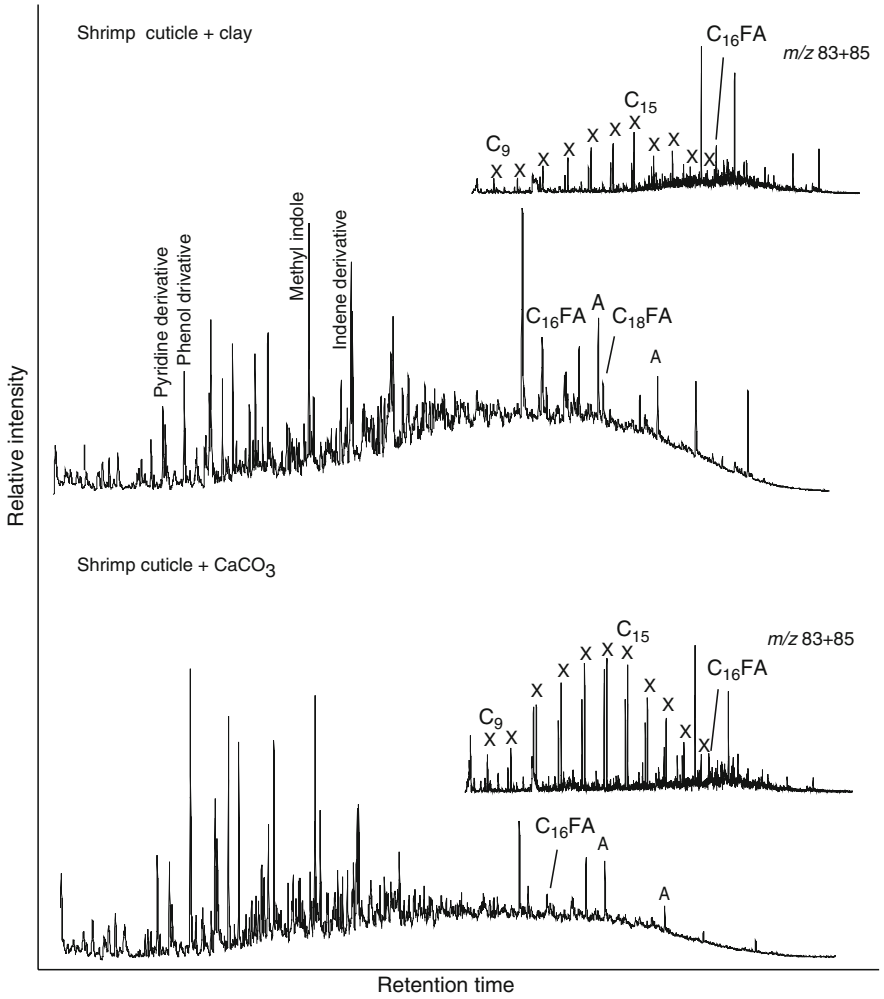

Fig. 8.4 Pyrolysis–gas chromatography–mass spectrometry analysis of shrimp cuticle heated in the presence of clay and calcium carbonate. Symbols same as in Figs. 8.2 and 8.3 (Adapted from Gupta et al. 2006a)

nitrogen-containing functional groups. Thus, both chitin and protein are nitrogen containing compounds. Amides are carboxylic acid derivatives, probably derived from nucleophilic reaction of N-bearing-components in chitin/protein complex of the cuticle with the fatty acyl components during maturation (Gupta et al. 2006). Indenes and their alkylated substituents, if present, are likewise derived from aromatization of compounds derived from chitin/protein in the cuticle. Indeed, Indene and its alkylated derivatives have been detected in Jurassic squid pens and Cretaceous shrimps (Stankiewicz et al. 1997c).

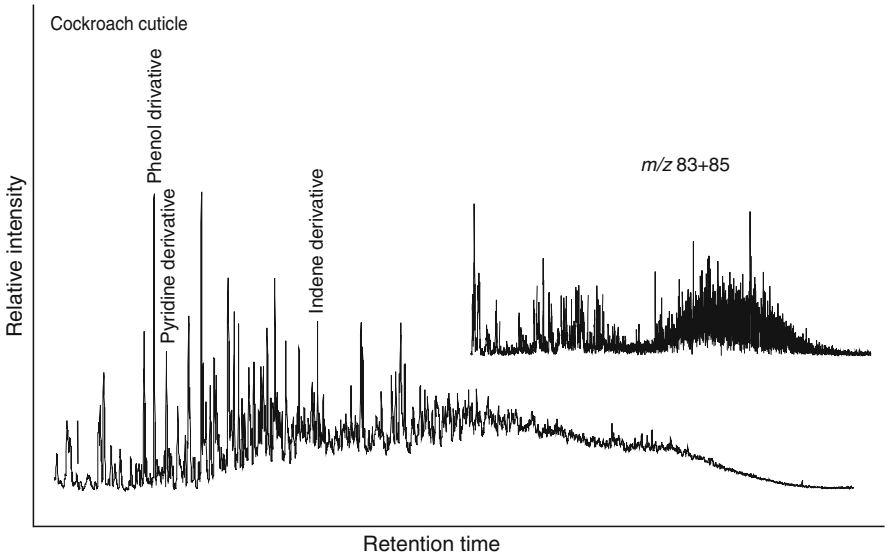

Fig. 8.5 Pyrolysis –gas chromatography–mass spectrometry analysis of cockroach cuticle that has been experimentally heated after removal of lipids. *Inset m/z* 85+83 does not reveal alkane/alkene homologues (x) present in heated shrimp and cockroach cuticle from which lipids have not been removed. Symbols same as in Figs. 8.2 and 8.3 (Adapted from Gupta et al. 2006a)

Shrimp cuticle matured in the presence of clay (Fig. 8.4) yielded a composition similar to untreated cuticle; however, cuticle matured in the presence of $CaCO_3$ (Fig. 8.4) showed reduction in the relative abundance of amides and *n*-alkane/alk-1-ene homologues. Thus, the presence of $CaCO_3$ may inhibit the production and formation of these components during the maturation experiment and/or during pyrolysis. Importantly, although the relative abundance was affected alkane/alkene homologues formed even in the presence of these matrix minerals (Stankiewicz et al. 2000).

Experiment conducted on cuticle post extraction and saponification yielded moieties related solely to matured chitin/protein and no *n*-alkyl component. As commercial chitin matured at 350°C and 700 bars failed to yield an aliphatic component, these must have been derived from the other components in the cuticle. This provides direct experimental evidence that lipids present in the extractable and hydrolysable fraction of the cuticle are necessary for the formation of the aliphatic polymer.

The experiment shows that an arthropod cuticle in a closed system (eliminating contamination from an external source) can yield an aliphatic component (Gupta et al. 2006) that can be generated from constituents within the cuticle itself upon artificial maturation, confirming the results of Stankiewicz et al. (2000) and expanding them to two other arthropods. This confirms that the aliphatic component encountered in fossil insect tissues is not the result of migration from an external source (Baas et al. 1995) but rather a product of incorporation of lipids present in the organism itself.

8.6.1 Geochemistry of Plant Fossils

Cuticles of higher vascular plants have a heterogeneous composition, they consist of an organically soluble fraction (such as plant waxes; Eglinton and Hamilton 1967) and the structural biopolymer cutin that is hydorolysable in basic conditions (Kolatukuddy 1980). Additionally, Nip et al. (1986) isolated a non-hydrolysable aliphatic macropolymer (cutan) from the cuticle of *Agave americana*. Tegelaar et al. (1991) proposed that cutan is widespread in the plant kingdom and plants with cutan have a high probability of entering the fossil record. As fossil leaves and cuticles across the geologic time scale (especially those of pre-Tertiary age) have a partial aliphatic composition, this composition has been attributed to the selective preservation of cutan. However, recent analysis of a wide variety of Gymnosperms and Angiosperms has failed to detect the presence of cutan in plants previously thought to contain cutan (Mösle et al. 1998; Gupta et al. 2006b), despite their fossil equivalents revealing an aliphatic composition; instead it has been argued that cutan may be limited to draught-adapted plants with very thick cuticles (Boom et al. 2005). This has renewed interest in understanding the origin of aliphatics in fossil organic matter both in animals and in plants (Briggs 1999). In the absence of cutan, the occurrence of aliphatics in fossil plants could instead be explained by preservation of non-recalcitrant (i.e. extractable and non-hydrolysable) aliphatic moieties e.g., waxes, membrane lipids and cutin. A similar process of polymerisation involving free and ester bound cuticular lipids has been invoked to explain the aliphatic character of fossil insects, where a similar aliphatic composition is encountered in the fossils as discussed in this chapter earlier. Experimental evidence for this was provided by using gold tube artificial heating of modern scorpion cuticle (Stankiewicz et al. 2000; Gupta et al. 2006a). Such techniques have been successfully used to understand thermal maturation and fossilisation of Type II kerogens, alginite, shales (Michels et al. 1995), coal (Landais et al. 1989) and other type III organic matter. Indeed, comparison between natural coalification stages and those using confined pyrolysis have indicated close replication of the natural process (Monthioux et al. 1985).

8.7 Experimental Heating of Plant Tissue Constituents

This study applies the same approach used for arthropods to the artificial heating of leaf tissues at various levels of chemical pre-treatment to evaluate the source of the aliphatic polymer encountered in fossil plant organic matter.

Experimental heating was conducted on extant leaves and plant tissue constituents at 350°C, confined under 700 bars for a duration of 24 h similar to the arthropod cuticles (Gupta et al. 2006a; Gupta et al. 2007a). Tissue components were heated at various levels of chemical treatment to evaluate the fate of various constituent biopolymers and determine their possible role in contributing to the formation of an aliphatic polymer. Whole leaves of extant *Castanea* were heated to understand

the overall distribution of products derived from various constituents: lignin, polysaccharides, cutin, cuticular lipids and internal lipids. The leaf tissues were also matured after lipid extraction (i.e. in the absence of internal+cuticular lipids) and saponification (i.e. in the absence of lipids and cutin, see Gupta et al. 2007a for conditions). In addition, cutin was isolated from tomato cuticle (by mechanical isolation followed by lipid extraction) and pure model compounds lignin and cellulose (Sigma-Aldrich) were also heated to assess if these can yield aliphatics under these pressure–temperature conditions. To assess the role of internal lipids internal tissue of tomato pulp was also heated (Fig. 8.1). The cuticle of *Agave americana* and associated tissue was heated similar to *Castanea* to determine to survival of cutan at these conditions.

Thus, this investigation attempts to approximate organic plant tissue fossilisation in the laboratory and evaluates fate of constituent biopolymers.

8.8 Transformation of Plant Tissue Constituents

Note that all pyrolysis results follow thermodesorption of extractable components (at 310°C for 10 s) and thus represents macromolecular component.

Pyrolysis of the modern leaf tissues (Fig. 8.6) yielded predominantly carbohydrate, lignin (guaiacyl and syringyl-related components), and protein moieties together with C_{16} and C_{18} fatty acids, reflecting the bulk composition of the leaf (Ralph and Hatfield 1991; Gupta and Pancost 2004). The fatty acyl moieties are derived from the biopolyester cutin Tegelaar et al. (1989) and internal lipids.

In contrast, heated *Castanea* tissues (without any chemical treatment) yielded chromatograms similar to those, commonly observed for fossil leaves, i.e. dominated by *n*-alkane/alkene homologues representing an *n*-alkyl component (Fig. 8.6). The *n*-alkanes range from C_9 to C_{31} and the *n*-alkenes from C_9 to C_{29}. The most abundant *n*-alkane is C_{27} homologue. Of the fatty acids released during pyrolysis, the C_{16} and C_{18} straight-chain homologues were the most abundant, with the straight chain C_{12}, C_{13}, C_{14}, and C_{15} components also were found to be present. Apart from the aliphatics other important pyrolysis products included phenol and its alkyl derivatives, benzene and its alkyl derivatives and indoles. Guaiacyl and syringyl related lignin moieties, as seen in the modern leaf tissue were not observed in detectable amounts in the matured leaves.

Interestingly, the analysis of leaf tissue matured after extraction and hydrolysis revealed that *n*-alkane/alkene homologues were absent in detectable amounts (including the short chain ones) and only phenols, benzene derivatives, etc. were present (Fig. 8.6). Thus, the absence of long chain *n*-alkanes in the pyrolysate suggests that their presence in untreated artificially heated leaves is due to contribution from the lipids in the soluble fraction.

The analysis of matured tomato internal tissue reveals a distinct aliphatic component (Fig. 8.7); the *n*-alkane/alkene homologues range from $C_{8\text{ to }26}$ (Fig. 8.7), Those with carbon chain length $C_{13,\ 14}$ and C_{15} have a high relative abundance.

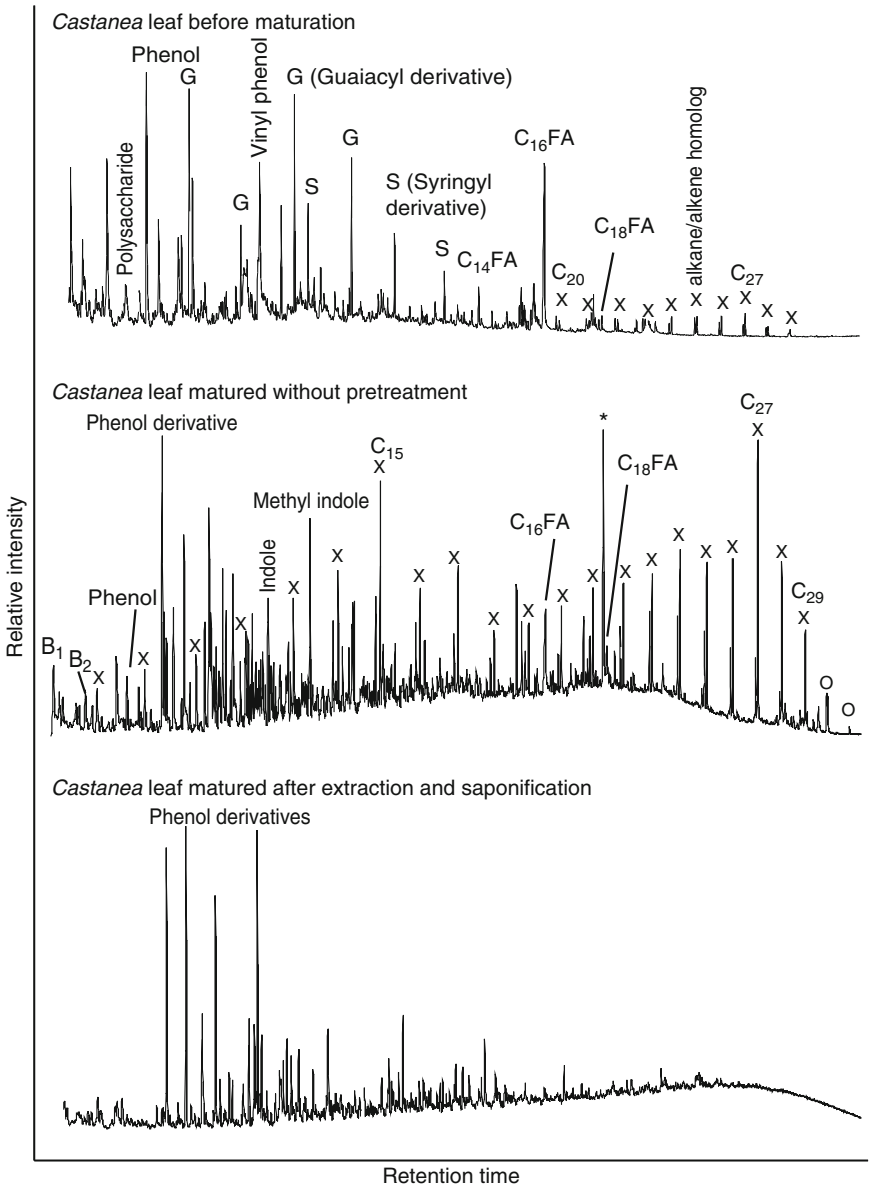

Fig. 8.6 Pyrolysis–gas chromatography–mass spectrometry analysis of modern untreated *Castenea* and samples that have been subjected to chemical pre-treatments before being experimentally heated. Note lack of alkane alkene peaks (x) after lipids have been removed from sample prior to experimental heating. B_1 toluene and B_2 dimethyl benzene. Symbols same as in Figs. 8.2 and 8.3 (Adapted from Gupta et al. 2007b)

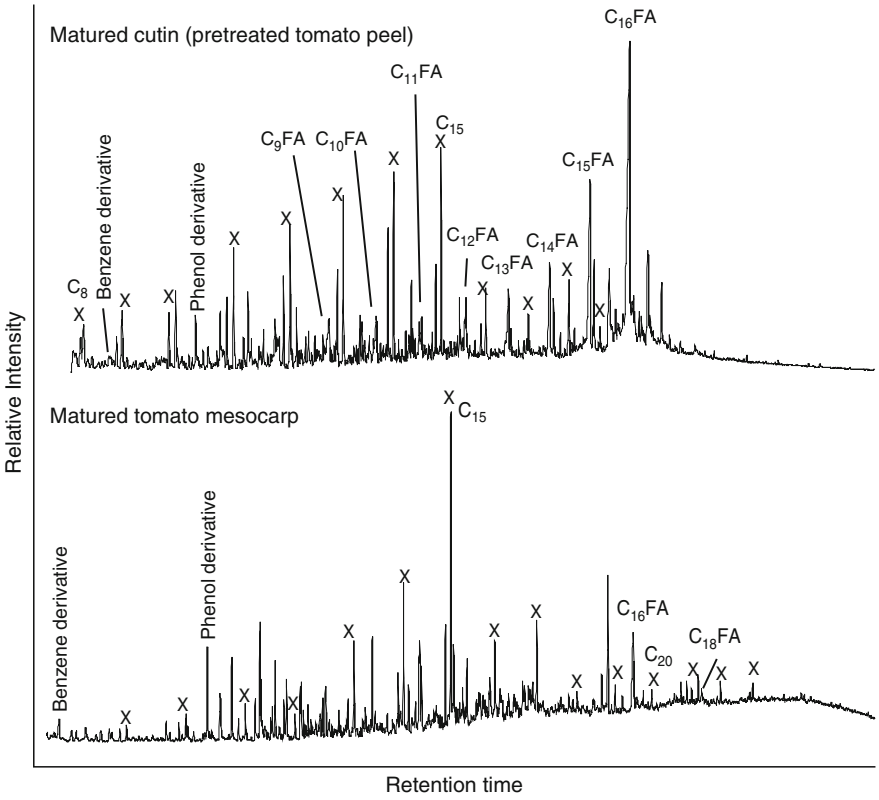

Fig. 8.7 Pyrolysis–GC–MS analysis of matured tomato peel/cutin and tomato mesocarp (internal tissue), showing distribution of alkane alkene peaks (x). Symbols same as in Figs. 8.2 and 8.3. Symbols same as in Figs. 8.2 and 8.3 (Adapted from Gupta et al. 2007b)

Model compounds such as lignin and cellulose were also heated. In the pyrolysates of these aromatic and phenolic moieties were detected; neither fatty acids nor *n*-alkanes were found. As, these failed to generate any aliphatic polymer, these do not contribute to any aliphatic component.

To understand the behaviors of cutin, isolated tomato peel was heated and it generated alkane/alkene homologues up to C_{19} and additional fatty acids.

To understand the behaviour of cutan, cuticle and associated tissue from *Agave americana* was heated. *Agave* matured without any treatment revealed the presence of *n*-alkane/alkene homologues ranging from $C_{8\text{ to }35}$ (Fig. x). Benzene derivatives, phenols and fatty acyl moieties were also observed as with the other plants. The *n*-alkane/alkene homologues (including those with carbon number > *n*-C_{20}) persisted in the tissue matured after both lipid extraction and saponification (Fig.), unlike the other plant tissues (Gupta et al. 2007a). Thus, cutan survives at these pressure temperature conditions. The absence of aliphatic component in *Castanea* matured after hydrolysis attests to the lack of cutan in it.

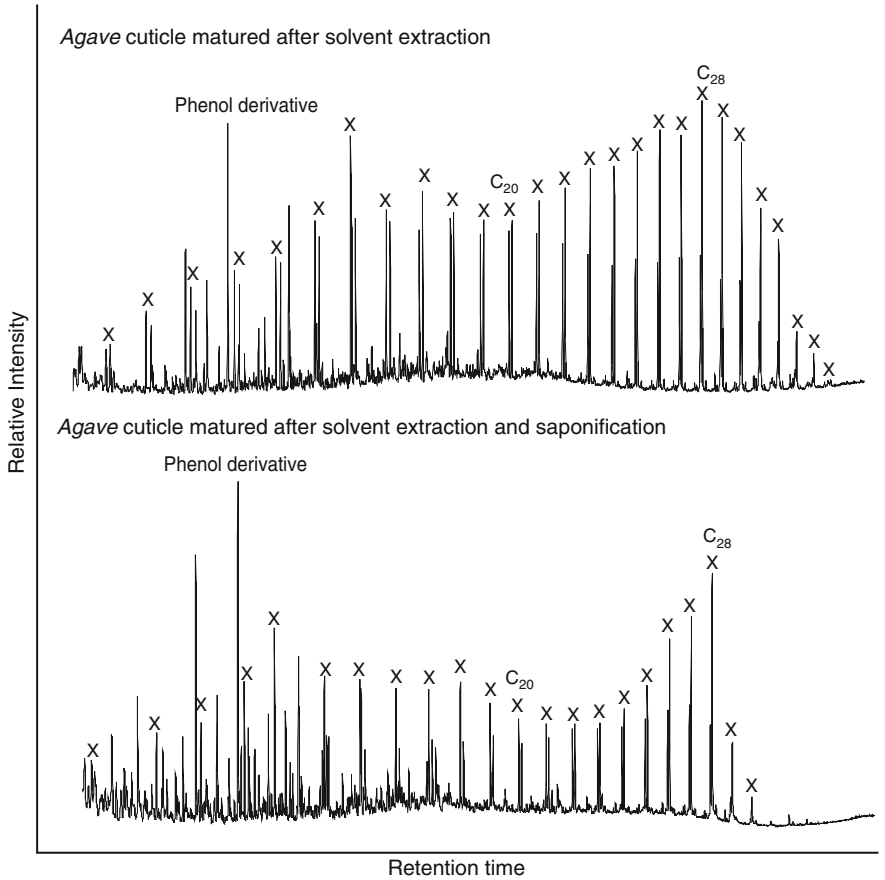

Fig. 8.8 Pyrolysis–GC–MS analysis of *Agave* matured after solvent extraction and after extraction and saponification showing presence of alkane alkene homologues even in samples from which lipids have been removed. Symbols same as in Figs. 8.2 and 8.3. Symbols same as in Figs. 8.2 and 8.3 (Adapted from Gupta et al. 2007b)

All previously reported pyrolysates of fossil leaves and cuticles in the Cenozoic, irrespective of age, plant type or enclosing lithology, show the presence of aliphatic components (Nip et al. 1986; Tegelaar et al. 1991; Mösle et al. 1998; Gupta et al. 2007b). This experimental study clearly demonstrates that in the absence of cutan; cutin, higher plant waxes and internal lipid components can serve as a source for the aliphatic component commonly observed in plant fossils. A similar explanation has been invoked for explaining the aliphatic composition of arthropod fossils earlier (Briggs 1999; Stankiewicz et al. 2000 none of which has a recalcitrant aliphatic precursor. This experiment provides evidence for such a process. The experiment provides a closed system without any incorporation of agents from an external source proving that the cuticle and associated tissue is capable of producing an aliphatic

component from constituents within the cuticle/tissue itself without migration from an external source.

It has been proposed that autoxidation can lead to polymerization of fatty acids, yielding structures containing aliphatic and, to a lesser extent, aromatic moieties. Recently, analysis of fossil dinoclasts indicated formation by oxidative polymerization of lipids, derived from cellular membranes and storage vesicles (de Leeuw et al. 2006). Oxidative crosslinking has been observed to contribute significantly to kerogen formation, where the role of selective preservation is limited (Riboulleau et al. 2001), and also in early stages of the formation of coorongite (Gatellier et al. 1993). This experimentally supported investigation provides further evidence that lipid incorporation can play an important role in fossilization of plant and arthropod constituents and this process may be of widespread importance.

References

Baas M, Briggs DEG, van Heemst JDH, Kear AJ, de Leeuw JW (1995) Selective preservation of chitin during the decay of shrimp. Geochim Cosmochim Acta 59:945–951

Boom A, Sinninghe Damsté JS, de Leeuw JW (2005) Cutan, a common aliphatic biopolymer in cuticles of droughtadapted plants. Org Geochem 36:595–601

Briggs DEG (1999) Molecular taphonomy of animal and plant cuticles: selective preservation and diagenesis. Philos Trans R Soc Lond 354:7–16

Briggs DEG, Kear AJ (1993) Fossilization of soft-tissue in the laboratory. Science 259:1439–1442

de Leeuw JW, Versteegh GJM, van Bergen PF (2006) Biomacromolecules of algae and plants and their fossil analogues. Plant Ecol 182:209–233

Duncan IJ, Titchener F, Briggs DEG (2003) Decay and disarticulation of the cockroach: implications for the preservation of the blattoids of Writhlington (Upper Carboniferous), UK. Palaios 18:256–265

Eglinton G, Hamilton RJ (1967) Leaf epicuticular waxes. Science 156:1322–1334

Gatellier J-PLA, de Leeuw JW, Sinninghe Damsté JS, Derenne S, Largeau C, Metzger P (1993) A comparative study of macromolecular substances of a Coorongite and cell walls of the extant alga Botryococcus braunii. Geochim Cosmochim Acta 57:2053–2068

Gupta NS, Pancost RD (2004) Biomolecular and physical taphonomy of angiosperm leaf during early decay: implications for fossilisation. Palaios 19:428–440

Gupta NS, Michels R, Briggs DEG, Evershed RP, Pancost RD (2006a) The organic preservation of fossil arthropods: an experimental study. Proc R Soc Lond B 273:2777–2783

Gupta NS, Collinson ME, Briggs DEG, Evershed RP, Pancost RD (2006b) Re-investigation of the occurrence of cutan in plants: implications for the leaf fossil record. Paleobiology 32:432–449

Gupta NS, Briggs DEG, Collinson ME, Evershed RP, Michels R, Jack KS, Pancost RD (2007a) Evidence for the in situ polymerisation of labile aliphatic organic compounds during the preservation of fossil leaves: Implications for organic matter preservation. Org Geochem 38:499–522

Gupta NS, Michels R, Briggs DEG, Collinson ME, Evershed RP, Pancost RD (2007b) Experimental evidence for the formation of geomacromolecules from plant leaf lipids. Org Geochem 38:28–36

Hof CHJ, Briggs DEG (1997) Decay and mineralization of mantis shrimps (Stomatopoda: Crustacea) – a key to their fossil record. Palaios 12:420–438

Kolatukuddy PE (1980) Biopolyester membranes of plants: cutin and suberin. Science 208: 990–1000

Landais P, Michels R, Poty B (1989) Pyrolysis of organic matter in cold-seal autoclaves. Experimental approach and application. J Anal Appl Pyrol 16:103–115

Michels R, Landais P, Torkelson BE, Philp RP (1995) Effects of confinement and water pressure on oil generation during confined pyrolysis, hydrous pyrolysis and high pressure hydrous pyrolysis. Geochim Cosmochim Acta 59:1589–1604

Monthioux M, Landais P, Monin JC (1985) Comparison between natural and artificial maturation series of humic coals from the Mahakam delta, Indonesia. Org Geochem 8:275–292

Mösle B, Collinson ME, Finch P, Stankiewicz BA, Scott AC, Wilson R (1998) Factors influencing the preservation of plant cuticles: a comparison of morphology and chemical composition of modern and fossil examples. Org Geochem 29:1369–1380

Nip M, Tegelaar EW, Brinkhuis H, de Leeuw JW, Schenk PA, Holloway PJ (1986) Analysis of modern and fossil plant cuticles by Curie point Py-GC and Curie point Py-GC–MS: recognition of a new, highly aliphatic and resistant biopolymer. Org Geochem 10:769–778

Ralph J, Hatfield RD (1991) Pyrolysis-GC–MS characterization of forage materials. J Agric Food Chem 39:1426–1437

Riboulleau A, Derenne S, Largeau C, Baudin F (2001) Origin of contrasting features and preservation pathways in kerogens from the Kashpir oil shales (Upper Jurassic, Russian Platform). Org Geochem 32:647–665

Sagemann J, Bale SJ, Briggs DEG, Parkes RJ (1999) Controls on the formation of authigenic minerals in association with decaying organic matter: an experimental approach. Geochim Cosmochim Acta 63:1083–1095

Stankiewicz BA, Briggs DEG, Evershed RP, Duncan IJ (1997a) Chemical preservation of insect cuticles from the Pleistocene asphalt deposits of California, USA. Geochim Cosmochim Acta 61:2247–2252

Stankiewicz BA, Briggs DEG, Evershed RP, Flannery MB, Wuttke M (1997b) Preservation of chitin in 25-million-year-old fossils. Science 276:1541–1543

Stankiewicz BA, Briggs DEG, Evershed RP (1997c) Chemical composition of Paleozoic and Mesozoic fossil invertebrate cuticles as revealed by pyrolysis-gas chromatography/ mass spectrometry. Energy Fuels 11:515–521

Stankiewicz BA, Mastalerz M, Hof CHJ, Bierstedt A, Briggs DEG, Evershed RP (1998) Biodegradation of chitin protein complex in crustacean cuticle. Org Geochem 28:67–76

Stankiewicz BA, Briggs DEG, Michels R, Collinson ME, Evershed RP (2000) Alternative origin of aliphatic polymer in kerogen. Geology 28:559–562

Tegelaar EW, de Leeuw JW, Holloway PJ (1989) Some mechanisms of flash pyrolysis of naturally occurring higher plant polyesters. J Anal Appl Pyrol 15:289–295

Tegelaar EW, Kerp H, Visscher H, Schenk PA, de Leeuw JW (1991) Bias of the paleobotanical record as a consequence of variations in the chemical composition of higher vascular plant cuticles. Paleobiology 17:133–144

Index